Electronic Thesis and Dissertation Repository

10-6-2011 12:00 AM

Maternal and Fetal Plasma Protein Changes in Fetal Growth Restriction

Maxim D. Seferovic, *The University of Western Ontario*

Follow this and additional works at: https://ir.lib.uwo.ca/etd

■ Part of the Female Urogenital Diseases and Pregnancy Complications Commons

Maternal and Fetal Plasma Proteome Changes in Fetal Growth Restriction

Plasma proteome changes in FGR

An Integrated-Article Thesis

by

Maxim D. Seferovic

Graduate Program in Biochemistry

Submitted in partial fulfillment
of the requirements for the degree of
Doctor of Philosophy

The School of Graduate and Postdoctoral Studies
The University of Western Ontario
London, Ontario, Canada

THE UNIVERSITY OF WESTERN ONTARIO
SCHOOL OF GRADUATE AND POSTDOCTORAL STUDIES

CERTIFICATE OF EXAMINATION

Supervisor

_____
Dr. Victor Han

Co-Supervisor

_____
Dr. Madhulika Gupta

Supervisory Committee

_____
Dr. Ken Yeung

_____
Dr. David Litchfield

Examiners

_____
Dr. Anthony Rupar

_____
Dr. Walter Siqueira

_____
Dr. Tim Regnault

_____
Dr. John Wilkins

The thesis by

Maxim Daniel Seferovic

entitled:

Maternal and fetal plasma proteome changes in fetal growth restriction

is accepted in partial fulfilment of the
requirements for the degree of
Doctor of Philosophy

Date_____   _____
                                              Chair of the Thesis Examination Board

Abstract

Fetal Growth Restriction (FGR) is caused by impaired maternal-fetal exchange of oxygen and nutrients causing fetal hypoxia and starvation. A functional failure of the placenta is the underlying cause, however the pathophysiology remains unknown. The fetus adapts by limiting growth, reducing demand for metabolic substrates. Monitoring the fetal size is the primary clinical method of FGR detection, though it does not distinguish a constitutionally small fetus from a pathological. Proteomic profiling of fetal and maternal plasma was therefore undertaken for discovery of biomarkers and pathological mechanisms. As a model of hepatic secreted fetal plasma proteins, HepG2 cell secretion changes in hypoxia were also investigated.

Profiling mother's plasma revealed altered expression of vascular regulatory proteins VCAM-1 and haptoglobin. VCAM-1 positively correlated to placental size. Profiling of HepG2 secreted proteins in hypoxia revealed increased angiogenic protein PAI-1, and the growth inhibitor IGFBP-1. Fetal plasma PAI-1 levels were found to be oxygen dependent, and the levels determinant of plasma's *in vitro* angiogenic potency. For IGFBP-1, increased phosphorylation was found at four discrete sites, leading to increased affinity for IGF-I, and mitigation of IGF-I stimulated cell proliferation *in vitro*.

Increased VCAM-1 relative to placental size in FGR has potential as a marker of placental health. Fetal plasma PAI-1 levels mediating angiogenesis is a newly discovered mechanism in FGR. PAI-1's hypoxia-dependent hepatic induction and consequent angiogenic effect may have significance to placental maldevelopment. Discovery of

increased IGFBP-1 phosphorylation in hypoxia, and its inhibition of IGF-I mediated

proliferation, may be an adaptive mechanism limiting fetal growth in FGR.

Co-Authorship Statement

Chapter 7 was written by Dr. Madhulika Gupta with sections and the figures written and prepared by me, and modified based on review by Dr. Victor Han. Chapter 2 was co-written with Dr. Madhulika Gupta and modified based on review by Dr. Victor Han. Chapters 3 and 4 were written by me and modified based on reviews by Dr. Madhulika Gupta. All other chapters were written by me and modified based on review by Dr. Victor Han.

Chapter 2

Dr. Suya Liu performed all mass spectrometry (Figure 2.2). Dr. Robert Gratton assessed the clinical charts. Jamie Seabrook performed the statistical analysis. A small part of this work was done as part of my fourth year honours project in the Department of Biochemistry.

Chapter 3

Violet Krughkov optimized the amount of denaturant to add to the depletion buffer.

Chapter 4

The mass spectrometry was done in collaboration with Dr. Devanand Pinto. Shali Chen provided a protocol, reagents, and cells for the angiogenic assays.

<u>Chapter 7</u>

Rashad Ali completed some of the hypoxia and leucine deprivation experiments before my taking over the project upon his departure. His and my experiments together were used for Figures 7.1 A and B, 7.2, 7.3, and 7.4. Dr. Javad Khosravi performed the IGFBP-1 ELISA on our samples (Figure 7.3) using an assay he developed. Suya Liu performed all mass spectrometry on our samples (Figure 7.4). Using our experiments, Hiroyasu Kamei performed the functional assays (Figure 7.6), and Dr. Madhulika Gupta performed the Biacore analysis (Figure 7.5).

Acknowledgements

I would like to recognize the contributions of my supervisors; **Dr. Madhulika Gupta,** particularly for her instruction, and patient consultation; **Dr. Victor Han**, for his guidance and judicious oversight, and for entrusting me with this research project in the very beginning. The completion of this thesis is a shared accomplishment with them.

From National Research Council in Halifax, I thank **Dr. Devanand Pinto,** for graciously taking me on in his lab, and also, **Ken Chisholm** for teaching me the fundamental techniques of tandem mass spectrometry.

From the Department of Biochemistry, I thank my graduate committee members **Dr. David Litchfield** and **Dr. Ken Yeung** for their stewardship over the years.

From the Han Lab I thank **Dr. Christiana Iosef** for our many useful conversations, and for being an indispensible reference on laboratory techniques and best practice. I also thank all the **members of the Han and Gupta Labs**, including the many medical and graduate students whom have come and gone, for making my time enjoyable. Among them, I particularly thank **Amer Youseff** and **Majida Abu Shehab** for their help, opinions, and fellowship.

Table of Contents

List of Figures

List of Tables

List of Appendices

List of Abbreviations, Symbols, and Nomenclature

2-D	2-dimensional
3-D	3-dimensional
2-DGE	2- dimensional gel electrophoresis
Ab	Antibody
ABC	Ammonium bicarbonate
ACN	Acetonitrile
AKP	Alkaline phosphatase
ARED	Absent or reversed end diastolic flow
ASP-N	Aspartate N-endoproteinase
B	Bound fraction
BCA	Bicinchoninic acid
BPS	Biophysical profile score
BSA	Bovine serum albumin
CAM	Cellular adhesion molecule
CE	Collision energy
CHAPS	3-[(3-cholamidopropyl)dimethylammonio]-1-propanesulfonate
CID	Collision-induced dissociation
CM	Conditioned media (Media containing secreted proteins)
D	Depleted fraction
DMEM/F-12	Dulbecco's modified eagle medium with nutrient mixture F-12
DOHaD	Developmental origins of health and disease
DTT	Dithiothreitol
ECL	Enhanced chemiluminescence
ECM	Extracellular matrix
EDTA	Ethylenediaminetetraacetic acid
EDV	End diastolic velocity
EGM	Endothelial growth media
ELISA	Enzyme-linked immunosorbant assay
ESI	Electrospray ionization

ExPASy	Expert protein analysis system (a website of proteomic analysis tools)
FBS	Fetal bovine serum
FGF-2	Fibroblast growth factor 2
FGR	Fetal growth restriction
FH	Fetal heart rate
GA	Gestational age
GAPDH	Glyceraldehyde 3-phosphate dehydrogenase
Glu	Glutamine
GE	Gel electrophoresis
HBS-EP	HEPES buffer saline with EDTA and polysorbate
hCG	Human chorionic gonadotropin
HEK	Human embryonic kidney cells
HELLP	Hemolytic anemia, elevated liver enzymes, and low platelet count
HEPES	4-(2-hydroxyethyl)-1-piperazineethanesulfonic acid
HepG2	Hepatoma G2 cells
HIF	Hypoxia-inducible factor
Hp	Haptoglobin
HPLC	High performance liquid chromatogroph(er/y)
HRE	Hypoxia response element (HIF complex promoter region)
HRP	Horseradish peroxidase
HUVEC	Human umbilical vein endothelial cells
ICAM-1	Intra-cellular adhesion molecule 1
IEF	Isoelectric focusing
IGF-I	Insulin-like growth factor-1
IGFBP-1	IGF binding protein-1
IGFs	Insulin-like growth factors
IgG	Immunoglobin G
IL-1β	Interleukin-1 beta
IL-6	Interleukin-6
IPG	Immobilized pH gradient
KA	Equilibrium association constant

KD	Equilibrium dissociation constant
LC	Liquid chromatograph(er/y)
LC-MS	Liquid chromatography mass spectromet(er/ry)
LC-MS/MS	Liquid chromatography tandem mass spectromet(er/ry)
Leu	Leucine
Mab	Monoclonal antibody
MALDI	Matrix-assisted laser desorption/ionization
MARS	Multiple affinity removal system
MMP	Matrix metalloproteinase
MRM	Multiple reaction monitoring
MS	Mass spectromet(er/ry)
MS/MS	Tandem mass spectromet(er/ry)
MTS	(3-(4,5-dimethylthiazol-2-yl)-5-(3-carboxymethoxyphenyl)-2-(4-sulfophenyl)-2H-tetrazolium)
MW	Molecular weight
MWCO	Molecular weight cut-off
NCBI	National center for biotechnology information
NF-κB	Nuclear factor kappa-light-chain-enhancer of activated B cells
NL	Non-linear
NS	No significance
OD	Optical density
PAI-1	Plasminogen activator inhibitor-1
PAPP-A	Pregnancy-associated plasma protein A
PBS	Phosphate buffer saline
PE	Preeclampsia
PED	Preserved end diastolic flow (opposite of ARED)
PHD	Hydroxylase domain containing enzyme
pI	Isoelectric point
PI	Propidium Iodide
PlGF	Placental growth factor
pS/pSer	Phosphoserine

PTM	Post-translational modification
PVDF	Polyvinylidene fluoride
pVHL	von Hippel–Lindau protein
Q-TOF	Quadrupole time of flight
Q-Trap	Quadrupole linear trap
RBP	Retinol binding protein
RH	Rehydration
RHB	Rehydration buffer
rIGF-I	Recombinant human IGF-I
ROS	Reactive oxygen species
RP-HPLC	Reverse phase high performance liquid chromatogroph(er/y)
SD	Standard deviation
SDS	sodium dodecyl sulfate
SEM	Standard error of the mean
Ser	Serine, with sequential amino acid position (e.g. 98/101/119/169)
SF	Serum free
SOCS	Suppressors of cytokine signaling
SPR	Surface plasmon resonance
TBS	Tris buffer saline
TFA	Trifluoroacetic acid
TNF-α	Tumour necrosis factor alpha
TOF	Time of flight
Tris	tris(hydroxymethyl)aminomethane
TTR	Transthyretin
UA	Umbillical artery
US	Ultrasonographic or ultrasound
UV	Ultra-violet or Umbillical vein
VCAM-1	Vascular cellular adhesion molecule 1
VEGF	Vascular endothelial growth factor
WP	Whole plasma

CHAPTER 1

Introduction

1.1. FETAL GROWTH RESTRICTION

1.1.1. Definition and outcome

Fetal growth restriction (FGR) is defined by the estimated fetal weight during gestation or birth weight being below the tenth percentile (1, 2). It is a condition that affects 5-7% of all pregnancies in Canada and it is a major contributor to both perinatal morbidity and mortality (3). Fetal growth restriction has been associated with significantly increased risk of perinatal death (3). Many FGR babies recover and undergo "catch-up growth" in the post-natal period, but the effects of this have health consequences in adulthood, with higher rates of disease in later life (4). They have increased risk for neurological and metabolic problems, type II diabetes, and especially, cardiovascular diseases such as hypertension, coronary heart disease and stroke (4, 5, 6). This process is termed the developmental origins of health and disease (DOHaD).

FGR, or intrauterine growth restriction (IUGR) as it is used interchangeably, does not have a single pathology; rather, it is a term used to describe a multitude of etiologies that manifest as poor fetal growth. It is also distinct from small for gestational age (SGA), which is a more inclusive term used to describe babies born small with birth weights below the tenth percentile, but may include both healthy but constitutionally small, as well as those who result from pathological pregnancies. Specifically, FGR describes fetuses whose growth is limited by pathologies during pregnancy of either intrinsic fetal (genetic or infective) or extrinsic problems in the gestational
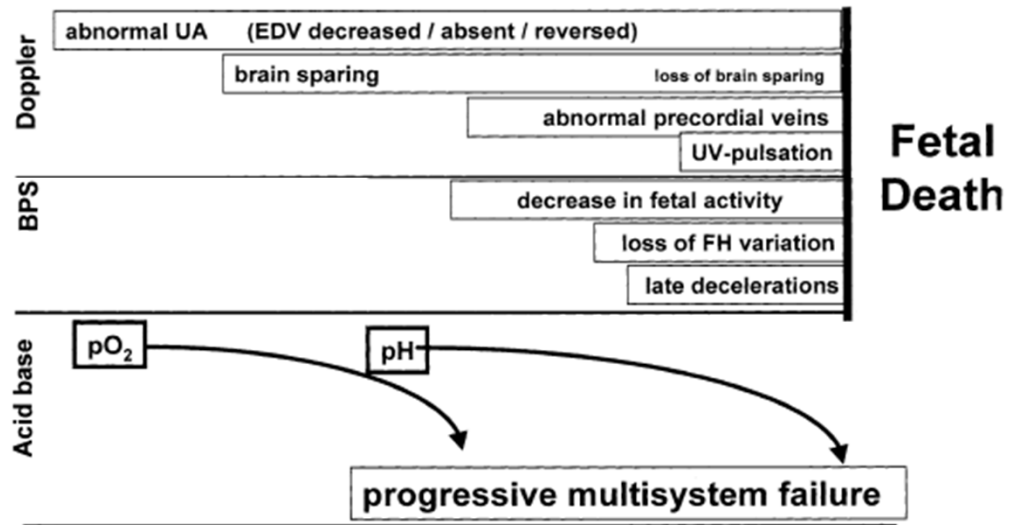
FIGURE 1.1. A progressive deterioration in fetal variables indicating declining metabolic status and possible death. Using Doppler, a measure of blood flow, abnormalities in blood flow. With increasing umbilical artery Doppler resistance, vascular adaptations lead to brain sparing at the expense of other organs. With more severe resistance, there is a decline in the biophysical profile (BPS), as these vascular adaptations fail. Declining O_2 and pH become take hold. The Decline of the biophysical variables are related to the acid-base status, and can ultimately result in fetal death

UA, umbilical artery; UV, umbilical vein; EDV, end diastolic velocity; FH, fetal heart rate; BPS, biophysical profile score.

Reproduced from *Seminars in Perinatology* 28(1). Baschat, A.A., and Hecher, K., Fetal growth restriction due to placental disease. pgs 67-80. Copyright 2004, with permission from Elsevier.

environment. Generally then, FGR babies are restricted to those whose growth do not achieve their normal potential *in utero* due to pathological factors (1).

1.1.2. Etiology

The etiology of FGR is highly diverse. Broadly, it can be broken down into causes intrinsic to the fetus or extrinsic, which are either maternal or placental. The latter causes are more common, and perhaps, more amenable to intervention. Fetal factors account for 10-20% of cases and are either genetic, such as chromosomal anomalies, mutations of growth factor or receptor genes, or congenital infections, most commonly viral (7). Maternal factors account for another 20-30% of cases, of which hypertensive disorders such as preeclampsia is most common (7). Other maternal factors include diabetes, poor nutrition, smoking, and drug and alcohol abuse (2, 8). The remainder and most common etiology is of placental origin of which the most common cause is uteroplacental or placental insufficiency. FGR caused by placental factors is the etiology of which this thesis will focus. In a broad sense, the placenta is unable to provide sufficient oxygen and nutrients to the fetus to achieve its growth potential. This arises when the fetal-placental vasculature does not adequately develop to facilitate maternal/fetal exchange. This failure of the placenta is therefore termed placental insufficiency, and is the most common etiology in FGR (9, 10, 11). The restricted exchange leads to conditions of acidosis and hypoxia, spurring fetal adaptation to the environment (Figure 1.1). Vascular and cardiac adaptations to the reduced blood flow result in brain sparing mechanisms, whereby blood is shunted

towards the brain at the expense of other organs, particularly the lungs and gastrointestinal organs, including liver and kidney. The growth of the fetus is limited to reduce the demand for metabolic substrates. If adaptive mechanisms become inadequate, the low oxygen conditions can no longer be accommodated, resulting in fetal death.

The fetal-placental vasculature is compromised in placental insufficiency, causing poor maternal/fetal exchange. Morphological evidence shows the villous tree of the chorionic villi in the fetal-placental vasculature to be poorly developed. Specifically there is a reduction in the volume density, the length ratio, and the degree of branching (12). Generally, this lower degree of branching results in longer villi, increasing vascular resistance. This increase in resistance is detected clinically by umbilical cord Doppler blood flow measurement. An increase in resistance leads to a decrease or even reversal of blood flow, and it is diagnostic of placental insufficiency (13).

As might be expected, it has long been theorized that abnormal angiogenic regulation in the microvilli of these pregnancies causes the vascular malformation, leading to placental insufficiency and FGR. The changing levels of VEGF, PlGF, and FGF-2 are thought to be important in the normal development of the placental vasculature. Abnormally low levels of VEGF have been observed, while levels of PIGF have been seen to increase. Despite this, the precise molecular mechanisms by which placental insufficiency arises are not well characterized (14).

1.1.3. Diagnosis and biomarkers

Current diagnosis of FGR relies on clinical assessment of the progression of biometric criteria. A stalled progression of the symphisis-fundal height late in gestation, which is observable from a routine exam, is often the first indication of FGR. A more precise estimation of fetal size is obtained by ultrasound (US) - based fetal biometry. The estimated size and weight is compared against standardized charts to estimate the percentile fetal weight given its GA (15, 16). A fetus below or close to the 10th percentile is suspected of FGR. To determine the presence of placental insufficiency, umbilical artery Doppler (17) is used, and the waveforms are analyzed to determine fetal blood flow to and from the placenta. Higher resistance of the placental vasculature, measured by umbilical Doppler resistance index (RI), indicates placental insufficiency. At birth, the birthweight and GA are used to calculate the percentile, below the 10th being diagnosed as SGA.

Although the diagnostic methods can determine the presence of FGR, there are limitations. Firstly, the fetal biometric measurements are entirely dependent on the growth of the fetus being perturbed to an advanced degree before detection is feasible. Presuming that an effective intervention is available, earlier diagnosis would clearly be critical to the outcome of the pregnancy and wellbeing of the fetus. Secondly, the criterion that the fetus (or newborn) is below the tenth percentile for GA is inherently over-inclusive. The definition does not differentiate a constitutionally small healthy baby from one with pathological growth restriction. Finally, the observation of a perturbation in fetal growth is dependent on close monitoring of the

pregnancy, including timely ultrasound analysis, and particularly use of specialized Doppler, which is not routinely monitored in late gestation.

For these reasons, there is a need for an easily administered blood test in the mother, so that FGR and placental health can be routinely screened for as part of normal pregnancy monitoring. If the basis of the test is rooted in the pathology, it will alert the clinicians to etiological information, as well as potentially have prognostic value. A biomarker present in the mother's blood plasma is first needed to form the basis of such a screening test. Based on the significance of specific factors in the growth and development of the fetus, several peptides have been proposed as likely candidates (18). Pre-albumin remains an option for non-specific detection of fetal defects and pregnancy complications (19). Plasma leptin reflects a generalized response to hypoxic stimuli (20), while free beta-hCG and PAPP-A levels in serum have been associated with general fetal abnormality (21). Using invasive amniocentesis, the elevated levels of alpha-fetoprotein in amniotic fluid was used for detection of FGR by some physicians (22). Biomarkers that prove more reliable and specific in their diagnostic value therefore remain to be identified. Proteomic approaches offer new opportunities for potential biomarker discovery in FGR (23).

1.2.   THE PLACENTAL VASCULATURE

1.2.1. Vascular formation of the chorionic villi
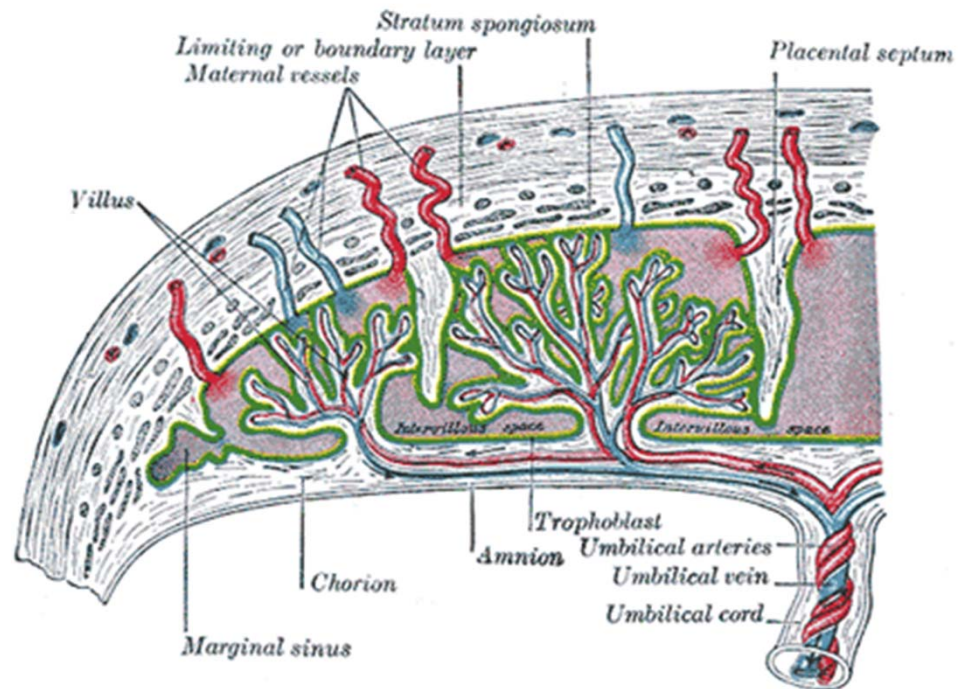
FIGURE 1.2. The maternal and fetal placental vasculature. The intervillous space is perfused with maternal blood supplied by the maternal spiral arteries. The chorionic villi bathe in the maternal blood to exchange waste products and nutrients. Exchange takes place across the syncitiotrophoblast layer which comprises the maternal-fetal blood burier. A failure in the proper formation of the chorionic villi is responsible for the increased placental resistance in placental insufficiency.

This is a reproduction from the 20th U.S. edition of Gray's Anatomy of the Human Body. Published 1918, public domain.

Maternal-fetal exchange of nutrients and waste products takes place across the placenta. Spiral arteries supply maternal blood to the intervillous space (Figure 1.2.). The fetal chorionic villi contained within compose the exchange surface across the trophoblast layers. The structure of these villi is critical to maximize the surface area, and thereby maximize exchange. Poor vascular formation of these villi is the cause of placental insufficiency and FGR.

The vasculature is formed by both angiogenesis and vasculogenesis. Angiogenesis is defined as the creation of blood vessels from existing vessels, while vasculogenesis is the creation of blood vessels from progenitor cells. These two processes are distinct. They are separate from vascular remodeling in that it is the structural change of existing vessels, so that they adopt different dimensions, or phenotypes. Vasculogenesis is important in the early phases of development (<6 weeks) (Figure 1.3 a). FGF-2 regulates the recruitment of haemangiogenic stem cells and other vascular progenitors in this stage. These cells differentiate and form haemangiogenic strands, which stretch out and eventually form tube-like structures of vascular endothelial cells with lumens, starting in week 3 (24).

Later in gestation, vasculogenesis is largely supplanted by angiogenic processes (25) (Figure 1.3 b – d). From the existing vessels then, the bulk of placental vascular development takes place in either sprouting or non-sprouting form. The balance of the two types of angiogenesis determines the character of the resulting placental villi (Figure 1.4). Normal villi have a mixture of sprouting and non-sprouting angiogenesis that leads to a mixture of branched and elongated villi. Branching angiogenesis takes
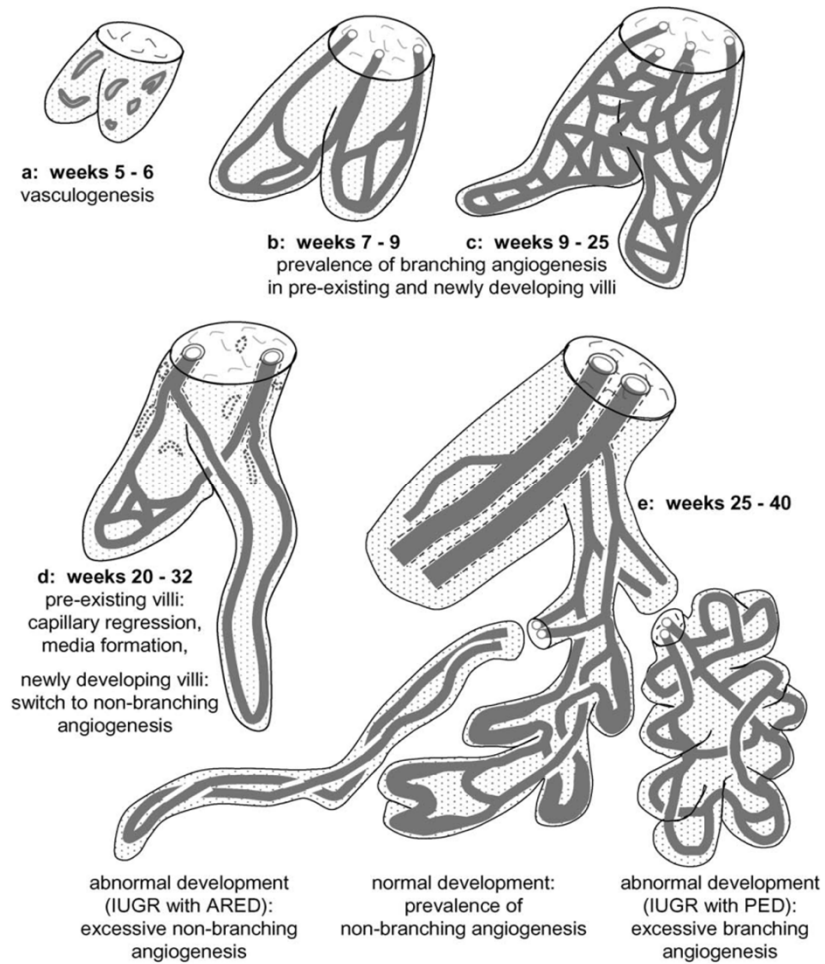
FIGURE 1.3. Patterns of villous development in relation to gestational phases of fetal vascular development. ARED; absent or reversed end diastolic flow; PED, preserved end diastolic flow

Reproduced from *Placenta* 25(2-3), Kaufmann P, Mayhew TM, Charnock-Jones DS., Aspects of human fetoplacental vasculogenesis and angiogenesis. II. Changes during normal pregnancy, pages 114-26 Copyright 2004, with permission from Elsevier.
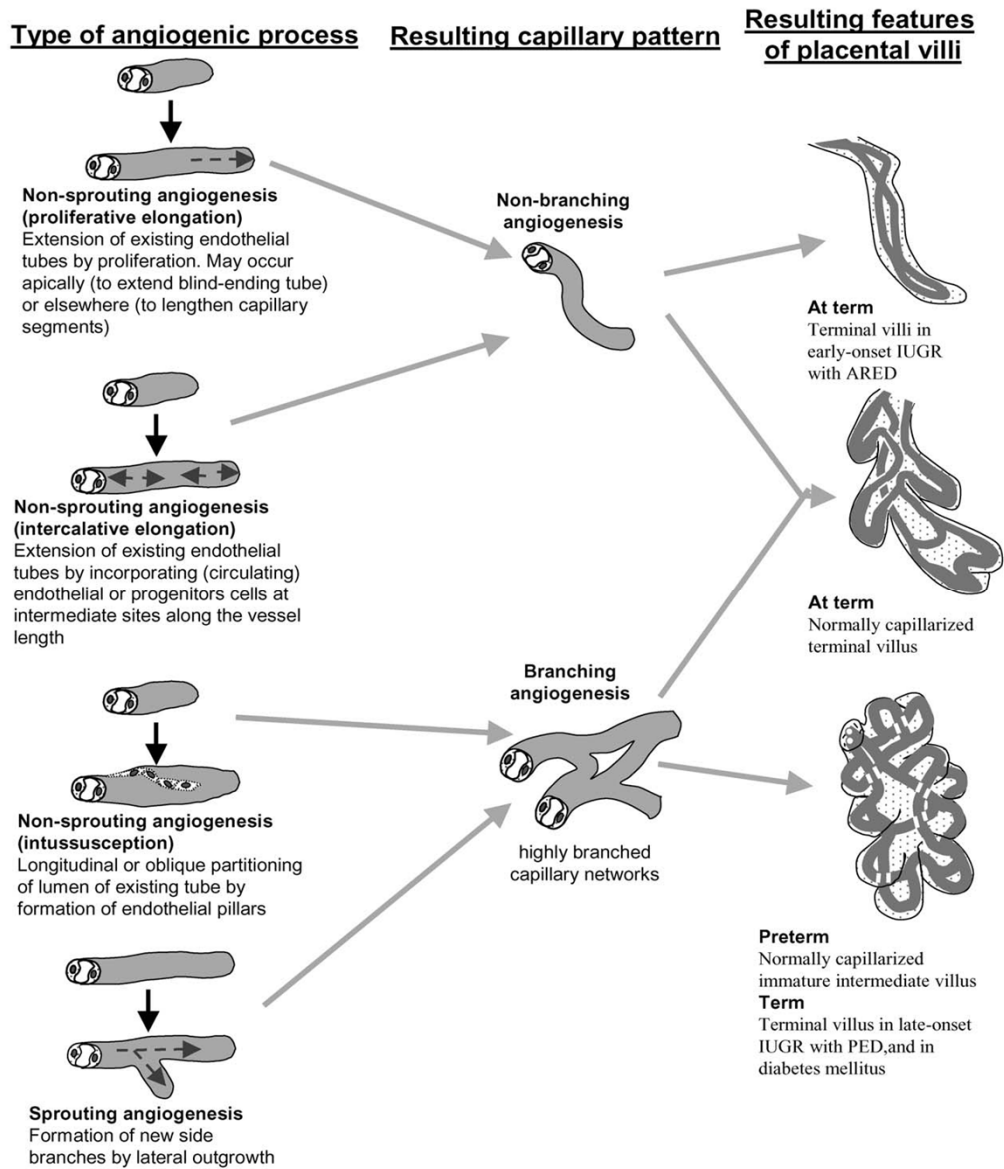
FIGURE 1.4. Different types of angiogenesis and the accompanying features of villous vascularization and development. ARED denotes absent or reversed end-diastolic flow in umbilical arteries whilst PED denotes preserved or persistent end-diastolic flow in the same arteries.

Reproduced from *Placenta* 25(2-3), Charnock-Jones, D.S., Kaufmann, P., Mayhew, T.M. Aspects of human fetoplacental vasculogenesis and angiogenesis. I. Molecular regulation, *Pages* 103-13, copyright 2004, with permission from Elsevier.

place between weeks 7-25 (Figure 1.3 b and c). Beyond 25 weeks, non-branching angiogenesis is predominant, leading to the formation of capillary loops (24) (Figure 1.3 e).

Normally, a balance of sprouting and non-sprouting angiogenesis produces the ideal placental vascular structure. In FGR without placental resistance, a more dominant sprouting angiogenesis manifests as a highly branched placental villi. In FGR with placental insufficiency however, an absence of sprouting angiogenesis in favor of either proliferative or intercalative elongation leads to long, non-branched terminal villi (Figure 1.3 e, Figure 1.4). These two characteristics of the villi lead to increased flow resistance seen by umbilical artery Doppler - the greater the vessel length and the smaller the vessel, the higher the resistance to flow in accordance with the Poiseuille equation (24). In the most severe cases, umbilical artery diastolic flow can stop or even reverse (referred to as ARED – absent or reversed end diastolic flow). The failure of branching angiogenesis then, and the predominance of vessel elongation, is thought to be causal of placental insufficiency.

1.2.2. Molecular regulation of placental angiogenesis

The fundamental steps in normal placental vessel branching angiogenesis were defined in a review by Charnock-Jones and others (25) - initially, there is vasodilatation and endothelial activation. This leads to increased degradation of the extra-cellular matrix by matrix metalloproteinases (MMPs) and an increase in

membrane permeability. The endothelial cells then proliferate and migrate, to form tube structures, and subsequently recruit pericytes, forming a mature vessel.

The angiogenic process is therefore regulated at several steps. As mentioned earlier, angiogenic cytokines VEGF, PlGF, and FGF-2 are very important in regulating the endothelial cells towards vascular growth and proliferation. VEGF, PIGF, and FGF-2 have a similar potency in inducing angiogenesis when overexpressed in rabbit cornea (26). VEGF has been shown to induce highly branched type angiogenesis, and is in higher concentration in the earlier stages of pregnancy, while PlGF increases later in gestation (24). The relative levels of VEGF and PlGF are theorized to determine the branched versus linear phenotype to a degree, however there are other unknown regulatory factors (24). Their placental expression may be oxygen dependent, as VEGF increases drastically in hypoxia, while PIGF decreases (24, 27). The regulation of the matrix surrounding the endothelial cells is thought to be an important regulatory mechanism that drives angiogenesis. The expression of extracellular matrix remodeling proteins such as MMPs and their inhibitors degrade the matrix so that new vessels can migrate and form in their place. Additionally, levels of protease inhibitors, like plasminogen activator inhibitors 1 and 2, have significant potential for angiogenic regulation in the placenta (25). Circulating levels of PAI-1 for example have shown to be potent regulators of angiogenesis in tumors and other tissues (28, 29, 30). PAI-1 deficient mice have also recently been shown to have altered placental vasculature (31).

1.3. ADAPTATION TO HYPOXIA

1.3.1. Effect on the fetus and liver

With placental insufficiency, the exchange of metabolic substrates and waste products is compromised. Therefore blood flowing from the placenta to the fetus in the umbilical vein post-exchange is abnormally low in oxygen, amino acids, fatty acids, and glucose. It is high in carbon dioxide and other waste products, and is consequently also more acidic. The fetus must therefore adapt to these environmental conditions to survive.

To accommodate oxygenated blood fed from the umbilical vein instead of the lungs, the fetal circulation has significant differences from that of the adult. These unique circulatory characteristics also function to maximize the utility of deficient oxygen and nutrients by diverting blood to where it is most needed, and therefore plays a large role in fetal adaptation. In the fetus, blood leaving the placenta through the umbilical vein travels to the liver, and the hepatic portal vein, from where it perfuses the fetus (Figure 1.5). Preceding this, however, a vessel unique to the fetus, the *ductus venosus*, bypasses the normal circulation and circulates the newly oxygenated blood directly to the inferior vena cava (Figure 1.5). From the inferior vena cava, this highly oxygenated blood travels to the heart, where through another shunt, the *ductus arteriosus*, blood passes from the pulmonary vein to the aortic arch (bypassing the lungs). The effect of these alterations is that the fetal brain is perfused directly with the newly oxygenated blood from the placenta. In conditions of hypoxia, it has been shown in animal models that the *ductus venosus* dilate leading to increased
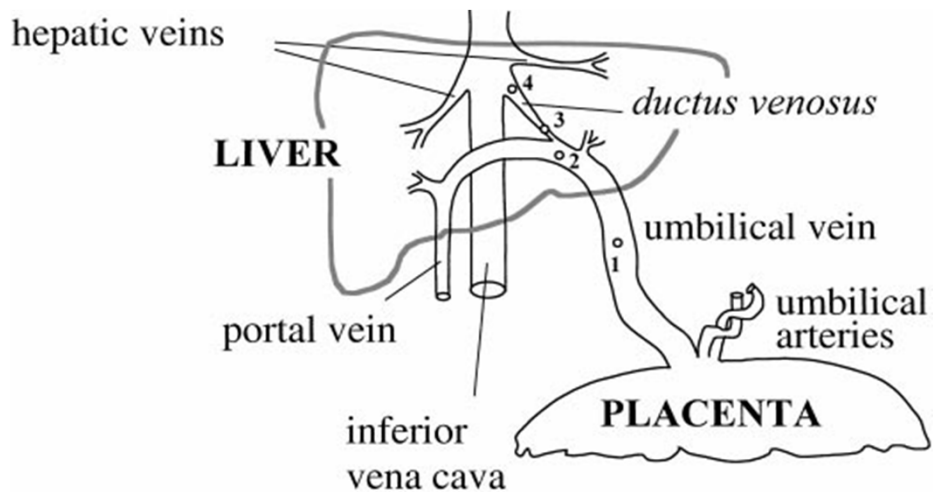
FIGURE 1.5. Anatomic scheme of the umbilical venous return indicating the direct perfusion of the liver with newly exchanged umbilical vein blood. Dilation of the ductus venosus leads to increased shunting of blood to the inferior vena cava. Blood flow is therefore directed to the heart at the expense of the liver's blood supply.

perfusion of the brain (32, 33). It is this "brain sparing" mechanism that leads to the disproportionately large head circumference in FGR fetuses and newborns, and the absence of which is associated with negative outcome, as growth restriction surpasses the fetus's capacity to adapt (Figure 1.1). These adaptations are of consequence to the liver, as it receives reduced blood flow, it creates localized conditions of even greater hypoxia and nutrient starvation (34).

Effectively, the brain is spared of starvation and hypoxia at the expense of the other fetal tissues, especially the liver. Although many of the metabolic/digestive functions of the liver are not critical during gestation, the liver likely remains sensitive to the levels of metabolic substrates and alters its protein synthesis accordingly. The liver is also particularly significant as the primary source of synthesis of plasma proteins, and therefore changes in its protein synthesis and secretion have effects throughout the body.

The effects of changes in liver secretion are apparent in adults, and provide clues to proteins changes potentially observable in the fetus. It is widely known, for example, that impaired secretion of blood clotting factors and other regulators in many liver diseases, leads to clotting disorders and internal bleeding (35). As another example, inflammatory cytokine messengers IL-1, IL-6, IL-8 and TNF-α in the blood signal secretion changes of acute phase plasma proteins in the liver. These proteins support diverse functions at the primary site of inflammation that classically include immune regulation and coagulation (36). Recent findings have linked angiogenic function to several acute phase proteins (37, 38) and their altered expression has been linked to

disease (39, 40, 41). Furthermore, hypoxia on its own has been shown to be sufficient to trigger acute phase-like secretion changes from hepatocytes (42). It therefore seems very probable that altered liver secretion of plasma proteins in fetal hypoxia will lead to functional changes in other tissues, including fetal-placental angiogenesis, which is associated with FGR pathology.

One such liver-secreted protein is insulin-like growth factor binding protein-1 (IGFBP-1). Its fetal liver synthesis is increased under hypoxic condition (43). By binding to IGF-I with high affinity, IGFBP-1 sequesters IGF-I in the circulation, thereby limiting its bioavailability for binding to IGF receptor 1 (IGFRI) (44). IGFBP-1 expression functions in limiting fetal growth to within the limitations of the available metabolic substrates (45).

1.3.2. Mechanisms of hypoxic regulation of liver secreted proteins

IGFBP-1 is upregulated in the hypoxic liver of the fetus. It is expected that other liver secreted plasma proteins of functional consequence to the fetus, may be regulated through similar oxygen sensitive cellular processes. Altered protein synthesis via hypoxic regulation has been shown to take place via several ubiquitous regulatory mechanisms. One such mechanism is upregulation through the stabilization of mRNAs, which is seen in VEGF regulation (46). More classically described however, is hypoxia signaling through the family of Hypoxia-Inducible Factors (HIF).

HIF-1α is a transcription co-factor that after migrating to the nucleus dimerizes with HIF-β, in a transcription complex that recognizes hypoxic response elements (HRE)
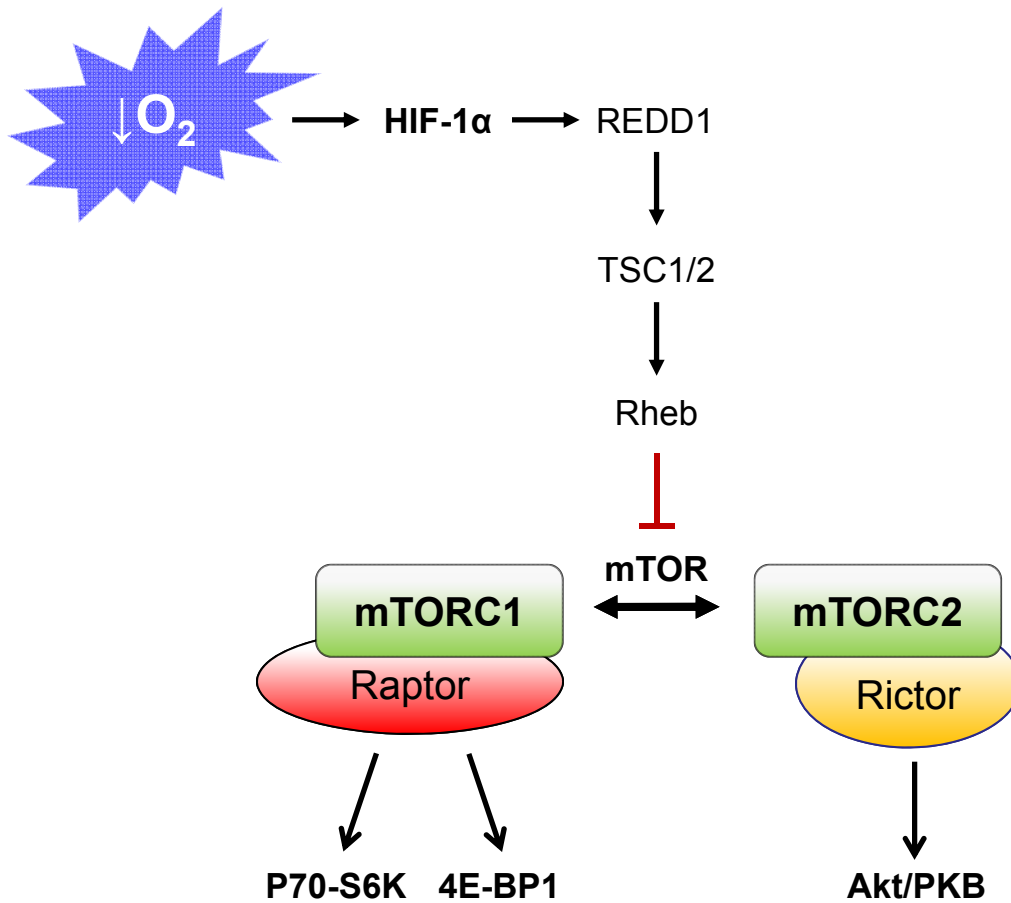
Figure 1.6. Hypoxic mediated signalling via mTOR. Inhibiting mTOR leads to signalling via kinase complexes with raptor or rictor that have diverse effects on transcription and translation. HIF-1α is upstream of mTOR signalling.

within the promoter sequence of target genes. However, in normal conditions when oxygen is abundant HIF-1α is degraded by the ubiquitin ligating von Hippel–Lindau (pVHL) protein complex, which recognizes hydroxyl groups on HIF-1α. These hydroxyl groups are in turn added by prolyl hydroxylase domain containing enzymes (PHDs). As oxygen is consumed directly as a substrate for the PHD enzymes, the levels of ambient O_2 are determinant of the HIF-1 hydroxylation and therefore O_2 dependent expression (47). It has been shown that the IGFBP-1 is downstream of an HRE, and that hypoxia leads to increased IGFBP-1 transcription, and protein secretion in hepatocytes.

Another potent molecular regulator of protein synthesis that is responsive to hypoxia is mammalian target of Rapamycin (mTOR) (48) (Figure 1.6). Hypoxia exerts inhibition on mTOR signaling via tumor suppressor complex 1/2 signaling, in a REDD1 upregulation dependent mechanism (48, 49, 50). REDD1 is transcribed in hypoxia via HRE dependent and independent regulation, either of which are sufficient to activate mTOR signaling (48, 51). mTOR is also well known to respond to nutritional and hormonal signals (52). Amino acid deprivation, especially leucine starvation, also causes changes in mTOR signaling (53).

mTOR functions through signaling pathways involving two major complexes: mTORC1 and mTORC2 that differ in their accessory proteins as well as their downstream effectors. mTOR activation regulates important pathways involved in diverse functions, among which are cellular growth and proliferation, cell survival, and protein synthesis. Interestingly, one of the many effects of mTOR signaling is

aortic arch

superior vena cava

foramen ovale
(becomes fossa ovalis)

right atrium

inferior vena cava

ductus venosus
(becomes ligamentum
venosum)

umbilical vein
(becomes ligamentum
teres)

pulmonary veins

pulmonary trunk

left atrium

left ventricle

right ventricle

abdominal aorta

Hypoxic liver

Fetal plasma proteome changes

umbilical vein

Maternal plasma proteome changes

umbilical arteries

Placental failure

Decreasing blood oxygen level

FIGURE 1.7. Fetal placental circulation showing origins of expected plasma protein changes in placental insufficiency. Placental insufficiency caused by malformed fetal chorionic villi will lead to secretion changes from the pathological fetal-placental tissues that will manifest as plasma proteome changes. Hypoxia of the liver will result in altered secretion of proteins that are circulated through the fetus and then placenta, before proteome sampling in the umbilical vein. Changes in secretion of the syncitiotrophoblsast or the maternal-placental tissues in adaptation to the fetal placental failure, reduced placental size or hypoxia will alter their secretion into the maternal plasma proteome.

transcription of HIF-1α through the activation of mTOR complex 1 (mTORC1) (54). This demonstrates that there is substantial positive feedback in the complex network of hypoxic-induced protein expression signaling pathways (Figure 1.6).

1.4.   SCOPE OF THESIS

Plasma, being in contact with all tissues, contains proteins representative of the whole body. Maternal plasma contains protein markers of maternal-placental changes in FGR at late gestation. Protein changes in the plasma particularly reflect changes in secretion from tissues affected by disease. For these reasons, maternal plasma is the ideal biological fluid to uncover biomarkers for diagnostic or prognostic test development of placental health (55).

Likewise, fetal plasma, conveniently accessed from the umbilical vein at delivery, contains fetal-placental proteins reflective of changes in FGR. The liver is the largest secretor of plasma proteins. It is also sensitive to the levels of metabolic substrates like hypoxia, and hepatocytes have been shown to drastically alter secretion *in vitro* (42). Finally, considering that the liver's blood supply is particularly compromised in FGR, it is expected that there will be altered secretion of proteins with hypoxia. These secretion changes will be reflected in the fetal plasma proteome (Figure 1.7). Changing secretion from the liver has been shown to have functional effects on fetal growth through IGFBP-1 regulation, and on the vasculature in adult liver disease (35). It is therefore expected that liver secreted protein changes identified in the fetal circulation may similarly be reflective of pathophysiological functional changes,

affecting the fetal and placental tissues. It is expected that these protein changes may be adaptive to metabolic substrate restriction (like changing IGFBP-1), and may regulate or otherwise be implicated in pathological vascular changes in the placenta in FGR. A discovery-based profiling approach will identify plasma protein changes in FGR, allowing for the formulation of new theories of hepatic involvement in the disease process.

The central hypothesis is that altered maternal and fetal plasma protein expression will result from placental insufficiency and/or the resultant hypoxia. The goal of this thesis is encapsulated with the overall objective of discovering and elucidating fetal and maternal plasma proteomic expression changes in FGR. Maternal plasma for the discovery of biomarkers, and fetal plasma for the discovery of hepatic, and other proteins related to the disease pathology. Furthermore, the consequences of the changing levels of fetal plasma proteins will be investigated using *in vitro* functional experiments to determine their significance in FGR pathophysiology.

The objective of profiling in fetal growth restriction is therefore twofold:

1. In Maternal Plasma:

   Identify candidate biomarkers of FGR. (Chapters 2 and 6)

2. In Fetal Plasma:

   a. Identify expression changes of proteins implicated in the fetal pathology of FGR by direct plasma profiling, and using a HepG2 model of hepatic secretion in hypoxia. (Chapters 3, 4, and 6)

b. Establish the functional effect of the identified protein changes.

(Chapter 5 and 7)

In this discovery-based approach, proteomic techniques are employed to broadly profile for changes of plasma directly, and additionally, the secretions of HepG2 cells in hypoxia will be profiled for changing proteins as a model of hepatic plasma proteins changing in the FGR fetus. The strategy of broad profiling allows the detection of unexpected changes, potentially signifying newly identifiable mechanisms involved in the disease.

1.5. REFERENCES

1. Cetin, I., Foidart, J. M., Miozzo, M., Raun, T., Jansson, T., Tsatsaris, V., Reik, W., Cross, J., Hauguel-de-Mouzon, S., Illsley, N., Kingdom, J., and Huppertz, B. (2004) Fetal Growth Restriction: A Workshop Report. *Placenta. 25*, 753-757.

2. Resnik, R. (2002) Intrauterine Growth Restriction. *Obstet. Gynecol. 99*, 490-496.

3. Garite, T. J., Clark, R., and Thorp, J. A. (2004) Intrauterine Growth Restriction Increases Morbidity and Mortality among Premature Neonates. *Am. J. Obstet. Gynecol. 191*, 481-487.

4. Barker, D. J. (1998) In Utero Programming of Chronic Disease. *Clin. Sci. (Lond). 95*, 115-128.

5. Jarvis, S., Glinianaia, S. V., Torrioli, M. G., Platt, M. J., Miceli, M., Jouk, P. S., Johnson, A., Hutton, J., Hemming, K., Hagberg, G., Dolk, H., Chalmers, J., and Surveillance of Cerebral Palsy in Europe (SCPE) collaboration of European Cerebral Palsy Registers. (2003) Cerebral Palsy and Intrauterine Growth in Single Births: European Collaborative Study. *Lancet. 362*, 1106-1111.

6. Jornayvaz, F. R., Selz, R., Tappy, L., and Theintz, G. E. (2004) Metabolism of Oral Glucose in Children Born Small for Gestational Age: Evidence for an Impaired Whole Body Glucose Oxidation. *Metabolism. 53*, 847-851.

7. Hendrix, N., and Berghella, V. (2008) Non-Placental Causes of Intrauterine Growth Restriction. *Semin. Perinatol. 32*, 161-165.

8. Ergaz, Z., Avgil, M., and Ornoy, A. (2005) Intrauterine Growth Restriction-Etiology and Consequences: What do we Know about the Human Situation and Experimental Animal Models? *Reprod. Toxicol. 20*, 301-322.

9. Cetin, I., Corbetta, C., Sereni, L. P., Marconi, A. M., Bozzetti, P., Pardi, G., and Battaglia, F. C. (1990) Umbilical Amino Acid Concentrations in Normal and Growth-Retarded Fetuses Sampled in Utero by Cordocentesis. *Am. J. Obstet. Gynecol. 162*, 253-261.

10. Jansson, T., Scholtbach, V., and Powell, T. L. (1998) Placental Transport of Leucine and Lysine is Reduced in Intrauterine Growth Restriction. *Pediatr. Res. 44*, 532-537.

11. Economides, D. L., and Nicolaides, K. H. (1989) Blood Glucose and Oxygen Tension Levels in Small-for-Gestational-Age Fetuses. *Am. J. Obstet. Gynecol. 160*, 385-389.

12. Mayhew, T. M., Charnock-Jones, D. S., and Kaufmann, P. (2004) Aspects of Human Fetoplacental Vasculogenesis and Angiogenesis. III. Changes in Complicated Pregnancies. *Placenta. 25*, 127-139.

13. Baschat, A. A., and Hecher, K. (2004) Fetal Growth Restriction due to Placental Disease. *Semin. Perinatol. 28*, 67-80.

14. Gagnon, R. (2003) Placental Insufficiency and its Consequences. *Eur. J. Obstet. Gynecol. Reprod. Biol. 110 Suppl 1*, S99-107.

15. Gaziano, E. P. (1995) Antenatal Ultrasound and Fetal Doppler. Diagnosis and Outcome in Intrauterine Growth Retardation. *Clin. Perinatol. 22*, 111-140.

16. Hobbins, J. (1997) Morphometry of Fetal Growth. *Acta Paediatr. Suppl. 423*, 165-8; discussion 169.

17. Barkehall-Thomas, A., Wilson, C., Baker, L., ni Bhuinneain, M., and Wallace, E. M. (2005) Uterine Artery Doppler Velocimetry for the Detection of Adverse Obstetric Outcomes in Patients with Elevated Mid-Trimester Beta-Human Chorionic Gonadotrophin. *Acta Obstet. Gynecol. Scand. 84*, 743-747.

18. Tjoa, M. L., Oudejans, C. B., van Vugt, J. M., Blankenstein, M. A., and van Wijk, I. J. (2004) Markers for Presymptomatic Prediction of Preeclampsia and Intrauterine Growth Restriction. *Hypertens. Pregnancy. 23*, 171-189.

19. Jain, R. K., Koenig, G. C., Dellian, M., Fukumura, D., Munn, L. L., and Melder, R. J. (1996) Leukocyte-Endothelial Adhesion and Angiogenesis in Tumors. *Cancer Metastasis Rev. 15*, 195-204.

20. Tommaselli, G. A., Pighetti, M., Nasti, A., D'Elia, A., Guida, M., Di Carlo, C., Bifulco, G., and Nappi, C. (2004) Serum Leptin Levels and Uterine Doppler Flow Velocimetry at 20 Weeks' Gestation as Markers for the Development of Pre-Eclampsia. *Gynecol. Endocrinol. 19*, 160-165.

21. Krantz, D., Goetzl, L., Simpson, J. L., Thom, E., Zachary, J., Hallahan, T. W., Silver, R., Pergament, E., Platt, L. D., Filkins, K., Johnson, A., Mahoney, M., Hogge, W. A.,

Wilson, R. D., Mohide, P., Hershey, D., Wapner, R., and First Trimester Maternal Serum Biochemistry and Fetal Nuchal Translucency Screening (BUN) Study Group. (2004) Association of Extreme First-Trimester Free Human Chorionic Gonadotropin-Beta, Pregnancy-Associated Plasma Protein A, and Nuchal Translucency with Intrauterine Growth Restriction and Other Adverse Pregnancy Outcomes. *Am. J. Obstet. Gynecol. 191*, 1452-1458.

22. Roig, M. D., Sabria, J., Valls, C., Borras, M., Miro, E., Ponce, J., and Vicens, J. M. (2005) The use of Biochemical Markers in Prenatal Diagnosis of Intrauterine Growth Retardation: Insulin-Like Growth Factor I, Leptin, and Alpha-Fetoprotein. *Eur. J. Obstet. Gynecol. Reprod. Biol. 120*, 27-32.

23. Shankar, R., Gude, N., Cullinane, F., Brennecke, S., Purcell, A. W., and Moses, E. K. (2005) An Emerging Role for Comprehensive Proteome Analysis in Human Pregnancy Research. *Reproduction. 129*, 685-696.

24. Kaufmann, P., Mayhew, T. M., and Charnock-Jones, D. S. (2004) Aspects of Human Fetoplacental Vasculogenesis and Angiogenesis. II. Changes during Normal Pregnancy. *Placenta. 25*, 114-126.

25. Charnock-Jones, D. S., Kaufmann, P., and Mayhew, T. M. (2004) Aspects of Human Fetoplacental Vasculogenesis and Angiogenesis. I. Molecular Regulation. *Placenta. 25*, 103-113.

26. Ziche, M., Maglione, D., Ribatti, D., Morbidelli, L., Lago, C. T., Battisti, M., Paoletti, I., Barra, A., Tucci, M., Parise, G., Vincenti, V., Granger, H. J., Viglietto, G., and Persico, M. G. (1997) Placenta Growth Factor-1 is Chemotactic, Mitogenic, and Angiogenic. *Lab. Invest. 76*, 517-531.

27. Gobble, R. M., Groesch, K. A., Chang, M., Torry, R. J., and Torry, D. S. (2009) Differential Regulation of Human PlGF Gene Expression in Trophoblast and Nontrophoblast Cells by Oxygen Tension. *Placenta. 30*, 869-875.

28. Bajou, K., Maillard, C., Jost, M., Lijnen, R. H., Gils, A., Declerck, P., Carmeliet, P., Foidart, J. M., and Noel, A. (2004) Host-Derived Plasminogen Activator Inhibitor-1 (PAI-1) Concentration is Critical for in Vivo Tumoral Angiogenesis and Growth. *Oncogene. 23*, 6986-6990.

29. McMahon, G. A., Petitclerc, E., Stefansson, S., Smith, E., Wong, M. K., Westrick, R. J., Ginsburg, D., Brooks, P. C., and Lawrence, D. A. (2001) Plasminogen Activator Inhibitor-1 Regulates Tumor Growth and Angiogenesis. *J. Biol. Chem. 276*, 33964-33968.

30. Basu, A., Menicucci, G., Maestas, J., Das, A., and McGuire, P. (2009) Plasminogen Activator Inhibitor-1 (PAI-1) Facilitates Retinal Angiogenesis in a Model of Oxygen-Induced Retinopathy. *Invest. Ophthalmol. Vis. Sci. 50*, 4974-4981.

31. Labied, S., Blacher, S., Carmeliet, P., Noel, A., Frankenne, F., Foidart, J. M., and Munaut, C. (2011) Transient Reduction of Placental Angiogenesis in PAI-1-Deficient Mice. *Physiol. Genomics. 43*, 188-198.

32. Edelstone, D. I., Rudolph, A. M., and Heymann, M. A. (1980) Effects of Hypoxemia and Decreasing Umbilical Flow Liver and Ductus Venosus Blood Flows in Fetal Lambs. *Am. J. Physiol. 238*, H656-63.

33. Paulick, R. P., Meyers, R. L., Rudolph, C. D., and Rudolph, A. M. (1990) Venous Responses to Hypoxemia in the Fetal Lamb. *J. Dev. Physiol. 14*, 81-88.

34. Bellotti, M., Pennati, G., De Gasperi, C., Battaglia, F. C., and Ferrazzi, E. (2000) Role of Ductus Venosus in Distribution of Umbilical Blood Flow in Human Fetuses during Second Half of Pregnancy. *Am. J. Physiol. Heart Circ. Physiol. 279*, H1256-63.

35. Trotter, J. F. (2006) Coagulation Abnormalities in Patients Who have Liver Disease. *Clin. Liver Dis. 10*, 665-78, x-xi.

36. Gruys, E., Toussaint, M. J., Niewold, T. A., and Koopmans, S. J. (2005) Acute Phase Reaction and Acute Phase Proteins. *J. Zhejiang Univ. Sci. B. 6*, 1045-1056.

37. Mullan, R. H., Bresnihan, B., Golden-Mason, L., Markham, T., O'Hara, R., FitzGerald, O., Veale, D. J., and Fearon, U. (2006) Acute-Phase Serum Amyloid A Stimulation of Angiogenesis, Leukocyte Recruitment, and Matrix Degradation in Rheumatoid Arthritis through an NF-kappaB-Dependent Signal Transduction Pathway. *Arthritis Rheum. 54*, 105-114.

38. de Kleijn, D. P., Smeets, M. B., Kemmeren, P. P., Lim, S. K., Van Middelaar, B. J., Velema, E., Schoneveld, A., Pasterkamp, G., and Borst, C. (2002) Acute-Phase Protein Haptoglobin is a Cell Migration Factor Involved in Arterial Restructuring. *FASEB J. 16*, 1123-1125.

39. Festa, A., D'Agostino, R.,Jr, Tracy, R. P., Haffner, S. M., and Insulin Resistance Atherosclerosis Study. (2002) Elevated Levels of Acute-Phase Proteins and Plasminogen Activator Inhibitor-1 Predict the Development of Type 2 Diabetes: The Insulin Resistance Atherosclerosis Study. *Diabetes. 51*, 1131-1137.

40. Urieli-Shoval, S., Linke, R. P., and Matzner, Y. (2000) Expression and Function of Serum Amyloid A, a Major Acute-Phase Protein, in Normal and Disease States. *Curr. Opin. Hematol. 7*, 64-69.

41. Badolato, R., and Oppenheim, J. J. (1996) Role of Cytokines, Acute-Phase Proteins, and Chemokines in the Progression of Rheumatoid Arthritis. *Semin. Arthritis Rheum. 26*, 526-538.

42. Wenger, R. H., Rolfs, A., Marti, H. H., Bauer, C., and Gassmann, M. (1995) Hypoxia, a Novel Inducer of Acute Phase Gene Expression in a Human Hepatoma Cell Line. *J. Biol. Chem. 270*, 27865-27870.

43. Averous, J., Maurin, A. C., Bruhat, A., Jousse, C., Arliguie, C., and Fafournoux, P. (2005) Induction of IGFBP-1 Expression by Amino Acid Deprivation of HepG2 Human Hepatoma Cells Involves both a Transcriptional Activation and an mRNA Stabilization due to its 3'UTR. *FEBS Lett. 579*, 2609-2614.

44. Jones, J. I., Busby, W. H.,Jr, Wright, G., Smith, C. E., Kimack, N. M., and Clemmons, D. R. (1993) Identification of the Sites of Phosphorylation in Insulin-Like Growth Factor Binding Protein-1. Regulation of its Affinity by Phosphorylation of Serine 101. *J. Biol. Chem. 268*, 1125-1131.

45. Watson, C. S., Bialek, P., Anzo, M., Khosravi, J., Yee, S. P., and Han, V. K. (2006) Elevated Circulating Insulin-Like Growth Factor Binding Protein-1 is Sufficient to Cause Fetal Growth Restriction. *Endocrinology. 147*, 1175-1186.

46. Ikeda, E., Achen, M. G., Breier, G., and Risau, W. (1995) Hypoxia-Induced Transcriptional Activation and Increased mRNA Stability of Vascular Endothelial Growth Factor in C6 Glioma Cells. *J. Biol. Chem. 270*, 19761-19766.

47. Majmundar, A. J., Wong, W. J., and Simon, M. C. (2010) Hypoxia-Inducible Factors and the Response to Hypoxic Stress. *Mol. Cell. 40*, 294-309.

48. Arsham, A. M., Howell, J. J., and Simon, M. C. (2003) A Novel Hypoxia-Inducible Factor-Independent Hypoxic Response Regulating Mammalian Target of Rapamycin and its Targets. *J. Biol. Chem. 278*, 29655-29660.

49. DeYoung, M. P., Horak, P., Sofer, A., Sgroi, D., and Ellisen, L. W. (2008) Hypoxia Regulates TSC1/2-mTOR Signaling and Tumor Suppression through REDD1-Mediated 14-3-3 Shuttling. *Genes Dev. 22*, 239-251.

50. Brugarolas, J., Lei, K., Hurley, R. L., Manning, B. D., Reiling, J. H., Hafen, E., Witters, L. A., Ellisen, L. W., and Kaelin, W. G.,Jr. (2004) Regulation of mTOR Function in Response to Hypoxia by REDD1 and the TSC1/TSC2 Tumor Suppressor Complex. *Genes Dev. 18*, 2893-2904.

51. Shoshani, T., Faerman, A., Mett, I., Zelin, E., Tenne, T., Gorodin, S., Moshel, Y., Elbaz, S., Budanov, A., Chajut, A., Kalinski, H., Kamer, I., Rozen, A., Mor, O., Keshet, E., Leshkowitz, D., Einat, P., Skaliter, R., and Feinstein, E. (2002) Identification of a Novel Hypoxia-Inducible Factor 1-Responsive Gene, RTP801, Involved in Apoptosis. *Mol. Cell. Biol. 22*, 2283-2293.

52. Loewith, R., Jacinto, E., Wullschleger, S., Lorberg, A., Crespo, J. L., Bonenfant, D., Oppliger, W., Jenoe, P., and Hall, M. N. (2002) Two TOR Complexes, Only One of which is Rapamycin Sensitive, have Distinct Roles in Cell Growth Control. *Mol. Cell. 10*, 457-468.

53. Hay, N., and Sonenberg, N. (2004) Upstream and Downstream of mTOR. *Genes Dev. 18*, 1926-1945.

54. Hudson, C. C., Liu, M., Chiang, G. G., Otterness, D. M., Loomis, D. C., Kaper, F., Giaccia, A. J., and Abraham, R. T. (2002) Regulation of Hypoxia-Inducible Factor 1alpha Expression and Function by the Mammalian Target of Rapamycin. *Mol. Cell. Biol. 22*, 7004-7014.

55. Anderson, N. L., and Anderson, N. G. (2002) The Human Plasma Proteome: History, Character, and Diagnostic Prospects. *Mol. Cell. Proteomics. 1*, 845-867.

CHAPTER 2

2-DGE profiling of maternal plasma:
Haptoglobin α2 as a biomarker

2.1. INTRODUCTION

Fetal growth restriction (FGR) is a pregnancy condition where estimated fetal weight is below the 10th percentile expected for gestational age (GA) (1, 2). The condition affects 3–5% of pregnancies, and is associated with high perinatal morbidity and mortality (3). FGR infants may also have an increased risk of adverse neuro-developmental outcomes and of cardiovascular and metabolic diseases later in life (4, 5). Currently, fetal size is routinely ascertained using imaging technology; however, the differentiation of normal, constitutionally small fetuses from those with pathologic FGR remains a clinical challenge. Identification of proteins that can be used as biomarkers is an antecedent step in the development of non-invasive diagnostic or prognostic tests for FGR. Discovery of a candidate biomarker protein or a group of proteins that are associated with the pathophysiology of FGR, should lead to the development of rapid detection and quantification methods, for example immunoassays (6,7), for possible clinical screening. The measurement of biomarkers combined with advanced ultrasonographic (US) biometry and fetal Doppler technology in a temporal manner will provide the ability to more accurately and precisely detect the presence of FGR.

Clinically significant FGR is caused by reduced fetal growth resulting from maternal conditions such as under-nutrition, smoking, drugs, and pre-pregnancy or pregnancy diseases including chronic hypertension or preeclampsia (8). Although the etiology and pathophysiology of FGR may be varied (2), it is widely accepted that poor placental development and or placental disease is the major common factor that is

associated with abnormal fetal growth (8, 9). Once congenital infection and chromosomal or congenital anomalies have been ruled out, FGR is mostly a result of utero-placental insufficiency (10). Proteomic analysis of maternal plasma may also provide us with better understanding of the pathophysiology underlying FGR.

Profiles of plasma proteins can illustrate changes owing to altered metabolism and/or disease process. They may have a causal relationship and/or indicate disease severity. Differential expression of proteins in blood plasma has been widely used to study various diseases (11–13). The significance of several plasma peptides in gestational diseases with respect to biomarker discovery, and the importance of proteomics in identifying these candidate proteins have been well denoted (14).

Analysis of global plasma proteins is a challenge because of the complexity of the plasma proteome. Plasma has a large concentration range that spans 10 orders of magnitude from albumin, the most concentrated protein, to the least concentrated cytokines. Also, many of the proteins in blood share chemical similarities in their pI and structure compared to intracellular proteins. This is because of the need for consistency and neutrality of the pH in the blood environment. The prevalence of PTMs like deamidations and glycosylations, which are comparatively rare on intracellular proteins, further complicates the proteome. To overcome these difficulties, pre-fractionation and depletion is often employed to adequately quantify detectable spots. Because these strategies often lead to high variability, this study is focused on rapid screening of whole plasma using two-dimensional gel

electrophoresis (2-DGE) as a proteomic approach to detect changes in plasma proteome profiles associated with FGR.

2.2. MATERIALS AND METHODS

2.2.1. Materials

All chemicals for 2-DGE and LC-MS/MS analysis were of electrophoretic or analytical grade. The total plasma protein concentrations were measured using BCA Protein Assay Kit (Pierce Biotech Inc., Rockford, IL), following the microplate technique as outlined by the manufacturer. Bovine albumin was used as the standard. Replicates were analyzed in a Multiskan EX microplate reader (Thermo Electron Corp., Vantaa, Finland).

2.2.2. Sample collection

With approval from the University of Western Ontario, Health Sciences Research Ethics Board and written informed consent from participants, pregnant women were recruited at St. Joseph's Hospital, London, ON, Canada. Blood samples were collected prior to delivery from mothers who consented to participate in the study. Table 2.1A shows a summary of the characteristics of the patients studied, and the inclusion and exclusion criteria for subject recruitment. Gestational age (GA) was determined by certain last menstrual date of mothers or the first trimester US crown rump length. Etiologies of fetal origin, like congenital infection and chromosomal or congenital

anomalies were excluded. Information from the antenatal records including standard tests for the evaluation of fetal health and risk factors as part of normal surveillance was obtained. The diagnosis of FGR group was based on last trimester estimated fetal weight as determined by fetal US biometry (15) and calculated using the Hadlock II formula. Birth weight percentiles were calculated based on their respective gender and GA using a standardized growth chart (16, 17). Control group subjects consist of normal pregnancies without medical or obstetric problems and with fetuses within normal growth percentiles (>25th). Measurements less than the 10th percentile for GA at birth were confirmed to be growth restricted (Table 2.1B). Placental insufficiency was determined by abnormal umbilical artery Doppler (18). 1-2 mL of maternal venous blood from FGR and control subjects were collected in EDTA coated tubes. Blood was centrifuged (2000g, 10 min at 4°C) and plasma samples were saved in small aliquots at –70°C until analysis.

2.2.3. Gel electrophoresis

 All protein separations on 1D and 2D gels were conducted using 1.5 mm 12% SDS polyacrylamide gels, run for 20 min at 80 V followed by approx 1 h 15 min at 120 V. Pre-stained Broad Range SDS molecular weight (Mr) marker (Bio-Rad Labs, Hercules, CA) was used for estimation of Mr. All relevant reagents for 2-DGE were purchased from Bio-Rad and used according to manufacturer's instructions. First Dimension Isoelectric Focusing for 2-DGE The isoelectric focusing (IEF) was performed using

PROTEAN IEF cell with ReadyStrip immobilized pH gradient (IPG) strips, 7 cm, pH 3.0–10.0 nonlinear (NL), unless otherwise specified.

2-D gel electrophoresis separation

For first dimension separation, maternal plasma (1.5 μL, ~90 μg protein) was made up to 125 μL with rehydration buffer (8 M urea, 2% CHAPS, 50 mM dithiothreitol [DTT], 0.2% Biolyte pH 3.0–10.0 ampholyte, 0.001% bromophenol blue). Prior to IEF, IPG strips were rehydrated overnight using active or passive rehydration. Proteins were separated using a programmed voltage gradient in steps; S1, 200 V, 100 Vh; S2, 500 V, 250 Vh; S3, 1000 V, 500 Vh; S4, 8000 V, 8000 Vh; S5 500 V (holding step), with rapid ramping and a maximum current of 50 μA/strip throughout. Electrofocused strips were stored at –80°C until used.

For the second dimension, the 2-DGE focused strips were incubated for 20 min in 2.5 mL equilibration buffer (Tris, pH 8.8 [50 mM], urea [6 M], SDS [2% w/v], and glycerol [30% v/v] containing DTT [1% w/v]), followed by another 20 min incubation with 2.5 mL equilibration buffer containing iodoacetamide (2.5% w/v). The IPG strips were placed on the second dimensional gel using 0.5% low melting gel agarose in 1X Tris glycine SDS buffer with 0.003% bromophenol blue. Electrophoresis was performed on SDS gels with a narrow (7%) stacking gel. Fixation was for 30 min (10% methanol and 7% acetic acid) followed by staining overnight with SYPRO Ruby gel stain (Bio-Rad).

Destaining was done for a minimum of 1.5 h using 10% methanol and 7% acetic acid solution.

2-DGE image analysis

The 2D gels were stained with SYPRO Ruby Red and the monochromatic 16-bit digital images were acquired using the Fluorochem 8800 imaging system (Alpha Innotech Corp. San Leandro, CA) employing ultraviolet light excitation with a SYPRO-500 filter integrated with imaging software. Acquisition of all images was performed under controlled conditions with consistent exposure times. Phoretix 2D Expression Software Analysis Phoretix 2D Expression 2005 software (Nonlinear Dynamics Ltd., Newcastle Upon Tyne, UK) was used for image analysis of 2D gels using normalization of the spots on replicate gels. Preliminary mapping of plasma protein spots on 2D gels was performed based on the published plasma map (SWISS 2-DGE database available at the ExPASy (Expert Protein Analysis System) website (http://ca.expasy.org/ch2d).

2.2.4. LC-MS/MS spot identification

Specific spots containing proteins of interest were picked and manually excised for in-gel digestion. In brief, excised gel spots were transferred to siliconized tubes, de-stained, and washed. Proteins were reduced, alkylated, and then digested with sequencing grade trypsin (Promega, Madison, WI) overnight at 37°C. After extraction

of peptides from the gel, the samples were dried in a vacuum centrifuge and dissolved in 0.2% formic acid ready for LC-MS/MS analysis.

LC-MS/MS

LC-MS/MS analysis was carried out on a Q-TOF Global Ultima mass spectrometer (Waters Micromass® MS; Waters Corp., Milford, MA) coupled with a Waters CapLC. The LC system consisted of a C18 analytical column (75 μm × 15 cm, 5 μm, LC Packings, Amsterdam, Netherlands) and nano-ESI source. For the standard LC-MS/MS procedure, a gradient (solvent A, 0.2% formic acid in water, B, 0.2% formic acid in acetonitrile, 5% B to 90% B in 60 min) was used to elute the peptides. The data-dependent acquisition function was used to both detect and sequentially perform collision-induced dissociation (CID) on the multiply charged ions that satisfied the selection criteria. The mass spectrometer was operated in positive-ion mode with MS data acquisition range, 300 to 1900 and MS/MS data acquisition range, 50 to 1900. The collision energy (CE) for MS/MS experiments was determined by the charge state and/or by the m/z range of the precursor ion. The CE values were according to standard chargestate recognition and CE files recommended by Micromass (Waters Corp.). The MS to MS/MS switching was allowed for the four most abundant precursors in the survey experiment with a 30-s time period set for MS/MS data acquisition for each peptide. In some cases, a precise list of peptides was set so that specific precursor ions were targeted to undergo tandem MS preferentially. For the MS and MS/MS experiments, the time-of-flight (TOF) instrument was calibrated with

an MS/MS spectrum of Glu-fibrinopeptide-b. Data were acquired using MassLynx 4.0 software (Waters Corp.).

Analysis of MS/MS Data

Data was further analyzed using MassLynx 4.0 software (Waters Corp.) and Mascot (19) for database search on Swiss-Prot. The mass tolerance for precursor and fragment ions was set to1.2 and 0.1 Da, respectively. Carbamidomethylated cysteine residue was set as a variable modification. All identified peptides during Mascot or Peaks (Bioinformatics Solutions Inc. Waterloo, Canada) searching were verified by manual interpretation of the spectra.

2.2.5. Analysis of 1 and 2-D Haptoglobin immunoblots

The identity of Hp subtypes/subunits (α1, α2, and β) and qualitative assessment of their expression in select plasma samples was performed by 2D Western immunoblot analysis. An equal volume of maternal plasma (~45 µg protein) from a severe case of FGR and a GA matched control subject were compared using 7-cm IPG strips, pH 4.0–7.0 for 2-DGE. Proteins separated on the gels were transferred onto a PVDF membrane (0.45 µm) (Hoffmann- La Roche Ltd., Basel, Switzerland) using a semi-dry Transblot apparatus (Bio-Rad). The membrane was blocked with 5% non-fat dry milk in TBS (50 mM Tris, pH 7.5, 150 mM NaCl) for 2 h at room temperature, followed by incubation with the primary polyclonal rabbit anti-human Hp antibody that

recognizes all Hp subtypes (Dako, Glostrup, Denmark) (1:5000 in TBS containing 1% non-fat dry milk and 0.1% Tween-20) at 4°C for 3 h. Anti-rabbit IgG was used as a secondary antibody in 1:8000 dilution (TBS containing 5% non-fat dry milk) at room temperature for 1 h. The blot was rinsed in TBS containing 0.5% Tween-20, and proteins were visualized using ECL Western Blotting Detection System (GE Healthcare, Piscataway, NJ) according to manufacturer's instructions.

One-dimensional Western immunoblot analysis of maternal plasma was performed on five representative samples from FGR and three from the control group. The FGR subjects were the most severe cases with <3rd percentile newborn birth weight for GA, whereas controls were of appropriate for gestational age. The dilutions of the polyclonal rabbit, antihuman Hp antibody (Dako) and the conditions for immunoblotting were the same as described earlier for 2D immunoblots. The plasma samples in equal volumes (~5 µg protein) were pre-treated with 2-mercaptoethanol (final concentration 1%) and subjected to 1D-GE. The immunoblot consisted of 0.1 µg standard purified Hp (GE Healthcare) as a reference/ positive control. Optical densitometric analysis of bands corresponding to the three Hp subtypes (α1, α2, and β) in respective bands on the 1D immunoblot was performed using Phoretix 1D software. The background subtraction, selection of lanes analyzed and the detection of specific bands for software quantification were all done manually. The quantification of 1D immunoblots was performed by densitometry using Phoretix 1D advanced v5.10 software (Nonlinear Dynamics Ltd.).

2.2.6. Quantitative analysis of 2-DGE Hp spots

For quantification of intensities of the spots on 2D gels for the specified proteins, Phoretix 2D expression software was used to analyze replicate gels under identical conditions. The software includes automated spot detection, gel matching, background correction, and data normalization. For analysis in this study however, spots of interest were manually matched because of the complexity of the gel images. The background intensity for individual spots was based on the intensity in a radius that extended 45 pixels in all directions (mode of non-spot). The spot volume was denoted by the sum pixel intensity within a spot minus the background. Individual spot volumes were divided by the sum total of all spot volumes on a particular gel and multiplied by a constant (100). "Normalization of spot volumes" was carried out to correct for random error as well as inherent total protein variation, and was used for statistical comparison.

2.2.7. Statistical analysis

Chi-square test was used to compare categorical variables between the FGR and control groups, or the Fisher's exact test where appropriate. The independent samples t-test was used to compare mean differences in continuous variables between the two groups. The Pearson correlation coefficient assessed the relationship between two continuous variables and scatter plots were produced to test for linearity. Statistical significance was determined at $p \leq 0.05$. Because the

sample sizes based on GA grouping described in Table 2.1A were low in the respective groups, and the observations in each group did not follow a normal distribution, we employed a nonparametric procedure using the Mann-Whitney test.

2.3. RESULTS

The clinical characteristics of the subjects in this study are described in Table 2.1A, B. Pregnancies were categorized into two groups namely <28 wk or ≥28 wk gestation. The controls were of appropriate for GA. Based on the uterine artery Doppler velocimetry >50% of subjects were diagnosed with placental insufficiency, and the majority were in the ≥28 wk GA group. The placental weights of FGR pregnancies (336.7 ± 40.9 g) were significantly lower than those of controls (489.2 ± 137.1 g) (p = 0.006).

2.3.1. 2-DGE comparison between plasma of FGR and normal pregnancies

Initial evaluative studies showed that IEF with active rehydration provided a better resolution of proteins as compared to passive rehydration (data not shown). In addition, an improved resolution of proteins was attained on the 2D gels using IPG strips, pH 3.0–10.0 NL compared to linear that is currently not depicted. All subsequent 2-DGE analyses were thus performed using IPG strips pH 3.0–10.0 NL. A representative comparison of protein spots on 2-DGE maps of maternal plasma from GA matched FGR and control subjects is shown in Figure 2.1A (i) and (ii), respectively.

TABLE 2.1.A. Study group characteristics.

Subject Characteristics [a]		FGR	Control	P
Total subjects (n)		28	22	
Doppler	Abnormal	15		
	Normal	7		
	None	6		
Delivery	Vaginal	14 (50%)	16 (73%)	
	Cesarean	14 (50%)	6 (27%)	
Gender	Male	13 (46%)	18 (82%)	0.01
	Female	15 (54%)	4 (18%)	
Maternal age (18-37 y)		25.8 ($\pm$6.2)	25.9 ($\pm$4.6)	
GA (wk) (23-40 wk)	>28 Wks	25 (90%)	15 (68%)	
	<28 Wks	3 (11%)	7 (32%)	
Placental wt. (g)		337 ($\pm$41)	489 ($\pm$137)	0.006

TABLE 2.1.B. Distribution of percentile of the newborns based on GA for FGR group

FGR Newborn percentile	<28 wks GA (n)	>28 wks GA (n)
<5th	3	7
5th – 10th	4	9

[a] Inclusion and exclusion criteria: Singleton pregnancies with growth restricted fetus in North American population were included. The subjects with twins, premature ruptured membranes, abrupted placenta, fetal, congenital or genetic abnormalities, diabetes, thyroid disorder and chronic hypertensive disorders, chorioamnionitis, preeclampsia ,smoking, drug use, and subjects with malnutrition were excluded.
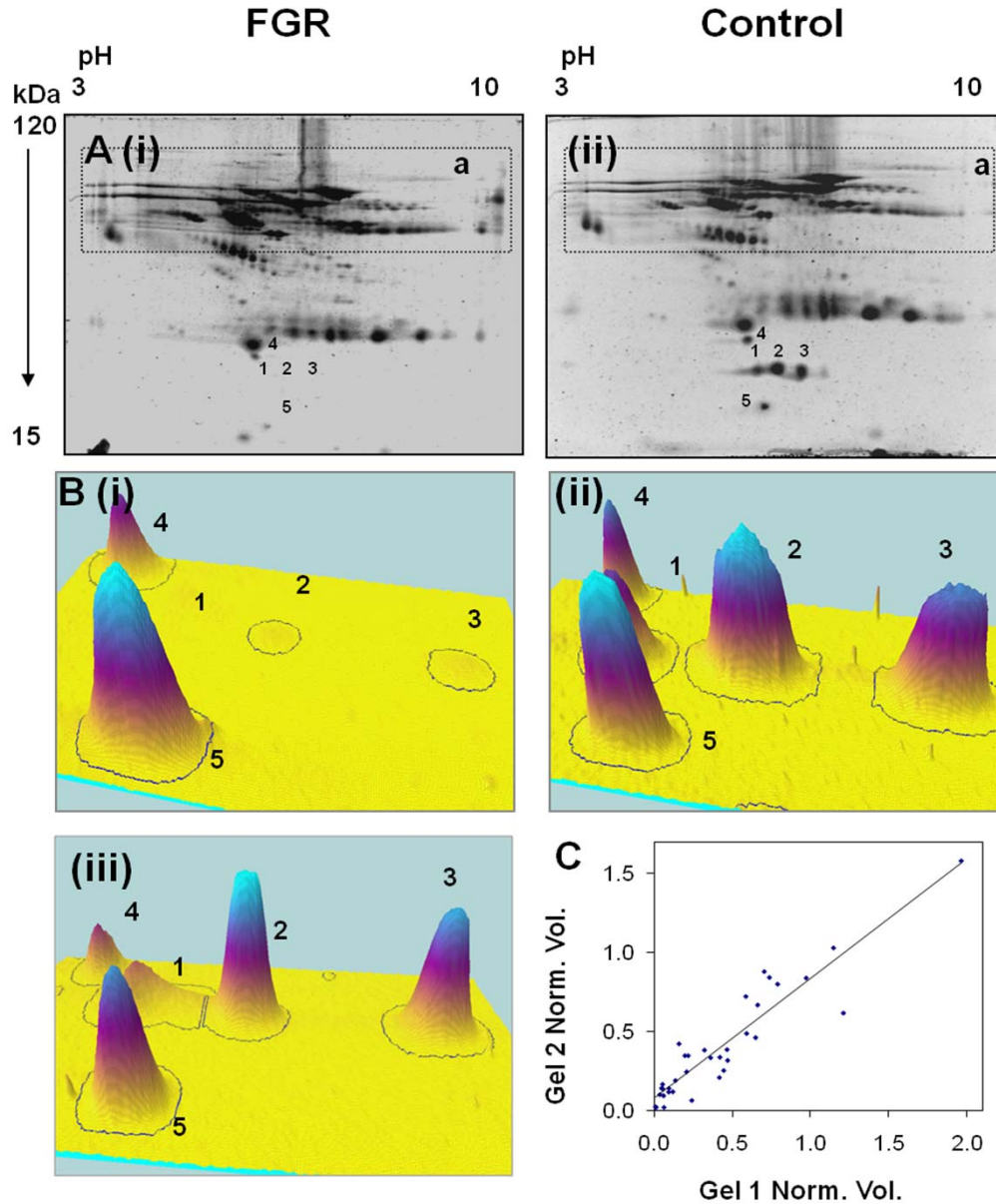
FIGURE 2.1. (A) Representation of comparison of 2D-GE maps using maternal plasma from FGR (i) and control (ii) subjects with matched GA. For FGR gels (i) spots 1, 2, and 3 (hp α2 variants) were absent as compared with the control (ii). Spot 4 (TTR) was moderately increased in FGR subjects while spot 5 (RBP) showed no detectable change in its expression. **(B)** A magnified, maximally contrasted three-dimensional rendering of 2D images for spots 1–5. The three different patterns primarily observed are represented. (i) 8/28 FGR, 7/22 controls, (ii) 4/28 FGR, 11/22 controls, (iii) 16/28 FGR, 4/22 controls. **(C)** Comparison of matched spots with normalized volumes detected on two 2D-GE maps of an identical maternal plasma sample prepared on separate occasions. The R squared for the trend-line was 0.86.

41

Although IPG strips, pH 3.0–10.0 NL provided better resolution of plasma proteins, the 7-cm strips did not optimally separate all abundant plasma proteins, specifically, in the higher Mr range. High abundant proteins, such as albumin and IgG, obscured the identification and quantification of minor proteins in and around this zone. The current protocol however, allowed successful discrimination of protein quantities between control and FGR samples, specifically in the lower Mr region. Only well separated and defined spots on the 2D gel images, quantifiable by software analysis, were further characterized. From the gel images, a set of five major visible spots in the lower Mr range, were prominent, labeled as 1–5 (Figure 2.1 [ii]). Comparison with the plasma map (EXPASY) indicated spots 1–3 as Hp α2 chain variants, spot 4 as transthyretin (TTR), and spot 5 as retinol binding protein (RBP).

The Hp α2 in plasma from FGR pregnancies showed three different patterns of expression. In the first pattern, Hp spots 1, 2, and 3 were near to, or below, the threshold of detection, as shown in Figure 2.1B (i), that was seen in 29% of FGR pregnancies. This pattern in controls was detected in 33% of pregnancies. In the second pattern, all three Hp spots (1, 2, and 3) were of relatively high intensity, as shown in Figure 2.1B (ii), was most commonly observed in controls (52% of pregnancies) and present in only in a small number (13%) of FGR pregnancies. In the third pattern, only spot 1 was reduced in intensity, as shown in Figure 2.1B (iii), was most prevalent (67%) in the FGR pregnancies, and was not commonly seen in the controls (14% of pregnancies). Shown in Figure 2.1C is the correlation of the same

TABLE 2.2. Summary of software spot quantitation of 2-D gels and MS/MS identification on specific protein spots from maternal plasma from FGR and control pregnancies representative of 3 MS experiments.

Spot #	ID	Observed		Coverage (%)	MS/MS ion & Sequence Tag		Mascot Score	Mean Vol. (SD)		p
		pI	Mr (KDa)		m/z (charge) a.a.	Sequence		FGR	Cont.	
1	Hp α2	5.8	18	6	720.33 (2+) 60-72 448.22 (2+) 95-102 656.79 (2+) 60-71 581.76 (2+) 142-151	TEGDGVYTLNNEK NPANPVQR TEGDGVYTLNDK LPECEAVCGK	145	0.12 (0.16)	0.26 (0.18)	0.006
2	Hpα2	6.4	18	11	720.33 (2+) 60-72 448.22 (2+) 95-102	TEGDGVYTLNNEK NPANPVQR	165	0.52 (0.55)	0.65 (0.47)	
3	Hp α2	6.9	18	6	336.7 (2+) 36-41 456.3 (2+) 42-54 787.4 (3+) 125-146	VLDAVR GSPAINVAVHVFR YTIAALLSPYSYST TAVVTNPK	85	0.29 (0.33)	0.38 (0.26)	
4	TTR	5.6	15	5.6	679.83 (2+) 26-38	AADDTWEPFASGK	156	0.63 (0.21)	0.44 (0.17)	0.001
5	RBP	5.2	20*	*	*	*		0.24 (0.12)	0.19 (0.09)	
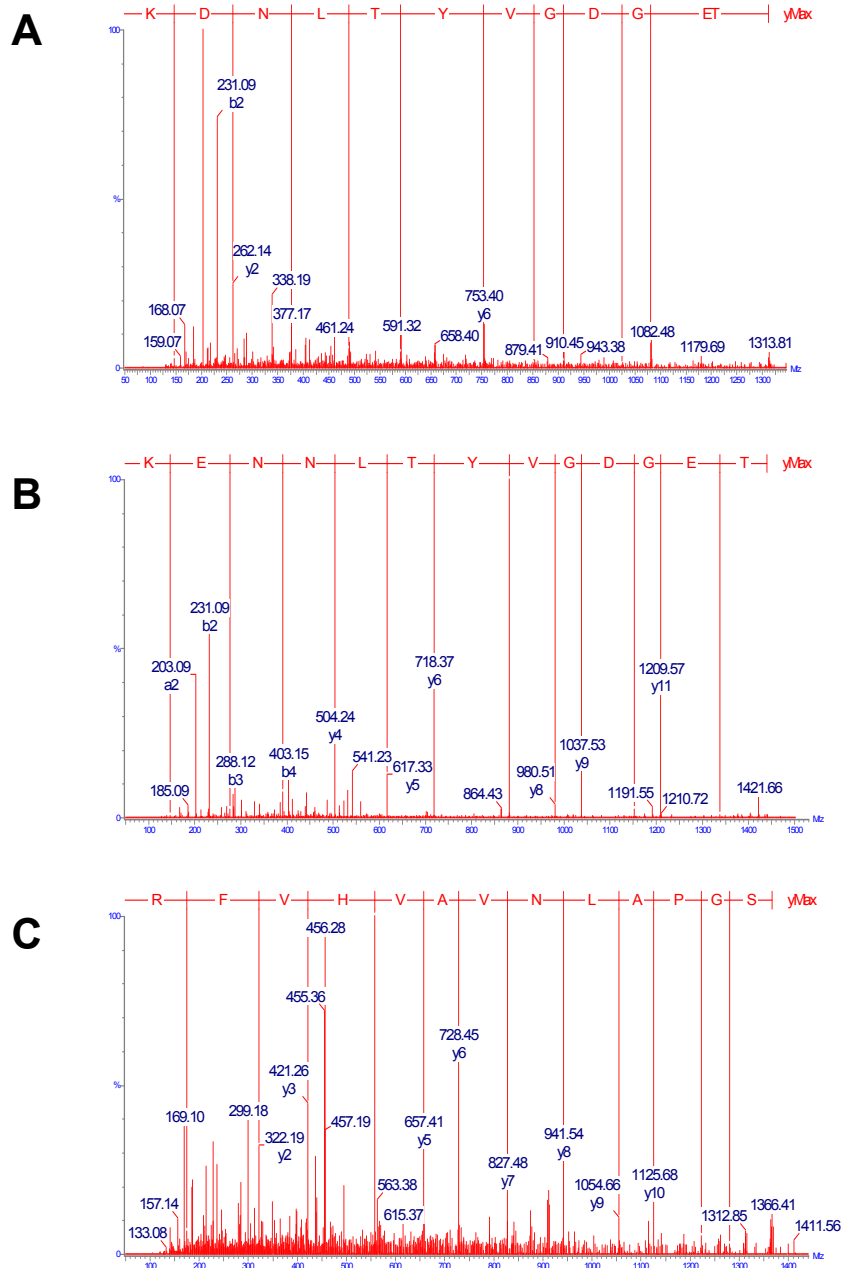
*not identified.

FIGURE 2.2. LC-MS/MS spectra for the identification of the tryptic peptide sequences of Hp α2 variants and TTR. MS/MS spectra of ion at m/z 656.31 (+2) **(A)** and 720.33 (2+) **(B)** from spot 1, 2, and 3 corresponding to Hp α2; and ion at m/z 683.88 (+2) **(C)** from spot 5 corresponding to TTR.

protein between two gels run under identical conditions. The R-squared for the linear plot was 0.86 suggesting relatively low inter-gel variability.

2.3.2. Identification of proteins spots

The identities of spots 1, 2, and 3 as variants of Hp α2 chain, and spot 4 as TTR were made by LC MS/MS followed by Mascot searches (Table 2.2). Although a low coverage (3–11%) for Hp α2 variants and (28%) for TTR were obtained, the high quality of MS/MS spectra (Figure 2.2) established the identity of these proteins in the select spots. No significant hits for other proteins were found in the region of these spots. Hp α2 variant proteins identified by MS were confirmed by 2D immunoblot analysis (Figure 2.3A [i]). Plasma from FGR and control subject showed variable intensities of protein species with Mr 16, 18, and 42 KDa, corresponding to α chains (α1 and α2) and a β chain of Hp, respectively (Figure 2.3A [i, ii]). Both Hp α1 and α2 variants were reduced significantly in FGR (Figure 2.3A [i]) compared to controls (Figure 2.3A [ii]). Immunoblotting corroborated the 2-DGE data with SYPRO Ruby stained gels (Figure 2.1A [i, ii]). Additional spots (a, b, and c) were detected compared to 2-DGE. As shown in Figure 2.3A (ii), spot (a) corresponded to the fourth variant of Hp α2, whereas spots (b) and (c) corresponded to two extra variants of Hp α1 in the control plasma. The additional spots (a), (b), and (c) seen in the controls were absent in the FGR.
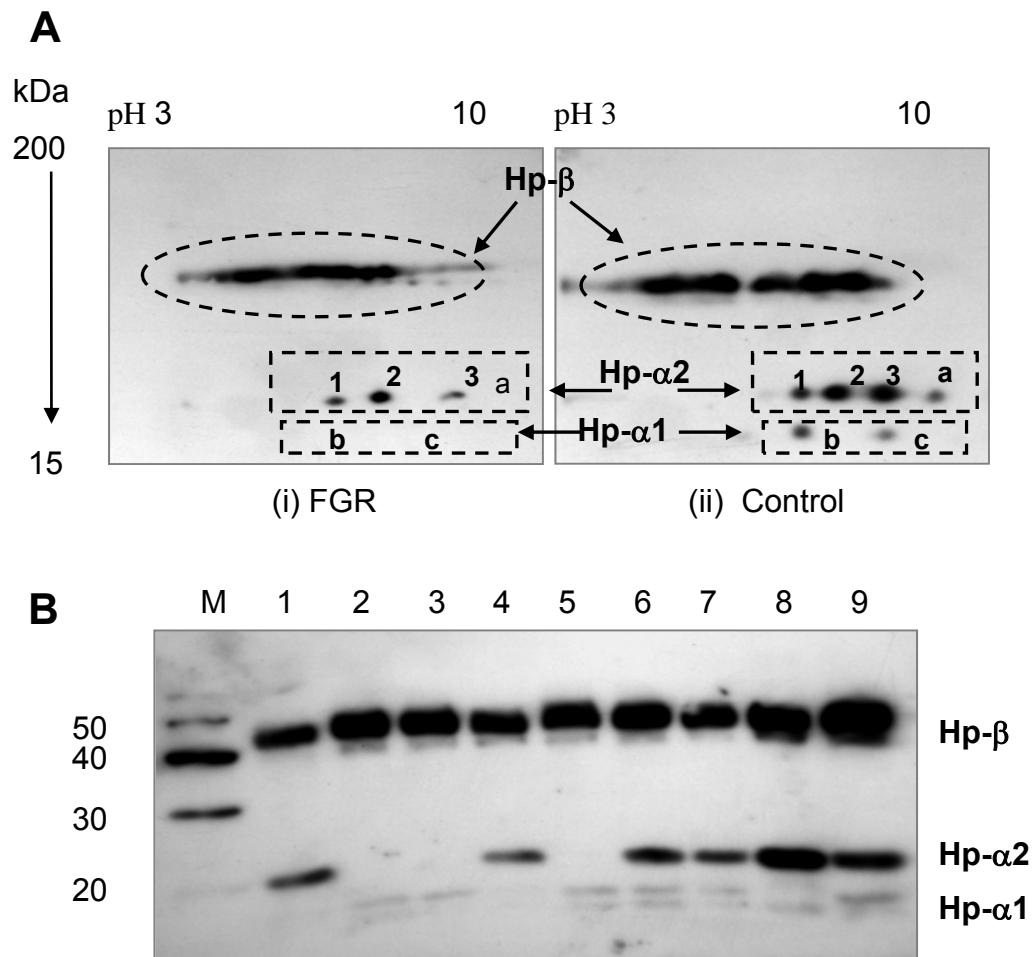
FIGURE 2.3. Western blots of maternal plasma for Hp. **(A)** Equal amounts of maternal plasma protein from a FGR (i) and a GA matched control (ii) were probed on a 2-D blot. A(i) shows significantly reduced spots 1, 2, and 3 corresponding to hp α2 variants as compared to the control (ii). An additional spot, denoted as (a) was detected in the control (ii) that represents the fourth variant of Hp α2 (plasma map, EXPASY). Spots (b) and (c), corresponding to Hp α1 variants, were only detected in the control (ii) sample. **(B)** Semiquantitative evaluation of Hp variants. Representative maternal plasma samples from FGR (n = 5) and control (n = 3) subjects were selected. Lanes 1–5 are FGR subjects with low birth weight newborns (<5th percentile for GA); lanes 6–8 from the control subjects with normal birth weight infants. Equal amount of total protein was loaded in lanes 1–8. Lane 9 consists of 0.1 μg pure Hp (Sigma), used as a positive control. Sample in lanes 4 and in 8 were common between 1D and 2D (A) immunoblot analysis.

2.3.3. Evaluation of Hp variants by immunoblotting

The specificity of the polyclonal antibody provided additional information on all Hp subtypes. The analysis of plasma samples from FGR and control subjects (Figure 2.3B) using anti-human Hp antibody showed variable intensities of three bands with Mr 16, 18, and 42, corresponding to Hp α1, α2, and β subtypes, respectively (Figure 2.3B, lanes 1–8). The Hp standard purified from pooled human plasma shown in lane 9 (Figure 2.3B) as a positive control, exhibited high intensity of 18 and 42 KDa bands but a fainter band at 16 KDa. Of the five samples representing the maternal plasma from FGR subjects in this study, three revealed Hp α2 to be absent in FGR (Figure 2.3B; lanes 2, 3, and 5). The band corresponding to Hp α1 however, was absent in two out of five FGR samples (Figure 2.3B; lane 1 and 4), whereas the intensity of this variant was relatively reduced in the remaining three samples (Figure 2.3B; lanes 2, 3, and 5). Although the representative samples from controls (lanes 6–8) showed varied signals, the intensities for both Hp α2 and Hp α1 bands were relatively higher than the FGR group. Quantitation of mean Hp band intensity using optical densitometry led to determine the reduction in Hp. A 25.6% reduction was observed for Hp β, 31.3% for Hp α1 and 93.0% for Hp α2 subtypes in FGR compared to the control. The data demonstrated a moderate or inconclusive reduction of Hp β and Hp α1 expression, nonetheless, a distinct reduction in Hp α2 in FGR.

2.3.4. Quantitative assessment of Hp α2 variants
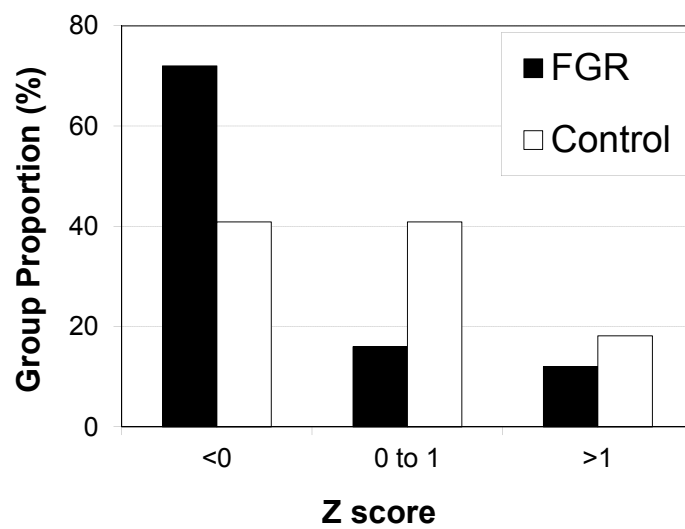
FIGURE 2.4. Quantitative distribution of significantly different Hp α2 variant 1 expression in maternal plasma from FGR (n=28) and control (n=22) subjects.

Statistical evaluation of normalized spot volumes for spots 1–3, (Hp α2 variants 1 to 3), spot 4 (TTR), and spot 5 (RBP) on 2D gels as represented in Figure 2.1A (i, ii) in FGR and control subjects is shown in Table 2.2. We used RBP as a quantitative control for a better indication of validity of evaluation of spots on the gels. The mean spot intensity for Hp variant 1 was significantly reduced in FGR compared to controls (p = 0.006), whereas TTR was higher in FGR compared to controls (p = 0.001). To further analyze the distribution of Hp variant 1 between control and FGR, the distribution of normalized volumes was plotted based on their z score, low (<0), medium (0–1 to 1) and high (normal) (>1). Figure 2.4 illustrates the intensity of Hp α2 variant 1 to be high or medium in the majority (59%) of controls, in comparison to only 28% of FGR subjects. As shown in Figure 2.4, the distribution of Hp α2 variant 1 volumes for FGR were negatively skewed, with 72% of Hp α2 variant 1 volumes being >1 SD below the overall mean compared to 40% in control.

Furthermore, we investigated the relationship between uterine artery Doppler flow velocimetry and the frequency of reduced Hp α2 variant 1 in FGR accompanied by abnormal Doppler. Hp spot 1 expressed as normalized volumes were low to medium (53.3% with low and 27% with medium) in 80% of FGR accompanied by abnormal Doppler, as compared to only 20% of FGR with normal Doppler.

2.4.   DISCUSSION

Our results suggest that 2-DGE combined with LC-MS/MS is a feasible approach to identify changes in relatively abundant low molecular weight proteins in un-fractionated plasma. Although 2-DGE analysis of whole plasma is a challenging and time consuming approach for comprehensive protein analysis, it allowed us to discover semiquantitative changes in the proteome of FGR pregnancies. New powerful image analysis software was crucial in the initial identification of changes in the plasma proteome and led us to determine that a specific variant of Hp α2 chain was reduced in the maternal plasma of FGR, but not of controls.

FGR is associated with increased mortality of the fetus and increased morbidity in the neonatal period and childhood, as well as in adulthood (4). Ultrasound fetal biometry is used for the estimation of fetal weight in fetuses (15–18, 20), and umbilical artery Doppler (18) is used to distinguish FGR fetuses owing to utero-placental insufficiency. Biophysical profile assessment is also used to determine fetal health and to provide indications for delivery. However, these tests reflect the condition of the fetus at the time of assessment and do not indicate the pathology or progression of the disease process that underlay FGR. Additional tests are, therefore, necessary to determine pathological FGR and its potential pathophysiology.

 FGR is a multifactorial disease with diverse etiology and pathophysiology (2), and therefore proteome changes may be etiologically dependent. Correspondingly, all subjects in this study were confirmed cases of FGR and the majority of them were the result of utero-placental insufficiency (21). To minimize heterogeneity and the effects of confounding factors in this study, the exclusion criteria used in the current

selection of subjects ensured requisite health and lifestyle factors that also include malnutrition. Because delivery was delayed if intervention was not necessary (2), most of the FGR pregnancies were ≥28 wk gestation. Poor placental growth has been shown to limit concurrent development of the fetus (21) and, as expected, our data shows the placental weight of FGR pregnancies to be significantly smaller than the matching controls. These results concur with the significance of abnormal placental development in FGR pregnancies (22).

Based on their relationship to growth and development of the fetus, several peptides have been proposed as potential biomarkers (23). Prealbumin has been suggested to be associated with fetal defects and pregnancy complications (24). Leptin may reflect a generalized response to hypoxic stimuli (25), and free β-hCG and PAPP-A levels have been associated with general fetal abnormality (26). Elevated α-fetoprotein levels in the amniotic fluid through amniocentesis have been suggested to be of potential use in the detection of FGR (27), however, its association with adverse pregnancy outcome has not been confirmed (28). Novel biomarkers that may be more reliable and specific in their diagnostic and prognostic value in FGR remain to be identified.

Proteomic approaches offer new opportunities for potential biomarker discovery in pregnancy disorders (14). When searching for diagnostic markers in plasma, depleting most abundant protein(s) may be valuable, however, it could also lead to variability and nonspecific protein loss (29). Although whole plasma analysis renders the possibility of detecting the desired biomarkers challenging (30, 31), it nonetheless

mitigates the complications associated with plasma pre-fractionation (32). Protein expression profiling using direct MS may be superior for identifying a larger number of total proteins (33), however, because of the lack of complete amino acid sequence coverage for a protein using either MALDI-MS or LC-MS/MS, there has been limited success in using MS based approach to identify the isoform and posttranslational modification in plasma (34). 2D gels on the other hand, generate different spots that correspond to a change in overall protein charge and/or molecular weight. In the current study, this technique has allowed the identification of Hp α2 as a differentially expressed protein in the plasma proteome, which was then confirmed by immunoblotting. This study was feasible because of the high abundance and adequately separate detectable spots for Hp which were discriminated by software analysis. These spots have previously been recognized as structurally different species of Hp α2 chain (11, 35, 36). Immunoblotting revealed additional Hp α2 and Hp α1 variants in the control plasma, which has been reported previously (35). Subsequent studies in a larger FGR population using an immunological assay with higher sensitivity and specificity will be crucial in determining the clinical utility of Hp α2.

Hp alpha is expressed via Hp α1 and α2 alleles. The absence of α2 in the plasma for many patients may be due to a lack of the allele (Figure 2.2Ai). Althogh nevertheless the majority of patients expressing the α2 allele had a significant reduction of variant 1 compared to other variants, which was not found in control (Figure 2.2B ii vs iii). Similar modifiacations resulting in a decreased isoform variant may be present on the

α1. Structural characterization of the modifications of the less common Hp α1 variant may determine if the changes are universal to other Hp types. Hp is a positive acute phase protein (37) that is variably expressed in maternal plasma during the course of pregnancy (38). Increased expression of serum Hp α2 has been detected in ovarian cancer and is used as a biomarker for screening this disease (39, 40). The specific reduction in Hp α2 variant, and possibly of Hp α1 protein chain, may not reflect a generalized positive acute phase response in the FGR.

Our data is the first to demonstrate consistently, the absence and/or suppression of only a specific variant of Hp α2 that migrates in the most acidic location of the three variants as identified on 2D gels. The differences in isoelectric points (pI) of Hp α2 variants may be because of its posttranslational modification, such as deamidation of asparagines (41, 42). Although the variability in intensity of Hp α2 variant 1 has been linked with a carboxypeptidase that leads to different turnover rates of this variant in blood (35), the pathophysiologic basis for the suppression of specific Hp variants in FGR is still unknown. The rates of deamidation of human proteins have been suggestive of a biologically relevant phenomenon that serves as molecular timer of biological events (43). It is possible that differences that lead to the separation or comigration of Hp α2 variants in FGR may be attributed to subtle structural modifications of the protein that occurs during the disease process. The site and the cause/effect for this modification in FGR are not known, however, it is likely that the placenta plays an important role in this process. Changes in posttranslational

processing and not in the synthesis or secretion of Hp have been shown in colon cancer (44).

Hp is an important protein in reproduction (45) and has been shown to be involved in the early signalling process during preimplantation (46). Hp is present in uterus and its role in endometrium has been suggested to be in protecting the fetus from a maternal allograft-like immune response (47). Hp is involved in HELLP syndrome, which is linked with haemolysis (48–50). It is also suggested to be involved in placental angiogenesis (51–53). Because placental insufficiency is the major common factor in FGR, it is logical to suggest the role of Hp in placental vessel remodelling. Given the contribution of Hp to placental development (47), it will be important to determine if Hp is a marker of placental insufficiency.

Clinically relevant biomarkers may however be of either causal or associative in nature (54). Based on our current findings, we have initiated a study to elucidate the mechanistic basis for Hp suppression in the pathophysiology of FGR using human hepatoma cells as hepatic synthetic machinery *in vitro* (55,56). Our on-going study shows that Hp biosynthesis in hepatoma cells is altered in a similar manner by hypoxia (unpublished data), a condition that is commonly associated with FGR.

In this study, we present evidence that expression of a specific variant of Hp α2, that is a high abundance protein, is uniquely expressed in FGR patients. This is the first report in our search toward discovery of biomarker(s) in FGR. However, for detection of larger number of plasma proteins, specifically of low molecular weight and low abundance, we propose to employ our recently established pre-fractionation

strategy in a follow up study to further elucidate the FGR proteome. Furthermore, identification of proteins in the plasma by 2-DGE followed by MS and the high throughput 2D LC-MS has demonstrated that the majority of the identified protein set was unique to each method (57) therefore, for a comprehensive coverage, as suggested by Choi et al. it will be ideal to apply the two methods to achieve optimal results for the analysis of the plasma proteome.

The maternal blood samples in this study were collected from pregnant women just before delivery. The results from this study are consistent among the subjects, who in our assessment represent the clinical population with the problem, and, therefore, strongly show that we have been successful in identifying a potential biomarker in maternal plasma indicative of a late manifestation of FGR. It is recognized that a differential expression does not positively identify any protein as a biomarker of FGR, fulfillment of other criteria such as a larger sample size, collection of maternal plasma prior to birth at different gestational ages and multifactorial analyses, will be essential before Hp α2 could be used in a clinical setting. The fact that the change in Hp α2 correlates with the Doppler outcomes suggests it can be a potential diagnostic and/or prognostic marker. If changes of Hp precede the clinical diagnosis of FGR and placental insufficiency, inclusion of this protein in routine antenatal estimation of fetal weight and/or umbilical artery Doppler examination could be useful clinically.

2.5.   REFERENCES

1. Cetin, I., Foidart, J. M., and Miozzo, M., et al. (2004) Fetal growth restriction: a workshop report. *Placenta. 25*, 753–757.

2. Resnik, R. (2002) Intrauterine growth restriction. Obstet. Gynecol. 99, 490–496.

3. Jarvis, S., Glinianaia, S. V., Torrioli, M. G., et al. (2003) Cerebral palsy and intrauterine growth in single births: European collaborative study. *Lancet. 362*, 1106–1111.

4. Barker, D. J. (2004) The developmental origins of well-being. *Philos. Trans. R. Soc. Lond. B. Biol. Sci. 359*, 1359–1366.

5. Jornayvaz, F. R., Selz, R., Tappy, L., and Theintz, G. E. (2004) Metabolism of oral glucose in children born small for gestational age: evidence for an impaired whole body glucose oxidation. *Metabolism. 53*, 847–851.

6. Abdo, M., Irving, B., Hudson, P., and Zola, H. (2005) Development of a cluster of differentiation antibody-based protein microarray. *J. Immunol. Methods. 305*, 3–9.

7. Abdolkhaleg D, Behrooz S. (2005) A sensitive immunoblotting method for screening of microalbuminuria in diabetic patients' urine. *Saudi Med. J. 26(7)*, 1075–1079.

8. Ergaz, Z., Avgil, M., and Ornoy, A. (2005) Intrauterine growth restriction-etiology and consequences: what do we know about the human situation and experimental animal models? *Reprod. Toxicol. 20*, 301–322.

9. Wilhelm, D., Mansmann, U., Neudeck, H., Matejevic, D., Vetter, K., and Graf, R. (2002) Decrease of elastic tissue fibres in stem villus blood vessels of the human placenta during IUGR and IUGR with concomitant preeclampsia. *Anat. Embryol. (Berl) 205*, 393–400.

10. Sibley, C. P., Turner, M. A., Cetin, I., et al. (2005) Placental phenotypes of intrauterine growth. *Pediatr. Res. 58*, 827–832.

11. Quero, C., Colome, N., Prieto, M. R., et al. (2004) Determination of protein markers in toxic oil syndrome studies. *Proteomics. 4*, 303–315.

12. Crameri, R. (2005) The potential of proteomics and peptidomics for allergy and asthma research. *Allergy. 60*, 1227–1237.

13. Davidsson, P. and Sjogren, M. (2005) The use of proteomics in biomarker discovery in neurodegenerative diseases. *Dis. Markers. 21*, 81–92.

14. Shankar, R., Gude, N., Cullinane, F., Brennecke, S., Purcell, A. W., and Moses, E. K. (2005) An emerging role for comprehensive proteome analysis in human pregnancy research. *Reproduction. 129*, 685–696.

15. Gaziano, E. P. (1995) Antenatal ultrasound and fetal Doppler. Diagnosis and outcome in intrauterine growth retardation. *Clin. Perinatol. 22*, 111–140.

16. Arbuckle, T. E., Wilkins, R., and Sherman, G. J. (1993) Birth weight percentiles by gestational age in Canada. Obstet. Gynecol. *81,* 39–48.

17. Gelbaya, T. A. and Nardo, L. G. (2005) Customised fetal growth chart: a systematic review. *J. Obstet. Gynaecol. 25*, 445–450.

18. Barkehall-Thomas, A., Wilson, C., Baker, L., ni Bhuinneain, M., and Wallace, E. M. (2005) Uterine artery Doppler velocimetry for the detection of adverse obstetric outcomes in patients with elevated mid-trimester betahuman chorionic gonadotrophin. *Acta. Obstet. Gynecol. Scand. 84*, 743–747.

19. Perkins, D. N., Pappin, D. J., Creasy, D. M., and Cottrell, J. S. (1999) Probability-based protein identification by searching sequence databases using mass spectrometry data. *Electrophoresis, 20*, 3551–3567.

20. Hobbins, J. (1997) Morphometry of fetal growth. *Acta. Paediatr. Suppl. 423,* 165–169.

21. Baschat, A. A. and Hecher, K. (2004) Fetal growth restriction due to placental disease. *Semin. Perinatol. 28,* 67–80.

22. Rutland, C. S., Mukhopadhyay, M., Underwood, S., Clyde, N., Mayhew, T. M., and Mitchell, C. A. (2005) Induction of intrauterine growth restriction by reducing placental vascular growth with the angioinhibin TNP-470. *Biol. Reprod. 73*, 1164–1173.

23. Tjoa, M. L., Oudejans, C. B., van Vugt, J. M., Blankenstein, M. A., and van Wijk, I. J. (2004) Markers for presymptomatic prediction of preeclampsia and intrauterine growth restriction. *Hypertens. Pregnancy. 23*, 171–189.

24. Jain, S. K., Shah, M., Ransonet, L., Wise, R., and Bocchini, J. A., Jr. (1995) Maternal and neonatal plasma transthyretin (prealbumin) concentrations and birth weight of newborn infants. *Biol. Neonate. 68*, 10–14.

25. Tommaselli, G. A., Pighetti, M., Nasti, A., et al. (2004) Serum leptin levels and uterine Doppler flow velocimetry at 20 weeks' gestation as markers for the development of preeclampsia. *Gynecol. Endocrinol. 19*, 160–165.

26. Krantz, D., Goetzl, L., Simpson, J. L., et al. (2004) Association of extreme first-trimester free human chorionic gonadotropin-beta, pregnancy-associated plasma protein A, and nuchal translucency with intrauterine growth restriction and other adverse pregnancy outcomes. *Am. J. Obstet. Gynecol. 191,* 1452–1458.

27. Roig, M. D., Sabria, J., Valls, C., et al. (2005) The use of biochemical markers in prenatal diagnosis of intrauterine growth retardation: insulin-like growth factor I, Leptin, and alphafetoprotein. *Eur. J. Obstet. Gynecol. Reprod. Biol. 120*, 27–32.

28. Ilagan, J. G., Stamilio, D. M., Ural, S. H., Macones, G. A., and Odibo, A. O. (2004) Abnormal multiple marker screens are associated with adverse perinatal outcomes in cases of intrauterine growth restriction. *Am. J. Obstet. Gynecol. 191*, 1465–1469.

29. Granger, J., Siddiqui, J., Copeland, S., and Remick, D. (2005) Albumin depletion of human plasma also removes low abundance proteins including the cytokines. *Proteomics, 5*, 4713–4718.

30. Wang, H., Clouthier, S. G., Galchev, V., et al. (2005) Intact-protein-based high-resolution three-dimensional quantitative analysis system for proteome profiling of biological fluids. *Mol. Cell. Proteomics. 4*, 618–625.

31. Pieper, R., Su, Q., Gatlin, C. L., Huang, S. T., Anderson, N. L., and Steiner, S. (2003) Multicomponent immunoaffinity subtraction chromatography: an innovative step towards a comprehensive survey of the human plasma proteome. *Proteomics. 3*, 422–432.

32. Zolotarjova, N., Martosella, J., Nicol, G., Bailey, J., Boyes, B. E., and Barrett, W. C. (2005) Differences among techniques for high-abundant protein depletion. *Proteomics. 5*, 3304–3313.

33. Koller, A., Washburn, M. P., Lange, B. M., et al. (2002) Proteomic survey of metabolic pathways in rice. *Proc. Natl. Acad. Sci. USA. 99*, 11,969–11,974.

34. Person, M. D., Shen, J., Traner, A., et al. (2006) Protein fragment domains identified using 2D gel electrophoresis/MALDI-TOF. *J. Biomol. Tech. 17*, 145–156.

35. Mikkat, S., Koy, C., Ulbrich, M., Ringel, B., and Glocker, M. O. (2004) Mass spectrometric protein structure characterization reveals cause of migration differences of haptoglobin alpha chains in two-dimensional gel electrophoresis. *Proteomics. 4*, 3921–3932.

36. John, H. A. and Purdom, I. F. (1989) Elevated plasma levels of haptoglobin in Duchenne muscular dystrophy:electrophoretic variants in patients with a severe form of the disease. *Electrophoresis. 10*, 489–493.

37. Haram, K., Augensen, K., and Elsayed, S. (1983) Serum protein pattern in normal pregnancy with special reference to acute-phase reactants. *Br. J. Obstet. Gynaecol. 90*, 139–145.

38. Gatzka, C., Bremerich, D., Kaufmann, M., and Ahr, A. (2002) Isolated decrease of Haptoglobin during pregnancy: diagnosis by chance or pathological? *Zentralbl. Gynakol. 124*, 120–122.

39. Ahmed, N., Barker, G., Oliva, K. T., et al. (2004) Proteomic-based identification of haptoglobin- 1 precursor as a novel circulating biomarker of ovarian cancer. *Br. J. Cancer. 91*, 129–140.

40. Ahmed, N., Oliva, K. T., Barker, G., et al. (2005) Proteomic tracking of serum protein isoforms as screening biomarkers of ovarian cancer. *Proteomics. 5*, 4625–4636.

41. Sarioglu, H., Lottspeich, F., Walk, T., Jung, G., and Eckerskorn, C. (2000) Deamidation as a widespread phenomenon in two-dimensional polyacrylamide gel electrophoresis of human blood plasma proteins. *Electrophoresis. 21*, 2209–2218.

42. Robinson, N. E. and Robinson, A. B. (2001) Deamidation of human proteins. *Proc. Natl. Acad. Sci. USA. 98*, 12,409–12,413.

43. Robinson, N. E. and Robinson, A. B. (2001) Molecular clocks. *Proc. Natl. Acad. Sci. USA. 98*, 944–949.

44. Bresalier, R. S., Byrd, J. C., Tessler, D., et al. (2004) A circulating ligand for galectin-3 is a haptoglobin-related glycoprotein elevated in individuals with colon cancer. *Gastroenterology. 127*, 741–748.

45. Ueda, K., Yamamasu, S., Nakamura, Y., et al. (2001) Involvement of phenotypes and serum levels of haptoglobin in the outcome of in vitro fertilization and embryo transfer. *Gynecol. Obstet. Invest. 51*, 219–222.

46. Herrler, A., von Wolff, M., and Beier, H. M. (2002) Proteins in the extraembryonic matrix of preimplantation rabbit embryos. *Anat. Embryol. (Berl). 206*, 49–55.

47. Berkova, N., Lemay, A., Dresser, D. W., Fontaine, J. Y., Kerizit, J., and Goupil, S. (2001) Haptoglobin is present in human endometrium and shows elevated levels in the decidua during pregnancy. *Mol. Hum. Reprod. 7*, 747–754.

48. Wilke, G., Rath, W., Schutz, E., Armstrong, V. W., and Kuhn, W. (1992) Haptoglobin as a sensitive marker of hemolysis in HELLP-syndrome. *Int. J. Gynaecol. Obstet. 39*, 29–34.

49. Raijmakers, M. T., Roes, E. M., te Morsche, R. H., Steegers, E. A., and Peters, W. H. (2003) Haptoglobin and its association with the HELLP syndrome. *J. Med. Genet. 40*, 214–216.

50. Yamamoto, H., Nishikawa, S., Yamazaki, K., and Kudo, R. (2000) Efficacy of Haptoglobin administration in the early postoperative course of patients with a diagnosis of HELLP syndrome. *J. Obstet. Gynaecol. 20*, 610–611.

51. Cid, M. C., Grant, D. S., Hoffman, G. S., Auerbach, R., Fauci, A. S., and Kleinman, H. K. (1993) Identification of haptoglobin as an angiogenic factor in sera from patients with systemic vasculitis. *J. Clin. Invest. 91*, 977–985.

52. Dobryszycka, W. (1997) Biological functions of haptoglobin: new pieces to an old puzzle. *Eur. J. Clin. Chem. Clin. Biochem. 35*, 647–654.

53. de Kleijn, D. P., Smeets, M. B., Kemmeren, P. P., et al. (2002) Acute-phase protein Haptoglobin is a cell migration factor involved in arterial restructuring. *FASEB J. 16*, 1123–1125.

54. Rapkiewicz, A. V., Espina, V., Petricoin, E. F., 3rd, and Liotta, L. A. (2004) Biomarkers of ovarian tumours. *Eur. J. Cancer. 40*, 2604–2612.

55. Elliott, H. G., Elliott, M. A., Watson, J., Steele, L., and Smith, K. D. (1995) Chromatographic investigation of the glycosylation pattern of alpha-1-acid glycoprotein secreted by the HepG2 cell line; a putative model for inflammation? *Biomed. Chromatogr. 9*, 199–204.

56. Popovici, R. M., Lu, M., Bhatia, S., Faessen, G. H., Giaccia, A. J., and Giudice, L. C. (2001) Hypoxia regulates insulin-like growth factorbinding protein 1 in human fetal

hepatocytes in primary culture: suggestive molecular mechanisms for in utero fetal growth restriction caused by uteroplacental insufficiency. *J. Clin. Endocrinol. Metab. 86*, 2653–2659.

57. Choi, K. S., Song, L., Park, Y. M., et al. (2006) Analysis of human plasma proteome by 2DEand 2D nanoLC-based mass spectrometry. *Prep. Biochem. Biotechnol. 36*, 3–17.

CHAPTER 3

Quantitative 2-D gel electrophoresis-based expression proteomics of albumin and IgG immunodepleted plasma

3.1. INTRODUCTION

Differential profiles of plasma proteins can illustrate changes due to altered metabolism or disease development. Consequently, these proteins are highly relevant both in diagnosis and in therapeutics (1, 2). Our specific interest is in analyzing maternal plasma by 2-D gel electrophoresis (2-DGE) to uncover potential markers of fetal growth restriction (3). However, proteomic analysis of plasma is challenging due to the plasma proteome's large dynamic range and the presence of highly abundant proteins, such as albumin and IgG (2). Their presence, and that of other high abundance proteins, is a major ongoing technical impediment to detecting less abundant proteins (4-12).

Immunoaffinity depletion of albumin and IgGs, or as many as 20 abundant proteins from plasma, is a preferred method of removal due to the relative specificity of the procedure over others (10, 13). Concomitant loss of non-target proteins through protein-protein interactions has thus far proven inevitable (6, 14), even though the addition of acetonitrile (ACN) appears to mitigate this loss (15). Improved post-depletion resolution in subsequent 2-DGE or in mass spectrometry (MS)-based analysis has been demonstrated (10, 16). In expression proteomics, however, these challenges are further compounded by the need to obtain quantitative data with high reproducibility. Although, the utility of the depletion process for improving spot resolution analysis of 2-DGE has been demonstrated (4, 10, 12, 15, 17, 18), its compatibility in quantitative 2-DGE expression proteomics has been largely unaddressed.

With albumin and IgG representing as much as 85% of plasma protein, any variability in their depletion substantially affects the remaining protein loaded on the gels. Densitometric quantitation of 2-DGE is ultimately no more reliable than the consistency in sample loading. The most critical aspects are therefore to establish and minimize the non-specific loss of proteins at the depletion step, as well as attain high efficiency and reproducibility with the subsequent quantitative analyses.

Proceeding with conventional immunodepletion using a commercial kit, this study evaluates the outcome of depletion and its reproducibility using 2-DGE followed by computerized image analysis. It furthermore identifies some proteins removed nonspecifically during depletion.

3.2. MATERIALS AND METHODS

3.2.1. Samples, reagents and equipment

A single blood sample was taken with informed consent and approval as described previously (3). Electrophoretic equipment and reagents were from Bio-Rad (Hercules, CA, USA) and all procedures were according to manufacturer's instructions unless otherwise specified. Protein measurements were made by Bradford assay.

3.2.2. Albumin and IgG depletion

Depletion of albumin and IgG from whole plasma was performed using the Qproteome Albumin/IgG Depletion Kit (Qiagen, Valencia, CA, USA). Buffer 2 (250

mM Tris HCl, 4% (w/v) CHAPS and 200 mM urea, pH 7.5) was used with 5% ACN added for maximal recovery (15). Additional washes (2 x 0.25 mL and 1 x 0.5 mL) were essential for optimal recovery of the protein in the depleted fraction. The albumin and IgG bound to the resin were eluted using 3 x 0.5 mL washes with 20 mM glycine buffer (pH 1.5) in a total volume of 1.5 mL. An adjustment for pH (neutral) was made with ~0.05 mL of 1.5 M Tris HCl buffer (pH 8.8) added to the final sample.

3.2.3. Immunoassays

1-D gels were transferred to PVDF membrane for Western blotting as described previously (3). Blocking was with 0.5% gelatin for albumin or 2% Polyvinyl Pyrrolidone (PVP) for IgG. Immunoblots were developed using primary goat (anti-human albumin) and rabbit (anti-human IgG) polyclonal antibodies (Bethyl Laboratories, Montgomery, TX, USA) (1:15000), and HRP conjugated goat anti-rabbit or mouse anti-goat IgG secondary antibodies (1:8000). Western lighting Enhanced Chemiluminescence (ECL) Reagent plus (Perkin Elmer) and Kodak XOMAT LS films were used.

Albumin and IgG quantification was performed employing respective ELISA kits for human albumin and IgG according to manufacturer's instructions (Bethyl Labs). Samples in ninety-six well microplates were quantified using a MultiSkan Ascent (Thermo Electron Corp. Waltham, MA, USA).

3.2.4. 2-DGE

Nanosep Omega 3K MWCO Centricons (PALL) were used to desalt and concentrate protein prior to 2-DGE. Samples (300 μg protein) were reconstituted in rehydration buffer (0.45 mL), and rehydrated actively onto 24 cm ReadyStrip™ immobilized pH gradient (IPG) strips (pH 3-10NL). Triplicate gels of a sample depleted three separate times were analyzed for reproducibility. The gels were stained with SYPRO Ruby protein stain.

2-DGE images were captured using a Fluorochem 8800 imaging system (Alpha Innotech Corp. San Leandro, CA, USA), with consistent exposure time in the linear range. Images were analyzed using Progenesis SameSpots software (Nonlinear Dynamics, Durham, NC, USA). All gels were warped to a single whole plasma gel template. The data analysis for densitometric aspects of the study was typical for expression proteomics. Matching was automatic but verified manually: artifacts, or spots that could not be confidently verified as true matches, were disregarded rather than manually edited and misalignments were corrected by manual warping when appropriate.

3.2.5. LC-ESI-MS/MS analysis

Excised spots were digested in-gel, using a Waters MassPREP aumtomated digestor (Waters, Milford, MA, USA). Samples were analysed by LC-ESI-MS/MS using a 2000 QTrap coupled to a LC Packings Ultimate HPLC system equipped with a 100 m x 15
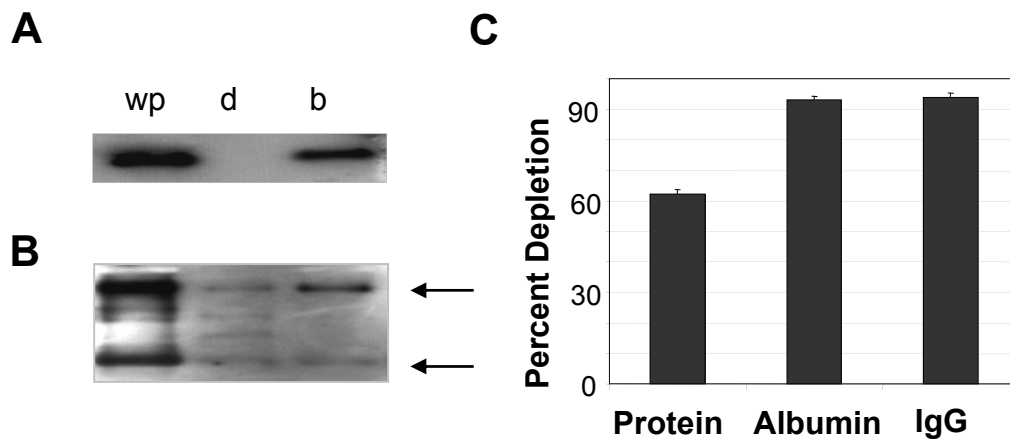
FIGURE 3.1. Western blots for albumin **(A)** and IgG **(B)** are shown with whole plasma (wp), depleted fraction (d), and bound fraction (b). To determine relative quantities of albumin and IgG contents in fractionated samples, proportionate volumes were loaded so that each lane has 0.01% of its fraction's total volume on immunoblot with albumin **(A)** and 0.03% for IgG **(B)**, respectively. Arrows show heavy and light chains of IgG. **(C)** Residual quantities of total protein (Bradford), albumin and IgG (ELISAs) of a sample after depletion of plasma in presence of acetonitrile (n=6) are shown as percent depletion. Error bars are SD.

cm CapRod RP-HPLC column (Merck, Whitehouse Station, NJ, USA) operated at a flow rate of 1 µl/min as previously described (19). A linear gradient from 5-50% B over 30 minutes (A: 5% ACN, 0.5% formic acid, B: 90% ACN, 0.5% formic acid). The LC was interfaced to the mass spectrometer via a nanoflow source equipped with a 15 µm internal diameter spray tip (New Objective, Woburn, MA, USA). The resulting tandem MS data was searched against NCBI protein sequence database. All identified peptides during Mascot (Matrix Science, London, UK) or Peaks (Bioinformatics Solutions Inc., Waterloo, ON, Canada) searching were verified by manual interpretation of the data.

3.3.   RESULTS

3.3.1. Level of immunoaffinity depletion

To visualize depletion prior to 2-DGE, 1-D immunoblot analysis of bound, depleted and whole plasma fractions was performed for albumin and IgG, respectively (Figure 3.1 A and B). As expected, albumin was highly abundant in both whole plasma (Figure 3.1A, lane wp), and the bound fraction (Figure 3.1A, lane b). Albumin was not detected in the depleted plasma (Figure 3.1A, lane d). Intense bands corresponding to IgG light and heavy chain proteins were prominent in both whole plasma (Figure 3.1B, lane, WP) and the bound fraction (Figure 3.1B, lane b). The corresponding light and heavy chain bands were, however, greatly reduced in the depleted plasma (Figure 3.1B, lane d), suggesting significant removal of IgG overall. Figure 3.1C is an
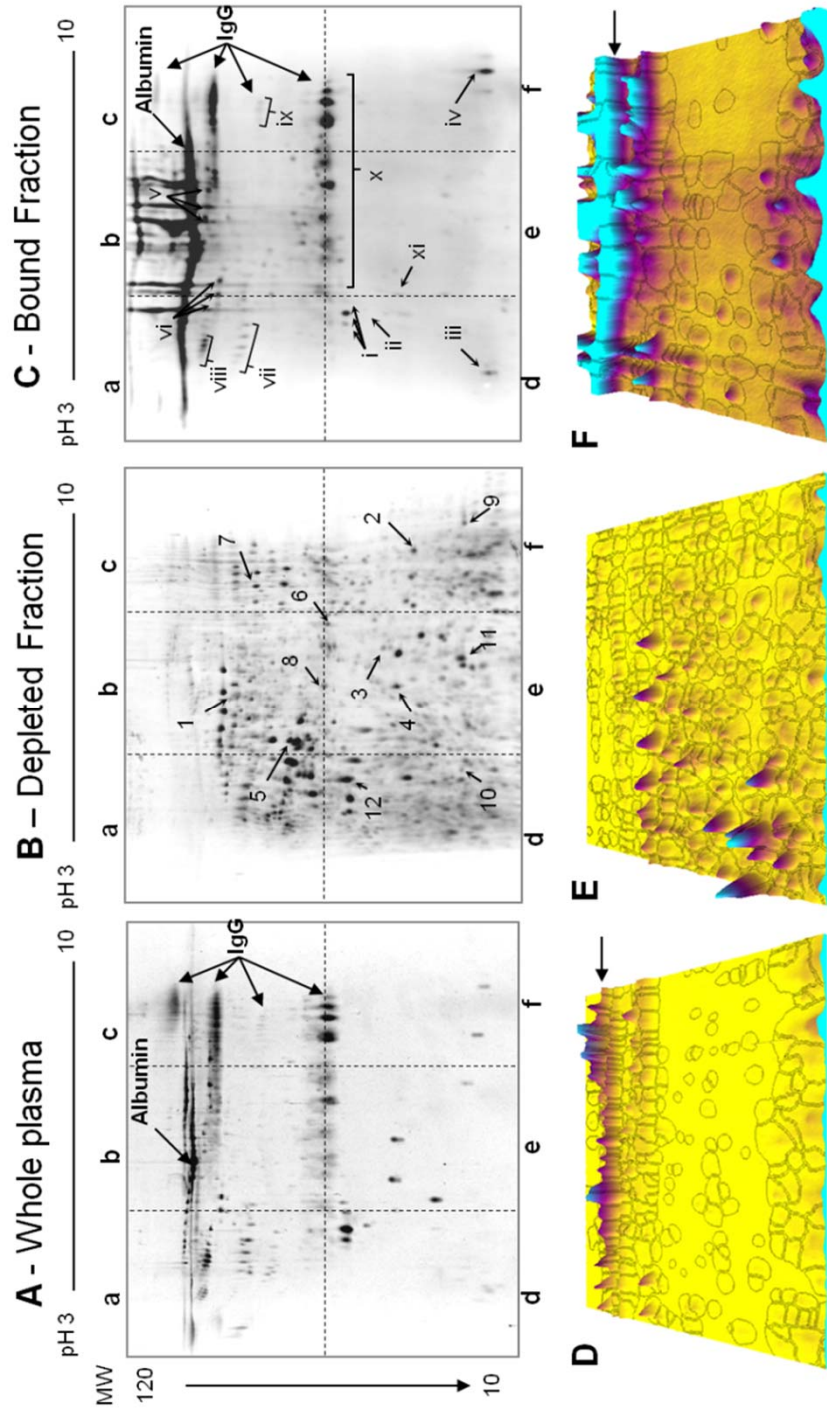
FIGURE 3.2. 2-D gels (24 cm) equally loaded with protein (300 µg) and warped to overlay alignment. Whole plasma **(A)**, depleted **(B)**, and bound **(C)** fraction images were divided in six **(a-f)** and their spots counted (Table 3.1). Spots identified by LC-ESI-MS/MS are labeled in the depleted fraction **(B)** (Table 3.2). Proteins identified based on migration comparison to the Swiss-2-D PAGE plasma protein map are labeled in the bound fraction **(C)**. **i** Apolipoprotein A-I (P02647), **ii** Plasma retinol-binding protein (P02753), **iii** Apolipoprotein C-II (P02655), **iv** Hemoglobin subunit β (P68871), **v** Fibrinogen β chain (P02675), **vi** Fibrinogen γ chain (P02679), **vii** Haptoglobin (P00738), **viii** Alpha-1-antitrypsin (P01009), **ix** Immunoglobulin heavy chain γ (P99008), **x** Immunoglobulin light chain (P99007) and **xi** Haptoglobin (P00738). **(D)**, **(E)** and **(F)** show area **b** from each **A**, **B** and **C** respectively, rendered in 3-D for spot density. Arrows in **D** and **F** point to spot density. Arrows in **D** and **F** point to smeared albumin.

68

TABLE 3.1. Comparison of the number of spots detected on 2-D gels in regions **a - f** from whole plasma, depleted, and bound fractions (Figure 3.2. A - C).

	a	b	c	d	e	f	Total
Whole	175 (57/0)	227 (75/0)	93 (65/44)	53	76	51	675
Depleted	212	254	233	197	225	204	1325
Increase from whole to depleted	37	27	140	144	149	153	650
Bound	42 (57/0)	55 (185/0)	30 (78/59)	30	50	36	243

Maximizing resolution of spots in whole plasma typically involves tolerating the overloading of abundant proteins, albumin and IgG. Spots identified by the software that resulted from smears due to albumin or IgG (Figure 3.2 arrows) were inconsistent from gel to gel and therefore not compatible with expression analysis. Accordingly, spots from smears are listed in brackets (albumin/IgG) but otherwise excluded from analysis.

assessment of the level of albumin and IgG depletion by ELISA (n=6); 38±1.2% of total protein was recovered, however 93±1.4% of albumin and 94±1.5% of IgG was removed (Figure 3.1C).

3.3.2. Improvement in 2-DGE spot resolution

2-D gels of the whole, the depleted, and the bound fractions of plasma are shown in Figure 3.2 A, B, and C, respectively. Spots from smears of albumin and IgG were discounted (Table 3.1, parenthesis) as they do not represent true resolution of proteins. There was a considerable increase in the number of spots resolved in all six areas on the depleted gel (Figure 3.2B), and overall the number of spots nearly doubled (n=675 to n=1325) (Table 3.1), thereby increasing the potential to identify new proteins. The alkaline region (area c), had considerably higher gains than other high Mr regions (a and b). The enhancement was accounted for partly by the significant amounts of albumin and the majority of IgG that would otherwise be present, and occlude other spots in this field. The greatest improvement in spot resolution was in the lower Mr regions (d–e). This is largely attributed to the relative enrichment of proteins after the removal of the high abundance proteins.

3.3.3. Relative protein enrichment

The relative enrichment is most apparent in three-dimensional images. Area b of Figure 3.2 A, B, and C is shown in Figure 3.2 D, E, and F respectively, with the third

TABLE 3.2. Identification of spots excised from an albumin and IgG depleted gel (Figure 3.2B) by LC-ESI-MS/MS.

2-D Spot #	Migration		Database	ID	M score	Protein	Vol. (fold change)
	pI	MW (KDa)					
Matched Spots							
1	5.7	50	NCBInr	gi|45708661	134	α2 Macroglobulin	5.6
2	8.5	17	NCBInr	gi|119626068	63	Albumin, isioform CRA_e	22.8
3	6.3	19	NCBInr	gi|119599289	54	Ceruloplasmin (ferroxidase), isoform CRA c	12.9
4	5.9	18	NCBInr	gi|119625312	108	Fibrinogen γ, isoform CRA_c	1.8
5	5.6	35	NCBInr	gi|119625326	127	Fibrinogen γ, isoform CRA_o	7.3
6	6.4	26	NCBInr	gi|577055	56	Fibrinogen γ, chain fragment	-1.8
7	7.0	42	NCBInr	gi|10121059	44	IgG1 Fc fragement γ receptor III complex	4.3
8	5.8	27	NCBInr	gi|118137965	99	Chain B, complement C3b	4.0
			NCBInr	gi|119625335	118	Fibrinogen β chain, isoform CRA_a	
			NCBInr	gi|119625336	118	Fibrinogen β chain, isoform CRA_b	
Unmatched Spots							
9	9.3	12	NCBInr	gi|119625338	51	Fibrinogen β chain, isoform CRA_d	-
10	5.4	12	NCBInr	gi|119579598	50	Haptoglobin, isoform CRA_a	-
11	6.2	13	NCBInr	gi|33337724	90	FWP007	-
12	5.2	23	NCBInr	gi|119625320	169	Fibrinogen γ, CRA_j	-

Matched spots are those that could be matched to the whole plasma 2-D gel (Figure 3.2A). The spots were quantified by optical densitometry using SameSpots software. Volumes of spots on gel from depleted fraction are expressed here as fold change from corresponding matches on the whole plasma gel (Figure 3.2A) from triplicate gels. See Figure 3.2B for the labeled spots corresponding to the spot numbers.

dimension as density, which is proportional to the amount of protein for the spot. The area in the depleted fraction (Figure 3.2E) clearly shows an increase in the low level proteins compared to the same area in whole plasma (Figure 3.2D). As calculated from the total protein and ELISA data (Figure 3.1C), an increase of 7.3-fold in relative abundance of residual proteins was expected due to enrichment. When matched spots, corresponding to proteins present on both gels, were compared for density, it was established that the spot density on average increased 8±3-fold (Table 3.2, matched), which was consistent with the theoretical expectation. However, the moderately high variance suggests that some proteins were preferentially retained. These proteins were subsequently identified by LC-ESI-MS/MS along with others (Figure 3.2B, numbered) (Table 3.2).

3.3.4. Non-targeted protein loss

Large smears of albumin and IgG were clearly present in the bound fraction (Figure 3.2 C and F, arrows) compared to whole plasma (Figure 3.2 A and D, arrows), and especially the depleted fraction (Figure 3.2 B and E). However, other protein spots were visible in the depleted fraction contrary to expectation (Figure 3.2C). By comparing the gel to the Swiss-2-D PAGE human plasma protein map by matching through our whole plasma gel (Figure 3.2A), we were able to set probable identities for many of the visible protein spots in the depleted fraction (Figure 3.2C, numerals).
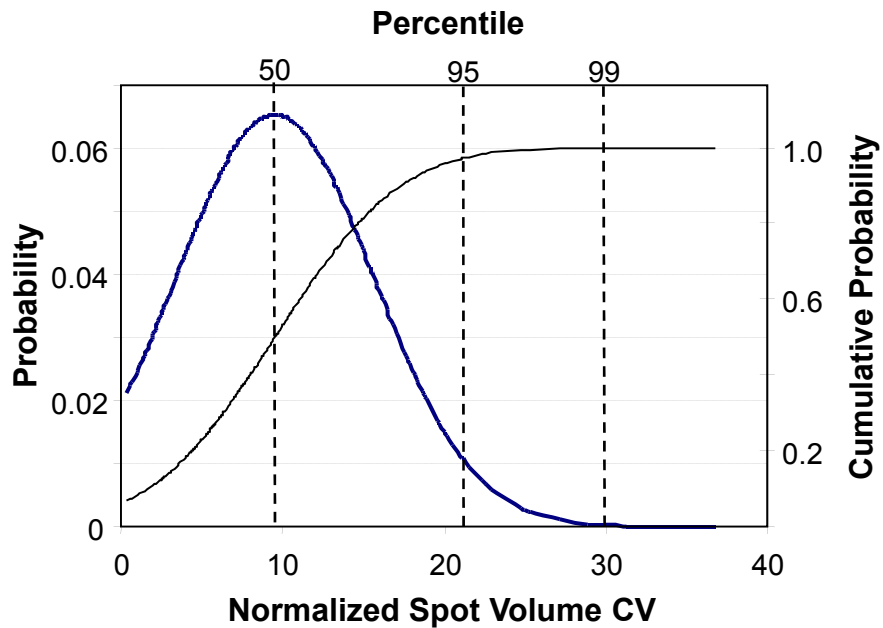
FIGURE 3.3. Probability distribution for the coefficient of variation of the normalized volume of matched spots from three replicate (depleted fraction) gels (Figure 3.2B). The mean coefficient of variation is 10% (SD 6.1) for spots verified as matched. The 95th and 99th percentiles are marked. Of manually verified matching spots, 95% of spots had a coefficient of variation <21% and 99% had a coefficient of variability <30%.

The major spots identified were typically high abundance proteins (Figure 3.2C), none

of which are known to directly bind albumin for transport. Of the proteins identified,

i, iv, v, vi, vii, viii, x, and xi, are among the ten most abundant proteins in plasma (20).

Only three proteins were not, although one of the three, hemoglobin (iv), may

circulate bound to haptoglobin (vii). Some proteins (i, xi, xii) were identified in both

the bound and the depleted fractions, indicating that their elution from the bound

fraction was incomplete. Hemoglobin (iv) appeared relatively enriched in the bound

compared to both depleted and whole fractions, indicating its preferential retention.

The data therefore suggests that although some proteins lost may couple with

albumin and in this manner may be distinctively retained through protein-protein

interactions (14), there was largely non-specific loss of proteins.

3.3.5. 2-DGE quantitative reproducibility

To analyze the quantitative spot reproducibility, three replicates of the depleted

fraction (Figure 3.2B) were produced and analyzed by 2-DGE. The distribution of the

variation between matching spots is plotted in Figure 3.3. The mean variability was

10+6%, while 95% of matching spots had a variability of less than 21% and the

probability of the variability exceeding 35% was <0.0001.

3.4.   DISCUSSION

Immunoaffinity depletion prior to 2-DGE has been shown to be a powerful fractionation technique in the identification of new proteins (21). In this study, we were able to demonstrate a much improved number of useful identifiable spots (n= 1325) resolved on a single 24 cm 2-D gel. As reported by others (4, 10, 12, 15, 17, 18), the achievement of high resolution on 2-DGE was attributable to a substantial improvement in dynamic range post-depletion, but additionally to the combined use of 24 cm 2-D gels over the more commonly used 18 cm gels.

This study demonstrates the quantitative feasibility of depletion in combination with high resolution 2-DGE. Evaluation of depletion for the MARS LC column (Agilent, Santa Clara, CA, USA) was reported to eliminate >99% for albumin and IgG, measured using the same ELISA kits (6). In our study, we found considerably less complete depletion, although neither protein was prominent on 2-D gels. A possible explanation may be the use of less sensitive antibody in the Qproteome kit, or the lower sensitivity or binding capacity of the spin column-based depletion compared to the LC technique, which is inherently more efficient. Reproducibility as measured by 2-DGE spot variance (Figure 3.3) was nevertheless better than reported for 2-DGE without fractionation, albeit with modest differences in methodology (22).

Multiple protein affinity columns may achieve even greater improvements in resolution, for as many as 20 of the most concentrated proteins are depleted, which accounts for >99% of plasma protein. The corollary of higher levels of depletion however, is that much greater sample volumes are required to yield several hundred micrograms of depleted protein required for large-format 2-DGE applications. A

substantial amount of pooling of depleted fractions or a very high capacity LC affinity column would be required.

The flexibility in spot alignment enabled comparison of the depleted and bound fractions of whole plasma, and tentative spot assignment using 2-D maps rather than spot excision and MS analysis. This facilitated the identification of proteins lost during depletion and the estimation of the relative protein enrichment post-depletion at the 2-D gel level.

Using this method, we were able to confidently interpret the protein loss inherent to depletion. Many proteins were lost that may not have been due to specific interactions with albumin or the depletion antibodies. Variations in the number of washes during the depletion process or the composition of the buffers have a strong influence on the proportion of non-targeted proteins retained on the resin (15). However, for maximal recovery, conditions were currently implemented as per Huang et al. (15), as well as our own optimizations. Despite removal of proteins that were identifiable, and undoubtedly others that were not, the depleted sample exhibited dramatic improvement in the number of spots resolved (Table 3.1) and reproducibility in spot density (Figure 3.3).

Albumin and IgG removal improves 2-DGE spot resolution. However, the application of immunodepletion of plasma samples to quantitative densitometric 2-DGE analysis further demonstrates its reproducibility. Proteins in the resulting 2-D gels were identifiable by LC-ESI-MS/MS despite the low density of some specific spots (Figure 3.2B spots 1, 3 and 10). Together, these aspects of the study illustrate that

quantitative 2-DGE of depleted plasma is an effective expedient to identifying plasma

proteome expression changes in clinical investigations.

3.5. REFERENCES

1. Shankar, R., Gude, N., Cullinane, F., Brennecke, S., Purcell, A. W., and Moses, E. K. (2005) An Emerging Role for Comprehensive Proteome Analysis in Human Pregnancy Research. *Reproduction. 129*, 685-696.

2. Anderson, N. L., and Anderson, N. G. (2002) The Human Plasma Proteome: History, Character, and Diagnostic Prospects. *Mol. Cell. Proteomics. 1*, 845-867.

3. Gupta, M. B., Seferovic, M. D., Liu, S., Gratton, R. J., Doherty-Kirby, A., Lajoie, G. A., and Han, V. K. M. (2006) Altered Proteome Profiles in Maternal Plasma in Pregnancies with Fetal Growth Restriction. *Clinical Proteomics. 2*, 169-184.

4. Darde, V. M., Barderas, M. G., and Vivanco, F. (2007) Depletion of High-Abundance Proteins in Plasma by Immunoaffinity Subtraction for Two-Dimensional Difference Gel Electrophoresis Analysis. *Methods Mol. Biol. 357*, 351-364.

5. Altintas, E. B., and Denizli, A. (2006) Efficient Removal of Albumin from Human Serum by Monosize Dye-Affinity Beads. *J. Chromatogr. B. Analyt Technol. Biomed. Life. Sci. 832*, 216-223.

6. Brand, J., Haslberger, T., Zolg, W., Pestlin, G., and Palme, S. (2006) Depletion Efficiency and Recovery of Trace Markers from a Multiparameter Immunodepletion Column. *Proteomics. 6*, 3236-3242.

7. Gong, Y., Li, X., Yang, B., Ying, W., Li, D., Zhang, Y., Dai, S., Cai, Y., Wang, J., He, F., and Qian, X. (2006) Different Immunoaffinity Fractionation Strategies to Characterize the Human Plasma Proteome. *J. Proteome Res. 5*, 1379-1387.

8. Liu, T., Qian, W. J., Mottaz, H. M., Gritsenko, M. A., Norbeck, A. D., Moore, R. J., Purvine, S. O., Camp, D. G.,2nd, and Smith, R. D. (2006) Evaluation of Multiprotein Immunoaffinity Subtraction for Plasma Proteomics and Candidate Biomarker Discovery using Mass Spectrometry. *Mol. Cell. Proteomics. 5*, 2167-2174.

9. Barnea, E., Sorkin, R., Ziv, T., Beer, I., and Admon, A. (2005) Evaluation of Prefractionation Methods as a Preparatory Step for Multidimensional Based Chromatography of Serum Proteins. *Proteomics. 5*, 3367-3375.

10. Bjorhall, K., Miliotis, T., and Davidsson, P. (2005) Comparison of Different Depletion Strategies for Improved Resolution in Proteomic Analysis of Human Serum Samples. *Proteomics. 5*, 307-317.

11. Cho, S. Y., Lee, E. Y., Lee, J. S., Kim, H. Y., Park, J. M., Kwon, M. S., Park, Y. K., Lee, H. J., Kang, M. J., Kim, J. Y., Yoo, J. S., Park, S. J., Cho, J. W., Kim, H. S., and Paik, Y. K. (2005) Efficient Prefractionation of Low-Abundance Proteins in Human Plasma and Construction of a Two-Dimensional Map. *Proteomics. 5*, 3386-3396.

12. Echan, L. A., Tang, H. Y., Ali-Khan, N., Lee, K., and Speicher, D. W. (2005) Depletion of Multiple High-Abundance Proteins Improves Protein Profiling Capacities of Human Serum and Plasma. *Proteomics. 5*, 3292-3303.

13. Steel, L. F., Trotter, M. G., Nakajima, P. B., Mattu, T. S., Gonye, G., and Block, T. (2003) Efficient and Specific Removal of Albumin from Human Serum Samples. *Mol. Cell. Proteomics. 2*, 262-270.

14. Granger, J., Siddiqui, J., Copeland, S., and Remick, D. (2005) Albumin Depletion of Human Plasma also Removes Low Abundance Proteins Including the Cytokines. *Proteomics. 5*, 4713-4718.

15. Huang, H. L., Stasyk, T., Morandell, S., Mogg, M., Schreiber, M., Feuerstein, I., Huck, C. W., Stecher, G., Bonn, G. K., and Huber, L. A. (2005) Enrichment of Low-Abundant Serum Proteins by albumin/immunoglobulin G Immunoaffinity Depletion Under Partly Denaturing Conditions. *Electrophoresis. 26*, 2843-2849.

16. Choi, K. S., Song, L., Park, Y. M., Marshall, J., Lund, A. L., Shion, H., Park, E. M., Chae, H. Z., and Park, J. H. (2006) Analysis of Human Plasma Proteome by 2DE- and 2D nanoLC-Based Mass Spectrometry. *Prep. Biochem. Biotechnol. 36*, 3-17.

17. Kim, H. J., Kim, M. R., So, E. J., and Kim, C. W. (2007) Comparison of Proteomes in various Human Plasma Preparations by Two-Dimensional Gel Electrophoresis. *J. Biochem. Biophys. Methods. 70*, 619-625.

18. Hinerfeld, D., Innamorati, D., Pirro, J., and Tam, S. W. (2004) Serum/Plasma Depletion with Chicken Immunoglobulin Y Antibodies for Proteomic Analysis from Multiple Mammalian Species. *J. Biomol. Tech. 15*, 184-190.

19. Ebanks, R. O., Chisholm, K., McKinnon, S., Whiteway, M., and Pinto, D. M. (2006) Proteomic Analysis of Candida Albicans Yeast and Hyphal Cell Wall and Associated Proteins. *Proteomics. 6*, 2147-2156.

20. Baussant, T., Bougueleret, L., Johnson, A., Rogers, J., Menin, L., Hall, M., Aberg, P. M., and Rose, K. (2005) Effective Depletion of Albumin using a New Peptide-Based Affinity Medium. *Proteomics. 5*, 973-977.

21. Pieper, R., Gatlin, C. L., Makusky, A. J., Russo, P. S., Schatz, C. R., Miller, S. S., Su, Q., McGrath, A. M., Estock, M. A., Parmar, P. P., Zhao, M., Huang, S. T., Zhou, J., Wang, F., Esquer-Blasco, R., Anderson, N. L., Taylor, J., and Steiner, S. (2003) The Human Serum Proteome: Display of nearly 3700 Chromatographically Separated Protein Spots on Two-Dimensional Electrophoresis Gels and Identification of 325 Distinct Proteins. *Proteomics. 3*, 1345-1364.

22. Hunt, S. M., Thomas, M. R., Sebastian, L. T., Pedersen, S. K., Harcourt, R. L., Sloane, A. J., and Wilkins, M. R. (2005) Optimal Replication and the Importance of Experimental Design for Gel-Based Quantitative Proteomics. *J. Proteome Res. 4*, 809-819.

CHAPTER 4

Altered Liver Secretion of Vascular Regulatory Proteins in Hypoxic Pregnancies Stimulate Angiogenesis *in vitro*

4.1. INTRODUCTION

Fetal hypoxia arises in Fetal Growth Restriction (FGR), a common pregnancy complication wherein the placenta fails to provide sufficient exchange of oxygen and nutrients to meet the metabolic needs of the developing fetus. A reduction in the villous tree of the placental vasculature leads to vascular resistance of the placenta, and consequently reduced blood flow (1, 2, 3). Ultimately, the reduced maternal/fetal exchange causes fetal nutrient starvation, acidosis, and critically, hypoxia. FGR babies have an abnormally low birthweight for their gestational age (<10th percentile), and often suffer perinatal morbidities. FGR is a leading cause of perinatal death (4).

Many common glycosylated plasma proteins, which originate primarily from liver secretions, have been shown to promote or inhibit angiogenesis, specifically through endothelial or smooth muscle migration regulation, or as proteins involved in vascular cell wall regulation. These include clusterin (5), fibrinogen (6), haptoglobin (7), high-density lipoprotein (8), high molecular weight kinogen (9), plasminogen activator inhibitor-1 (PAI-1) (10), pregnancy associated plasma protein A (PAPP-A) (11), transferrin (12), and vitronectin (13), among others. Haptoglobin, for example, has been identified as an angiogenic factor, and its elevated levels in plasma have been implicated in vascular disease (14). The expression of many of these liver proteins during hypoxic pregnancies and their potential role in FGR is unknown. The ability of the haemostatic system to regulate angiogenesis has been demonstrated extensively in vessel repair and in tumor development, where a balance of factors
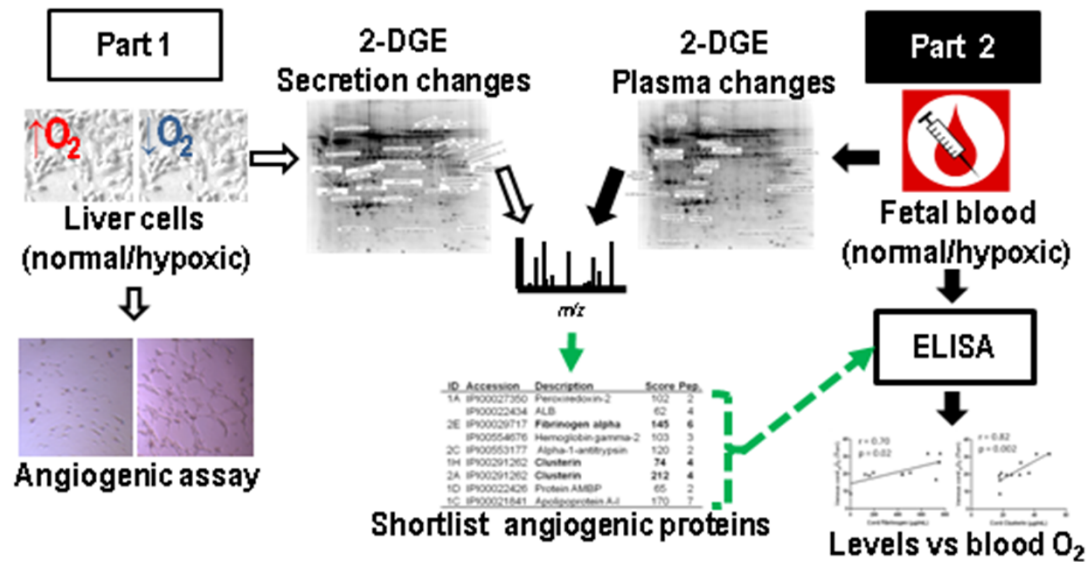
FIGURE 4.1. Overview of experimental design. Liver cells are treated with 1% and 20% O_2. Secretions are assessed for their ability to promote or inhibit angiogenesis in an *in vitro* tube formation assay. Differences in cell secretion are identified by 2-DGE followed by ESI-MS/MS. Changing proteins with angiogenic function are shortlisted together with changing angiogenic proteins identified by directly profiling fetal plasma from control and hypoxic pregnancies with 2-DGE. ELISAs then more precisely assess the levels of the shortlisted proteins in fetal plasma. The levels of the angiogenic proteins are then correlated to the fetal blood oxygen level measured at birth.

has been shown to be critical for vascular development. The levels of these proteins

is also highly dependent on liver function, as patients with compromised livers often

have poor haemostatic control due to the altered protein secretion.

In the fetal circulation, the liver is the first organ to receive newly oxygenated blood

from the placenta through the umbilical vein. In hypoxic pregnancies, increased

shunting of blood towards critical organs like the brain and heart spares them from

starvation, at the expense of the liver (15, 16). The liver is the central metabolic

organ and the primary secretor of plasma proteins, many with angiogenic function.

Therefore, the liver is uniquely positioned to regulate plasma proteins in order to

adapt to the metabolic environment under hypoxic conditions. Analogous

mechanisms have been shown to regulate fetal growth. IGF-I induced growth in the

fetus has been shown to be reduced by the altered liver secretion of insulin-like

growth factor binding protein-1 (IGFBP-1) in an oxygen-dependant fashion (17, 18,

19, 20).

Hypoxia induces changes in the liver secretome and, consequently, in the plasma

proteome, that will likely cause angiogenic changes in the fetal and placental

vasculature. Accordingly, we set out to discover whether hepatic secretions in

hypoxic conditions could affect angiogenic potency and to identify those oxygen-

regulated, angiogenic proteins in plasma of FGR newborns. We then correlated the

levels of these proteins in the fetal blood plasma to the oxygen level of the fetal

blood supply (venous umbilical cord). Associating the protein changes with the

characteristic physiological measures of FGR will indicate the identified protein's

physiological significance in the disease. An experimental outline is described in Figure 4.1.

4.2. METHODS

4.2.1. HepG2 cell culture and secretome

HepG2 cells procured from ATCC were grown in DMEM/F-12 culture media (Invitrogen, San Diego, Ca, USA) with 10% FBS (Invitrogen) to ~70% confluence, washed twice in FBS-free media, and subsequently cultured in FBS-free media. The cells were allowed to acclimatize for three hours in before the media was changed once more with FBS-free media, containing 50 mM HEPES buffer, and oxygen treatments commenced. Cells were placed in sealed chambers and flushed with 1% or 4% O_2 (5% CO_2, and the balance N_2) or placed in the incubator (20% O_2). The cells were placed on an orbital shaker at low speed to facilitate continued gas exchange between the cell environment and the surrounding air.   The procedure was conducted as described previously (20). Conditioned media (CM) was collected after 24 hours, and dissolved oxygen was measured using an ABL 700 blood gas analyzer. The samples were then desalted, concentrated, and buffer exchanged into 2-DGE rehydration buffer (Bio-Rad, Hercules, CA, USA), using 3 KDa molecular weight cut off filter (Pall, Port Washington, NY, USA). Urea (200 mM) was used for wash steps (5x), and a final wash with rehydration buffer. The sample was then reconstituted in 450 μL rehydration buffer to perform 2-DGE.

Flow cytometry for the detection of apoptosis and necrosis via annexin-V labeling was performed on live cells using Annexin-V-FLUOS Staining Kit (Roche, Penzberg, Germany) according to manufacturer's instructions. Cells were detached and separated using TripleXExpress (Invitrogen). The re-suspended cells were then incubated for 15 min with labeling reagents, annexin-V-fluos and propidium iodide. Flow cytometry was then performed using an Epics XL-MCL (Beckman Coulter, Brea, CA, USA) according to manufacturer's recommendation.

4.2.2. Human vascular endothelial cell (HUVEC) culture and angiogenic assays

Media from HepG2 cells cultured under various oxygen conditions was concentrated and buffer exchanged into Endothelial Growth Media (Lonza, Basel, Switzerland) (FBS-free) using a 30 KDa molecular weight cut-off filter (Pall, Port Washington, NY, USA). The concentrated samples were then diluted with culture media to 200 µg/mL of secreted protein (approximately equivalent to 1% of normal plasma). HUVECs (Lonza) were plated on ECMatrix at a density of 3 x 10^4 cells per well (96 well plate) together with 100 µL of the media containing the secreted proteins, and allowed to grow for several hours according to the *In Vitro* Angiogenesis Assay Kit (Millipore, MA, USA). Images were taken when the FBS-free negative control started exhibiting tube formation. The tube length and cell area were quantified using Axiovision software (v4.7.1, Carl Zeiss, Germany) from three fields per well, and branches were counted manually as per the Angiogenesis Assay Kit.

4.2.3. 2-D gel electrophoresis

Generally, 2-DGE was conducted using Bio-Rad reagents and equipment unless otherwise stated. Samples of HepG2 secretory proteins (400 μg) or depleted plasma (350 μg) were separated on 24 cm ReadyStrip™ immobilized pH gradient (IPG) strips (pH 3-10, non-linear). 2-D gels were stained with SYPRO Ruby (Invitrogen). Imaging was performed under UV excitation using a Fluorchem imager (Alpha Innotech Corp San Leandro, Ca, USA). The images of the stained gels were captured using UV trans-illuminator of Fluorchem 8800 imaging software (Alpha Innotech Corp San Leandro, Ca, USA). The detailed procedure, including the software analysis and an assessment of the quantitative reproducibility, has been described previously (21). All images were analyzed with Progenesis SameSpots (non-Linear, New Castle upon Tyne, UK). Paired t-test, with pairing based on gestational age matched paring of each FGR sample to its corresponding control, was used to assess changes between control and FGR groups for cord plasma. One-way ANOVA was used to compare spot means from 1, 4, and 20% O_2 triplicate gels. Spot density changes with $p<0.05$ were considered significant.

4.2.4. In-gel digestion and mass spectrometry

Excised spots were digested in-gel, using a Waters MassPREP automated digester (Waters, Milford, MA, USA). Samples were analyzed by LC-ESI-MS/MS using a 4000

QTrap coupled to an Agilent 1100 cap LC system equipped with a 100 μm x 15 cm monolithic HPLC column (Phenomenex, Torrance, CA, USA) operated at a flow rate of 1 μL/min as previously described (22). A linear gradient from 5-50% B over 30 minutes (A: 5% ACN, 0.5% formic acid, B: 90% ACN, 0.5% formic acid) was used. The LC was interfaced to the mass spectrometer via a nanoflow source equipped with a 15 μm internal diameter spray tip (New Objective, Woburn, MA, USA). The resulting tandem MS data was searched against NCBI protein sequence database (03032009) and IPI Human (3.59) databases. All identified peptides during Mascot (Matrix Science, London, UK) or Peaks (Bioinformatics Solutions Inc., Waterloo, On, Canada) searching were verified by manual interpretation of the data.

4.2.5. Plasma collection and sample preparation

Fetal plasma was collected from the venous umbilical cord at the time of delivery from FGR (n=12) and gestational age matched control (n=12) pregnancies at St Joseph's Hospital, in London, Ontario, Canada. Pregnancies with fetal growth restriction resulting from placental insufficiency were included. Subjects with fetal, congenital or genetic abnormalities, *in utero* infection, diabetes, thyroid disorders, drug abuse, chronic hypertensive disorders, or preeclampsia were excluded.

Samples were collected in EDTA coated tubes, centrifuged at 2000 g for 15 min at 4°C and clear plasma samples saved in small aliquots at -80°C. Collection criteria and procedures for collection took place as described in detail previously (23). The

average birthweight was less than the 2nd percentile (below the 10th widely considered the diagnostic threshold for FGR). Nearly all FGR subjects (10/12) and the majority of control subjects (8/12) were delivered by caesarean section. All deliveries were performed under epidural or spinal anesthetic, or were natural deliveries. Healthy pregnancies were selected for controls based on matching gestational age to the FGR pregnancies, all with birthweights above the 25th percentiles.

Plasma for 2-DGE was depleted of albumin and IgG with disposable spin columns (QProteome, Qiagen, Venlo, The Netherlands) using our previously established protocol (21). After depletion, 350 µg of protein from the flow-through fraction was desalted, concentrated and buffer exchanged with 2-DGE rehydration buffer as described for CM.

4.2.6. Protein measurements and statistical evaluations

All total protein quantifications were by Bradford method (Bio-Rad). ELISA kits were commercially obtained to determine the concentration of specific proteins; clusterin (BioVendor, Evropska, Czech Republic), fibrinogen (Innovative Research, MI, USA), transferrin (AssayPro, St. Charles, MO, USA), albumin and IgG (Bethyl Labs, TX, USA). Samples were assessed in duplicates using a Multiskan EX micro-plate reader (Thermo Electron Corp. Waltham, MA, USA) following manufacturer's instructions. Plasminogen activator inhibitor-1 (PAI-1) and VEGF were measured as part of an immunological-based fluorescent multiplex assay (Human CDV1, Millipore, Billerica,
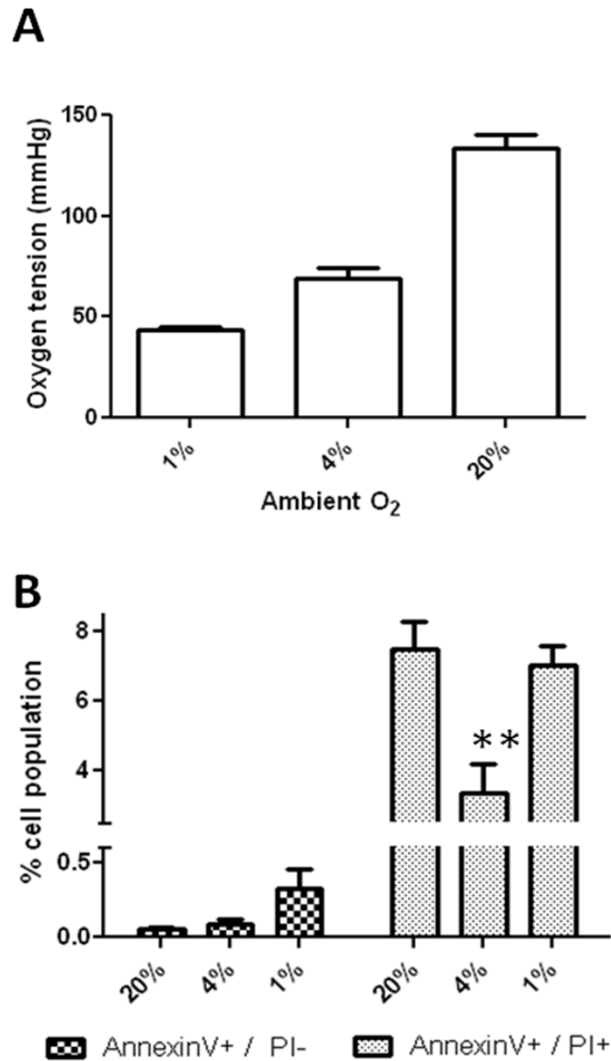
FIGURE 4.2. Culture conditions of HepG2 cells treated with hypoxia to mimic fetal growth restricted conditions. **(A)** Dissolved oxygen levels were measured after 24 h to compare oxygen treatments to physiological exposure of the fetus *in vivo* (Table 4.2). **(B)** Flow cytometry cell counts for triplicate experiments of annexin V and propidium iodide stained cells to determine the levels of apoptosis and necrosis taking place with hypoxic treatment. Significant change determined by ANOVA (**$p<0.001$). Both 1 and 20% O_2 showed elevated necrosis compared to 4% O_2 condition.

MA, USA) using a Bio-Plex 200 system (Bio-Rad), which utilizes Luminex® xMAPTM fluorescent bead-based technology (Luminex Corp., Austin, TX). Levels were automatically calculated from standard curves using Bio-Plex Manager software (v.4.1.1, Bio-Rad). All statistics (excluding 2-DGE densitometry) were done using GraphPad Prism 5 (Graph Pad Software Inc, CA, USA). To compare means, t-tests, paired t-tests, or one-way ANOVAs were used where appropriate. Pearson's Correlation compared proteins' levels to blood oxygen levels, as well as other quantitative clinical criteria in Table 4.2.

4.3. RESULTS

4.3.1. HepG2 secretions in low oxygen induce angiogenesis

To assess the influence of liver hepatocyte protein secretion changes in hypoxia on potential angiogenic regulation via the fetal plasma, we used an established cell model for hepatic protein expression (20). HepG2 cells were exposed to 20%, 4%, or 1% O_2 for 24 hours in FBS-free conditions. Measurements of dissolved oxygen in the conditioned media (CM) from these samples showed that decreasing the ambient oxygen levels to 1% lowered the tension to 40 Torr (Figure 4.2A), which approximates normal *in utero* oxygen levels (Table 4.2). Tension readings for ambient levels of oxygen at 20%, although typical in cell culture, were substantially increased above physiological levels both for fetal and adult blood (24). Flow cytometry analyzing markers of apoptosis and necrosis revealed overall a minimal amount of apoptosis
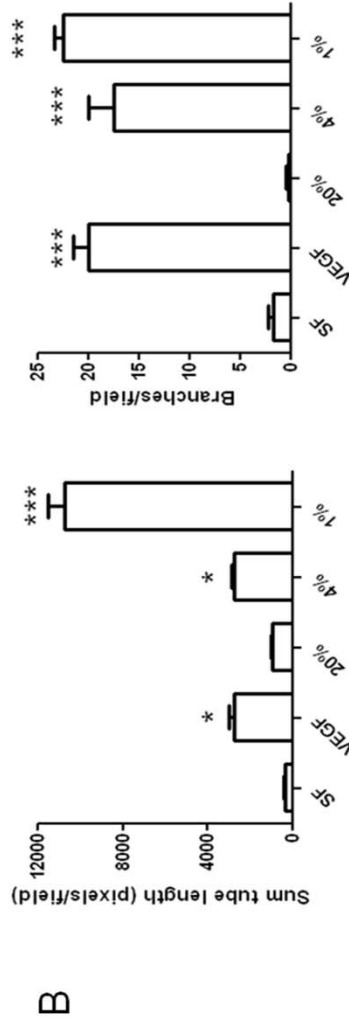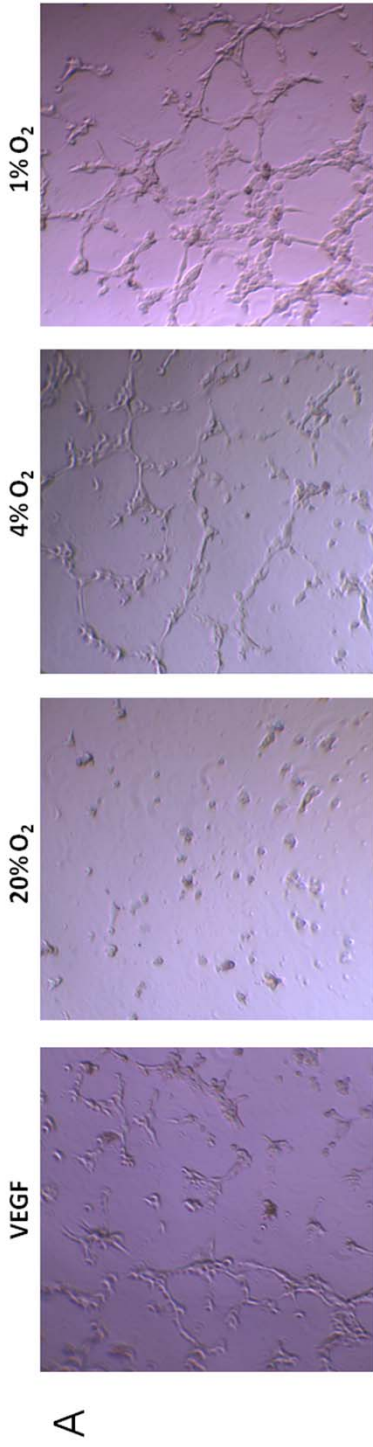
FIGURE 4.3. *In vitro* angiogenic tube formation assay of HepG2 secreted proteins. HUVEC cells after 3 h in the presence of 500 µg/mL of conditioned media proteins (~1% normal serum concentration) from hypoxic treated HepG2 cells. VEGF (10 ng/mL) and serum free conditions were used as controls (n=3). **(A)** Representative fields are shown. **(B)** Total length of all tubes formed and the total number of branches per field were used for quantitative comparison of angiogenic induction. ANOVA compared the treatments. Significant changes from the 20% HepG2 conditioned media treatment are shown (* $p < 0.05$, ***$p < 0.0001$).

(AnnexinV+/PI-) after 24 hours across treatments (Figure 4.2B). Apoptosis at 1% O_2 appeared elevated, however it was not significantly different. Necrosis (AnnexinV+/PI+) was significantly elevated in both 1% and 20% compared to 4% O_2.

HUVECs were subsequently treated with the CM from HepG2 cells exposed to hypoxia to assess the potential changes in angiogenic induction following low oxygen treatment. After three hours of CM treatment, relative tube formation and degree of tube branching (Figure 4.3) using 1% O_2 treatment were both significantly larger than either 4% or 20% oxygen treatment. The 1% O_2 treatment CM also induced more tube formation than VEGF alone. Measurements of VEGF levels were from 10 to 100-fold less in the CM of 1% and 20% O_2 treatments than the VEGF positive control (10 ng/mL).

4.3.2. Identification of changing hepatic secreted angiogenic proteins

To identify candidate proteins changing due to the hypoxia, secretome profiling of HepG2 cells in low oxygen conditions was undertaken. Using samples isolated from three separate HepG2 cell cultures, equal amounts of protein (400 µg) were separated on large 2-D gels in triplicate. Figures 4.4 A and B show a representative gel image of the HepG2 secretome. When the spot density of triplicate gels from all three treatment conditions (20% and 4%, relative to 1% O_2) was assessed using 2-DGE densitometric software, many protein spots were revealed as changing between the three groups. In all, approximately 1200 spots were separated and detected by
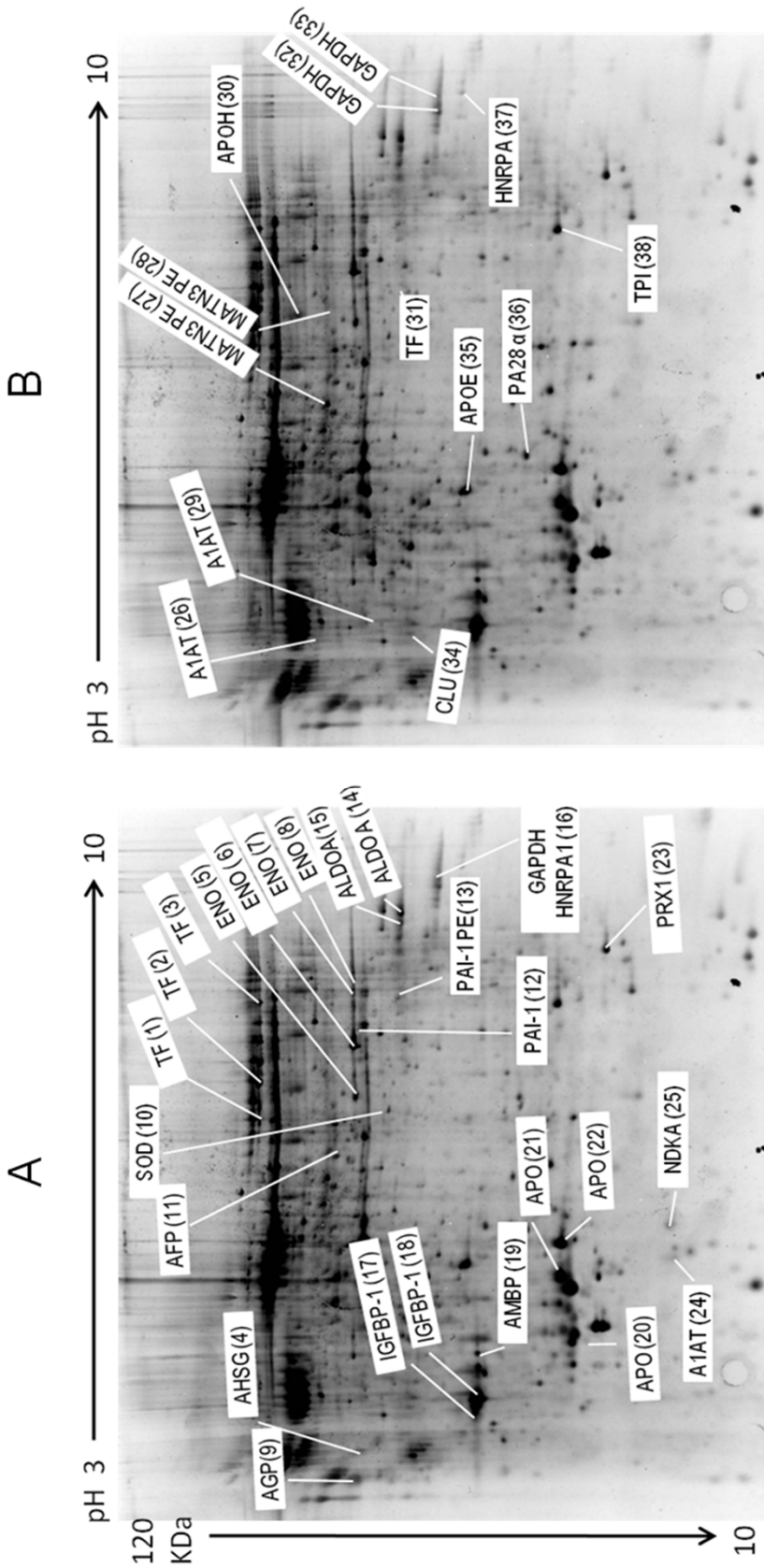
Figure. 4.4. Representative 2-D gel pH 3-10NL of conditioned media from HepG2 cells treated with varying conditions of hypoxia in serum free conditions. Triplicate gels from separate 1, 4, or 20% ambient air cell culture experiments were subjected to 2-DGE. Spots indicated are significantly changing in density by paired ANOVA ($p < 0.05$). Proteins indicated are top scoring identifications by LC-MS/MS. **(A)** Increasing spots and **(B)** decreasing spots in 1% from either 4%, or 20% O2 treatment. Complete MS and quantitative data are listed in Table 4.2.

TABLE 4.1. Identification of the protein spots by LC-MS/MS that were found to be significantly changing in hypoxia by ANOVA in Figure 4.4.[a]

Spot ID	Accession	Description	Score	Peptides	Fold Change			ANOVA (p)
					20%	4%	1%	
1	IPI00022463	**Transferrin**	**399**	**14**	**1.00**	**2.09**	**1.34**	**0.034**
	IPI00305457	Alpha-1-antitrypsin precursor 4	53	2				
2	IPI00022463	**Transferrin**	**479**	**16**	**1.00**	**2.13**	**1.45**	**0.029**
3	IPI00022463	**Transferrin**	**320**	**13**	**1.00**	**1.97**	**2.55**	**0.0003**
4	IPI00022431	Alpha-2-HS-glycoprotein like	233	6	1.00	1.74	1.41	0.026
	IPI00305457	Alpha-1-antitrypsin precursor 4	41	1				
5	IPI00465248	Alpha-enolase	204	6	1.00	0.83	1.72	0.039
6	IPI00465248	Alpha-enolase	558	13	1.00	0.80	1.38	0.004
7	IPI00465248	Alpha-enolase	448	11	1.00	0.65	1.06	0.001
8	IPI00465248	Alpha-enolase	85	3	1.00	0.50	1.45	0.001
9	IPI00020091	Alpha-1-acid glycoprotein 2	44	1	1.00	1.02	1.44	0.041
10	IPI00218733	Superoxide dismutase [Cu-Zn]	50	2	1.00	0.73	2.52	0.001
11	IPI00022434	Putative uncharacterized protein ALB	104	4	1.00	1.55	1.50	0.005
12	IPI00007118	**Plasminogen activator inhibitor 1**	**213**	**8**	**1.00**	**1.46**	**2.41**	**0.016**
	IPI00216773	Albumin	48	1				
	IPI00470629	Uncharacterized protein C2orf34	37	1				
	IPI00465248	Alpha-enolase	89	1				
13	IPI00007118	**Plasminogen activator inhibitor 1**	**102**	**6**	**1.00**	**1.55**	**3.57**	**0.043**
14	IPI00465439	Fructose-bisphosphate aldolase A	214	8	1.00	0.83	0.78	0.021
	IPI00418262	Fructose-bisphosphate aldolase	59	3				
15	IPI00465439	Fructose-bisphosphate aldolase A	350	11	1.00	0.49	1.23	0.006
	IPI00418262	Fructose-bisphosphate aldolase C like	126	3				
16	IPI00219018	Glyceraldehyde-3-phosphate dehydrogenase	88	2	1.00	1.11	1.19	0.024
	IPI00419373	Heterogeneous nuclear ribonucleoprotein A3	39	1				
17	IPI00031086	Insulin-like growth factor-binding protein 1	210	6	1.00	2.07	1.42	0.002
	IPI00022426	Alpha-1-microglobulin/bikunin precursor	77	2				

Table Continued...

TABLE 4.1. Continued.

Spot ID	Accession	Description	Score	Peptides	Fold Change 20%	4%	1%	ANOVA (p)
18	IPI00031086	Insulin-like growth factor-binding protein 1	210	5	1.00	1.86	1.51	0.022
	IPI00022426	Alpha-1-microglobulin/bikunin precursor	46	1				
19	IPI00022426	Alpha-1-microglobulin/bikunin precursor	53	1	1.00	1.71	1.30	0.044
	IPI00010896	Chloride intracellular channel protein 1	224	6				
20	IPI00021841	Apolipoprotein A-I	162	6	1.00	0.98	1.20	0.038
	IPI00022434	Putative uncharacterized protein Albumin	43	1				
21	IPI00021841	Apolipoprotein A-I	132	4	1.00	1.10	1.88	0.003
	IPI00022434	Putative uncharacterized protein Albumin	41	1				
22	IPI00021841	Apolipoprotein A-I	58	2	1.00	0.92	1.97	0.014
23	IPI00000874	Peroxiredoxin-1	138	8	1.00	0.57	0.80	0.004
24	IPI00553177	Alpha-1-antitrypsin	102	4	1.00	1.18	1.10	0.009
25	IPI00012048	Nucleoside diphosphate kinase A	97	3	1.00	1.32	1.43	0.028
26	IPI00553177	Alpha-1-antitrypsin	376	15	1.00	1.75	0.69	0.049
	IPI00022431	Alpha-2-HS-glycoprotein like	69	2				
	IPI00030702	Isocitrate dehydrogenase [NAD] α, mitochondrial	56	1				
27	IPI00005690	Matrilin-3	230	5	1.00	0.73	0.68	0.007
28	IPI00005690	Matrilin-3	90	2	1.00	0.78	0.57	0.007
29	IPI00553177	Alpha-1-antitrypsin	125	5	1.00	0.62	0.43	0.013
30	IPI00298828	Beta-2-glycoprotein 1	60	1	1.00	0.51	0.97	0.021
31	IPI00022463	**Transferrin**	**203**	**4**	**1.00**	**0.91**	**0.97**	**0.021**
32	IPI00219018	Glyceraldehyde-3-phosphate dehydrogenase	72	1	1.00	0.39	0.82	0.002
33	IPI00219018	Glyceraldehyde-3-phosphate dehydrogenase	169	5	1.00	0.33	0.95	0.000
34	IPI00291262	**Clusterin**	**125**	**4**	**1.00**	**0.56**	**0.64**	**0.005**
35	IPI00021842	Apolipoprotein E	193	7	1.00	0.87	0.72	0.029
	IPI00006114	Pigment epithelium-derived factor	102	6				
	IPI00303482	Fibrinogen-like protein 1 precursor	67	3				
36	IPI00479722	Proteasome activator complex subunit 1	94	4	1.00	0.64	0.79	0.010
37	IPI00396378	Heterogeneous nuclear ribonucleoproteins A2/B1	132	3	1.00	1.22	1.18	0.007
38	IPI00465028	Triosephosphate isomerase	234	5	1.00	0.67	0.76	0.031

[a] Proteins with known function in vessel regulation were selected for subsequent ELISA determination of their fetal cord plasma levels are in bold.

2-DGE software, from which, 196 were identified as either increasing or decreasing significantly between the three groups, of these, 38 were identified using LC-MS/MS. The significant matches to the NCBI database searches and the relative fold-change and significance of the densitometric analysis are indicated in Table 4.1. The top scoring hits for each excised spot from Table 4.1 are indicated for proteins interpreted as significantly upregulated with decreasing oxygen (Figure 4.4A) and those downregulated with decreasing oxygen (Figure 4.4B). Corresponding spots and table entries are labeled by number in column 1 of Table 4.1. For a broader characterization of the HepG2 secretome, additional spots were identified that were not changing significantly. These are included as Supplemental Figure 4.1 and Supplemental Table 4.1.

Several of the identified changing proteins were glycolysis proteins, such as enolase, adolase, GAPDH, and triphosphate isomerase (Figure 4.4, Table 4.1). Spots of these proteins were typically decreasing with 4% treatment from 20%, but increasing again with 1% O_2 treatment. Most other protein spots, as shown in Table 4.1, either decreased or increased across the three treatments, or for some, changed in only one of the three treatment conditions (typically 1% or 20% O_2). Of the increasing proteins in hypoxia, peroxiredoxin–1, dismutase superoxide, and IGFBP-1 are known to be oxygen-sensitive proteins. Plasminogen activator inhibitor-1 (PAI-1) has been shown to be upregulated in placenta of FGR pregnancies (25) and is known to be regulated by hypoxic-inducible factors. Here there are two PAI-1 isoforms identified as increasing 2.4 and 3.6 fold from 20% to 1% O_2 (Spots 12 and 13) (p=0.02 and 0.04).
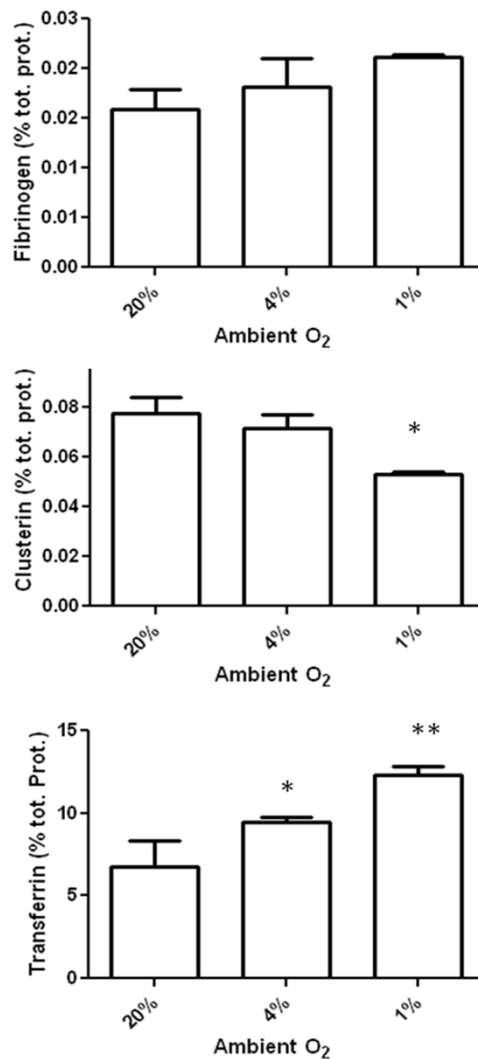
FIGURE 4.5. ELISA values for total clusterin, fibrinogen ,and transferrin in conditioned media from triplicate experiments of HepG2 cells in different ambient oxygen environments. Changes were assessed by ANOVA (*p<0.05, **p<0.01). Clusterin isoforms were seen to decrease in the HepG2 conditioned media by 2-DGE while transferrin isoforms were seen to increase in hypoxia (Figure 4.4 and Table 4.1), Fibrinogen was unchanged in the conditioned media, but an isoform was changed in the fetal plasma between control and FGR (Supplemental Figure 4.2 and Supplemental Table 4.2).

Several isoforms of transferrin were also seen to increase from 20 to 1% O_2, by 1.3, 1.5, and 2.5-fold (Spots 1, 2, and 3) (p=0.03, 0.03, and 0.0003). One additional low molecular weight spot identified as a transferrin isoform was decreased, however by only 10% (Spot 31). Additionally, clusterin was shown to be decreased nearly 2-fold in 1 and 4% compared to 20% (Spot 34) (p=0.005).

To verify that the overall levels of these proteins were changing in the CM, in a manner that matched the spot changes seen by 2-DGE densitometry, ELISA measurements were performed (Figure 4.5). Clusterin and transferrin, were shown to decrease 1.7 fold (p<0.05) and increase 2.1 fold (p<0.01) with hypoxia (20% to 1% O_2), respectively. Although fibrinogen was identified as changing in plasma between control and FGR subjects by 2-DGE (Supplemental Table 4.2, Spot 2), it did not change significantly in the CM by ELISA (Figure 4.5), nor was it identified as changing in the 2-DGE analysis of CM (Figure 4.4, Table 4.1). PAI-1 has previously been characterized to increase in hypoxic HepG2 CM under the regulation of the hypoxic inducible factor-1 (HIF-1) (26).

4.3.3. Patient selection and clinical characteristics

To assess the change in levels *in vivo* of angiogenic proteins identified in hepatic secretion, plasma was collected at birth from the umbilical vein of hypoxic FGR newborns. To minimize the potential confounding effects of changing protein levels with fetal development, each FGR sample was paired to a control sample gestational

TABLE 4.2. Clinical characteristics of FGR pregnancies from which fetal blood samples were collected.

		Control	FGR	p
Subjects (n)	Male	7	8	
	Female	5	4	
	Total	12	12	
Birthweight (g)		2214 (764)	1335 (600)	0.0002
Gestational age (wks)		33.9 (4.3)	33.3 (4.2)	
Birthweight percentile		47.1 (26)	1.9 (2.7)	0.0001
Maternal age (y)		27.33 (5.6)	29.0 (6.4)	
Placental weight (g)		519 (151)	352 (159)	0.03
Placental Resistance*		0.63 (0.10)	0.96 (0.24)	0.04
Blood gas				
Arterial:	pO_2 (Torr)	17.9 (5.4)	12.7 (4.7)	0.02
	pCO_2 (Torr)	50.1 (5.8)	55.8 (4.6)	
	pH	7.28 (0.03)	7.26 (0.04)	
Venous:	pO_2 (Torr)	33.1 (6.7)	21.7 (6.6)	0.004
	pCO_2 (Torr)	35.55 (7.3)	46.1 (4.7)	0.002
	pH	7.34 (0.03)	7.32 (0.04)	0.05
Gravida		1.9 (1.3)	1.5 (0.8)	
Term		0.3 (0.7)	0.4 (0.7)	
Preterm		0.0	0.2 (0.4)	
Abortions		0.6 (1.0)	0.0	
Living		0.3 (0.5)	0.5 (0.8)	
APGAR (5 min)		8.9 (0.3)	8.3 (1.4)	

Paired t-test, based on gestational age matches, was used to determine differences between groups. Standard deviation is shown in brackets. *Umbilical cord Doppler ultrasound was performed on 10 FGR samples and only 4 controls. The resistance index from the last Doppler ultrasound waveforms prior to delivery is indicated.
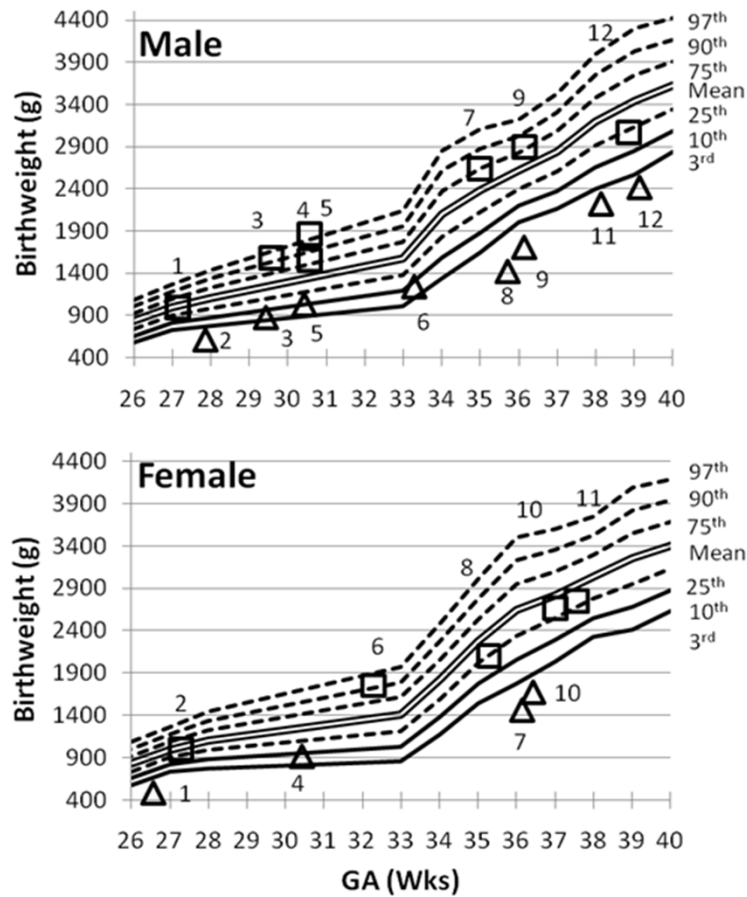
FIGURE 4.6. Birthweight versus gestational age for FGR pregnancies from which fetal plasma was collected at birth. The standardized percentile of birthweight for a Canadian population is indicated. To control for the effects of gestational age, samples from FGR pregnancies were paired with a matching gestational age control pregnancy. Paired FGR (triangle) and control (square) pregnancies are indicated by a shared number. Only severe FGR pregnancies were recruited. Controls are healthy pregnancies that matched the gestational age of each FGR pregnancy within 4 days.

age (GA) matched to within 4 days. The pairing of the GA matched samples is shown in Figure 4.6. The clinical characteristics of the patients abstracted from patient charts and diagnostic lab results including blood oxygen levels are shown in Table 4.2. The GA at birth spans from pre-term to term (27 to 39 weeks). Differences between GA-paired subject's characteristics were assessed by paired t-test. The selected patients represent severe FGR pregnancies with the average percentile of birthweight for GA of 1.9, which was drastically lower than control at 47.1 (p<0.0001), where >10th percentile is generally considered normal. The average oxygen level of the fetal blood supply (venous umbilical cord pO_2 - placenta to fetus) was 36% lower (p=0.004), and the returning blood for exchange (arterial umbilical pO_2 - fetus to placenta) reduced by 29% (p=0.02) in FGR pregnancies compared to control. The venous pH was decreased by 0.02 (p=0.05) and carbon dioxide level elevated by an average of 30% (p=0.002) in the venous umbilical blood. These findings are consistent with reduced exchange taking place across the FGR placenta. Further indication of reduced placental vasculature is seen in the measure of placental resistance to blood flow measured by umbilical cord Doppler ultrasound. The prenatal measurement was performed on most FGR pregnancies (n=10), and some control pregnancies (n=5). The resistance index (which increases due to inadequate placental vasculature, and leads to reduced blood flow to the fetus) was significantly elevated between the four paired FGR and GA matched controls (p=0.04, paired t-test) as well as the overall group means (p=0.01, t-test).

4.3.4. 2-DGE profiling for FGR plasma identified changing hepatic secreted proteins

Venous umbilical cord plasma was also profiled by 2-DGE after depletion of albumin and IgG in an effort to directly identify angiogenic plasma protein changes.   Each of the 12 FGR gels was paired to its corresponding GA matched control sample gel for quantitative comparison and statistical evaluation by paired t-test. In all, about 700 spots were separated, from which 42 were identified as either increasing or decreasing significantly by the software. Following visual verification, spot excision, and trypsin digestion, ten of the spots were identified using LC-MS/MS. The significant matches based on NCBI database searching and the relative fold-change and significance of the densitometric analysis are indicated in Supplemental Table 4.2, a representative gel is shown in Supplemental Figure 4.2. An interpretation of the most significant protein identifications and the increase or decrease taking place is depicted in Supplemental Table 4.2. Two isoforms of clusterin were detected, which were found to be significantly decreasing, as was seen in CM of hypoxic HepG2 cells (1.8 and 1.5 fold, Spots 4 and 5, p=0.04 and 0.03). An isoform of fibrinogen was also found to decrease significantly (2.2 fold, Spot 2, p=0.02). Of the ten identified proteins changing in fetal plasma, all were of hepatic origin.

4.3.5. Plasma levels of hepatic angiogenic proteins is dependent on blood oxygen levels
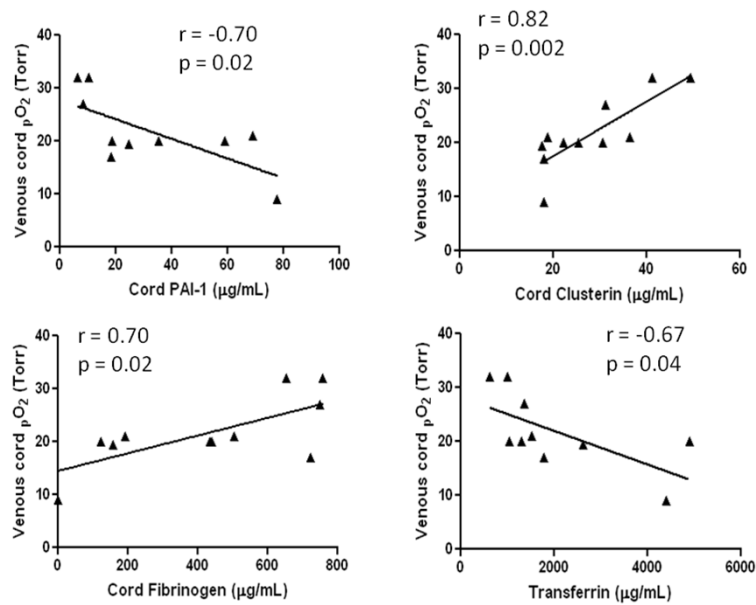
FIGURE 4.7. Immunological based measurement from control and FGR cord plasma samples (Table 4.2 and Figure 4.6), analyzing levels of PAI-1, fibrinogen, clusterin, and transferrin. Pearson's correlation of protein levels with venous oxygen level was measured at delivery.

The proteins selected for further quantitative evaluation are proteins known to function in angiogenesis. The levels of angiogenic proteins changing in hypoxic CM of HepG2 cells, as well as fibrinogen, which was identified as changing by 2-DGE profiling of the fetal plasma directly, were measured by immunoassay in venous umbilical cord plasma. This was done to determine if their levels were changing with *in utero* low oxygen conditions of FGR pregnancies. Proteins assessed were PAI-1 and transferrin, which were identified as increasing in the CM of hypoxic treated HepG2 cells (Figure 4.4, Table 4.1). Fibrinogen, which was shown to decrease in 2-DGE of fetal plasma (Supplemental Figure 4.2 and Supplemental Table 4.2), was also selected. Finally clusterin, which was shown to decrease both in secretions of hypoxic HepG2 cells, and in the fetal plasma, was assessed as well. Following immunoassay, correlation of the proteins' levels with many of the clinical characteristics listed in Table 4.2 was then performed. These included placental size, birthweight, gestational age, and arterial and venous oxygen levels. The venous, rather than arterial oxygen level's was of particular interest, as the venous cord is the immediate blood supply of the fetal liver, and the blood immediately leaving the placenta following gas exchange. Figure 4.7 shows the correlation of the levels of PAI-1, fibrinogen, clusterin, and transferrin, with venous oxygen levels. Specifically for the FGR group, PAI-1 and transferrin exhibited a significant negative correlation with venous oxygen levels (r=-0.70, p=0.02 and r=-0.67, p=0.04), indicating their increase with hypoxia. The correlations for these two however, appeared to be dependent on one, and two data points respectively, whose plasma levels were elevated from the

mean. The levels of fibrinogen and clusterin exhibited strong positive correlations with the dissolved venous oxygen (r=0.70, p=0.02 and r=0.82, p=0.002), indicating their decrease with hypoxia in FGR (Figure 4.7).

To check for any relationship of the angiogenic proteins with growth and development, their levels were also correlated with placental size, birthweight, and GA. Both clusterin and transferrin, correlated with GA (r=0.68, p=0.01 and r=-0.71, p=0.01) and birthweight (r=0.65, p= 0.02 and r=-0.66, p=0.03). There was no relation to any other factors for PAI-1 or fibrinogen. None of the proteins' levels correlated with umbilical artery oxygen level. To control for overall hepatic protein secretion changes or overall plasma protein levels being decreased in FGR, albumin (hepatic secreted) and IgG (non-hepatic secreted) were assessed as controls. Both albumin and IgG were strongly associated with GA (r=0.76, p=0.004 and r=0.69, p=0.01), birthweight (r=0.80, p=0.002 and r=0.76, p=0.004), and placental weight (r=0.69, p=0.01 and r=0.81, p=0.001), in FGR. Neither however, exhibited any correlation with the oxygen levels of the FGR samples.

4.4. DISCUSSION

This study identifies liver secretions to be pro-angiogenic under hypoxic conditions. The discovery of the changing levels of angiogenic proteins fibrinogen, clusterin, transferrin, and especially, the potent vascular regulator PAI-1, in a manner consistent with pro-angiogenesis, explains this finding. The same proteins were also

identified as changing in an oxygen-dependant manner, and in the corresponding directions, in the fetal blood plasma of hypoxic pregnancies. Together, this strongly suggests that fetal liver secretions have a role in vascular regulation of the fetal/placental vasculature in hypoxia. The findings are highly relevant to FGR pregnancies where chronic hypoxia and blood deprivation to the liver arise from a reduced placental vasculature, and the consequent fetal adaptations. The pro-angiogenic liver protein expression in response to a hypoxic environment in late gestation may be acting as an adaptive mechanism in an attempt to rescue the inadequate vasculature, formed earlier in gestation.

4.4.1. Angiogenic protein changes in HepG2 secretions as a model for plasma proteome changes

Given the complexity of direct profiling of plasma, and the involvement of hepatic proteins, a cell-based model for hypoxia-induced hepatic expression was used. Changes in the secretion of angiogenic regulators from the liver were profiled, in complement to direct profiling of hypoxic FGR plasma. HepG2 secretome profiling separated more spots relative to direct plasma profiling, which was challenging despite depletion of albumin and IgG from the samples (Supplemental Figure 4.2). HepG2 cells have been established as a viable model of hepatic secretion changes in hypoxia (27, 28). HepG2 cells' protein expression is sensitive to oxygen (29, 30), and these cells have been used extensively for fetal IGFBP-1 expression studies in a model of fetal hypoxia (18, 20).

The treatments of the HepG2 cells with various levels of oxygen in this study altered the dissolved gas environment of the cells (Figure 4.2A). A concentration of 90 Torr is normal *in vivo* radial artery oxygen content (24), while this drops to approximately 60 Torr in the uterine vein (31), corresponding to the 4% oxygen treatment. The 1% treatment at 40 Torr therefore represents physiological hypoxia for most tissues, and it is somewhat higher than the venous umbilical cord supply seen in normal pregnancy (Table 4.2). A better indication of oxygen state or sensitivity is ascertained from the HepG2 physiological response to the oxygen level. There appears to be an increase in apoptosis, indicating a degree of cellular stress, in the 1% O_2 treatment condition. The level of necrosis, which was significantly elevated in 1% and 20% O_2, indicates a HepG2 natural preference for 4% O_2 condition. 1% and 20% O_2 can therefore be considered hypoxic and supraoxic, respectively, within the context of this experiment (Figure 4.2B).

The degree of hypoxic sensitivity of HepG2 cells appears in the 2-DGE profiling as well. Several glycolysis related proteins changed with hypoxic treatment (Table 4.4). In many instances, the glycolysis proteins (GAPDH, enolase, adolase, triphosphate isomerase) were at their lowest expression for the 4% condition and increased in expression for both the 20% and 1% O_2 conditions. In the context of hypoxia, an upregulation of these proteins is to be expected given the increasing reliance on glycolysis in hypoxic conditions. In super-physiological conditions, an upregulation of these enzymes is expected, as the demands for substrate from a more active citric acid cycle increase with the abundance of oxygen. Although some of this change

may be due to increased spilling of cellular contents into the media in necrosis, this alone cannot account for the large changes observed in this study. Indeed, other non-glycolysis cytosolic proteins, like nuclear ribonucleoprotein, cofilin, and peptidyl-prolyl cis-trans isomerase, where identified, did not show any apparent change (Supplemental Figure 4.1 and Supplemental Table 4.1).

4.4.2. Plasma protein changes reflect altered angiogenic function in hypoxic pregnancies

PAI-1 is an important regulator of the extracellular matrix. It regulates fibrinolysis, an important process in clotting, vessel remodeling and angiogenesis (reviewed) (10). PAI-1 was also shown to be increased in placental villous samples at the maternal-fetal interface in FGR pregnancies, and is suggested to be contributing to the pathology of the disease (25). Mutations in its gene have been associated with increased incidence of FGR (32). Its role in FGR has been speculated to be through thrombophilia in the placenta, contributing to placental malfunction (25, 33). Our finding that circulating PAI-1 is increased, and is correlated with the severity of venous hypoxia in FGR (Figure 4.7), supports the evidence that PAI-1 is linked to the disease. As PAI-1 regulates fibrinogen deposition, the increased levels of PAI-1 also explain decreasing circulating levels of fibrinogen with hypoxia. Indeed, fibrinogen levels showed a strong negative correlation to PAI-1 levels (r =-0.76, p=0.006) (graph not shown). The negative relationship is consistent with PAI-1 mediated extracellular matrix remodeling. Fibrinogen acts as an important scaffold for vascular endothelial

cells, and itself plays a role in regulating endothelial migration and angiogenesis through αvβ3 integrin (6).

Clusterin and transferrin, which are decreasing and increasing with hypoxia, are known to inhibit and stimulate, respectively, vascular endothelial cell migration and endothelial cell adhesion to the extracellular matrix (5, 12, 34). Clusterin has been shown to bind, and be endocytosed, by the same vascular endothelial receptor as PAI-1 (35), and is altered in the plasma of mothers with preeclampsia, another pregnancy complication with 20% co-presentation in FGR (36). Transferrin, like PAI-1, is downstream of hypoxia response elements, and is known to be regulated by hypoxia inducible factor-1 (37). A decrease in clusterin with an increase in transferrin is therefore consistent with vascular changes that are pro-angiogenic.

The finding of these protein changes is in addition to other findings of increased localized expression of angiogenic cytokines in hypoxic conditions that also act on the endothelium. Vascular endothelial growth factor (VEGF) and placental growth factor (PIGF), which are sensitive to oxygen, have been suggested to play a role in FGR (3). PIGF has been shown to correlate to vascular resistance in the FGR fetus (38), although no change in the circulating levels of VEGF are observed (39).

4.4.3. Conclusions

Here we link the protein changes of important liver secreted angiogenic proteins directly to the metabolic restriction of oxygen. Linking the pro-angiogenic changes in

the plasma expression of PAI-1, clusterin, fibrinogen, and transferrin in late gestation hypoxia implicates the fetal liver in vascular regulation. Hypoxia is critical to an angiogenic response in wound healing. The protein changes in this study suggest analogous vascular changes; PAI-1 mediated extracellular matrix remodeling and fibrinogen deposition, and an increase in endothelial activity. The data therefore strongly supports the interaction of the haemostatic and angiogenic mechanisms in regulating the placental vasculature. However, it is not known that these changes act to improve the placental vasculature for increased blood flow to the fetus. Conversely, their expression may in fact be maladaptive, by contributing to haemostatic dysregulation, which has already been identified in FGR placentas (25, 33). The late gestation remodeling of the vasculature could have significant implications in the pathophysiology of FGR, and potentially in the fetal origins of cardiovascular disease that develop in adult life.

4.5. REFERENCES

1. Mayhew, T. M., Wijesekara, J., Baker, P. N., and Ong, S. S. (2004) Morphometric Evidence that Villous Development and Fetoplacental Angiogenesis are Compromised by Intrauterine Growth Restriction but Not by Pre-Eclampsia. *Placenta. 25*, 829-833.

2. Gagnon, R. (2003) Placental Insufficiency and its Consequences. *Eur. J. Obstet. Gynecol. Reprod. Biol. 110 Suppl 1*, S99-107.

3. Zygmunt, M., Herr, F., Munstedt, K., Lang, U., and Liang, O. D. (2003) Angiogenesis and Vasculogenesis in Pregnancy. *Eur. J. Obstet. Gynecol. Reprod. Biol. 110 Suppl 1*, S10-8.

4. M Kady, S., and Gardosi, J. (2004) Perinatal Mortality and Fetal Growth Restriction. *Best Pract. Res. Clin. Obstet. Gynaecol. 18*, 397-410.

5. Sivamurthy, N., Stone, D. H., LoGerfo, F. W., and Quist, W. C. (2001) Apolipoprotein J Inhibits the Migration and Adhesion of Endothelial Cells. *Surgery. 130*, 204-209.

6. Thiagarajan, P., Rippon, A. J., and Farrell, D. H. (1996) Alternative Adhesion Sites in Human Fibrinogen for Vascular Endothelial Cells. *Biochemistry. 35*, 4169-4175.

7. Cid, M. C., Grant, D. S., Hoffman, G. S., Auerbach, R., Fauci, A. S., and Kleinman, H. K. (1993) Identification of Haptoglobin as an Angiogenic Factor in Sera from Patients with Systemic Vasculitis. *J. Clin. Invest. 91*, 977-985.

8. Sumi, M., Sata, M., Miura, S., Rye, K. A., Toya, N., Kanaoka, Y., Yanaga, K., Ohki, T., Saku, K., and Nagai, R. (2007) Reconstituted High-Density Lipoprotein Stimulates Differentiation of Endothelial Progenitor Cells and Enhances Ischemia-Induced Angiogenesis. *Arterioscler. Thromb. Vasc. Biol. 27*, 813-818.

9. Liu, Y., Cao, D. J., Sainz, I. M., Guo, Y. L., and Colman, R. W. (2008) The Inhibitory Effect of HKa in Endothelial Cell Tube Formation is Mediated by Disrupting the uPA-uPAR Complex and Inhibiting its Signaling and Internalization. *Am. J. Physiol. Cell. Physiol. 295*, C257-67.

10. Stefansson, S., McMahon, G. A., Petitclerc, E., and Lawrence, D. A. (2003) Plasminogen Activator Inhibitor-1 in Tumor Growth, Angiogenesis and Vascular Remodeling. *Curr. Pharm. Des. 9*, 1545-1564.

11. Jadlowiec, J., Dongell, D., Smith, J., Conover, C., and Campbell, P. (2005) Pregnancy-Associated Plasma Protein-a is Involved in Matrix Mineralization of Human Adult Mesenchymal Stem Cells and Angiogenesis in the Chick Chorioallontoic Membrane. *Endocrinology. 146*, 3765-3772.

12. Carlevaro, M. F., Albini, A., Ribatti, D., Gentili, C., Benelli, R., Cermelli, S., Cancedda, R., and Cancedda, F. D. (1997) Transferrin Promotes Endothelial Cell Migration and Invasion: Implication in Cartilage Neovascularization. *J. Cell Biol. 136*, 1375-1384.

13. Stefansson, S., Petitclerc, E., Wong, M. K., McMahon, G. A., Brooks, P. C., and Lawrence, D. A. (2001) Inhibition of Angiogenesis in Vivo by Plasminogen Activator Inhibitor-1. *J. Biol. Chem. 276*, 8135-8141.

14. Cid, M. C., Grant, D. S., Hoffman, G. S., Auerbach, R., Fauci, A. S., and Kleinman, H. K. (1993) Identification of Haptoglobin as an Angiogenic Factor in Sera from Patients with Systemic Vasculitis. *J. Clin. Invest. 91*, 977-985.

15. Nathanielsz, P. W., and Hanson, M. A. (2003) The Fetal Dilemma: Spare the Brain and Spoil the Liver. *J. Physiol. 548*, 333.

16. Kiserud, T., Kessler, J., Ebbing, C., and Rasmussen, S. (2006) Ductus Venosus Shunting in Growth-Restricted Fetuses and the Effect of Umbilical Circulatory Compromise. *Ultrasound Obstet. Gynecol. 28*, 143-149.

17. Watson, C. S., Bialek, P., Anzo, M., Khosravi, J., Yee, S. P., and Han, V. K. (2006) Elevated Circulating Insulin-Like Growth Factor Binding Protein-1 is Sufficient to Cause Fetal Growth Restriction. *Endocrinology. 147*, 1175-1186.

18. Tazuke, S. I., Mazure, N. M., Sugawara, J., Carland, G., Faessen, G. H., Suen, L. F., Irwin, J. C., Powell, D. R., Giaccia, A. J., and Giudice, L. C. (1998) Hypoxia Stimulates Insulin-Like Growth Factor Binding Protein 1 (IGFBP-1) Gene Expression in HepG2 Cells: A Possible Model for IGFBP-1 Expression in Fetal Hypoxia. *Proc. Natl. Acad. Sci. U. S. A. 95*, 10188-10193.

19. Crossey, P. A., Pillai, C. C., and Miell, J. P. (2002) Altered Placental Development and Intrauterine Growth Restriction in IGF Binding Protein-1 Transgenic Mice. *J. Clin. Invest. 110*, 411-418.

20. Seferovic, M. D., Ali, R., Kamei, H., Liu, S., Khosravi, J. M., Nazarian, S., Han, V. K., Duan, C., and Gupta, M. B. (2009) Hypoxia and Leucine Deprivation Induce Human Insulin-Like Growth Factor Binding Protein-1 Hyperphosphorylation and Increase its Biological Activity. *Endocrinology. 150*, 220-231.

21. Seferovic, M. D., Krughkov, V., Pinto, D., Han, V. K., and Gupta, M. B. (2008) Quantitative 2-D Gel Electrophoresis-Based Expression Proteomics of Albumin and IgG Immunodepleted Plasma. *J. Chromatogr. B. Analyt Technol. Biomed. Life. Sci. 865*, 147-152.

22. Ebanks, R. O., Chisholm, K., McKinnon, S., Whiteway, M., and Pinto, D. M. (2006) Proteomic Analysis of Candida Albicans Yeast and Hyphal Cell Wall and Associated Proteins. *Proteomics. 6*, 2147-2156.

23. Gupta, M. B., Seferovic, M. D., Liu, S., Gratton, R. J., Doherty-Kirby, A., Lajoie, G. A., and Han, V. K. M. (2006) Altered Proteome Profiles in Maternal Plasma in Pregnancies with Fetal Growth Restriction. *Clinical Proteomics. 2*, 169-184.

24. Crapo, R. O., Jensen, R. L., Hegewald, M., and Tashkin, D. P. (1999) Arterial Blood Gas Reference Values for Sea Level and an Altitude of 1,400 Meters. *Am. J. Respir. Crit. Care Med. 160*, 1525-1531.

25. Estelles, A., Gilabert, J., Keeton, M., Eguchi, Y., Aznar, J., Grancha, S., Espna, F., Loskutoff, D. J., and Schleef, R. R. (1994) Altered Expression of Plasminogen Activator Inhibitor Type 1 in Placentas from Pregnant Women with Preeclampsia and/or Intrauterine Fetal Growth Retardation. *Blood. 84*, 143-150.

26. Fink, T., Kazlauskas, A., Poellinger, L., Ebbesen, P., and Zachar, V. (2002) Identification of a Tightly Regulated Hypoxia-Response Element in the Promoter of Human Plasminogen Activator Inhibitor-1. *Blood. 99*, 2077-2083.

27. Maruyama, M., Matsunaga, T., Harada, E., and Ohmori, S. (2007) Comparison of Basal Gene Expression and Induction of CYP3As in HepG2 and Human Fetal Liver Cells. *Biol. Pharm. Bull. 30*, 2091-2097.

28. Kelly, J. H., and Darlington, G. J. (1989) Modulation of the Liver Specific Phenotype in the Human Hepatoblastoma Line Hep G2. *In Vitro Cell. Dev. Biol. 25*, 217-222.

29. Wenger, R. H., Rolfs, A., Marti, H. H., Bauer, C., and Gassmann, M. (1995) Hypoxia, a Novel Inducer of Acute Phase Gene Expression in a Human Hepatoma Cell Line. *J. Biol. Chem. 270*, 27865-27870.

30. Sonna, L. A., Cullivan, M. L., Sheldon, H. K., Pratt, R. E., and Lilly, C. M. (2003) Effect of Hypoxia on Gene Expression by Human Hepatocytes (HepG2). *Physiol. Genomics. 12*, 195-207.

31. Pardi, G., Cetin, I., Marconi, A. M., Bozzetti, P., Buscaglia, M., Makowski, E. L., and Battaglia, F. C. (1992) Venous Drainage of the Human Uterus: Respiratory Gas Studies in Normal and Fetal Growth-Retarded Pregnancies. *Am. J. Obstet. Gynecol. 166*, 699-706.

32. Glueck, C. J., Kupferminc, M. J., Fontaine, R. N., Wang, P., Weksler, B. B., and Eldor, A. (2001) Genetic Hypofibrinolysis in Complicated Pregnancies. *Obstet. Gynecol. 97*, 44-48.

33. Kupferminc, M. J., Many, A., Bar-Am, A., Lessing, J. B., and Ascher-Landsberg, J. (2002) Mid-Trimester Severe Intrauterine Growth Restriction is Associated with a High Prevalence of Thrombophilia. *BJOG. 109*, 1373-1376.

34. Sivamurthy, N., Rohan, D. I., Stone, D. H., Quist, W. C., and LoGerfo, F. W. (2000) Inhibition of Vascular Smooth Muscle and Endothelial Cell Migration by Apolipoprotein J. *J. Am. Coll. Surg. 191*, S2-S2.

35. Kounnas, M. Z., Loukinova, E. B., Stefansson, S., Harmony, J. A., Brewer, B. H., Strickland, D. K., and Argraves, W. S. (1995) Identification of Glycoprotein 330 as an Endocytic Receptor for Apolipoprotein J/clusterin. *J. Biol. Chem. 270*, 13070-13075.

36. Watanabe, H., Hamada, H., Yamada, N., Sohda, S., Yamakawa-Kobayashi, K., Yoshikawa, H., and Arinami, T. (2004) Proteome Analysis Reveals Elevated Serum Levels of Clusterin in Patients with Preeclampsia. *Proteomics. 4*, 537-543.

37. Rolfs, A., Kvietikova, I., Gassmann, M., and Wenger, R. H. (1997) Oxygen-Regulated Transferrin Expression is Mediated by Hypoxia-Inducible Factor-1. *J. Biol. Chem. 272*, 20055-20062.

38. Schlembach, D., Wallner, W., Sengenberger, R., Stiegler, E., Mortl, M., Beckmann, M. W., and Lang, U. (2007) Angiogenic Growth Factor Levels in Maternal and Fetal Blood: Correlation with Doppler Ultrasound Parameters in Pregnancies Complicated by Pre-Eclampsia and Intrauterine Growth Restriction. *Ultrasound Obstet. Gynecol. 29*, 407-413.

39. Wallner, W., Sengenberger, R., Strick, R., Strissel, P. L., Meurer, B., Beckmann, M. W., and Schlembach, D. (2007) Angiogenic Growth Factors in Maternal and Fetal Serum in Pregnancies Complicated by Intrauterine Growth Restriction. *Clin. Sci. (Lond). 112*, 51-57.

CHAPTER 5

Oxygen dependent increase in fetal-placental plasma PAI-1 stimulates angiogenesis in placental insufficiency

5.1. INTRODUCTION

A compromised vasculature leading to placental insufficiency is a leading cause of Fetal Growth Restriction (FGR). The reduced volume and degree of branching of the chorionic villous tree (1) leads to increased vascular resistance of the fetal-placental circulation. The reduced circulation leads to reduced maternal/fetal exchange, creating conditions of hypoxia and acidosis for the fetus. There is a significantly elevated risk of perinatal death, or long-term complications for the infant. The primary causes of the placental vascular deficiency, as well as the vascular regulatory response to hypoxic changes in placental insufficiency, are therefore of considerable research interest.

The changing expression of pro-angiogenic cytokines VEGF and FGF-2 are important to normal development of the placental vasculature (2, 3). The role of placental oxygen in angiogenic regulation is presumed to be acting via upregulation of VEGF and its receptors, or through increased sensitivity of endothelial cells to FGF-2 (4, 5). The fetal-placental VEGF expression levels have been variably reported as higher (6), lower (7), or unchanged (8) in its expression in FGR pregnancies. An ovine model of placental insufficiency revealed VEGF expression to be decreased (9). FGF-2 expression levels are reported to be higher in FGR pregnancies (6). Despite the changing levels of these factors in placental insufficiency, the precise angiogenic regulation mechanisms leading to the vascular pathology are unknown (2). The relative increase or decrease of VEGF and other factors in FGR is compounded by the

115

different etiologies: increased circulating levels of VEGF are shown to play a role in the pathogenesis of FGR pregnancies with preeclampsia (10).

VEGF and FGF-2 signal endothelial cellular migration and secretion of matrix metalloproteinases (MMPs). Remodeling of the ECM by proteins in circulation and secreted from endothelial cells is critical to endothelial cell migration and therefore integral to angiogenesis. VEGF also signals the production of plasminogen activator inhibitor 1 (PAI-1) (11). PAI-1 levels are potent regulators of fibrinolysis and extracellular matrix (ECM) remodeling. It has pro-angiogenic effects, which is a factor in tumorigenesis (12). Using knockout mice, PAI-1 was demonstrated to regulate retinal vascularization (13). Furthermore, it has recently been shown that PAI-1 deficient mice have reduced placental angiogenesis and an altered vascular morphology (14). Its increased transcription in syncitiotrophoblast has been reported in FGR (15). Our recent data has also shown that its plasma levels in the FGR fetus increase with hypoxia (16).

In addition to VEGF-mediated expression, PAI-1 is strongly induced via hypoxic-mediated mechanisms. PAI-1, like VEGF, is downstream of a hypoxic response element, and is therefore upregulated via HIF-1 mediated induction (17). We therefore hypothesized that changing PAI-1 levels in hypoxic pregnancies with placental insufficiency may be contributing to the pathological vascular changes of the placenta. Using the blood immediately effluent from the placenta collected from the venous umbilical cord following delivery, we sought to determine if (i) PAI-1 is

increasing or decreasing in the plasma, (ii) its relationship to oxygen, VEGF and FGF-2

levels, and (iii) determine the effect of its changing levels on angiogenic regulation.

5.2. MATERIALS AND METHODS

5.2.1. Subject recruitment and plasma collection

The study recruited pregnant women from St. Joseph's Hospital, London, ON Canada

with written and informed consent and with approval from the Human Ethics Review

Board of The University of Western Ontario. Women suspected of severe fetal

growth restriction with placental insufficiency were included in the study (n=12).

Mothers with FGR pregnancies were otherwise healthy. Exclusion criteria included

preeclampsia, abrupted placenta, fetal congenital abnormalities, fetal or placental

infection, and maternal diabetes. Mothers with healthy pregnancies with gestational

ages (GA) that matched the FGR pregnancies within 4 days were recruited as controls

(n=12). Women with suspected FGR had estimated weights determined by fetal

biometric ultrasound measurements, with estimated fetal weight well below the

tenth percentile for GA (18). Umbilical Doppler was measured a maximum of three

days prior to delivery to determine the placental resistance in FGR pregnancies. GA

was determined by last menstrual date of mothers or the first trimester ultrasound

crown rump length.

Maternal blood was collected by venipuncture just prior to delivery. At delivery the

umbilical cord was clamped and fetal blood removed from the fetal umbilical cord

vein by venipuncture in EDTA coated tubes. Some of the blood was analyzed at St Joseph's Hospital as part of normal neonatal care, and blood gas values were abstracted from fetal charts. The remaining blood was centrifuged at 3500 x g for 15 min at 4°C, and the plasma supernatants saved for subsequent analysis at -80°C.

The final percentiles were calculated following birth by comparing birthweight for given GA and gender to standardized growth charts (18). All FGR pregnancies were confirmed to be <3rd percentile and all control pregnancies used were >25th percentile for GA and gender. Pathological examination of the majority of the placentas (9 of 12 control and 10 of 12 FGR) was undertaken at St Joseph's Hospital. Based on review of the pathological reports and other information in the patient charts, some subjects were excluded. In 2 of the 12 FGR patients fetal congenital anomalies were found, and an additional patient was excluded due to infection. One maternal control sample was excluded due to the finding of funisitis (infection/inflammation of the umbilical cord). All other placentas were negative for signs of infection. Umbilical blood gas levels were also abstracted from the chart for (8 of 9 FGR and 11 of 11 controls pregnancies).

5.2.2 HUVEC culture and angiogenic assays

Human umbilical vein endothelial cells (HUVECs) (Lonza, Basel, Switzerland) were grown in Endothelial Growth Media (Lonza) supplemented with 10% FBS, using CELL+ growth surface coated flasks (Sarstedt, Numbrecht, Germany). For treatments,

HUVECs were plated on ECMatrix (Millipore, MA, USA) at a density of 1 x 10^4 or 3 x 10^4 cells per well (96 well plate) with 50 μL of FBS-free media. The plasma collected was added to Endothelial Base Media (Lonza, Basel, Switzerland) (FBS-free) for a final concentration of 1% in 100 μL of media. The cells were then allowed to grow from 2 to 12 hours depending on the cell density, and as per the *In Vitro* Angiogenesis Assay Kit protocol (Millipore, MA, USA). For antibody inhibitor treatments, antibodies were added to the plasma in 30 μL of base media, and incubated at RT for 1 hour. Cells were then added to the tubes, and incubated for a further 10 minutes prior to plating. Three bright field images were taken using an inverted microscope. Leica FireCam software was used to capture the images (v3.4, Leica Microsystems, Wetzlar, Germany). The tube length and cell area were quantified using Axiovision software (v4.7.1, Carl Zeiss, Germany), and branches were counted manually as per the Angiogenesis Assay Kit.

5.2.3 Protein measurements and statistical evaluations

All total protein quantifications were by Bradford method (BioRad). FGF-2, VEGF, and PAI-1 were measured by an immunological-based fluorescent multiplex assays (Human CDV1, Millipore, Billerica, MA, USA) using a Bio-Plex 200 system (BioRad), which utilizes Luminex® xMAPTM fluorescent bead-based technology (Luminex Corp., Austin, TX). Levels were automatically calculated from standard curves using Bio-Plex Manager software (v.4.1.1, Bio-Rad). All statistics were done using GraphPad Prism 5 (Graph Pad Software Inc, CA, USA). To compare means, t-tests, Mann-Whitney, or

TABLE 5.1. Clinical characteristics of FGR and gestational age matched control pregnancies from which cord blood samples were collected.

		Control	FGR
Subjects (n)	*Male*	6	5
	Female	5	4
	Total:	11	9
Birthweight (g)		2170 (670)	**1453* (624)**
Gestational age (wk)		33.7 (3.7)	34.0 (4.3)
Birthweight percentile		53 (19)	**1.7*** (2.9)**
Maternal age (y)		27 (5)	29 (7)
Placental weight (g)		533 (125)	**385** (172)**
Placental Resistance⁺		0.63 (0.09)	**0.99* (0.24)**
Maternal BP			
	Systolic	113 (11)	130 (16)
	Diastolic	71 (8)	81 (15)
APGAR (5 min)		8.8 (0.4)	8.4 (1.1)

Comparison of means by t-test (*p<0.05, **p<0.01, ***p<0.001). Standard deviation is indicated in brackets. ⁺Placental resistance index from the last umbilical cord Doppler ultrasound prior to delivery. Doppler was performed for 8 of 9 FGR and 5 of 11 controls.
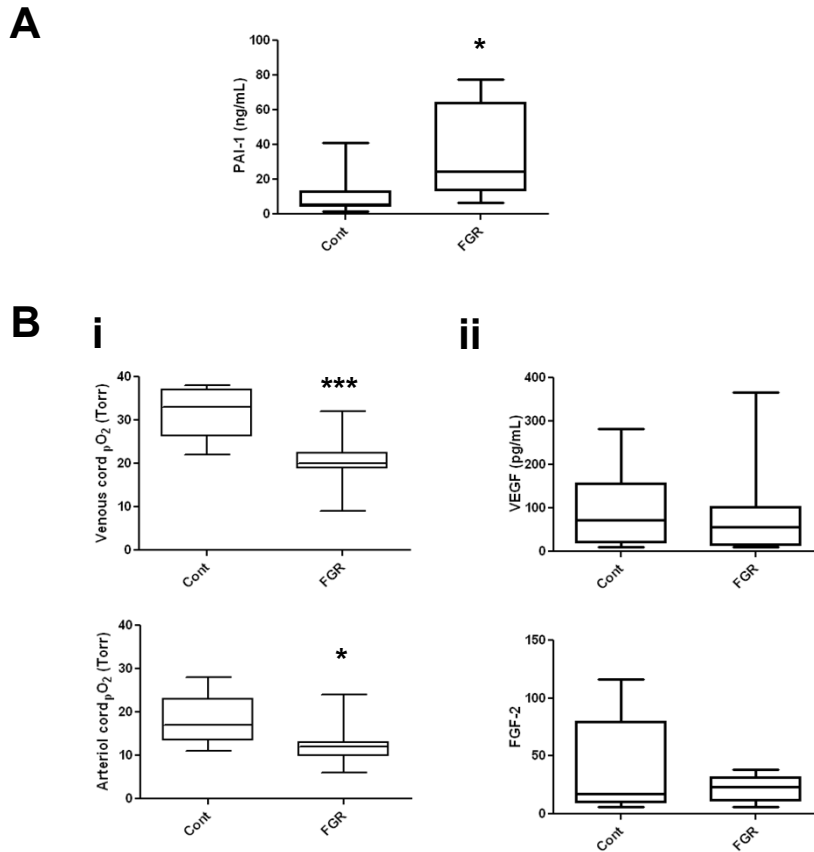
FIGURE 5.1. Fetal umbilical cord plasma levels of PAI-1 and its oxygen and cytokine regulators, in placental insufficiency compared to controls. **(A)** PAI-1 is increased in fetal circulation in placental insufficiency. **(B)** Oxygen levels in both the venous and arterial umbilical cord were decreased in placental insufficiency (i), while VEGF and FGF-2 levels were unchanged (ii). (t-test, *p<0.05, **p<0.01, ***p<0.001).

one-way ANOVAs were used where appropriate. Pearson's Correlation compared proteins' levels to blood oxygen levels, as well as other quantitative criteria abstracted from the clinical charts, and the degree of angiogenesis measured in the angiogenic assay.

5.3. RESULTS

Effluent placental blood samples were collected at the time of delivery from the umbilical cord vein. Mothers with FGR and placental insufficiency were selected for the study, and represent the span of gestational age from 27 to 39 weeks. Healthy controls were selected to match based on gestational age (GA) within 4 days of delivery. The characteristics of the pregnancy and neonates for the groups are summarized in Table 5.1. FGR babies were severely growth restricted, with birthweight percentiles averaging less than the 2nd percentile for GA. The placentae also weighed ~150 g less on average, which was significantly smaller ($p<0.01$). Placental resistance of the vasculature by umbilical Doppler was substantially increased in FGR babies just prior to delivery. Although the maternal systolic blood pressure (BP) was slightly elevated in FGR, the overall normal BP levels indicate the absence of preeclampsia in both FGR and control groups. The degree of restricted exchange across the placenta was also apparent in the levels of umbilical oxygen, which were significantly reduced (both venous and arterial, $p<0.001$ and 0.05 respectively) in FGR (Figure 5.1Bi). Together these characteristics indicate fetal growth restricted pregnancies with placental insufficiency.
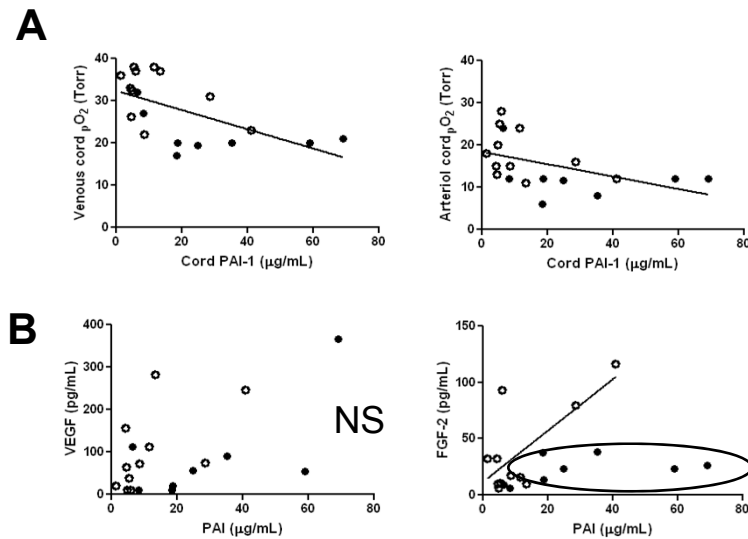
FIGURE 5.2. Circulating levels of PAI-1 in the fetus correlate to its molecular regulators *in vivo*. **(A)** The circulating levels of PAI-1 increase in proportion to the degree of hypoxia. There is a moderately negative correlation to the venous umbilical cord oxygen level (r=-0.60 , p<0.01), and modest correlation to the arterial umbilical cord oxygen levels (r=-0.48, p<0.05). **(B)** In contrast, angiogenic cytokines VEGF and FGF-2 exhibit a poor relationship to levels of PAI-1. VEGF did not correlate to increased PAI-1. Increased FGF-2 correlates to increased PAI-1 in controls only (r=0.72, p<0.01). In FGR, PAI-1 expression is unrelated to levels of FGF-2 (circle). (open: control, closed: FGR).

We analyzed the placental effluent blood (umbilical cord plasma) for evidence of increased PAI-1 in the FGR placentas. We also measured the levels of its regulators, VEGF and FGF-2, using the same highly sensitive fluorescent multiplex immunoassay. It was found that PAI-1 was significantly increased (>4-fold, $p<0.05$) in FGR compared to control (Figure 5.1A). However there was no change in its angiogenic cytokine regulators VEGF and FGF-2 (Figure 5.1Bii). The levels of PAI-1 however appeared to be closely related to the amount of blood oxygen, especially venous oxygen ($r=0.60$), as determined by their significant correlations (Figure 5.2A). The levels of PAI-1, however, did not correlate to the levels of VEGF in the plasma ($p<0.01$ and 0.05 respectively) (Figure 5.2B). Although PAI-1 correlated strongly to the levels of FGF-2 in control pregnancies ($r=0.72$, $p<0.01$), the levels of FGF-2 in FGR pregnancies was completely independent of the PAI-1 expression in plasma (Figure 5.2B circle).

The unchanged level of VEGF was surprising given VEGF's upregulation in hypoxia, and the significantly lower levels of oxygen both entering and leaving the placenta (Figure 5.1Bi) in our FGR samples with compromised vasculature. Nonetheless, given that pro-angiogenic PAI-1 is increasing in plasma concentration (Figure 5.1A), we set out to measure the effects of the effluent placental blood on angiogenesis, using an *in vitro* angiogenic assay. HUVEC cells plated on ECMatrix were subjected to a 1% concentration of the placental effluent blood plasma taken from the umbilical cords of FGR and control pregnancies. Representative images from the assay are shown in Figure 5.3A. The amount of angiogenic potency of the FGR plasma relative to control was quantified using software with total length of tube formation and number of

A
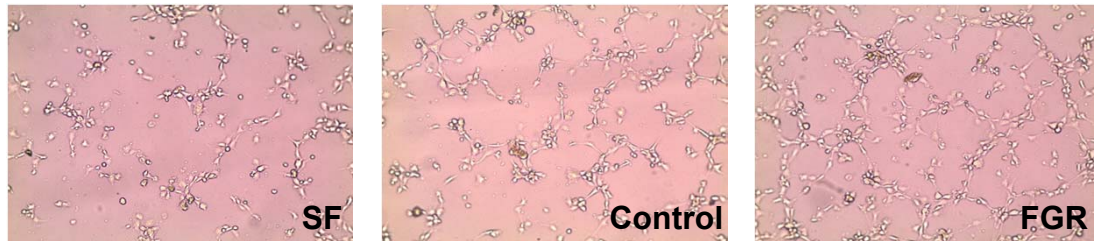
B
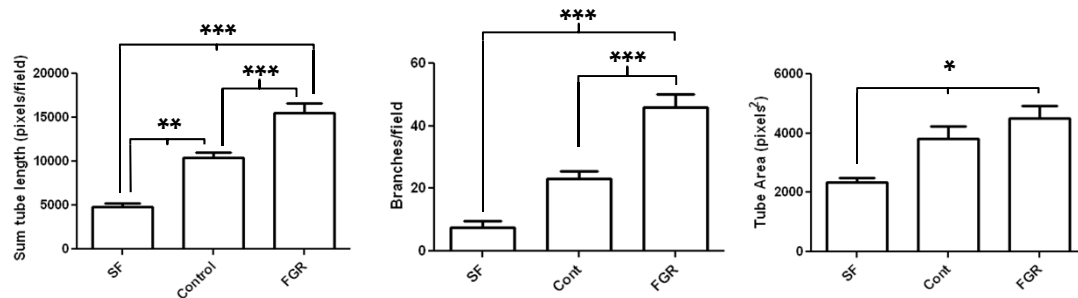
FIGURE 5.3. Angiogenic tube formation assay of HUVECs in the presence of 1% venous umbilical cord plasma from 12 FGR and 12 gestational age matched control newborns. **(A)** Representative fields are shown from serum free control (SF) as well as control, and FGR groups. **(B)** The total length of all tubes formed and the total number of branches per field were used for quantitative comparison of the relative angiogenic potency of the plasma induced changes (One-way ANOVA, *p<0.05, **p<0.01, and ***p<0.001).
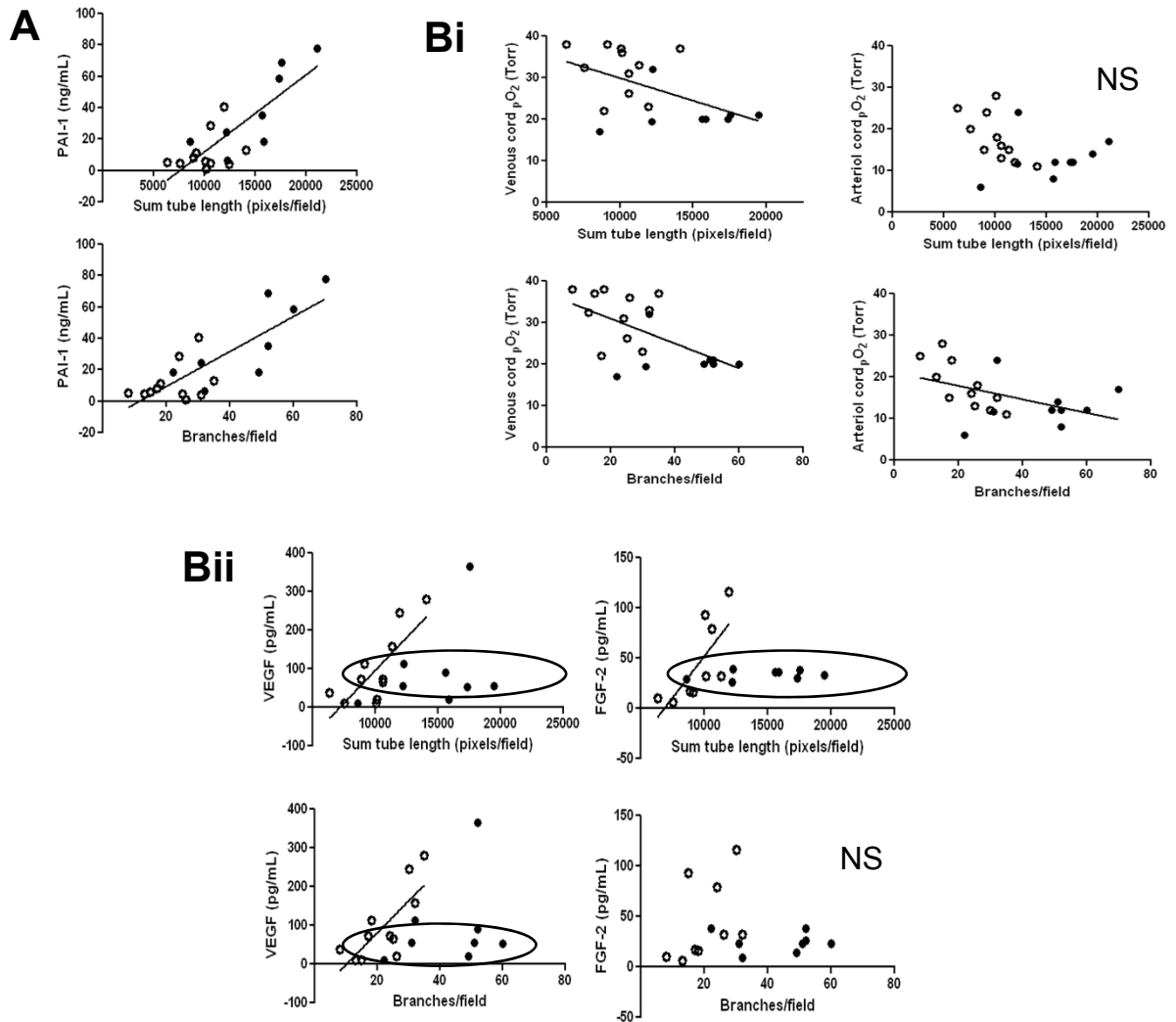
FIGURE 5.4. Plasma levels of PAI-1 and its molecular regulators, oxygen, VEGF, and FGF-2 correlate to the angiogenic potency of the plasma. **(A)** PAI-1 very strongly correlated to both tube formation and the number of branches (r= 0.82 and 0.81, P<0.001 and 0.0001 respectively). **(B)** (i) The angiogenic potency was related to the blood's oxygen levels at birth. Tube length and branching increased in hypoxia as measured in the umbilical vein (r=-0.64 and -0.70, P<0.001 and 0.0001 respectively), and also to some degree, the umbilical artery (r=-0.47, P<0.05). **(B)** (ii) VEGF and FGF-2 regulated angiogenesis however in control only. Both tube length and branching correlated to VEGF levels in control fetus' (r=0.75 and 0.76, p<0.05 and 0.01 respectively). For FGF-2, a correlation only existed with tube length in control pregnancies (r=0.73, p<0.05). The relationship between VEGF and FGF-2 levels and PAI-1 expression was apparent in controls, but broke down in FGR. (open: Control, closed: FGR).

branches per field as metrics. The FGR plasma from pregnancies with placental insufficiency induced 1.5-fold greater tube length (p<0.01) and 2-fold greater degree of tube branching (p<0.001) compared to control (Figure 5.3B). The overall proliferation of the cells appeared to be unchanged, as the tube area remained unchanged (Figure 5.3B).

When correlated to the degree of angiogenic induction by the plasma, it was revealed that PAI-1 is very strongly pro-angiogenic. PAI-1 correlated strongly to both tube formation (r= 0.82, P<0.001), and the degree of branching (r= 0.81, P<0.0001) (Figure 5.4A). Placental hypoxia, a determinant of PAI-1 expression (Figure 5.2A), correlated to the increased angiogenesis. Venous umbilical blood oxygen correlated with tube length and the degree of branching (r=-0.64 and -0.70, P<0.001 and 0.0001 respectively) (Figure 5.4Bi). Arterial umbilical blood oxygen also correlated mildly to the degree of branching (r=-0.47, P<0.05) (Figure 5.4Bi).

It was surprising that no apparent relationship with angiogenesis was found with overall levels of VEGF and FGF-2 given their strong angiogenic potency. When these cytokines were analyzed separately for control and FGR groups however, it became apparent that a significant relationship indeed exists in normal pregnancy. Levels of VEGF and FGF-2 correlated very strongly with tube formation in controls (r=0.75 and 0.73, p<0.05), however this relationship was decoupled in FGR (Figure 5.4Bii, circles). VEGF also correlated strongly to the degree of branching in control pregnancies (r=0.76, p<0.01).

	3 hours	6 hour	9 hours
Plasma -			
Plasma +			
0.05 PAI-1 ab			
0.25 PAI-1 ab			
1.25 PAI-1 ab			
1.25 GAPDH ab			
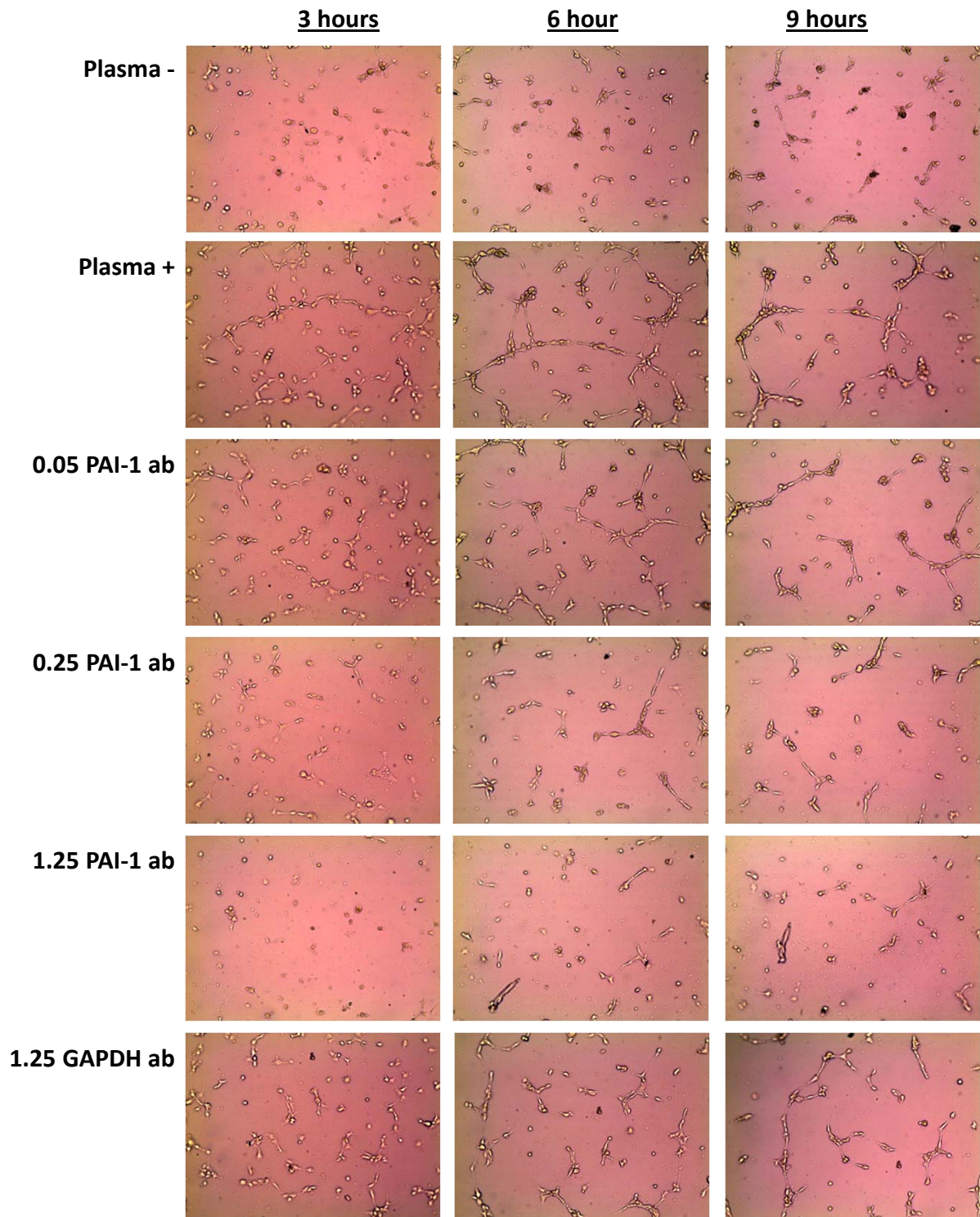
FIGURE 5.5. Angiogenic tube formation assay of HUVECs in the presence of 1% venous umbilical cord plasma. PAI-1 antibody was added in indicated amounts (μg/mL) in triplicate wells, and compared to serum free and a GAPDH antibody control. Representative fields (100x magnification) are shown from one of three experiments. Quantification of replicate fields is indicated in Figure 5.6.
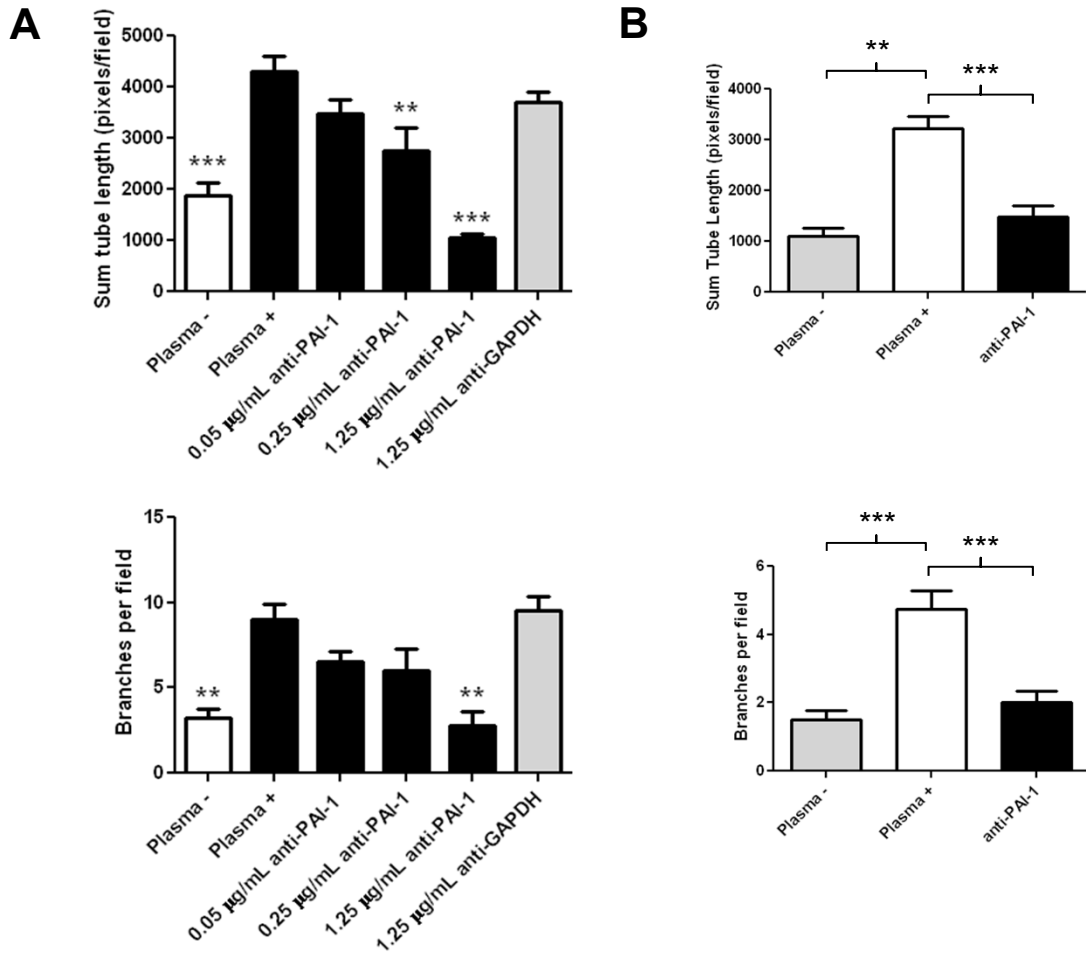
FIGURE 5.6. PAI-1 inhibition decreases angiogenesis *in utero.* Angiogenic tube formation assay of HUVECs in the presence of 1% venous umbilical cord plasma. PAI-1 antibody was added in indicated amounts, as well as plasma-free, and GAPDH antibody control. **(A)** Quantification of a single experiment after 9 hours incubation. Representative fields are shown in Figure 5.5. Significant differences from the Plasma + by one-way ANOVA are indicated. PAI-1 inhibited angiogenesis measured both by total tube length and branching. **(B)** Experiments were repeated for six fetal umbilical cord plasma samples, with and without 1 µg/mL of PAI-1 inhibiting antibody. Inhibiting PAI-1 decreased total tube length and number of branches significantly (one-way ANOVA). (*p<0.05, **p<0.01, ***p<0.001)

To determine if the angiogenic changes observed were directly related to PAI-1 levels, umbilical blood plasma was subjected to various concentrations of a PAI-1 activity inhibiting antibody. Representative fields from the tube formation assay are shown in Figure 5.5. Incubating umbilical cord with 0.25 µg/mL of antibody was sufficient to inhibit tube formation, 1.25 µg/mL inhibited tube formation to levels similar to cells grown in the absence of plasma. Quantifying the inhibition proved the changes to be significant: 1.25 µg/ml of anti-PAI-1 inhibited the total tube length and the branches per field ~2-fold ($p<0.001$ and 0.01 respectively) (Figure 5.6A). The finding was reproducible across six umbilical plasma samples (Figure 5.6B). PAI-1 inhibition completely disrupted endothelial tube formation to levels similar to plasma-free conditions, demonstrating the significance of extracellular circulating PAI-1 levels to angiogenesis.

5.4. DISCUSSION

The finding that the effluent blood plasma from pregnancies with placental insufficiency is pro-angiogenic is, at first glance, paradoxical, as placental insufficiency is characterized by diminished chorionic villi. Stimulators of placental angiogenesis FGF-2 and VEGF were associated with increased angiogenesis in controls, but were not responsible for the increased angiogenesis observed with FGR plasma. Thus, although our findings confirm that the role of VEGF in placental insufficiency is diminished, the discovery that levels of circulating PAI-1 are significantly elevated in FGR, and that the PAI-1 levels were strongly, positively associated with angiogenesis

in FGR is novel. Inhibition of PAI-1 reveals the extent of the angiogenic regulatory role circulating PAI-1 may be playing in the chorionic villi of placental insufficiency, as well as in other diseases like tumor vascularization. The association of increased PAI-1 expression with hypoxia demonstrates that its levels are directly regulated by hypoxic conditions in placental insufficiency through HIF-1 mediated transcription. Upregulation of PAI-1 in hypoxic conditions of FGR may be an adaptive mechanism to mitigate the poorly branched placental vasculature in late gestational hypoxia. Alternatively it may be maladaptive, whereby indiscriminate angiogenesis acts to the detriment of placental exchange, contributing to poorly branched chorionic villi, and exacerbating the pathology. It is unknown whether increased fetal PAI-1 in development may have a negative long-term effect on cardiovascular health in adulthood.

5.4.1 Sample selection

The samples selected are representative of very severe cases of FGR with placental insufficiency. The severely reduced umbilical oxygen levels and high carbon dioxide are indicative of the severely reduced exchange in the placenta. The venous umbilical cord pO_2 approximates that of placental oxygen, correlating 0.80 to the placental levels (19). Similarly, the low birthweight, percentile birthweight, placental weight, and particularly the increased placental resistance as measured by umbilical Doppler are hallmarks of FGR pregnancies with placental insufficiency. Increased vascular resistance in the placenta has been attributed to poor vascularization of the chorionic

villi (20). Particularly, an absence of branching and an abnormally long capillary tube lead to increased resistance in the terminal villous tree (1).

5.4.2. Vascular Regulation via VEGF/FGF-2

Angiogenesis in the branching phase is largely attributable to VEGF and FGF-2 (21). Although the levels of these cytokines did not change between control and FGR pregnancies, the levels of VEGF and FGF-2 correlated with angiogenic potency in controls (Figure 5.4Bii). PAI-1 expression is upregulated by VEGF and FGF-2 (11). The levels of FGF-2, but not VEGF, correlated modestly with PAI-1 levels (Figure 5.2B) (which in turn were strongly related to angiogenic potency (Figure 5.4A)) in controls only. This indicates a modest relationship between the expression of angiogenic cytokines, PAI-1 expression, and angiogenesis in normal pregnancy. Considering that inhibition of PAI-1 led to decreased angiogenesis, the evidence suggests that plasma PAI-1 levels are a potent central angiogenic mediator in normal cytokine mediated angiogenesis in the placenta.

Because neither VEGF nor FGF-2 increase in FGR, nor correlate to angiogenesis, nor PAI-1 expression in FGR, it is also apparent that changing levels of angiogenic cytokines do not account for the increase in angiogenesis seen in FGR. Since VEGF is regulated downstream of HIF-1, it is surprising that it does not increase in hypoxic conditions of FGR. Likewise, levels of VEGF (or FGF-2) do not correlate to the level of hypoxia in the blood (data not shown). Although this is surprising, it mirrors findings

by others who have also observed similar phenomena in FGR (7, 8). Thus while VEGF and FGF-2 are strong plasma mediators of angiogenesis in normal pregnancy, alternative mechanisms regulate the increased angiogenesis in FGR.

5.4.3. Vascular regulation via PAI-1 in hypoxic conditions

Angiogenesis is negatively regulated by hypoxia. The oxygen saturation in our blood samples (Figure 5.2C) directly correlated to tube length and the degree of branching (Figure 5.4Bi). PAI-1, like VEGF, is also upregulated via HIF-1 in hypoxia (17). PAI-1 levels moderately negatively correlated with venous oxygen levels (Figure 5.2A). PAI-1 levels in turn, were most strongly associated with angiogenesis (Figure 5.4A). The inhibition of PAI-1 led to drastically decreased angiogenic potential, demonstrating clearly the significance of circulating levels of PAI-1 to angiogenic regulation. Dosing umbilical plasma with 1.25 µg/mL of inhibiting antibody was sufficient to largely reverse plasma-induced angiogenesis *in vitro*. This is especially significant when considering the range of PAI-1 in normal pregnancy, compared to FGR with placental insufficiency. The range spans ~0-40 ng/ml in normal pregnancy, while in FGR it reaches nearly double that (Figure 5.1A). The total inhibition of PAI-1 then is not dissimilar to the PAI-1 levels in some control pregnancies (< 1µg/mL). Nor is the difference between control and FGR levels miniscule; a 4-fold increase in circulating PAI-1 levels in FGR could very plausibly have an effect on regulation of the chorionic villi based on these findings.

PAI-1 has been shown to be potently pro-angiogenic in doses approximating physiological. PAI-1 is thought to be pro-angiogenic by blocking excessive plasmin degradation of the ECM providing a stable platform for cell migration, proliferation, and vessel maturation (22). It additionally has a vitronectin binding function that may block the binding of endothelial integrins. PAI-1 is strongly associated with tumor vascularization, where its increased levels have been associated with poor prognosis (12, 23, 24). Mice lacking PAI-1 prevent invasion and vascularization of transplanted malignant tumors (25). It is required for post-ischemic injury angiogenesis in the retina in a murine model of angiogenesis (13). Recent studies have found that PAI-1 knockout mice have transiently reduced maternal and fetal-placental vasculature (14). Although it is unknown to what extent PAI-1 levels may affect angiogenesis in the chorionic villi of human pregnancies, it can be inferred from the preceding studies and the findings presented here that it is very likely to have a strong regulatory role.

5.4.4. Summary

Elevated PAI-1 is a negative prognostic indicator for cancer, and it has been hypothesized that the levels of PAI-1 promote tumor vascularization. Here, circulating PAI-1 levels were directly correlated to their angiogenic potency. Specifically, PAI-1 was found to be elevated in effluent placental plasma of newborns with fetal growth restriction caused by placental insufficiency. It was shown that PAI-1 levels determined the angiogenic potency of the placental plasma. Finally, this

increase in PAI-1 was demonstrated to be related to the hypoxic conditions of the pregnancy. These data together show that circulating fetal PAI-1 levels are a central mediator of angiogenesis, dually regulated by angiogenic cytokines VEGF and FGF-2 in normal pregnancy, and highly upregulated via hypoxia in placental insufficiency. PAI-1 may be contributing to the vascular pathology of the placental chorionic villi vasculature in FGR pregnancies with placental insufficiency. It remains to be determined whether the upregulation may have a mitigating effect on placental exchange or exacerbate the pathological blood flow resistance by contributing to elongated, but poorly branched, chorionic villi observed in placental insufficiency.

5.5. REFERENCES

1. Mayhew, T. M., Charnock-Jones, D. S., and Kaufmann, P. (2004) Aspects of Human Fetoplacental Vasculogenesis and Angiogenesis. III. Changes in Complicated Pregnancies. *Placenta. 25*, 127-139.

2. Charnock-Jones, D. S., Kaufmann, P., and Mayhew, T. M. (2004) Aspects of Human Fetoplacental Vasculogenesis and Angiogenesis. I. Molecular Regulation. *Placenta. 25*, 103-113.

3. Zygmunt, M., Herr, F., Munstedt, K., Lang, U., and Liang, O. D. (2003) Angiogenesis and Vasculogenesis in Pregnancy. *Eur. J. Obstet. Gynecol. Reprod. Biol. 110 Suppl 1*, S10-8.

4. Wang, K., Jiang, Y. Z., Chen, D. B., and Zheng, J. (2009) Hypoxia Enhances FGF2- and VEGF-Stimulated Human Placental Artery Endothelial Cell Proliferation: Roles of MEK1/2/ERK1/2 and PI3K/AKT1 Pathways. *Placenta. 30*, 1045-1051.

5. Pugh, C. W., and Ratcliffe, P. J. (2003) Regulation of Angiogenesis by Hypoxia: Role of the HIF System. *Nat. Med. 9*, 677-684.

6. Barut, F., Barut, A., Gun, B. D., Kandemir, N. O., Harma, M. I., Harma, M., Aktunc, E., and Ozdamar, S. O. (2010) Intrauterine Growth Restriction and Placental Angiogenesis. *Diagn. Pathol. 5*, 24.

7. Khaliq, A., Dunk, C., Jiang, J., Shams, M., Li, X. F., Acevedo, C., Weich, H., Whittle, M., and Ahmed, A. (1999) Hypoxia Down-Regulates Placenta Growth Factor, Whereas Fetal Growth Restriction Up-Regulates Placenta Growth Factor Expression: Molecular Evidence for "Placental Hyperoxia" in Intrauterine Growth Restriction. *Lab. Invest. 79*, 151-170.

8. Malamitsi-Puchner, A., Boutsikou, T., Economou, E., Sarandakou, A., Makrakis, E., Hassiakos, D., and Creatsas, G. (2005) Vascular Endothelial Growth Factor and Placenta Growth Factor in Intrauterine Growth-Restricted Fetuses and Neonates. *Mediators Inflamm. 2005*, 293-297.

9. Regnault, T. R., de Vrijer, B., Galan, H. L., Davidsen, M. L., Trembler, K. A., Battaglia, F. C., Wilkening, R. B., and Anthony, R. V. (2003) The Relationship between Transplacental O_2 Diffusion and Placental Expression of PlGF, VEGF and their Receptors in a Placental Insufficiency Model of Fetal Growth Restriction. *J. Physiol. 550*, 641-656.

10. Cetin, I., Foidart, J. M., Miozzo, M., Raun, T., Jansson, T., Tsatsaris, V., Reik, W., Cross, J., Hauguel-de-Mouzon, S., Illsley, N., Kingdom, J., and Huppertz, B. (2004) Fetal Growth Restriction: A Workshop Report. *Placenta. 25*, 753-757.

11. Pepper, M. S., Ferrara, N., Orci, L., and Montesano, R. (1991) Vascular Endothelial Growth Factor (VEGF) Induces Plasminogen Activators and Plasminogen Activator Inhibitor-1 in Microvascular Endothelial Cells. *Biochem. Biophys. Res. Commun. 181*, 902-906.

12. Bajou, K., Maillard, C., Jost, M., Lijnen, R. H., Gils, A., Declerck, P., Carmeliet, P., Foidart, J. M., and Noel, A. (2004) Host-Derived Plasminogen Activator Inhibitor-1 (PAI-1) Concentration is Critical for in Vivo Tumoral Angiogenesis and Growth. *Oncogene. 23*, 6986-6990.

13. Basu, A., Menicucci, G., Maestas, J., Das, A., and McGuire, P. (2009) Plasminogen Activator Inhibitor-1 (PAI-1) Facilitates Retinal Angiogenesis in a Model of Oxygen-Induced Retinopathy. *Invest. Ophthalmol. Vis. Sci. 50*, 4974-4981.

14. Labied, S., Blacher, S., Carmeliet, P., Noel, A., Frankenne, F., Foidart, J. M., and Munaut, C. (2011) Transient Reduction of Placental Angiogenesis in PAI-1-Deficient Mice. *Physiol. Genomics. 43*, 188-198.

15. Estelles, A., Gilabert, J., Keeton, M., Eguchi, Y., Aznar, J., Grancha, S., Espna, F., Loskutoff, D. J., and Schleef, R. R. (1994) Altered Expression of Plasminogen Activator Inhibitor Type 1 in Placentas from Pregnant Women with Preeclampsia and/or Intrauterine Fetal Growth Retardation. *Blood. 84*, 143-150.

16. Seferovic, M. D., Chen, S., Pinto, D. M., and Gupta, M. B. (2011) Altered Liver Secretion of Vascular Regulatory Proteins in Hypoxic Pregnancies Stimulate Angiogenesis in Vitro. *J. Proteome Res. 10*, 1495-1504.

17. Fink, T., Kazlauskas, A., Poellinger, L., Ebbesen, P., and Zachar, V. (2002) Identification of a Tightly Regulated Hypoxia-Response Element in the Promoter of Human Plasminogen Activator Inhibitor-1. *Blood. 99*, 2077-2083.

18. Arbuckle, T. E., Wilkins, R., and Sherman, G. J. (1993) Birth Weight Percentiles by Gestational Age in Canada. *Obstet. Gynecol. 81*, 39-48.

19. Nodwell, A., Carmichael, L., Ross, M., and Richardson, B. (2005) Placental Compared with Umbilical Cord Blood to Assess Fetal Blood Gas and Acid-Base Status. *Obstet. Gynecol. 105*, 129-138.

20. Mayhew, T. M., Wijesekara, J., Baker, P. N., and Ong, S. S. (2004) Morphometric Evidence that Villous Development and Fetoplacental Angiogenesis are Compromised by Intrauterine Growth Restriction but Not by Pre-Eclampsia. *Placenta. 25*, 829-833.

21. Kaufmann, P., Mayhew, T. M., and Charnock-Jones, D. S. (2004) Aspects of Human Fetoplacental Vasculogenesis and Angiogenesis. II. Changes during Normal Pregnancy. *Placenta. 25*, 114-126.

22. Bajou, K., Masson, V., Gerard, R. D., Schmitt, P. M., Albert, V., Praus, M., Lund, L. R., Frandsen, T. L., Brunner, N., Dano, K., Fusenig, N. E., Weidle, U., Carmeliet, G., Loskutoff, D., Collen, D., Carmeliet, P., Foidart, J. M., and Noel, A. (2001) The Plasminogen Activator Inhibitor PAI-1 Controls in Vivo Tumor Vascularization by Interaction with Proteases, Not Vitronectin. Implications for Antiangiogenic Strategies. *J. Cell Biol. 152*, 777-784.

23. McMahon, G. A., Petitclerc, E., Stefansson, S., Smith, E., Wong, M. K., Westrick, R. J., Ginsburg, D., Brooks, P. C., and Lawrence, D. A. (2001) Plasminogen Activator Inhibitor-1 Regulates Tumor Growth and Angiogenesis. *J. Biol. Chem. 276*, 33964-33968.

24. Duffy, M. J. (2002) Urokinase Plasminogen Activator and its Inhibitor, PAI-1, as Prognostic Markers in Breast Cancer: From Pilot to Level 1 Evidence Studies. *Clin. Chem. 48*, 1194-1197.

25. Bajou, K., Noel, A., Gerard, R. D., Masson, V., Brunner, N., Holst-Hansen, C., Skobe, M., Fusenig, N. E., Carmeliet, P., Collen, D., and Foidart, J. M. (1998) Absence of Host Plasminogen Activator Inhibitor 1 Prevents Cancer Invasion and Vascularization. *Nat. Med. 4*, 923-928.

CHAPTER 6

Maternal and fetal vascular inflammation in placental insufficiency: VCAM-1 as a marker of placental health

6.1. INTRODUCTION

Endothelial activation has important roles in angiogenesis and in vascular reorganization. The cellular adhesion molecules (CAMs) E-selectin, VCAM-1 and ICAM-1 are up-regulated by the endothelium, and are known to recruit leukocytes following injury. More recently they have been shown to contribute to angiogenesis by recruitment of endothelial progenitors in circulation (1, 2, 3). Soluble levels of VCAM-1 and ICAM-1 have been demonstrated to up-regulate angiogenesis (4, 5). Their involvement in tumor vascularization is an area of ongoing interest (6, 7).

In the placenta, CAMs are thought to be critical for normal vascular function. VCAM-1, for example, is required for blood vessel formation (8). A murine model lacking VCAM-1 results in embryonic lethality due to vascular malformations in the placenta (9, 10). ICAM-1 up-regulation is critically important for angiogenesis following ischemic injury (1, 2). CAMs E-selectin, VCAM-1 and ICAM-1 are expressed with increasing levels of VEGF and FGF-2 via NF-κB (11, 12). They are also potently upregulated by inflammatory cytokines.

The perturbation of normal vascular development in placental insufficiency leads to malformation of the placental vasculature. Elongated, poorly branched chorionic villi exhibit increased resistance, leading to absent or reversed blood flow and poor perfusion of the fetal-placenta. In these conditions, there is strong evidence of maternal or fetal placental-vascular inflammation (13). Inflammation leads to endothelial activation, marked by expression of cellular adhesion molecules (CAMs). Continuous activation causes endothelial dysfunction and aberrant angiogenesis,

which contributes to the pathology of many diseases, such as rheumatoid arthritis and inflammatory bowel disease (12, 14, 15). Aberrant inflammation leading to endothelial dysfunction is hypothesized to be contributing to placental insufficiency, and there has been much evidence to suggest maternal and fetal-placental inflammation is occurring.

Bartha and others found elevated levels of TNF-α in mother's serum of 14 FGR women with placental insufficiency, but not without (16). Maternal polymorphisms in anti-inflammatory or inflammatory cytokines has been associated with increased risk of FGR (17, 18, 19). There is increased endothelial activation as well. It was found that all three of VCAM-1, ICAM-1 and E-selectin were increased 1.5 to 3-fold in the maternal plasma of pregnancies with FGR, however there was no change in the levels of IL-6 and TNF-α. In FGR with preeclampsia, all of the three CAMs as well as IL-6 and TNF-α were increased (20).

In the fetal placenta, the inflammation may be more pronounced. Holcberg and others found a 10-fold increase in secretion of TNF-α in vascular perfusions of FGR placenta compared to control pregnancies (21). A recent study found levels of IL-6 but not TNF-α to be elevated in the umbilical cords of SGA infants compared to AGA (22). The expression of inflammatory cytokines IL-6, Il-8, and the suppressors of cytokine signaling (SOCS) 2 and 3 were found to be increased in the endothelium of the fetal-placental microvasculature in placental insufficiency (23).

The increased inflammation may be brought about by conditions of hypoxia. Hypoxic treatment of placental villous explants has been shown to induce expression of

inflammatory cytokines (24). In the maternal intervillous space in placental insufficiency, poor exchange leads to supraoxic conditions as the fetus fails to extract oxygen from the maternal supply (25). Maternal inflammation then may be associated with localized supraoxic conditions.

Markers of placental inflammation detectable in the placental blood that correlate to hypoxia would be ideally suited as a marker of placental health. There has been considerable interest in the discovery of biomarkers of FGR (7, 26, 27, 28, 29). The discovery of a biomarker that may be used in a maternal blood based screening test for the detection of FGR however remains to be elucidated. In this study, we determined the suitability of vascular CAMs as markers of placental health. We first established the degree of maternal and fetal vascular inflammation in severe FGR pregnancies with placental insufficiency by measuring soluble CAMs. We then determined the association of inflammatory cytokines IL-6 and TNF-α expression to hypoxic conditions at delivery, and the degree to which these cytokines are associated with altered CAM expression.

6.2.   MATERIALS AND METHODS

6.2.1. Subject recruitment

Pregnant women admitted for care at St. Joseph's Hospital, London, ON Canada were recruited for this study. This study was approved by the Human Ethics Review Board of The University of Western Ontario and conducted with written informed consent

from participants. Pregnancies with placental insufficiency and suspected growth restricted fetus were included. Antenatal identification of pregnant women in the FGR group was based on last trimester-estimated weights of the fetuses as determined by fetal biometric ultrasound measurements. Gestational age (GA) was determined by certain last menstrual date of mothers or the first trimester ultrasound crown rump length. Placental insufficiency was determined by abnormal umbilical artery Doppler (30). Fetal growth was compared using the Canadian growth chart for estimation of fetal weight less than the 10th percentile (31). At birth, the percentiles were calculated and confirmed based on their respective gender and GA using standardized growth charts for birth weight (31). Mothers of FGR pregnancies were otherwise healthy. Abruption placenta, fetal congenital abnormalities, fetal infection, preeclampsia, drug use, and maternal diabetes were all exclusion criteria for the study.

6.2.2. Plasma collection

Plasma was collected by venipuncture from the mother just prior to delivery, and from the fetus via the venous umbilical cord immediately following delivery of the placenta, after clamping the vessel. Healthy pregnancies were selected for controls based on matching gestational age. Samples were collected in EDTA coated tubes, centrifuged at 2000 x g for 15 min at 4°C and clear plasma samples saved in small aliquots at -80°C.

Birthweight percentiles were calculated post-delivery. The average birthweight was less than the 2nd percentile for FGR patients, and all GA matching control birthweights selected to be above the 25th percentile. All deliveries were performed with either epidural or spinal anesthetic or were natural deliveries. Pathological reports for the placentas were negative for signs of infection, major infarcts, or other gross anomalies. Umbilical blood gas levels were also abstracted from the chart for all but one patient (FGR group).

6.2.3. Protein measurements and statistical evaluations

All total protein quantifications were by Bradford method (BioRad). IL-1β, IL-6, TNF-α, E-selectin, VCAM-1, and ICAM-1 were measured by an immunological-based fluorescent multiplex assays (Human CVD and MPXHCYTO, Millipore, Billerica, MA, USA) using a Bio-Plex 200 system (Bio-Rad), which utilizes Luminex® xMAPTM fluorescent bead-based technology (Luminex Corp., Austin, TX). Levels were automatically calculated from standard curves using Bio-Plex Manager software (v.4.1.1, Bio-Rad). Statistics were performed using GraphPad Prism 5 (Graph Pad Software Inc, CA, USA). To compare means, t-tests, paired t-tests, Mann-Whitney, or one-way ANOVAs were used where appropriate. Pearson's Correlation compared proteins' levels to each other, to the blood oxygen levels, placenta weight, birthweight, and several other metrics abstracted from the clinical charts.

TABLE 6.1. Characteristics of FGR and gestational age-matched control pregnancies from which maternal and venous umbilical cord blood samples were collected.

		Fetal		Maternal	
		Control	FGR	Control	FGR
Subjects (n)	*M/F*	6/5	6/3	6/6	5/4
	Total:	11	9	12	9
Delivery	Vag./ces.	6/5	7/2	7/5	4/5
Birthweight (g)		2170 (670)	**1453* (624)**	2343 (854)	1738 (733)
Gestational age (wks)		33.7 (3.7)	34.0 (4.3)	34.5 (4.7)	35.6 (4.9)
Birthweight percentile		53 (19)	**1.7*** (2.9)**	40.0 (25)	**1.0*** (1.5)**
Placental weight (g)		532 (124)	**385* (173)**	514 (121)	**385* (170)**
Placental Resistance[+]		0.63 (0.09)	**0.99**(0.24)**	0.63 (0.10)	**0.92* (0.28)**
Blood gases					
Arterial:	*pO2 (Torr)*	19.6 (6.2)	**13.2* (4.7)**	17.4 (4.0)	14.6 (4.1)
	pCO2 (Torr)	47.9 (6.2)	**55.1* (4.9)**	51.1 (6.3)	51.7 (7.7)
	pH	7.29 (0.04)	7.25 (0.05)	7.28 (0.05)	7.26 (0.04)
Venous:	*pO2 (Torr)*	34.7 (6.5)	**22.6*** (4.5)**	35.6 (7.4)	**25.1** (6.3)**
	pCO2 (Torr)	32.6 (6.7)	**45.0*** (3.9)**	32.4 (9.8)	**42.0* (5.1)**
	pH	7.34 (0.03)	**7.32* (0.03)**	7.34 (0.02)	7.33 (0.03)
Maternal BP	*Systolic*	113 (11)	**133* (17)**	117 (13)	124 (23)
	Diastolic	71 (8)	81 (17)	72 (110)	85 (20)
APGAR (5 min)		8.8 (0.4)	8.3 (1.4)	8.7 (0.8)	8.4 (1.0)

Comparison of means by t-test (*p<0.05, **p<0.01, ***p<0.001). Standard deviation is indicated in brackets. [+]Placental resistance index from the last umbilical cord Doppler ultrasound prior to delivery, which was performed for all FGR, but only 7 controls.
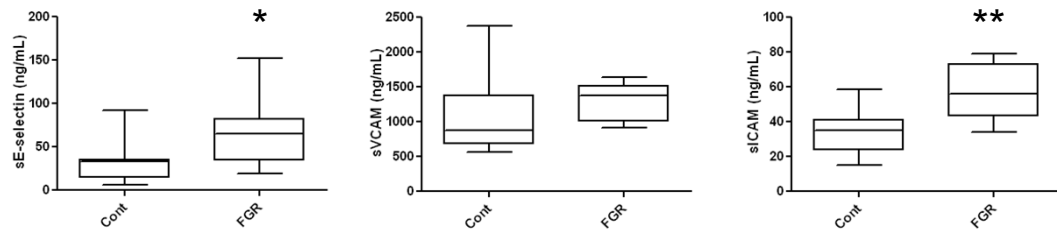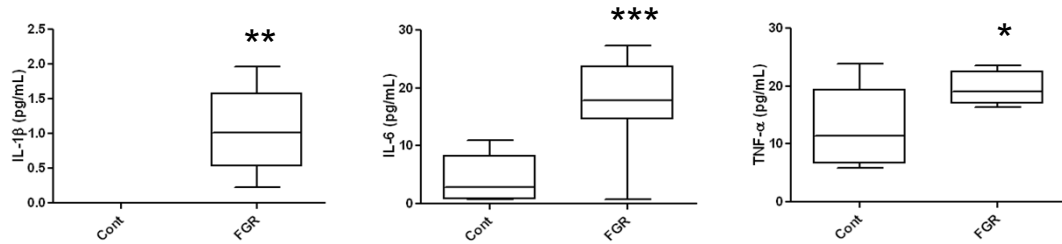
FIGURE 6.1. Fetal venous umbilical cord plasma levels of proteins in FGR (n=9) samples compared to controls (n=11). **(A)** Endothelial activation markers **(B)** Inflammatory cytokines. (t-test, *p<0.05, **p<0.01. Whiskers indicate range.)

6.3.   RESULTS

Maternal blood was collected by venipuncture at time of delivery from severe FGR mothers with placental insufficiency. Following delivery, effluent placental blood was taken from the umbilical vein. Healthy pregnancies were selected based on matching GA within one week for each of the FGR samples collected. FGR pregnancies were very severe with a significantly smaller percentile birthweight compared to controls, which on average was much lower than the 3rd percentile (Table 6.1). FGR pregnancies also had significantly smaller placental weight. The placental resistance index for FGR pregnancies was significantly higher for FGR patients when measured in the week prior to delivery. All FGR patients were determined to have placental insufficiency, and an absence of preeclampsia. The reduced venous oxygen and increased carbon dioxide in venous umbilical cord is indicative of the poor maternal/fetal exchange.

The levels of markers of vascular inflammation E-selectin, VCAM-1 and ICAM-1, along with their inflammatory cytokine regulators Il-1ß, Il-6, and TNF-α were measured using a highly sensitive Luminex multiplex fluorescent assay. The cellular adhesion molecules E-Selectin and ICAM-1 increased ~2-fold in FGR compared to control ($p<0.05$ and $p<0.01$ respectively) (Figure 6.1A). Their inflammatory cytokine regulators were also increased (Figure 6.1B). IL-1β increased at least 3-fold, although it is impossible to determine precisely as all controls were below the sensitivity limits of the assay ($p<<0.01$) (Figure 6.1B). Cytokines Il-6 and TNF-α, also increased approximately 5-fold and 2-fold ($p<0.001$ and 0.05 respectively) (Figure 6.1B).
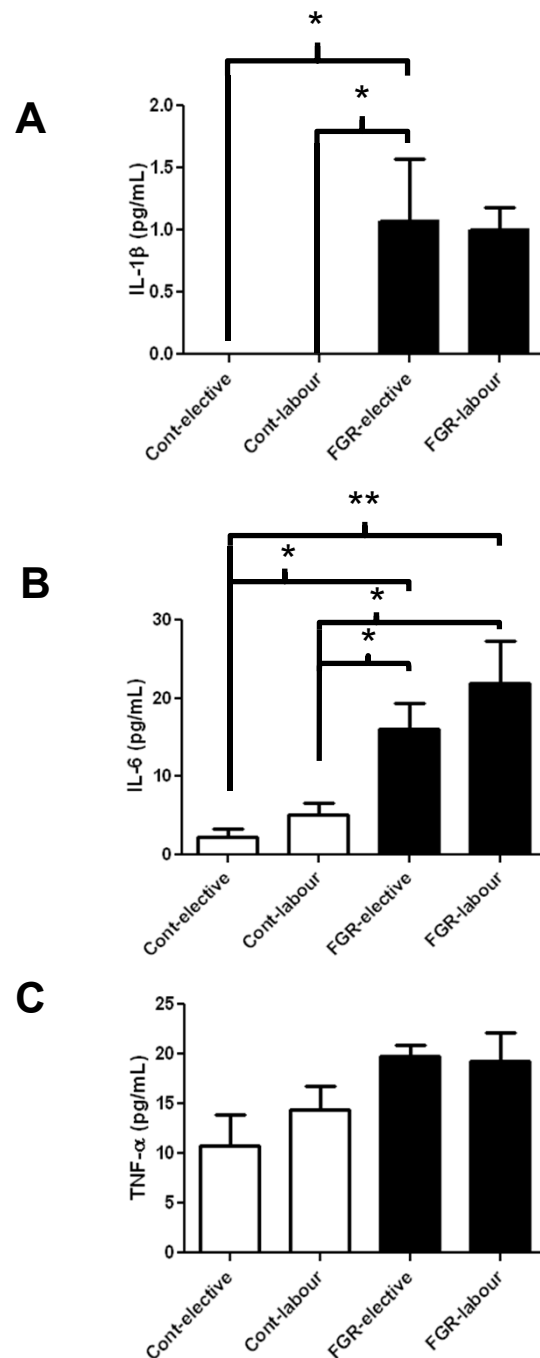
Figure 6.2. Changing levels of inflammatory cytokines by delivery type. Labor (either induced or spontaneous) compared to elective deliveries. **(A)** There was no difference in IL-1β in the FGR group. **(B)** Controls had significantly reduced levels of IL-6 regardless of labor mode. **(C)** Levels of TNF-α were unchanged. (one-way ANOVA, Tukey's post test, *$p<0.05$, **$p<0.01$. Standard error indicated).
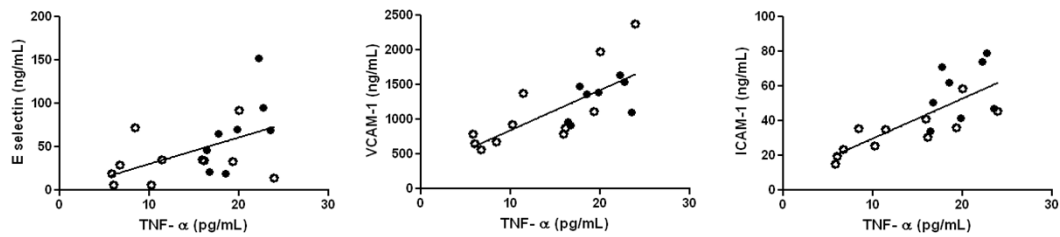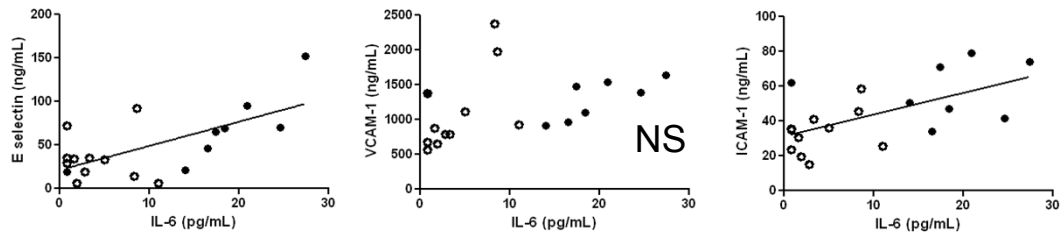
Figure 6.3. Increased levels of circulating cytokines strongly relate to increased endothelial activation. **(A)** TNF-α increased expression of E-Selectin, VCAM-1, and ICAM-1 strongly (r=0.50, 0.75, and 0.73, p<0.05, 0.001, and 0.001 respectively). **(B)** IL-6 increased the expression of E-Selectin and ICAM-1 as well (r=0.66 and 0.60, respectively, p<0.01). (open: Control, closed: FGR).

As the levels of IL-6 have been reported to increase in labor (32), the measurements of cytokines were separated by delivery type. Delivery following labor (either induced or natural, either vaginal delivery or subsequent caesarean section), and elective caesarean section were evaluated separately (Figure 6.2). Although IL-6 appeared to increase between the labor and elective groups for both controls and FGR, the difference was not significant with the number of samples analyzed (elective caesarean n=4, labor n=7). Regardless of either labor or elective birth however, the FGR group was highly elevated compared to control for IL-6 (Figure 6.2).

The increased levels of cytokines appeared to be causing endothelial activation in the fetal-placental vasculature. Increased IL-6 in the fetus correlated with both E-selectin and ICAM-1 levels (r=0.57 and 0.55, p<0.01 and 0.05 respectively) (Figure 6.3B). Similarly increased levels of TNF-α were also correlated (r=0.49 and 0.74, p<0.05 and 0.001 respectively) (Figure 6.3A). Despite the levels of VCAM-1 not being significantly increased, the expression of VCAM-1 was highly dependent on the levels of circulating TNF-α levels in the fetus (r=0.73, p<0.001), but not levels of IL-6 (Figure 6.3A).

Increased cytokine-mediated vascular inflammation is partially caused by conditions of hypoxia. Both IL-6 and TNF-α levels increased as venous umbilical cord oxygen levels decreased (r=-0.51, and -0.71, p<0.05, and 0.001 respectively) (Figure 6.4). Similarly, levels of ICAM-1 were increased in hypoxia (Figure 6.4). The association of increased ICAM-1 levels with hypoxia may be a result of intermediary inflammatory
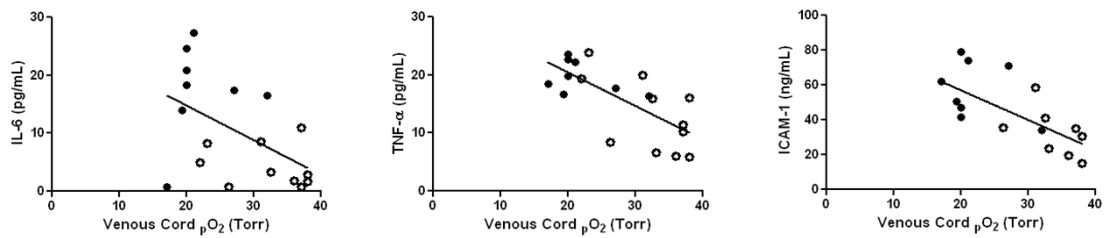
FIGURE 6.4. Inflammatory cytokines and ICAM-1 levels increase in the presence of hypoxia. Il-6, TNF-α, and ICAM-1 were increased as venous umbilical cord oxygen levels decreased (r=-0.51, -0.71, and -0.69, p<0.05, 0.001, and 0.001 respectively) (open: Control, closed: FGR).
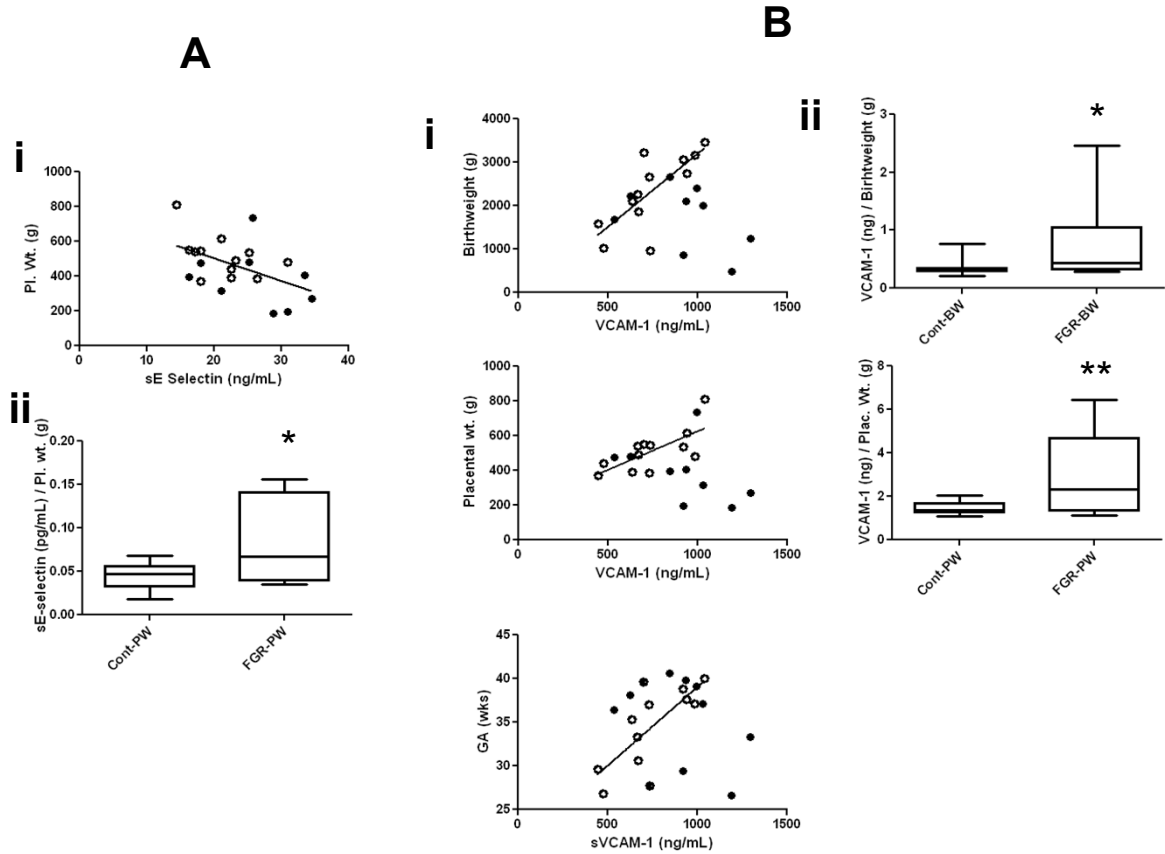
FIGURE 6.5. Maternal levels of cellular adhesion molecules (CAMs) correlate to physiologic metrics of the pregnancy. **(A)** E-selectin is negatively correlated to placental size (r=-0.50, p<0.05) (i). Its levels are increased in FGR relative to placental size (ii). **(B)** (i) Levels of VCAMs correlate to birthweight (r=0.75, p<0.01), placental weight (r=0.70, p<0.01) and gestational age (r=0.73, p<0.01) in normal (control) pregnancies. (ii) Maternal levels of VCAM-1 are stable and proportional to the size of either the fetus or the placenta in control pregnancies, but are upregulated in FGR pregnancies relative to fetal/placenta size (Wilcoxon, *p<0.05, **p<0.01. Whiskers indicate range) (open Control, closed FGR).

cytokines upregulation in hypoxia. ICAM-1 was strongly induced by IL-6 and particularly TNF-α level (Figure 6.3A).

To assess if the vascular inflammation was confined to the fetal-placental vasculature, the maternal plasma was assessed as well. None of the CAMs or inflammatory cytokines was increased (Supplemental Figure 6.1). Similarly, there was no correlation of maternal expression of any of the CAMs or inflammatory cytokines between mothers and the matching blood of their fetus (n=6 FGR and 6 control).

Nevertheless, there was a significant relationship between the expression of CAMs and metrics of fetal-placental size at birth. For E-selectin, there was increased circulating levels in the mother who had a smaller placentas (r=-0.50, p<0.05) (Figure 6.5Ai). This indicates a greater degree of endothelial activation in the placenta of FGR mothers with placental insufficiency. E-selectin is therefore increased with placental malfunction; smaller FGR placentas have disproportionately increased E-Selectin expression (~1.5 fold, p<0.05) (Figure 6.5Aii).

For VCAM-1 there was an increase in its expression strongly proportional to both placental weight (r=0.70, p<0.01), and also birthweight (r=0.75, p<0.01), as well as to gestational age (r=0.73, p<0.01) (Figure 6.5Bi). Unlike for E-selectin, these associations were observable very strongly in controls. FGR VCAM-1 levels were decoupled from these metrics, and instead appeared aberrantly elevated. This is suggestive that VCAM-1 expression increases as part of normal placental growth and development. Assuming the changing VCAM-1 levels are related to placental expression, increasing VCAM-1 with placental weight is logical as the vascular bed is
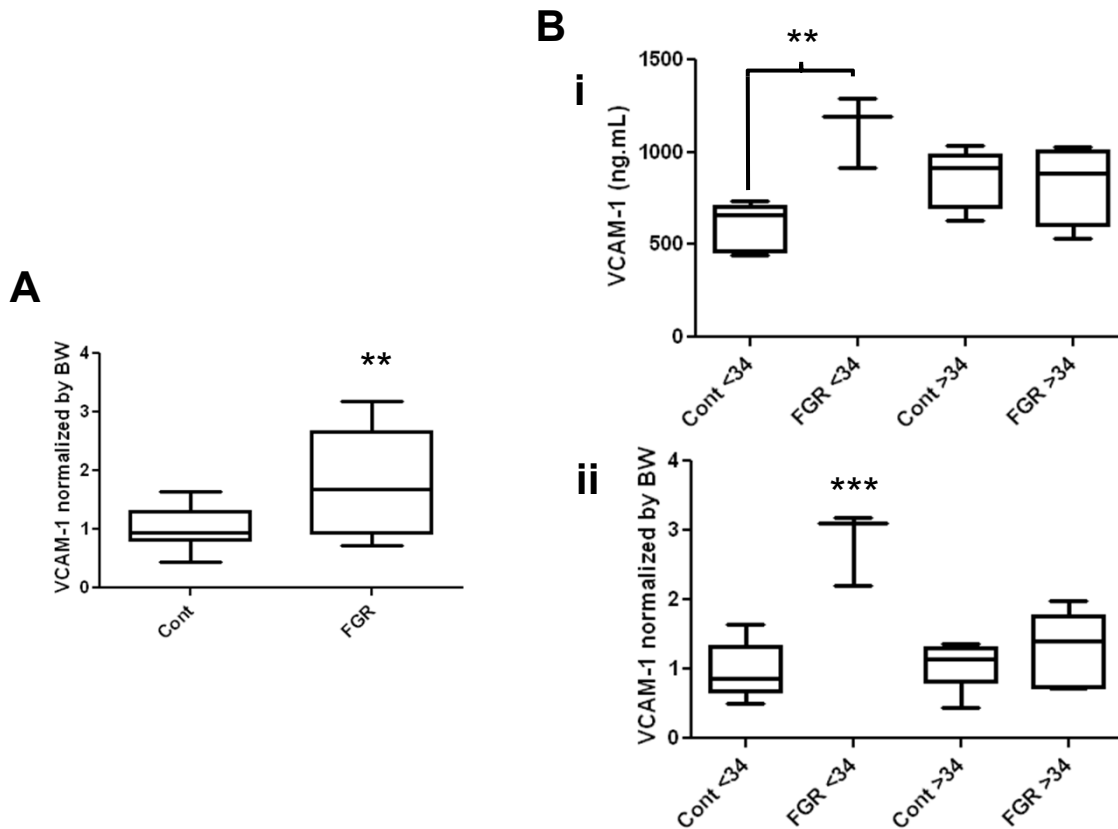
FIGURE 6.6. Maternal levels of VCAM-1, as a candidate biomarker of placental distress. **(A)** Close association of VCAM-1 with birthweight (Figure 6.5Bi) was used to normalize the control and FGR data for expected levels given birthweight. VCAM-1 levels normalized by birthweight show significant elevation of VCAM-1 in placental insufficiency. **(B)** (i) GA effects show that VCAM-1 is elevated in FGR, particularly before the last month of pregnancy. (ii) Normalizing by birthweight accentuates the GA differences between earlier GA FGR and later GA FGR. (Wilcoxon or ANOVA with Tukeys post test, *p<0.05, **p<0.01, ***p<0.001. Whiskers indicate range.) (Open: Control, Closed: FGR).

increased. Likewise, birthweight is strongly correlated to placental size, and increased VCAM-1 would also be expected as the placental vasculature continues to develop later in gestation. In FGR then, VCAM-1 is 1.5 to 2-fold more highly expressed in the maternal circulation relative to the size of the placenta (p<0.01) and also the fetus (birthweight, p<0.05) (Figure 6.5Bii).

Elevated levels of VCAM-1 in the mother's circulation relative to the fetal size may therefore be predictive of placental development. Although placental size is difficult to assess prior to delivery, fetal size is estimated routinely in pregnancy by ultrasound. A high level of VCAM-1 for the estimated fetal weight may therefore be a metric that distinguishes the control and placental insufficiency pregnancies more distinctly. To assess this possibility, we normalized the levels of VCAM-1 by birthweight, adjusting for the slope (0.1688 ng/mL VCAM-1 per g birthweight) of the line of best fit for the birthweight vs VCAM-1 relationship (Figure 6.5Bi). The results show clearly that in FGR there is a two fold increase in circulating maternal VCAM-1 relative to birthweight that is significant at delivery (p<0.01) (Figure 6.6A). To assess the differences before the prenatal period, when they would be of predictive value, the samples were separated into the perinatal period (>34 weeks) and pre-perinatal period (<34 weeks). VCAM-1 expression without normalizing by birthweight showed distinct, significant differences between control and FGR in the pre-perinatal period, but not in the perinatal period (Figure 6.6Bi). Normalizing by birthweight accentuated this difference from 2.5-fold (p<0.1) to 3.5-fold (p<0.001) (Figure 6.6Bii). VCAM-1, when normalized for birthweight, was also higher in FGR in pre-perinatal

period than it was in either control or FGR in the perinatal period (p<0.001) (Figure 6.6Bii).

The results suggest that VCAM-1 expression may peak relative to placental size in the pre-perinatal period when placental vascular development is most active. Whereas in normal pregnancy VCAM-1 expression may stay stable or increase from the pre-perinatal to perinatal period, the results show that in placental insufficiency, VCAM-1 is highly elevated in the pre-perinatal period, and may in fact decrease in the perinatal period.

6.4.   DISCUSSION

The results show there is substantial vascular inflammation of the fetal vasculature in placental insufficiency, and that this inflammation is closely correlated to a strong upregulation of inflammatory cytokines. Here we directly associated the vessel inflammation to hypoxic conditions of the placenta, measured in effluent placental blood at delivery. Hypoxic-mediated up-regulation of inflammatory cytokines is at least partially causal of vessel inflammation, as their expression negatively correlated to oxygen tension. The data furthermore confirm that there is some maternal vascular inflammation. The expression of CAMs relative to placental size indicates its localization at the maternal fetal interface. Finally we identify maternal soluble levels of VCAM-1 as a molecule with the potential for a predictive role in determining the presence of placental failure.

6.4.1. Fetal Inflammation

There is a large degree of vascular inflammation in the fetus, indicated by the highly elevated levels of the cytokines IL-1β, Il-6, and TNF-α, and CAMs E-selectin, and ICAM-1 in the FGR fetus. The results shown here are similar to previous findings of inflammation, however we were able to directly associate IL-6, TNF- α, and ICAM-1 expression with the degree of venous umbilical hypoxia. Venous umbilical cord pO_2 approximates that of the placenta, correlating 0.80 to the placental levels (33). Furthermore, there was a strong correlation of circulating Il-6 and TNF-α to the CAMs demonstrating that the upregulation of the CAMs is strongly related to cytokine-mediated inflammation in placental insufficiency.

Continual endothelial activation via TNF-α and IL-6 causes endothelial dysfunction. However, it has also been shown to induce endothelial sprouting (14). TNF-α has pro-angiogenic effects in the presence of cofactors *in vivo* (34). It has also been shown that TNF-α directly primes endothelial cells for an angiogenic response following inflammation, initially suppressing VEGF signaling until the inflammation has cleared (35). Recent findings have shown that TNF-α induces vascular remodeling in a murine model of chronic inflammation (36). Under conditions of chronic inflammation, normal angiogenesis may be suppressed and vessel remodeling induced in the placental microvasculature. Although it is apparent that inflammation has some pro-angiogenic effect, chronic inflammation, and the accompanying endothelial

dysfunction, in placental insufficiency may be detrimental to normal vascular development and maternal/fetal exchange.

6.4.2. Maternal Inflammation

Although vascular inflammation on the maternal side was not obvious from changing levels of CAMs or inflammatory cytokines, there was an increase of VCAM-1 and E-selectin expression relative to placental size. The inflammation therefore appears minimal compared to the fetal inflammation. Like others (20, 37), and unlike what is observed in the fetus, we found no relationship between the levels of cytokines and the CAM expression in the mother. Bartha and others found an increase in TNF-α levels in the maternal circulation (38). The disparity may be in the episodic nature of cytokine production compared to sustained tissue inflammation, the relatively short half-life in circulation compared to other proteins, and the proximity of the site of sampling in the mother's arm (antecubital venipuncture) from the site of inflammation, the maternal-placental circulation. In the fetus by comparison, there is greater inflammation apparent because the sampling is the effluent placental plasma directly, and also that chronic hypoxia may be leading to more systemic and severe inflammation.

In placental insufficiency, maternal blood in the intervillous space and blood returning to the mother's heart via the uterine veins is supraoxic as the fetal chorionic villi have failed to extract sufficient oxygen and nutrients from the maternal

supply (25). Oxidative stress causes inflammation and cytokine production via ROS-mediated NF-κB activation. The syncytiotrophoblast expresses E-Selectin, VCAM-1, and ICAM-1 (39), and therefore conditions of transient placental oxygen, or fetal hypoxia, may be leading to their production. Other factors may also be implicated. The release of syncytiotrophoblast membrane fragments has been suggested. It has also been shown that primary trophoblast cells from complicated pregnancies can induce endothelial activation in maternal post-placental vessels by secretion of chymotrypsin-like proteases (40, 41).

6.4.3. VCAM-1 as a Biomarker

Plasma levels of both soluble E-selectin and VCAM-1 are pro-angiogenic in a sialyl Lewis-X dependent mechanism (42). VCAM-1 is expressed only in very low amounts from endothelial cells in mature quiescent vasculature, however is rapidly up-regulated in inflammation or injury, or conversely in angiogenesis (8, 43). VCAM-1 deletion is embryonic lethal in mice due to its importance to vascular formation in the placenta (9, 10). Importantly, it is expressed from proliferating endothelial cells, and it is required for blood vessel formation (8). VCAM-1 expression correlates to placental weight in controls but not FGR, and increases with GA, indicating that VCAM-1 is functioning in normal placental vascular development. Taken together, it strongly suggests that VCAM-1 increases are indicative of ongoing vascular expansion associated with placental growth, and therefore VCAM-1 changes in circulation are caused by events in the placental vasculature. Although increased VCAM-1 with

placental size and GA may be normally related to angiogenesis, its increase in FGR was in a manner unrelated to GA or placental weight. Its increase in expression in FGR may be due to localized inflammation.

The discovery of VCAM-1 levels tracking the progression of placental vascular development reveals a potential biomarker for monitoring placental health. As VCAM-1 is expressed minimally in quiescent vasculature, its blood plasma levels may reflect placental angiogenic or inflammatory changes very sensitively. Indeed, the levels of VCAM-1 in normal pregnancies have minimal variability when birthweight and placental weight are considered (Figure 6.5Bii). By testing maternal plasma VCAM-1 levels at regular intervals throughout gestation, the detection of a decrease in VCAM-1, particularly late in gestation, may indicate placental failure. Establishing typical VCAM-1 levels by estimated fetal weight may increase the predictive power of VCAM-1. A large prospective study to monitor VCAM-1 throughout gestation is therefore suggested to establish its predictive potential. Furthermore, combining the fetal weight estimates, done routinely by ultrasound, with VCAM-1 levels into standardized expected VCAM-1 levels for the fetal size is the antecedent step in determining its baseline expression utility.

6.5. REFERENCES

1. Hristov, M., Zernecke, A., Liehn, E. A., and Weber, C. (2007) Regulation of Endothelial Progenitor Cell Homing After Arterial Injury. *Thromb. Haemost. 98*, 274-277.

2. Wu, Y., Ip, J. E., Huang, J., Zhang, L., Matsushita, K., Liew, C. C., Pratt, R. E., and Dzau, V. J. (2006) Essential Role of ICAM-1/CD18 in Mediating EPC Recruitment, Angiogenesis, and Repair to the Infarcted Myocardium. *Circ. Res. 99*, 315-322.

3. Oh, I. Y., Yoon, C. H., Hur, J., Kim, J. H., Kim, T. Y., Lee, C. S., Park, K. W., Chae, I. H., Oh, B. H., Park, Y. B., and Kim, H. S. (2007) Involvement of E-Selectin in Recruitment of Endothelial Progenitor Cells and Angiogenesis in Ischemic Muscle. *Blood. 110*, 3891-3899.

4. Koch, A. E., Halloran, M. M., Haskell, C. J., Shah, M. R., and Polverini, P. J. (1995) Angiogenesis Mediated by Soluble Forms of E-Selectin and Vascular Cell Adhesion Molecule-1. *Nature. 376*, 517-519.

5. Deng, C., Zhang, D., Shan, S., Wu, J., Yang, H., and Yu, Y. (2007) Angiogenic Effect of Intercellular Adhesion Molecule-1. *J. Huazhong Univ. Sci. Technolog Med. Sci. 27*, 9-12.

6. Francavilla, C., Maddaluno, L., and Cavallaro, U. (2009) The Functional Role of Cell Adhesion Molecules in Tumor Angiogenesis. *Semin. Cancer Biol. 19*, 298-309.

7. Jain, R. K., Koenig, G. C., Dellian, M., Fukumura, D., Munn, L. L., and Melder, R. J. (1996) Leukocyte-Endothelial Adhesion and Angiogenesis in Tumors. *Cancer Metastasis Rev. 15*, 195-204.

8. Garmy-Susini, B., Jin, H., Zhu, Y., Sung, R. J., Hwang, R., and Varner, J. (2005) Integrin alpha4beta1-VCAM-1-Mediated Adhesion between Endothelial and Mural Cells is Required for Blood Vessel Maturation. *J. Clin. Invest. 115*, 1542-1551.

9. Kwee, L., Baldwin, H. S., Shen, H. M., Stewart, C. L., Buck, C., Buck, C. A., and Labow, M. A. (1995) Defective Development of the Embryonic and Extraembryonic Circulatory Systems in Vascular Cell Adhesion Molecule (VCAM-1) Deficient Mice. *Development. 121*, 489-503.

10. Gurtner, G. C., Davis, V., Li, H., McCoy, M. J., Sharpe, A., and Cybulsky, M. I. (1995) Targeted Disruption of the Murine VCAM1 Gene: Essential Role of VCAM-1 in Chorioallantoic Fusion and Placentation. *Genes Dev. 9*, 1-14.

11. Kim, I., Moon, S. O., Kim, S. H., Kim, H. J., Koh, Y. S., and Koh, G. Y. (2001) Vascular Endothelial Growth Factor Expression of Intercellular Adhesion Molecule 1 (ICAM-1), Vascular Cell Adhesion Molecule 1 (VCAM-1), and E-Selectin through Nuclear Factor-Kappa B Activation in Endothelial Cells. *J. Biol. Chem. 276*, 7614-7620.

12. Szekanecz, Z., and Koch, A. E. (2007) Mechanisms of Disease: Angiogenesis in Inflammatory Diseases. *Nat. Clin. Pract. Rheumatol. 3*, 635-643.

13. Boutsikou, T., Mastorakos, G., Kyriakakou, M., Margeli, A., Hassiakos, D., Papassotiriou, I., Kanaka-Gantenbein, C., and Malamitsi-Puchner, A. (2010) Circulating Levels of Inflammatory Markers in Intrauterine Growth Restriction. *Mediators Inflamm. 2010*, 790605.

14. Rajashekhar, G., Willuweit, A., Patterson, C. E., Sun, P., Hilbig, A., Breier, G., Helisch, A., and Clauss, M. (2006) Continuous Endothelial Cell Activation Increases Angiogenesis: Evidence for the Direct Role of Endothelium Linking Angiogenesis and Inflammation. *J. Vasc. Res. 43*, 193-204.

15. Scaldaferri, F., Vetrano, S., Sans, M., Arena, V., Straface, G., Stigliano, E., Repici, A., Sturm, A., Malesci, A., Panes, J., Yla-Herttuala, S., Fiocchi, C., and Danese, S. (2009) VEGF-A Links Angiogenesis and Inflammation in Inflammatory Bowel Disease Pathogenesis. *Gastroenterology. 136*, 585-95.e5.

16. Bartha, J. L., Romero-Carmona, R., and Comino-Delgado, R. (2003) Inflammatory Cytokines in Intrauterine Growth Retardation. *Acta Obstet. Gynecol. Scand. 82*, 1099-1102.

17. Engel, S. A., Olshan, A. F., Savitz, D. A., Thorp, J., Erichsen, H. C., and Chanock, S. J. (2005) Risk of Small-for-Gestational Age is Associated with Common Anti-Inflammatory Cytokine Polymorphisms. *Epidemiology. 16*, 478-486.

18. Sata, F., Toya, S., Yamada, H., Suzuki, K., Saijo, Y., Yamazaki, A., Minakami, H., and Kishi, R. (2009) Proinflammatory Cytokine Polymorphisms and the Risk of Preterm Birth and Low Birthweight in a Japanese Population. *Mol. Hum. Reprod. 15*, 121-130.

19. Seremak-Mrozikiewicz, A., Dubiel, M., Drews, K., Gudmundsson, S., and Mrozikiewicz, P. M. (2008) TNF-Alpha Gene Polymorphism and Fetal Doppler Velocimetry in Intrauterine Growth Restriction. *Neuro Endocrinol. Lett. 29*, 493-499.

20. Johnson, M. R., Anim-Nyame, N., Johnson, P., Sooranna, S. R., and Steer, P. J. (2002) Does Endothelial Cell Activation Occur with Intrauterine Growth Restriction? *BJOG. 109*, 836-839.

21. Holcberg, G., Huleihel, M., Sapir, O., Katz, M., Tsadkin, M., Furman, B., Mazor, M., and Myatt, L. (2001) Increased Production of Tumor Necrosis Factor-Alpha TNF-Alpha by IUGR Human Placentae. *Eur. J. Obstet. Gynecol. Reprod. Biol. 94*, 69-72.

22. Amarilyo, G., Oren, A., Mimouni, F. B., Ochshorn, Y., Deutsch, V., and Mandel, D. (2011) Increased Cord Serum Inflammatory Markers in Small-for-Gestational-Age Neonates. *J. Perinatol. 31*, 30-32.

23. Wang, X., Athayde, N., and Trudinger, B. (2003) A Proinflammatory Cytokine Response is Present in the Fetal Placental Vasculature in Placental Insufficiency. *Am. J. Obstet. Gynecol. 189*, 1445-1451.

24. Benyo, D. F., Miles, T. M., and Conrad, K. P. (1997) Hypoxia Stimulates Cytokine Production by Villous Explants from the Human Placenta. *J. Clin. Endocrinol. Metab. 82*, 1582-1588.

25. Ahmed, A., and Kilby, M. D. (1997) Hypoxia Or Hyperoxia in Placental Insufficiency? *Lancet. 350*, 826-827.

26. Tjoa, M. L., Oudejans, C. B., van Vugt, J. M., Blankenstein, M. A., and van Wijk, I. J. (2004) Markers for Presymptomatic Prediction of Preeclampsia and Intrauterine Growth Restriction. *Hypertens. Pregnancy. 23*, 171-189.

27. Krantz, D., Goetzl, L., Simpson, J. L., Thom, E., Zachary, J., Hallahan, T. W., Silver, R., Pergament, E., Platt, L. D., Filkins, K., Johnson, A., Mahoney, M., Hogge, W. A., Wilson, R. D., Mohide, P., Hershey, D., Wapner, R., and First Trimester Maternal Serum Biochemistry and Fetal Nuchal Translucency Screening (BUN) Study Group. (2004) Association of Extreme First-Trimester Free Human Chorionic Gonadotropin-Beta, Pregnancy-Associated Plasma Protein A, and Nuchal Translucency with Intrauterine Growth Restriction and Other Adverse Pregnancy Outcomes. *Am. J. Obstet. Gynecol. 191*, 1452-1458.

28. Roig, M. D., Sabria, J., Valls, C., Borras, M., Miro, E., Ponce, J., and Vicens, J. M. (2005) The use of Biochemical Markers in Prenatal Diagnosis of Intrauterine Growth Retardation: Insulin-Like Growth Factor I, Leptin, and Alpha-Fetoprotein. *Eur. J. Obstet. Gynecol. Reprod. Biol. 120*, 27-32.

29. Gupta, M. B., Seferovic, M. D., Liu, S., Gratton, R. J., Doherty-Kirby, A., Lajoie, G. A., and Han, V. K. M. (2006) Altered Proteome Profiles in Maternal Plasma in Pregnancies with Fetal Growth Restriction. *Clinical Proteomics. 2*, 169-184.

30. Barkehall-Thomas, A., Wilson, C., Baker, L., ni Bhuinneain, M., and Wallace, E. M. (2005) Uterine Artery Doppler Velocimetry for the Detection of Adverse Obstetric Outcomes in Patients with Elevated Mid-Trimester Beta-Human Chorionic Gonadotrophin. *Acta Obstet. Gynecol. Scand. 84*, 743-747.

31. Arbuckle, T. E., Wilkins, R., and Sherman, G. J. (1993) Birth Weight Percentiles by Gestational Age in Canada. *Obstet. Gynecol. 81*, 39-48.

32. Duncombe, G., Veldhuizen, R. A., Gratton, R. J., Han, V. K., and Richardson, B. S. (2010) IL-6 and TNFalpha Across the Umbilical Circulation in Term Pregnancies: Relationship with Labour Events. *Early Hum. Dev. 86*, 113-117.

33. Nodwell, A., Carmichael, L., Ross, M., and Richardson, B. (2005) Placental Compared with Umbilical Cord Blood to Assess Fetal Blood Gas and Acid-Base Status. *Obstet. Gynecol. 105*, 129-138.

34. Frater-Schroder, M., Risau, W., Hallmann, R., Gautschi, P., and Bohlen, P. (1987) Tumor Necrosis Factor Type Alpha, a Potent Inhibitor of Endothelial Cell Growth in Vitro, is Angiogenic in Vivo. *Proc. Natl. Acad. Sci. U. S. A. 84*, 5277-5281.

35. Sainson, R. C., Johnston, D. A., Chu, H. C., Holderfield, M. T., Nakatsu, M. N., Crampton, S. P., Davis, J., Conn, E., and Hughes, C. C. (2008) TNF Primes Endothelial Cells for Angiogenic Sprouting by Inducing a Tip Cell Phenotype. *Blood. 111*, 4997-5007.

36. Baluk, P., Yao, L. C., Feng, J., Romano, T., Jung, S. S., Schreiter, J. L., Yan, L., Shealy, D. J., and McDonald, D. M. (2009) TNF-Alpha Drives Remodeling of Blood Vessels and Lymphatics in Sustained Airway Inflammation in Mice. *J. Clin. Invest. 119*, 2954-2964.

37. Heyl, W., Handt, S., Reister, F., Gehlen, J., Schroder, W., Mittermayer, C., and Rath, W. (1999) Elevated Soluble Adhesion Molecules in Women with Pre-Eclampsia. do Cytokines Like Tumour Necrosis Factor-Alpha and Interleukin-1beta Cause Endothelial Activation. *Eur. J. Obstet. Gynecol. Reprod. Biol. 86*, 35-41.

38. Bartha, J. L., Romero-Carmona, R., and Comino-Delgado, R. (2003) Inflammatory Cytokines in Intrauterine Growth Retardation. *Acta Obstet. Gynecol. Scand. 82*, 1099-1102.

39. Zygmunt, M., Wienhard, J., Boving, B., Munstedt, K., Braems, G., Bohle, R. M., and Lang, U. (1998) Expression of Cell Adhesion Molecules in the Extravillous Trophoblast in Placentas of Preterm Pregnancies and in Placentas at Term. *Zentralbl. Gynakol. 120*, 488-492.

40. Yang, G., Chang, L., Alexander, J. S., Groome, L. J., and Yuping, W. (2009) Chymotrypsin-Like Protease (Chymase) Mediates Endothelial Activation by Factors Derived from Preeclamptic Placentas. *Reprod. Sci. 16*, 905-913.

41. Wang, Y., Zhang, Y., Lewis, D. F., Gu, Y., Li, H., Granger, D. N., and Alexander, J. S. (2003) Protease Chymotrypsin Mediates the Endothelial Expression of P- and E-Selectin, but Not ICAM and VCAM, Induced by Placental Trophoblasts from Pre-Eclamptic Pregnancies. *Placenta. 24*, 851-861.

42. Koch, A. E., Halloran, M. M., Haskell, C. J., Shah, M. R., and Polverini, P. J. (1995) Angiogenesis Mediated by Soluble Forms of E-Selectin and Vascular Cell Adhesion Molecule-1. *Nature. 376*, 517-519.

43. Ulyanova, T., Scott, L. M., Priestley, G. V., Jiang, Y., Nakamoto, B., Koni, P. A., and Papayannopoulou, T. (2005) VCAM-1 Expression in Adult Hematopoietic and Nonhematopoietic Cells is Controlled by Tissue-Inductive Signals and Reflects their Developmental Origin. *Blood. 106*, 86-94.

CHAPTER 7

Hypoxia and leucine deprivation induce human insulin-like growth factor binding protein-1 hyperphosphorylation and increase its biological activity

7.1. INTRODUCTION

IGF binding protein (IGFBP)-1 is a major IGFBP in pregnancy that modulates the cellular actions of IGFs (1). IGFBP-1 is synthesized predominantly by the maternal and fetal liver and by the maternal decidua during pregnancy (2, 3). Recent *in vivo* data show that fetal overexpression of IGFBP-1 inhibits fetal growth in mice (4, 5) and that IGFBP-1 contributes to fetal growth restriction (FGR) by inhibiting IGF-mediated fetal growth (6-9).

IGFBP-1 is a metabolically regulated protein and is suggested to have an important role in glucose homeostasis (10). The expression of IGFBP-1 is dynamically influenced by nutritional status, increasing during fasting, malnutrition, and diabetes while decreasing upon insulin treatment (11-13). Inhibition of IGFBP-1 production by insulin (14, 15) is one of the potential mechanisms in regulation of fetal growth (16-18).

Recent studies also suggest that induction of the IGFBP-1 expression under hypoxia and other catabolic conditions is an evolutionarily conserved mechanism. The biological significance of IGFBP-1 induction is to reduce the availability of IGFs to their receptors, and to divert the limited energy resources away from growth and development toward those metabolic processes essential for survival (7, 9, 19, 20).

The biological effect of IGFBP-1 depends not only on the total protein levels, but also on its proteolysis (21) and phosphorylation state (22, 23). It has been reported that phosphorylation of IGFBP-1 at certain sites can increase its binding affinity for IGF-I

and, thus, restricts IGF-I's bioavailability for binding its receptor (24). In addition, phosphorylation makes IGFBP-1 more resistant to proteolysis (25), therefore, accentuating its inhibitory effect on IGF-I.

Exposing HepG2 cells to hypoxia and leucine derivation treatment significantly induced IGFBP-1 mRNA and protein expression (26-28), however, it is not clear whether hypoxia and leucine deprivation treatments also affect the phosphorylation states and biological activity of IGFBP-1. The objectives of this study were to examine possible changes in IGFBP-1 phosphorylation status induced by hypoxia and leucine deprivation, determine the major phosphorylation sites, and investigate the biological and physiological relevance.

7.2. MATERIALS AND METHODS

7.2.1. Materials

All chemicals used were of electrophoresis or analytical grade. Human hepatocellular carcinoma cell line HepG2 and human embryonic kidney (HEK) 293 cells were purchased from American Type Culture Collection (Manassas, VA). Anti-human IGFBP-1 monoclonal antibody (Mab 6303) was from Medix Biochemica (Kauniainen, Finland), and antihuman IGFBP-1 polyclonal was a gift from Dr. R. Baxter of the Kolling Institute of Medical Research (Sydney, Australia). Horseradish peroxidase (HRP)-conjugated secondary antibodies were goat anti-rabbit or goat anti-mouse (Bio-Rad Laboratories, Inc., Hercules, CA). ELISA kits for total, and serine

phosphorylated IGFBP-1, were obtained from Diagnostic Systems Laboratories, Inc. (Webster, TX). The total albumin ELISA kit was from Bethyl Laboratories, Inc. (Montgomery, TX). The total protein was measured by Bradford assay (Bio-Rad Laboratories).

Phosphopeptide enrichment was performed using titanium dioxide (TiO_2) (Titansphere TiO; GL Sciences Inc., Tokyo, Japan). The interaction of IGF-I and IGFBP-1 was analyzed using surface plasmon resonance (SPR) using Biacore X instrument (Biacore, Inc., Piscataway, NJ) with sensor chips CM5. The amine coupling was performed using N-hydroxysuccinimide, N-ethyl-N-(3-diethylaminopropyl) carbodiimide, and ethanolamine hydrochloride. The sensor chips and all the chemicals for Biacore were from GE Healthcare Bio-Sciences AB (Piscataway, NJ). Recombinant human IGF-I (rIGF-I) was a gift from Dr. George Bright of Tercica Inc. (Brisbane, CA).

7.2.2. HepG2 cell culture and treatment conditions

HepG2 cells were grown at 37°C under 95% air, 5% CO_2 in DMEM/F-12 with 10% (vol./vol.) fetal bovine serum (FBS) (Life Technologies, Inc.; Invitrogen Corp., Carlsbad, CA). Cells grown to approximately 90% confluence were trypsin digested, counted, re-plated on 100 x 20 mm plates (Falcon; BD Biosciences, Franklin Lakes, NJ) at a density of 1.4 x 10^4 cells per mL, and incubated in DMEM/F-12 containing 10% FBS for 24 h until approximately 70% confluence.

Hypoxic treatments

Before hypoxic treatment, the cells were rinsed twice and incubated for 3 h in FBS-free DMEM/F-12. The media were then replaced with new FBS-free DMEM/F-12 and cells immediately placed in a modular incubator chamber (Billups-Rothenberg Inc., Del Mar, CA) that was flushed with 1% O_2, and 5% CO_2 with the bulk N_2. The cells in the sealed hypoxic chamber were placed in the incubator (20% O_2) with cells cultured normally (controls). Oxygen content in the hypoxic chamber was monitored at 12-h intervals with a Hudson 5590 Oxygen Monitor (Hudson, Ventronics Division, Temecula, CA). The partial pressure measurements for pO_2 and pCO_2, as well as pH evaluations, were made using an ABL700 series blood gas analyzer (Radiometer, Copenhagen, Denmark). After treatment, conditioned media (CM) were collected at 48 h (26, 27). Samples were centrifuged at 1200 rpm for 10 min and aliquots of the supernatants stored at $-20°$ C.

Leucine deprivation treatments

Media containing various concentrations of the essential amino acid leucine were prepared from DMEM/F-12 lacking methionine, leucine, lysine, and glutamine, and various salts (Sigma-Aldrich Corp., St. Louis, MO). Cell media were formulated by adding the missing amino acids and salt components to make it consistent with normal DMEM/F-12, except for leucine, which was added in 450 (equivalent to

DMEM/F-12), 140, 70, and 0 µM concentrations. Once cells were approximately 70% confluent, they were washed and incubated for 3 h with the specially formulated FBS-free DMEM/F-12 (with 450 µM leucine). Cells were then rinsed with FBS-free DMEM/F-12 (0 µM leucine) and finally incubated with FBS-free DMEM/F-12 containing various concentrations of leucine as described earlier. The CM were collected after 16 h incubation (27), centrifuged at 1200 rpm for 10 min, and stored at −20° C.

7.2.3. Western immunoblot and ligand blot analysis for IGFBP-1

All protein separations were conducted using 1.5 mm 12% sodium dodecyl sulfate polyacrylamide gels using MagicMark XP (Invitrogen) MW marker. Crude amniotic fluid from a healthy pregnancy was used as a positive control. For IGFBP-1 expression, equal volumes (10 or 15 µl) of direct CM samples were obtained from cells grown in incubator air (20% O_2) and hypoxia (1% O_2), and from cells cultured with leucine (450 µM leucine) and leucine deprived (0 µM leucine) conditions in all analysis unless specified otherwise. Immunoblot analysis was performed using wet transfer (29), and membranes were blocked using 4% BSA. IGFBP-1 Mab 6303 (1:10,000 dilution) was used as the primary antibody and HRP-conjugated goat anti-mouse IgG (1:8,000 dilution) as the secondary antibody. Western Lighting Enhanced Chemiluminescence (ECL) Reagent Plus (PerkinElmer, Boston, MA) and Kodak XOMAT LS films (Eastman Kodak Co., Rochester, NY) were used for detection of proteins.

To detect other IGFBPs, 5 µl CM sample from HepG2 cells was used for ligand blot analysis using biotin-labeled rIGF-I (10 ng/ml) (30). Crude amniotic fluid was used as a positive control, and proteins were detected using HRP-conjugated streptavidin (1:1000 dilution) and the ECL Reagent Plus kit.

For 2-D immunoblots, equal volumes (100 µl) of CM were desalted and concentrated 10-fold using 10-kDa MW cut-off (MWCO) Centricon tubes (PALL Life Sciences, Ann Arbor, MI). Desalted samples were reconstituted with rehydration buffer {8 M urea, 2% (3-[(3-cholamidopropyl) dimethylammonio]- 1-propanesulfonate (CHAPS) (Bio-Rad), 50 mM dithiothreitol, 0.2% Biolyte (Bio-Rad), (pH 3–10 ampholyte), and 0.001% bromophenol blue} and transferred onto a polyvinylidene fluoride membrane by wet transfer (31). Membranes were blocked in 4% non-fat dry milk and then incubated overnight with IGFBP-1 polyclonal antibody (1:10,000 dilution). The goat anti-rabbit HRP-conjugated antibody (1:8000 dilution) was used as a secondary antibody, and proteins were visualized using the ECL Plus system.

The 16-bit digital images of the gels and immunoblots were acquired in the linear range under white light using the FluoroChem 8800 imaging system (Alpha Innotech Corp., San Leandro, CA). Three-dimensional (3-D) qualitative evaluation of IGFBP-1 isoforms on the blots was performed using PG220 software (Nonlinear Dynamics Ltd., Newcastle upon Tyne, UK).

The phosphorylation state of IGFBP-1 in CM was confirmed by pre-treatment of the samples (100 µl) with calf intestinal alkaline phosphatase (AKP) (Sigma-Aldrich) (200 U) for 6 h at 37 C. The reaction was stopped by addition of rehydration buffer. The

de-phosphorylated protein samples were further analyzed for IGFBP-1 isoforms using 2-D immunoblotting as described previously.

7.2.4. Immunoassays for total and phosphorylated IGFBP-1

The phosphorylated IGFBP-1 ELISA is based on first capturing total phosphorylated and non-phosphorylated IGFBP-1 with an anti-IGFBP-1 monoclonal antibody (32); the captured serine phosphorylated IGFBP-1 is then selectively detected by a specific anti-phosphoserine antibody labeled with HRP (33). Total IGFBP-1 levels in CM were normalized to total protein by the Bradford method. The total albumin levels in the same set of CM samples were analyzed by ELISA as per the manufacturer's instructions.

7.2.5. MS analysis of IGFBP-1 phosphorylation

Sample preparation

For MS analysis of IGFBP-1 phosphorylation, samples were from control (2O% O_2) and hypoxia (1% O_2) and from cells cultured with leucine treatments (450 and 0 µM leu) conditions. Equal volumes of CM (400 µl) were desalted (10 KDa MWCO) at 4° C with ammonium bicarbonate (ABC) buffer (pH 8.0). Samples were then separated on one-dimensional gels. To identify the band corresponding to IGFBP-1 on the gel, the lane with amniotic fluid (positive control) was excised for immunoblot analysis using Mab 6303. The remaining gel was fixed for 30 min (10% methanol and 7% acetic acid) and

stained overnight with SYPRO Ruby (Invitrogen) stain. Gel images were captured under UV excitation with a SYPRO-500 filter. Using the immunoblot as a guide, the specific band on the gel corresponding to IGFBP-1 [28 KDa molecular mass (MW)] from different treatments was manually excised under UV light.

For in-gel digestion, the gel slices were cut into small cubes (1 mm^3), transferred to siliconized Eppendorf tubes (Hamburg, Germany), and sequentially washed with 100 mM ABC buffer (pH 8.0), followed by acetonitrile (ACN). The samples were dried in a vacuum centrifuge. For reduction and alkylation, the gel pieces were treated with 10 mM dithiothreitol, followed by 100 mM iodoacetamide. Subsequently, proteins were digested with aspartate N-endoproteinase (Asp-N) (Sigma-Aldrich) (25 ng/µl), followed by sequencing grade trypsin (12.5 ng/µl) (Promega Corp., Madison, WI) at 37° C overnight. The gel was extracted with 30 µl ABC, 50% ACN, and 5% formic acid sequentially. The extracted peptides were dried and stored at −80° C.

Phosphopeptide enrichment

Phosphorylated IGFBP-1 peptides were enriched using TiO_2. In brief, the pelleted IGFBP-1 peptides after digestion were dissolved in 20 µl loading buffer [80% ACN and 1% trifluoroacetic acid (TFA)] and incubated with 1 µl TiO_2 slurry (5 µm, 1 mg, in 50% ACN) for 20 min at room temperature on a shaker. The solution and TiO_2 particles were transferred to a pipette tip with a piece of filter paper inserted at its end to serve as a frit. The tip was placed in a microcentrifuge tube and centrifuged for 5 min.

The particles were washed using 20 µl loading buffer (50 mg/ml dihydroxybenzoic acid and 0.2% TFA in 40% ACN) and centrifuged again. The phosphopeptides were eluted using 20 µl elution buffer [5% ammonium hydroxide (pH 11.0)] and centrifuged for 10 min. To the receiving tube, 5 µl 5% TFA was added before eluting the bound phosphopeptides. The samples were dried in SpeedVac and reconstituted in 0.1% formic acid in water or in 50 mM EDTA in water before liquid chromatography-mass spectrometry (LC-MS) or liquid chromatography-tandem mass spectrometry (LC-MS/MS) analysis.

LC-MS/MS and LC-MS phosphopeptide analysis

The enriched phosphopeptides were analyzed on a CapLC (Waters Corp., Milford, MA) coupled with a Quadrupole Time-of-Flight mass spectrometer (Global Ultima; Micromass, Manchester, UK) using a 5 µm x 0.5 mm C18 precolumn and a 75 µm x 150 mm analytical column (LC Packings, Amsterdam, The Netherlands) with a 300-nl/min flow rate through the analytical column. LC-MS/MS analysis was performed using a gradient elution and the data-dependent acquisition function (34). For estimations of the phosphorylation changes upon treatments, LC-MS analysis were performed on the same instrument setting. The selected ion chromatograms for different phosphopeptide peaks were plotted, and the spectra were summed. The intensities of the phosphopeptide peaks in the summed spectra were used for the semiquantitative determination of the relative amounts of phosphopeptide in the samples from control to treatment conditions.

LC-MS/MS spectra were processed using the Maxnt 3 function in Masslynx software (version 4.0; Waters). Mascot (Matrix Science, Boston, MA) and PEAKS software were used to search Swiss-prot database for protein identification. Peptide mass/charge (m/z) tolerance was set to 1.2 and the peptide fragment ion tolerance to 0.1 Da. Asp-N and/or trypsin was designated as the protease, and up to one missed cleavage was allowed. Carbamidomethylation on cysteine residue was included as a fixed modification, whereas oxidation of methionine and phosphorylation of serine/threonine/tyrosine and tyrosyl residues were selected as a variable modification. Phosphopeptides identified were manually inspected to verify that the majority of high abundance peaks were y or b sequence ions, or $y - H_2O/H_3PO_4$ or $b - H_2O/H_3PO_4$ ions when appropriate. For all the phosphopeptides, their phosphorylation sites were verified manually.

7.2.6. SPR for binding characteristics of IGFBP-1 with IGF-I

The comparative measurements of the binding rate constants characteristic of IGFBP-1 and rIGF-I were performed using a Biacore X instrument. 70 μL of rIGF-I (10 μg/ml) diluted in 100 mM acetate buffer (pH 4.0) were immobilized to the Sensor Chip CM5 surface by amine coupling as per the manufacturer's protocol. The rIGF-I immobilization was performed on a "sample flow cell," that achieved approximately 4000–5000 resonance unit signals in three different experiments.

All CM samples were buffer exchanged with HBS EP buffer (pH 7.4) [10 mM HEPES, 150 mM NaCl, 3.4 mM EDTA, and 0.005% surfactant P20 (pH 7.4)], concentrated 10-fold, and serially diluted at analysis in the HBS EP buffer. The overabundance of IGFBP-1 and negligible IGFBP-3 secreted by HepG2 cells (35) discounted interference if any in Biacore analysis. IGF-I binding assay was additionally performed on de-phosphorylated IGFBP-1, obtained by AKP treatment of hypoxia (1% pO_2) and leucine deprivation (0 µM leu) treated CM. The AKP reactions were performed as described earlier, except here the reactions were terminated using EDTA (final concentration, 50 mM) followed by immediate buffer exchange with HBS EP buffer.

In a typical binding experiment, 70 µl CM with various concentrations of analyte (70–700 nM) was injected for a 60-sec association phase in both reference and sample cells. The interaction of IGFBP-1 with the immobilized IGF-I was monitored until equilibrium was attained. The dissociation phase was initiated by passage of HBS EP buffer for a period of 1–3 min. The biosensor surfaces were regenerated by a 60-sec injection of 10–30 µl glycine buffer [50 mM (pH 2.0)] after each injection.

CM samples from three independent cell culture experiments for hypoxic and leucine deprivation treatments were analyzed in triplicate in random order and tested on at least three different sensor chips. A low immobilization level as well as a high flow rate (50 µl/min) and analyte concentrations limited the mass transport phenomenon. Furthermore, the resonance unit response was always reported as the difference between signals occurring from the sample and the reference cell (with no ligand). Therefore, bulk refractive index, background and nonspecific binding of the soluble

ligands were always subtracted. Representative curves were generated for the association and dissociation phases, and kinetic data were analyzed using the BIAevaluation software version 3.0 (Biacore) as per 1:1 Langmuir binding model.

7.2.7. Biological assay of IGFBP-1 activity

The biological activity of IGFBP-1 in CM samples from HepG2 cells was studied using MTS assay (CellTiter 96 AOueous Non-Radioactive Cell Proliferation Assay; Promega). HEK293 cells were cultured in DMEM supplemented with 10% FBS, penicillin, and streptomycin in a humidified-air atmosphere containing 5% CO_2. CM were collected from HepG2 cells grown in incubator air (2O% O_2) and hypoxia (1% O_2). The total IGFBP-1 concentrations in CM samples were estimated by ELISA as described previously. To eliminate possible effects of other factors in the CM from HepG2 cells, IGFBP-1 was depleted and used as a control. For this purpose, CM were incubated with a polyclonal rabbit anti-human IGFBP-1 antibody overnight at 4° C (1:500 dilution); 50 µl protein A-Sepharose was then added and rocked for another 4 h at 4° C. The CM were centrifuged, and the supernatants collected were used as controls. This IGFBP-1 depleted CM sample was also added to the IGF-I (25 nM) group. Various concentrations of IGFBP-1 (8.3, 25, or 75 nM) were added singly or with 25 nM IGF-I. The assays were terminated after 48 h following the manufacturer's instructions.

7.2.8. Statistical evaluation
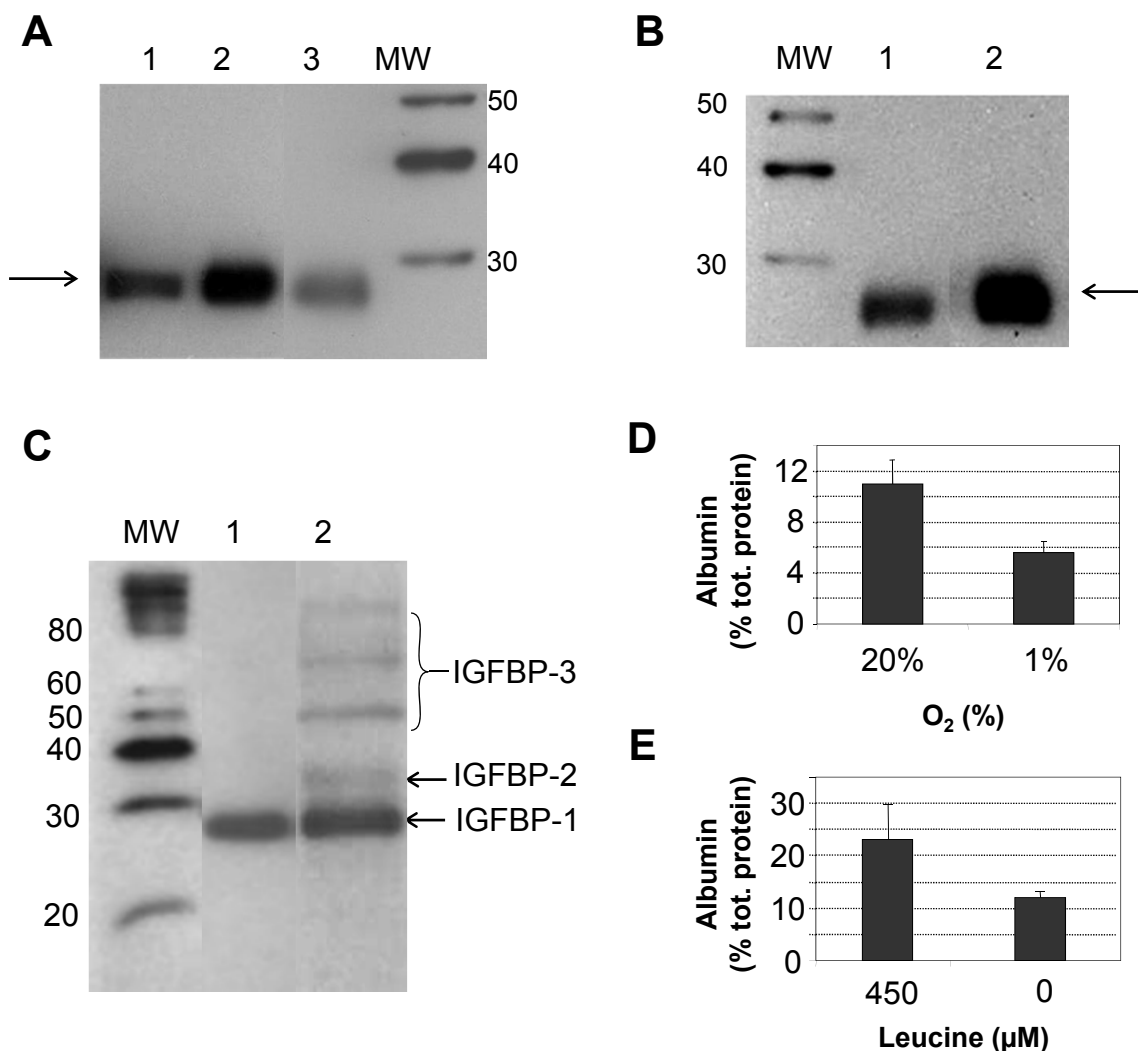
Figure 7.1. One-dimensional IGFBP-1 immunoblot. **(A)** Samples contain equal volumes of FBS-free CM from HepG2 cells cultured in incubator air (control, 20% O_2) (lane 1) or under hypoxic (1% O_2) (lane 2) conditions for 48 hr. Lane 3 is amniotic fluid as a positive control. **(B)** CM from HepG2 cells treated with 450 μM leucine (lane 1) and without (0 μM) leucine (lane 2). **(C)** IGF-I ligand blot of CM from HepG2 cells (lane 1) and amniotic fluid as a positive control (lane 2). IGFBPs identified by their M_r are indicated. ELISA data indicating concentration of albumin as percentage of total protein in samples from cells in incubator air (control, (20% O_2) and hypoxic (1% O_2) conditions, and with leucine (control, 450 μM) **(D)** and without (0 μM) leucine **(E)**. Decreased levels of albumin in CM confirmed the effectiveness of the treatment conditions.

Statistical significance among each experimental group was determined by the unpaired t test. Values are represented as means ± SD. Statistical analysis was performed using GraphPad Prism 3.0 software (GraphPad Software Inc., San Diego, CA), and significance was accepted at $P < 0.05$.

7.3. RESULTS

7.3.1. Effect of hypoxia and leucine deprivation on IGFBP-1 expression and phosphorylation in HepG2 cells

Air monitoring of the hypoxic chambers ensured desired levels of O_2 in hypoxic treatments. Upon completion of the treatments (48 h), pO_2 tension levels of CM showed an average (SEM) 43.3 (1.53) and 133.3 (7.36) Torr (mm Hg) for 1 and 20% O_2 levels, respectively. The levels of pCO_2 remained relatively stable within time points tested, and pHs of the media between the hypoxic and control treatments were also comparable.

In agreement with previous reports (17, 36, 37), immunoblot analysis qualitatively indicates (Figure 7.1A, lanes 1 and 2) that IGFBP-1 expression was induced in hypoxia (26, 27). Similarly, leucine deprivation (0 µM leucine) also increased IGFBP-1 levels compared with cells cultured with high concentrations of leucine (450 µM leucine) (Figure 7.1B, lanes 1 and 2). Modest increases in IGFBP-1 levels were found (data not shown) in cells cultured in lower leucine concentrations (70 and 140 µM leucine). Furthermore, ligand blot analysis results in Figure 7.1C show detection of mainly
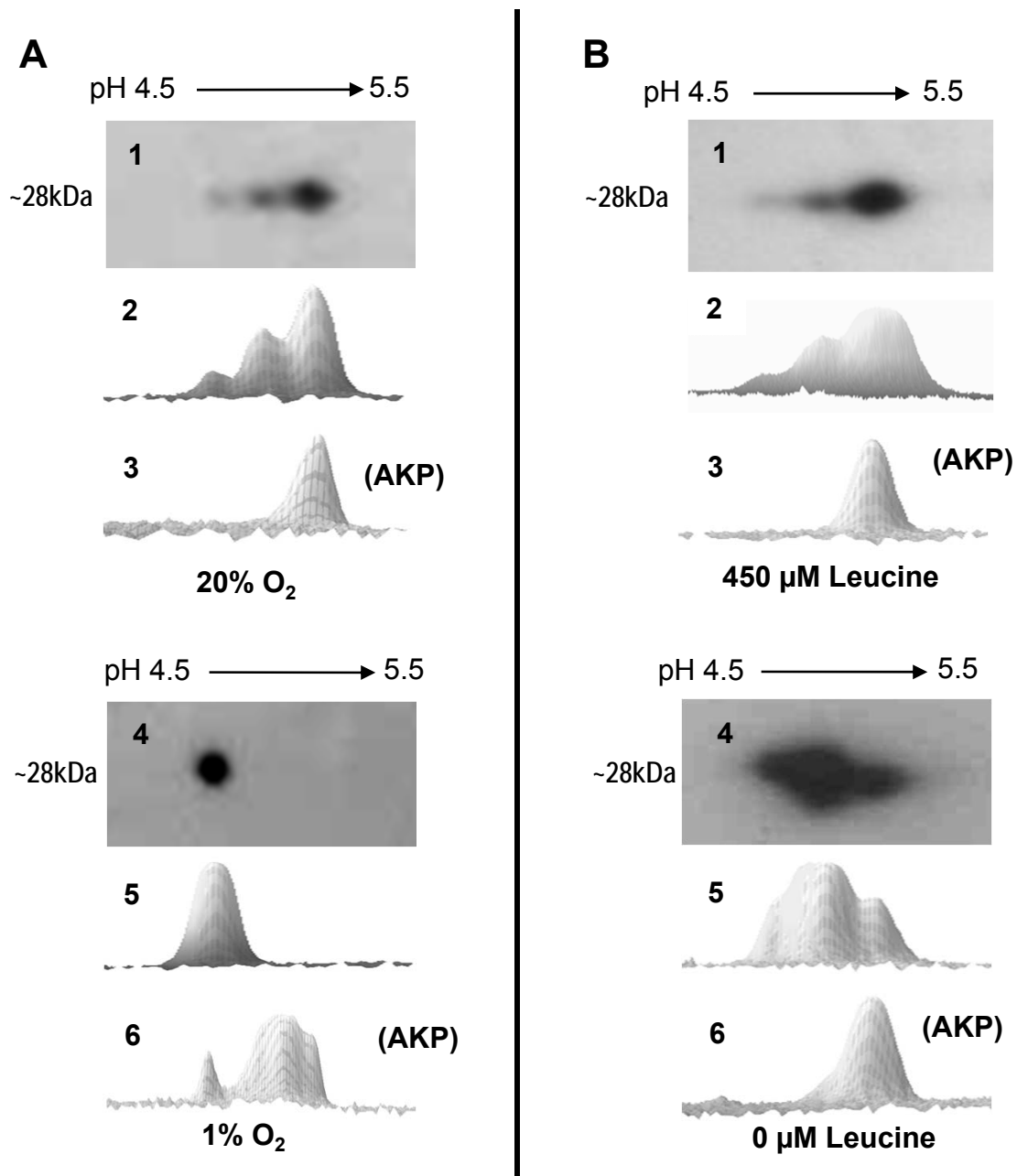
FIGURE 7.2. 2-D IGFBP-1 immunoblot showing separation of the IGFBP-1 phosphoisoforms based on pI using CM from HepG2 cells. **(A)** CM from cells grown in 20% O_2 or 1% O_2. The blot shown in A4 appears to have a higher intensity of IGFBP-1 with a single dominant phosphoisoforms shifted in pI towards the acidic end compared with the control (A1). **(B)** B1 shows CM from cells grown in 450 µM leucine, B4 in leucine deprived cells (0 µM leucine). 3-D densitometric views of the specified areas are shown in 2 and 5. Blots in 3 and 6 are the same sample of 2 and 4, after treatment with AKP.

IGFBP-1 (lane 1), suggesting a predominance of this protein and negligible levels of other IGFBPs in HepG2 CM (35).

ELISA estimations in Figure 7.1, D and E, show reduced concentration of albumin for both hypoxia and leucine deprivation. Albumin is a major mediator of the acute phase response to disturbances of homeostasis, mainly due to altered hepatic metabolism (38). Decreased plasma albumin being characteristic of a negative acute phase reaction and mimicked by HepG2 cells (37, 39) in hypoxia confirmed effectiveness of the treatment, physiologically.

7.3.2. Identification of various IGFBP-1 phosphoisoforms isoforms in hypoxia and leucine deprivation

2-D immunoblot analysis was performed qualitatively to examine possible differential phosphorylation states in IGFBP-1 induced under hypoxic and leucine deprivation conditions. Data with CM from the control HepG2 cells show three spots (28 KDa) between pH 4.5 and 5.5, representing a mixture of non and variably phosphorylated IGFBP-1 variants (Figure 7.2, A1 and B1). The 3-D densitometric view of the 2-D image shown in Figure 7.2, A and B (panel 2), showed three major peaks. The change in IGFBP-1 isoelectric point (pI) caused by phosphorylation is estimated to be pH –0.09 for the first phosphorylation, –0.08 for the second and third, and –0.07 for the fourth subsequent (Scansite MW and pI calculator; http://scansite.mit.edu.proxy2.lib.uwo.ca:2048). The pI difference between units

illustrated in the 3-D view was manually estimated as pH approximately 0.1. Greater

intensity toward the higher pH is indicative of less phosphorylated states (40). The

peak in the most alkaline region is the non-phosphorylated variant. The other two

spots represent medium and highly phosphorylated IGFBP-1 isoforms. It is evident

from these results that HepG2 cells secrete a mixture of three major forms of IGFBP-

1 with the non-phosphorylated isoform as the dominant one. To confirm this, the

same CM sample was treated with AKP. As shown in panel 3, AKP treatment resulted

in a single non-phosphorylated form. The results of the hypoxia group are shown in

Figure 7.2A, panels 4 and 5. There was an intense spot/peak in the more acidic

region, representing the dominance of a highly phosphorylated isoform of IGFBP-1.

AKP treatment shifted the majority of the IGFBP-1s to the alkaline region (panel 6),

confirming the phosphorylation status.

Figure 7.2B shows representative 2-D immunoblots of IGFBP-1 isoforms under the

control (450 µM leu) with three distinct IGFBP-1 isoforms (panel 1); the least or non-

phosphorylated isoform is clearly the dominant form (Figure 7.2B, panel 2). AKP

treatment resulted in shifting of the other spots to the alkaline region (Figure 7.2B,

panel 3). In the leucine-deprived group (0 µM leucine), a higher proportion of

medium and highly phosphorylated variants were observed. Two of the three spots

found at around pH 4.5 had higher intensity (Figure 7.2B, panels 4 and 5) compared

with those of the control (Figure 7.2B, panels 1 and 2). Although there was no

marked reduction in the levels of non-phosphorylated isoform as seen in hypoxic

experiments, a significant increase in intensity of some spots suggests higher levels of
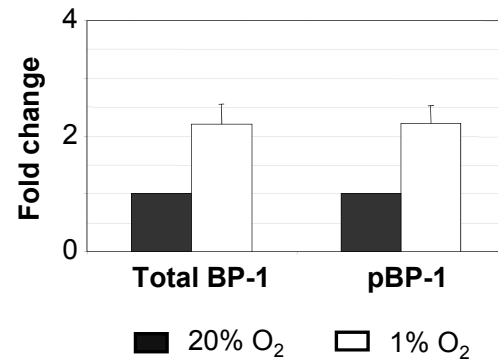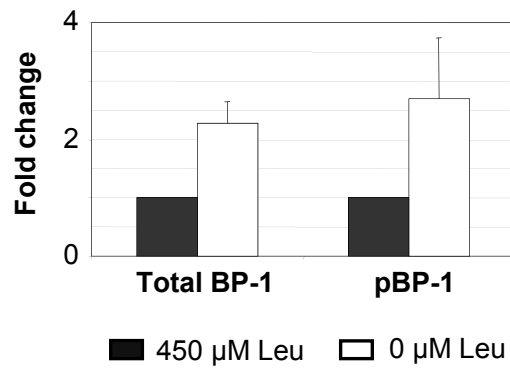
FIGURE 7.3. ELISA data indicating the change in total and phosphorylated IGFBP-1 isoforms from incubator air (control, 20% O_2) to hypoxic (1% O_2) conditions **(A)** and control [450 µM leucine (Leu)] to leucine deprived (0 µM Leu) conditions **(B)**.

phosphorylated isoforms. AKP treatment shifted these phospho-IGFBP-1s to the alkaline region (Figure 7.2B, panel 6). These data suggest that hypoxia and leucine deprivation increase the phosphorylation of IGFBP-1 in HepG2 cells.

It should be noted that a polyclonal IGFBP-1 is used in 2-D immunoblot analysis. The use of this polyclonal was essential because the monoclonal 6303 antibody was not efficient in detecting IGFBP-1 on 2-D immunoblots, possibly due to harsh sample preparation conditions in 2-D gel analysis.

7.3.3. Total and phosphorylated IGFBP-1 concentrations by ELISA

The effects of hypoxia and leucine deprivation on total IGFBP-1 and serine phosphorylated IGFBP-1 levels were determined and are represented as fold change in Figure 7.3. As anticipated, the concentrations of total IGFBP-1 increased in both hypoxia and in leucine deprivation group. The levels of serine phosphorylated IGFBP-1 relative to their respective controls showed proportional increases (Figure 7.3, A and B). The data indicate that an induction of total IGFBP-1 is accompanied by a proportional increase in IGFBP-1 phosphorylation.

7.3.4. Mass spectrometry for identification of IGFBP-1 phosphorylation sites

Three phosphorylation sites, Ser101, Ser119, and Ser169, have been reported for IGFBP-1 (41). Upon sequential Asp-N and trypsin digestions, the following three phosphopeptides were detected, and the amino acid sequences [phosphoserine (pS)
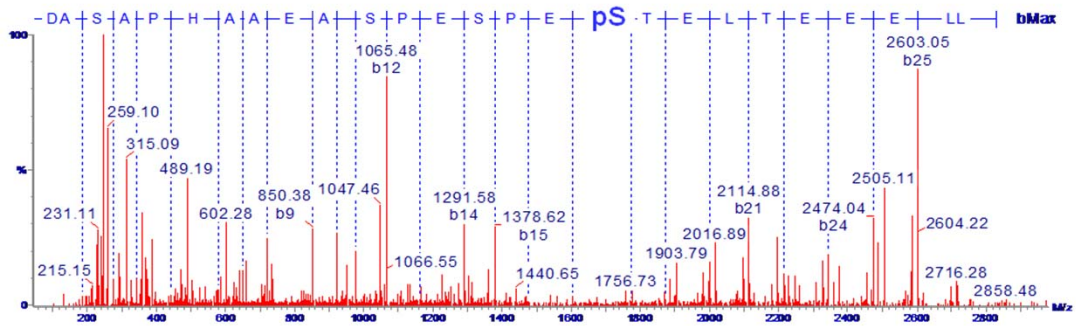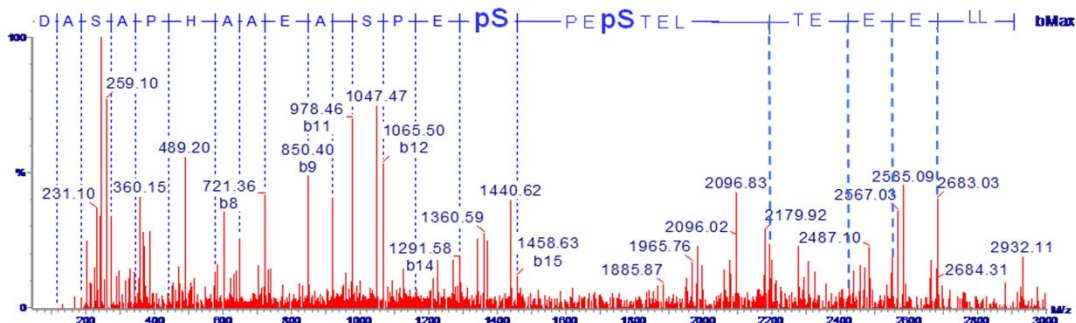
FIGURE 7.4. LC-MS/MS spectra showing newly identified phosphorylation site pSer98 for IGFBP-1 secreted from HepG2 cells under hypoxic (1% O_2) conditions. The deconvoluted spectra of ions at 949.73 m/z is for the singly phosphorylated pSer101 with peptide sequence shown in **A** and 976.42 m/z is for the doubly phosphorylated pSer101 together with pSer98 in **B**. Both ions were observed as triply charged ions. In spectrum **A**, intense b ions confirm the amino acid sequence of the peptide; the observed b18 ion at 1771.68 and the b18–98 ion at 1673.75 , derived from b18 ion with a loss of H_3PO_4, indicate the phosphorylation on Ser(101) residue. In spectrum **B**, the precursor ion is 80 Da heavier than the ion in the spectrum **A**, indicating an additional phosphorylation; the observed b15 ion at 1458.63 and the b15–98 ion at 1360.59 indicate the phosphorylation on the Ser(98) in addition to the Ser101.

TABLE 7.1. Ratios of IGFBP-1 phosphopeptide peak intensity in hypoxia (1% O_2) and leucine-deprived (0 µM leucine) samples relative to controls (20% O_2 and 450 µM leucine)

Treatment	IGFBP-1 phosphopeptide peak intensity change (fold change)		
20 to 1% O_2	*pSer 101*	*pS119[1]*	*pS169[1]*
Mean	3.17	2.07	4.22
SD	0.66	0.65	0.96
450 to 0 µM leu	*pSer 101[1]*	*pS119[2]*	*pS169[1]*
Mean	1.86	4.43	2.45
SD	1.10		0.28

The relative peak intensity measurements for each set (control and treatment condition) were done sequentially to ensure identical analytical conditions in an individual experiment. Three MS analyses were done separately using samples collected from three independent cell culture experiments for both hypoxic and leucine-deprived treatments.

[1] Two out of three experiments.

[2] SD not determined because the intensity in one of the two control samples (450 µM Leu) was lower than the detection level.

shown in parentheses] were confirmed by LC-MS/MS:

DASAPHAAEAGSPESPEpS(101)TEITEEELL, 949.73 m/z, +3; DNFHLMAPpS(119)EE, 685.30 m/z, +2; and AQETpS(169) GEEISK, 629.78 m/z, +2. The phosphopeptides shown with their mass to charge ratios (m/z) were detected in samples from hypoxic (control, 20% O_2 and hypoxia, 1% O_2) and in leucine deprivation (450 and 0 μM leucine) treatments.

A new doubly phosphorylated peptide, DASAPHAAEAGSPEpS(98)PEpS(101)TEITEEELL, 976.42 m/z. +3 was also detected but only when analyzed with EDTA added to the sample. The modified protocol (34) increases the detection sensitivity of multi-phosphorylated peptides. Using the CM from hypoxia treatments, the LC-MS/MS spectra are shown with a peak at 949.73 m/z for the single phosphorylated peptide at Ser101 (Figure 7.4A) and at 976.42 m/z for Ser98 with Ser101 (Figure 7.4B). This doubly phosphorylated phosphopeptide was detected in two out of three samples from hypoxia but not with the controls (20% O_2), or leucine deprivation (450 and 0 μM leucine) treatments.

7.3.5. Semiquantitation of the phosphorylation changes of IGFBP-1 induced by hypoxia and leucine deprivation

We next performed LC-MS analysis of TiO_2 enriched IGFBP-1 phosphopeptides in CM from different treatments. IGFBP-1 phosphopeptide peak intensity ratios were calculated from the relative phosphopeptide peak intensities between the control

and treated groups. The data from these experiments are summarized in Table 7.1. For the hypoxia experiment, pSer101, pSer119, and pSer169 all showed equal to or more than double increases in peak signal intensities relative to the control. Similarly, fold increases were also recorded for leucine deprivation from two out of three samples.

The doubly phosphorylated peptide with pSer98 and pSer101 was detected in the samples from hypoxia (1% O_2) as shown in Figure 7.4B. Due to the absence of pSer98 in the controls (20% O_2), the fold increase upon treatment was not discernable. However, these results clearly indicate that pSer98 was hyperphosphorylated in hypoxia. Being adjacent to the major site, it is possible that pSer98 acts with pSer101 in hypoxic stress to contribute to changes in IGFBP-1 functions.

It should be noted that the MS analysis was performed using three independent preparations from three separate cell culture experiments. Furthermore, the LC-MS analyses were performed using equal volumes of CM at different times; therefore, the data should be considered an estimate. Despite this caveat, the outcome of MS analysis is highly consistent with the results obtained by immunoblotting (Figure 7.2, A and B) and ELISA (Figure 7.3, A and B). Altogether, our LC-MS data clearly demonstrate (Table 7.1) that the phosphorylation of IGFBP-1 was consistently increased in hypoxia and in leucine deprivation treatment, but more prominently in hypoxia.

Table 7.2 The kinetics of the affinity of IGFBP-1 for IGF-I assessed in triplicate by Biacore analysis for CM in hypoxia (1% O_2) and leucine-deprived (450 µM leucine) samples relative to controls (incubator air, 20% O_2 and 450 µM leucine)

Treatment	Kd (M)	Treatment	Kd (M)
20% O_2		**450 µM Leu**	
Mean	1.54×10^{-7}	Mean	1.40×10^{-7}
SD	0.01×10^{-7}	SD	0.49×10^{-7}
1% O_2		**0 µM Leu**	
Mean	5.83×10^{-10}	Mean	0.64×10^{-10}
SD	0.02×10^{-10}	SD	0.00×10^{-10}
De-phos.		**De-phos.**	
Mean	7.09×10^{-7}	Mean	4.56×10^{-7}
SD	0.13×10^{-7}	SD	0.07×10^{-7}

CM from hypoxic or leucine-deprived conditions were dephosphorylated by AKP and the kinetics reassessed.
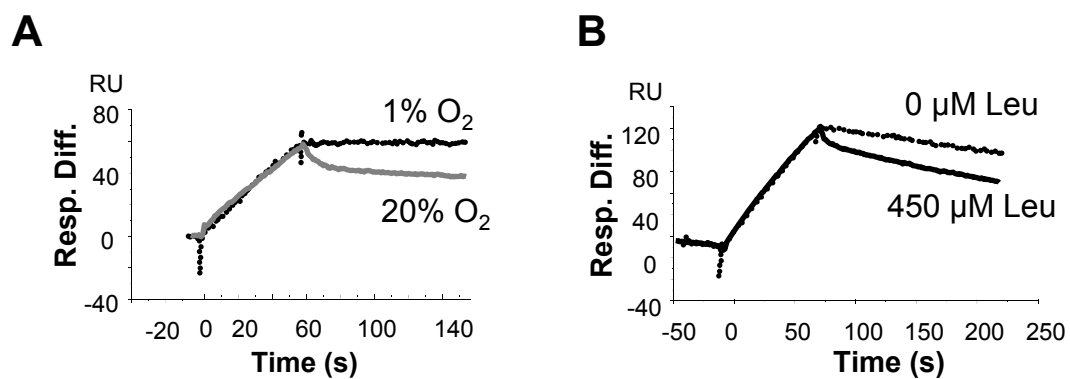
FIGURE 7.5. The association and dissociation phases of concentration-dependent binding of IGFBP-1 to immobilized rIGF-I, comparing hypoxic or leucine-deprived treatment of the HepG2 cells with controls. Analyte (IGFBP-1) is CM from HepG2 cells grown in incubator air (control, 20% O_2) or hypoxia (1% O_2) for 48 h **(A)** and control (450 µM Leu) and leucine-deprived (0 µM leucine) treatments **(B)** for 16 h. The kinetic analysis shows alterations in dissociation phases for both hypoxic and leucine (Leu) treatments. Resp. Diff., Response unit differences.

7.3.6. IGF-I binding kinetics using SPR analysis

Biacore biosensor measurements were performed to gain insight into the influences of phosphorylation on the ligand binding kinetics of the IGFBP-1 molecule. Hypoxia and leucine deprivation treatment lowered the equilibrium dissociation constant (KD) value of IGFBP-1 (Table 7.2). A representative comparison of association and dissociation phases of the interaction of IGFBP-1 with IGF-I, in control vs. the hypoxia group, is shown in Figure 7.5A, and with leucine (450 μM leu) and leucine deprivation (0 μM leu) groups in Figure 7.5B. Compared with IGFBP-1 prepared from the control cells, IGFBP-1 prepared from the hypoxic cells and the leucine-deprived cells exhibited slower dissociation rates, and the resultant complexes were more stable. Kinetic analysis of the biosensorgram curves demonstrates that the IGFBP-1 binding affinity for IGF-I under basal conditions was comparable to those reported previously using Biacore analysis (42). The estimations of the off rates suggest that binding interactions of IGFBP-1 with IGF-I were affected by both hypoxia and leucine deprivation but more significantly by leucine deprivation (Table 7.2). To ascertain that the changes in ligand binding kinetics were indeed due to elevated phosphorylation, these preparations were de-phosphorylated and analyzed. The results showed that KD values were returned to the control levels (Table 7.2), suggesting that the changes in phosphorylation states are responsible for the changes in IGF binding affinity.
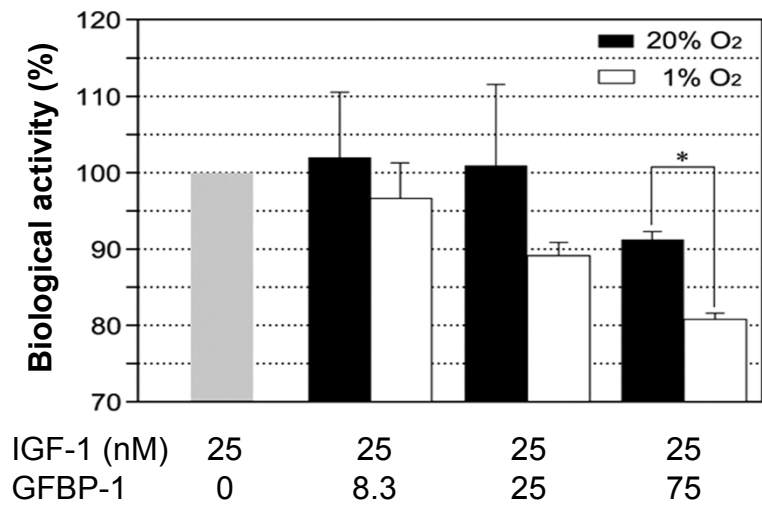
FIGURE 7.6. Hypoxia-induced IGFBP-1 phosphorylation increases its ability to inhibit IGF action. IGFBP-1 prepared from HepG2 cells grown under 20% O_2 (*solid*) and 1% O_2 (*open)* was added to cultured HEK293 cells with or with IGF-I at indicated concentrations. Values are represented as means with SD of two independent assays, each performed in triplicates. (*$p<0.05$).

7.3.7. Hypoxia treatment increases the biological potency of IGFBP-1 in inhibiting IGF actions

We next determined the functional significance of the hypoxia-induced IGFBP-1 hyperphosphorylation. Addition of IGF-I (25 nM) to cultured HEK293 cells resulted in a significant increase in cell number. Total IGFBP-1 isolated from direct CM from HepG2 cells grown in either incubator air (20% O_2), or hypoxia (1% O_2) inhibited IGF-I activity in a dose-dependent manner (Figure 7.6). The IGFBP-1 sample derived from the hypoxia group was more potent than that from the 20% O_2 group. At the highest dosage (75 nM) tested, it caused a 20% reduction in IGF-I-induced cell proliferation. In comparison, the less phosphorylated IGFBP-1 derived from the 20% O_2 group only caused a 9% reduction. The difference was statistically significant ($P < 0.05$). A similar trend was also observed at low doses (25 nM), although the difference was not statistically significant. These functional data together with the binding kinetics data indicate that the hypoxia-induced IGFBP-1 phosphorylation increases its ability to inhibit IGF actions.

7.4. DISCUSSION

Increased expression of IGFBP-1 has been considered a marker of metabolic irregularities in fetal nutrition (12, 43, 44) and in oxygen delivery (9, 45) that are strongly linked to FGR (46-48). By subjecting human HepG2 cells to hypoxia and leucine deprivation (27, 35, 49-51), we demonstrated that hypoxia and leucine

deprivation lead to altered phosphorylation states of IGFBP-1. We have identified pSer169 as a major site of phosphorylation that may, along with pSer101, be responsible for altering the affinity of hepatic IGFBP-1 with IGF-I. We have provided data suggesting that elevated phosphorylation of the IGFBP-1 molecule increases its IGF binding affinity. The highly phosphorylated IGFBP-1 also has greater biological activity in inhibiting IGF-I-stimulated cell proliferation. These findings suggest that IGFBP-1 phosphorylation may be a novel mechanism of fetal adaptive response to hypoxia and nutrient restriction.

Regulation of IGFBP-1 and modulation of IGF-I actions are highly dynamic and complex, particularly in human FGR (52). Besides the endocrine factors, IGFBP-1 is induced by a variety of catabolic conditions. For example, fasting, malnutrition, and protein restriction rapidly induce IGFBP-1 at the transcription level (19). The depletion of a single amino acid (arginine, cysteine, and all essential amino acids) is sufficient to induce IGFBP-1 expression in vitro. Other catabolic conditions regulating IGFBP-1 expression include endoplasmic reticulum stress and hypoxic stress (19).

Induction of IGFBP-1 to reduce IGF action is considered to be part of a regulatory mechanism during fetal development (17, 53). The stress signalling events that alter IGFBP-1 expression have thus far been shown to be highly significant in signal transduction events (54). The impacts of chronic hypoxia (7, 8, 17, 35, 55) and poor nutrient transfer (20) to the fetus on regulation of the IGFBP-1 gene at the transcription level are well studied. Tazuke and others (35) have identified a hypoxia response element located in intron 2 of the human IGFBP-1 gene responsible for the

hypoxia response in cultured human HepG2 cells. Likewise, recent studies using zebra fish embryo show that the induction of IGFBP-1 gene expression by hypoxia is mediated through hypoxia-inducible factor 1 (HIF-1) both in vitro and in vivo, and the HIF-1 pathway is established in early embryonic stages (56). The functional importance of the HIF-1 pathway in hypoxia-induced IGFBP-1 gene expression (8, 9) has been suggested to be a mechanism that in the human fetus could restrict IGF-mediated growth *in utero*.

The physiological role of IGFBP-1 depends not only on the levels of IGFBP-1 but also on its phosphorylation (57). Phosphorylation and glycosylation of proteins usually result in specific functional consequences or may be caused by a disease (58, 59). IGFBP-1 phosphorylation is suggested as a key mechanism in modulation of cellular responses to IGFs (60) and subsequently in restriction of IGF-I mediated fetal growth (25, 61).

HepG2 cells represent fetal liver metabolism in vitro (62-64) and have successfully been used in studies with IGFBP-1 involving fetal hypoxia (17, 36, 65). Furthermore, IGFBP-1 phosphoisoforms purified from HepG2 show similar IGF-I binding characteristics to that of the plasma (66). Considering that variable phosphorylation of IGFBP-1 could modulate IGF-I bioavailability in hypoxia, we selected HepG2 cells for the current study.

ELISA data revealed that the total serine phosphorylation of IGFBP-1 increased for hypoxia and leucine deprivation, proportional to the overall increases in IGFBP-1 secretion. Although total protein was decreased, qualitatively, IGFBP-1 and its

phosphorylation were concomitantly induced with both treatments. 2-D immunoblotting combined with the ELISA results suggest that despite modest changes detected in overall phosphorylation, the proportion of multi-phosphorylated isoforms is substantially increased. The affinity of IGFBP-1 for IGF-I was also increased for both hypoxic and leucine deprivation treatments, but more so, consequent to hypoxia.

The relative phosphopeptide intensity for pSer169 increased most dramatically under hypoxia. This was followed by pSer101. Protein phosphorylation being a complex dynamic process often involves multiple phosphorylation sites (67). Although technical challenges limit the identification of multiply phosphorylated peptides (34, 68), a doubly phosphorylated peptide was identified in hypoxia. With close proximity of pSer98 with the major functional site, pSer101 (41), it is conceivable that in hypoxia, interactions between the adjacent phosphoserines may be significant in the mechanism of kinase actions (69). Future mutagenesis study should clarify the importance of pSer98 in IGFBP-1 structure and in the functional responses (70, 71).

In the case of leucine deprivation, pSer119 appeared to increase the greatest proportion, followed by pS169. In addition, the effects on IGFBP-1 induction and its phosphorylation were not solely dose dependent (data not shown) when tested under physiologically relevant concentrations (72). These results suggest that possibly extreme nutrient restriction may be necessary to induce IGFBP-1 phosphorylation to exert any potential metabolic effects in regulation of IGF-I. The differences in IGFBP-1 phosphorylation sites induced by hypoxic and leucine

deprivation are of potential interest; distinct variations in IGFBP-1 phosphorylation were also consistent with its IGF-binding kinetics. A greater binding affinity of IGFBP-1 for IGF-I in hypoxia is also associated with stronger inhibitory activity to IGF actions.

During pregnancy, IGFBP-1 in plasma is in the non- and lesser-phosphorylated forms (66, 73). The putative mechanisms leading to hyperphosphorylated IGFBP-1 in stress conditions are unknown. IGFBP-1 is a substrate of multiple protein kinases (74-76). We speculate that the balance of kinases regulated by environmental stimuli is altered (35, 77, 78). As a result, the production and/or the activity of one or multiple protein kinases (79) may be induced (80). Alternatively, reduced dephosphorylation by AKP isoforms (81), such as due to aberrant glycosylation (58), may broaden action potentials resulting in hyperphosphorylated IGFBP-1. Assuming that hypoxic modulation of IGFBP-1 phosphorylation in cell culture reflects the *in vivo* situation, further investigations should have important implications for the mechanisms through which the fetus responds to low oxygen supply. Proteolysis and dephosphorylation of IGFBP-1 are two physiological processes that may have complementary roles in regulating the bioavailability of IGF-I. The widespread oxygen-sensing (82) and signalling mechanisms (83) together with increased phosphorylation in hypoxia could also affect IGFBP-1 proteolysis (25, 84).

Several factors have so far been associated with fetal stress that could contribute to elevated levels of IGFBP-1 mRNA and protein (85-87). This study provides the first biochemical and physiological evidence of altered IGFBP-1 phosphorylation as a regulatory mechanism of fetal adaptive response to hypoxia and possibly to severe

under nutrition in utero. Whether IGFBP-1 phosphorylation may be a potential

mechanism in other catabolic conditions, that lead to elevated IGFBP-1 production,

(88-91) needs to be investigated.

7.5. REFERENCES

1. Iwashita, M. (1994). [Physiological significance of IGF-I and its binding proteins on fetal growth and maturation]. *Nippon Sanka. Fujinka. Gakkai. Zasshi. 46*:660–672 (Japanese).

2. Martina, N.A., Kim, E., Chitkara, U., Wathen, N.C., Chard, T., Giudice, L.C. (1997) Gestational age-dependent expression of insulin-like growth factor-binding protein-1 (IGFBP-1) phosphoisoforms in human extraembryonic cavities, maternal serum, and decidua suggests decidua as the primary source of IGFBP-1 in these fluids during early pregnancy. *J. Clin. Endocrinol. Metab. 82*:1894–1898.

3. Sugawara J., Tazuke, S.I., Suen, L.F., Powell, D.R., Kaper, F., Giaccia, A.J., Giudice, L.C. (2000) Regulation of insulin-like growth factor-binding protein 1 by hypoxia and 3',5'-cyclic adenosine monophosphate is additive in HepG2 cells. *J. Clin. Endocrinol. Metab*. 85:3821–3827.

4. Ben Lagha, N., Seurin, D., Le Bouc, Y., Binouxm M., Berdal, A., Menuelle, P., Babajko, S. (2006) Insulin-like growth factor binding protein (IGFBP-1) involvement in intrauterine growth retardation: study on IGFBP-1 overexpressing transgenic mice. *Endocrinology. 147*:4730–4737.

5. Watson, C.S., Bialek, P., Anzo, M., Khosravi, .J, Yee, S.P., Han, V.K. (2006) Elevated circulating insulin-like growth factor binding protein-1 is sufficient to cause fetal growth restriction. *Endocrinology 147*:1175–1186.

6. Giudice, L.C., de Zegher, F., Gargosky, S.E., Dsupin, B.A., de las Fuentes, L., Crystal, R.A., Hintz, R.L., Rosenfeld, R.G. (1995) Insulin-like growth factors and their binding proteins in the term and preterm human fetus and neonate with normal and extremes of intrauterine growth. *J. Clin. Endocrinol. Metab. 80*:1548–1555.

7. Maures, T.J., Duan, C. (2002) Structure, developmental expression, and physiological regulation of zebrafish IGF binding protein-1. *Endocrinology 143*:2722–2731.

8. Huang, S.T., Vo, K.C., Lyell, D.J., Faessen, G.H., Tulac, S., Tibshirani, R., Giaccia, A.J., Giudice, L.C. (2004) Developmental response to hypoxia. *FASEB J 18*:1348–1365 .

9. Kajimura, S., Aida, K., Duan, C. (2005) Insulin-like growth factor-binding protein-1 (IGFBP-1) mediates hypoxia-induced embryonic growth and developmental retardation. *Proc. Natl. Acad. Sci. USA 102*:1240–1245 .

10. Rajkumar, K., Krsek, M., Dheen, S.T., Murphy, L.J. (1996) Impaired glucose homeostasis in insulin-like growth factor binding protein-1 transgenic mice. *J. Clin. Invest. 98*:1818–1825.

11. Finlay, D., Patel, S., Dickson, L.M., Shpiro, N., Marquez, R., Rhodes, C.J., Sutherland, C. (2004) Glycogen synthase kinase-3 regulates IGFBP-1 gene transcription through the thymine-rich insulin response element. *BMC Mol. Biol.* 5:15 .

12. Langford, K., Blum, W., Nicolaides, K., Jones, J., McGregor, A., Miell, J. (1994) The pathophysiology of the insulin-like growth factor axis in fetal growth failure: a basis for programming by undernutrition? *Eur. J. Clin. Invest. 24*:851–856.

13. Tapanainen, P.J., Bang, P., Wilson, K., Unterman, T.G., Vreman, H.J., Rosenfeld, R.G. (1994) Maternal hypoxia as a model for intrauterine growth retardation: effects on insulin-like growth factors and their binding proteins. *Pediatr. Res. 36*:152–158.

14. Unterman, T.G., Oehler, D.T., Murphy, L.J., Lacson, R.G. (1991) Multihormonal regulation of insulin-like growth factor-binding protein-1 in rat H4IIE hepatoma cells: the dominant role of insulin. *Endocrinology 128*:2693–2701.

15. Lee, P.D., Giudice, L.C., Conover, C.A., Powell, D.R. (1997) Insulin-like growth factor binding protein-1: recent findings and new directions. *Proc. Soc. Exp. Biol. Med. 216*:319–357.

16. Gibson, J.M., Westwood, M., Lauszus, F.F., Klebe, J.G., Flyvbjerg, A., White, A. (1999) Phosphorylated insulin-like growth factor binding protein 1 is increased in pregnant diabetic subjects. *Diabetes. 48*:321–326.

17. Popovici, R.M., Lu, M., Bhatia, S., Faessen, G.H., Giaccia, A.J., Giudice, L.C. (2001) Hypoxia regulates insulin-like growth factor-binding protein 1 in human fetal hepatocytes in primary culture: suggestive molecular mechanisms for *in utero* fetal growth restriction caused by uteroplacental insufficiency. *J. Clin. Endocrinol. Metab. 86*:2653–2659.

18. Lindsay, R.S., Westgate, J.A., Beattie, J., Pattison, N.S., Gamble, G., Mildenhall, L.F., Breier, B.H., Johnstone, F.D. (2007) Inverse changes in fetal insulin-like growth factor (IGF)-1 and IGF binding protein-1 in association with higher birth weight in maternal diabetes. *Clin. Endocrinol. (Oxf) 66*:322–328.

19. Kajimura, S., Duan, C. (2007) An evolutionarily conserved fine tuner of IGF actions under catabolic conditions. *J. Fish Biol.* 94:E46–E54.

20. Fowden, A.L., Giussani, D.A., Forhead, A.J. (2006) Intrauterine programming of physiological systems: causes and consequences. *Physiology (Bethesda) 21*:29–37.

21. Firth, S.M., Baxter, R.C. (2002) Cellular actions of the insulin-like growth factor binding proteins. *Endocr. Rev. 23*:824–854.

22. Westwood, M., Gibson, J.M., Davies, A.J., Young, R.J., White, A. (1994) The phosphorylation pattern of insulin-like growth factor-binding protein-1 in normal

plasma is different from that in amniotic fluid and changes during pregnancy. *J. Clin. Endocrinol. Metab. 79*:1735–1741.

23. Loukovaara, M., Leinonen, P., Teramo, K., Nurminen, E., Andersson, S., Rutanen, E.M. (2005) Effect of maternal diabetes on phosphorylation of insulin-like growth factor binding protein-1 in cord serum. *Diabet. Med. 22*:434–439.

24. Jones, J.I., Busby, Jr. W.H., Wright, G., Smith, C.E., Kimack, N.M., Clemmons, D.R. (1993) Identification of the sites of phosphorylation in insulin-like growth factor binding protein-1. Regulation of its affinity by phosphorylation of serine 101. *J. Biol. Chem. 268*:1125–1131 .

25. Gibson, J.M., Aplin, J.D., White, A., Westwood, M. (2001) Regulation of IGF bioavailability in pregnancy. *Mol. Hum. Reprod. 7*:79–87.

26. Eghbali-Fatourechi, G., Conover, C.A., Sieck, G.C., Gores, G.J., Fitzpatrick, L.A. (1994) Secretion of insulin-like growth factor binding protein-1 from individual hepatocytes. *Res. Commun. Mol. Pathol. Pharmacol. 85*:243–259.

27. Averous, J., Maurin, A.C., Bruhat, A., Jousse, C., Arliguie, C., Fafournoux, P. (2005) Induction of IGFBP-1 expression by amino acid deprivation of HepG2 human hepatoma cells involves both a transcriptional activation and an mRNA stabilization due to its 3'UTR. *FEBS Lett. 579*:2609–2614.

28. El Khattabi, I., Remacle, C., Reusens, B. (2006) The regulation of IGFs and IGFBPs by prolactin in primary culture of fetal rat hepatocytes is influenced by maternal malnutrition. *Am. J. Physiol. Endocrinol. Metab. 291*:E835–E842.

29. Seferovic, M.D., Krughkov, V., Pinto, D., Han, V.K., Gupta, M.B. (2008) Quantitative 2-D gel electrophoresis-based expression proteomics of albumin and IgG immunodepleted plasma. *J. Chromatogr. B Analyt. Technol. Biomed. Life. Sci. 865*:147–152.

30. Grulich-Henn, J., Spiess, S., Heinrich, U., Schonberg, D., Bettendorf, M. (1998) Ligand blot analysis of insulin-like growth factor-binding proteins using biotinylated insulin-like growth factor-I. *Horm. Res. 49*:1–7.

31. Gupta, M.B., Seferovic, M.D., Liu, S., Gratton, R.J., Doherty-Kirby, A., Lajoie, G.A., Han, V.K.M. (2006) Altered proteome profiles in maternal plasma in pregnancies with fetal growth restrictions. *Clin. Proteomics. 2*:169–184.

32. Khosravi, M.J., Diamandi, A., Mistry, J. (1997) Immunoassay of insulin-like growth factor binding protein-1. *Clin. Chem. 43*:523–532.

33. Khosravi, J., Krishna, R.G., Bodani, U., Diamandi, A., Khaja, N., Kalra, B., Kumar, A. (2007) Immunoassay of serine-phosphorylated isoform of insulin-like growth factor (IGF) binding protein (IGFBP)-1. *Clin. Biochem. 40*:86–93.

34. Liu, S., Zhang, C., Campbell, J.L., Zhang, H., Yeung, K.K., Han, V.K., Lajoie, G.A. (2005) Formation of phosphopeptide-metal ion complexes in liquid

chromatography/electrospray mass spectrometry and their influence on phosphopeptide detection. *Rapid Commun. Mass Spectrom. 19*:2747–2756.

35. Tazuke, S.I., Mazure, N.M., Sugawara, J., Carland, G., Faessen, G.H., Suen, L.F., Irwin, J.C., Powell, D.R., Giaccia, A.J., Giudice, L.C. (1998) Hypoxia stimulates insulin-like growth factor binding protein 1 (IGFBP-1) gene expression in HepG2 cells: a possible model for IGFBP-1 expression in fetal hypoxia. *Proc. Natl. Acad. Sci. USA 95*:10188–10193.

36. Scharf, J.G.,Unterman, T.G., Kietzmann, T. (2005) Oxygen-dependent modulation of insulin-like growth factor binding protein biosynthesis in primary cultures of rat hepatocytes. *Endocrinology 146*:5433–5443.

37. Wenger, R.H., Rolfs, A., Marti, H.H., Bauer, C., Gassmann, M. (1995) Hypoxia, a novel inducer of acute phase gene expression in a human hepatoma cell line. *J. Biol. Chem. 270*:27865–27870.

38. Gabay, C., Kushner, I. (1999) Acute-phase proteins and other systemic responses to inflammation. *N. Engl. J. Med. 340*:448–454.

39. Sonna, L.A., Cullivan, M.L., Sheldon, H.K., Pratt, R.E., Lilly, C.M. (2003) Effect of hypoxia on gene expression by human hepatocytes (HepG2). *Physiol. Genomics. 12*:195–207.

40. Halligan, B.D., Ruotti, V., Jin, W., Laffoon, S., Twigger, S.N., Dratz, E.A. (2004) ProMoST (Protein Modification Screening Tool): a web-based tool for mapping protein modifications on two-dimensional gels. *Nucleic Acids Res. 32*:W638–W644.

41. Jones, J.I., Busby, Jr. W.H., Wright, G., Clemmons, D.R. (1993) Human IGFBP-1 is phosphorylated on 3 serine residues: effects of site-directed mutagenesis of the major phosphoserine. *Growth Regul. 3*:37–40.

42. Wong, M.S., Fong, C.C., Yang, M. (1999) Biosensor measurement of the interaction kinetics between insulin-like growth factors and their binding proteins. *Biochim. Biophys. Acta. 1432*:293–301.

43. Chard, T. (1994) Insulin-like growth factors and their binding proteins in normal and abnormal human fetal growth. *Growth Regul. 4*:91–100.

44. El Khattabi, I., Remacle, C., Reusens, B. (2006) The regulation of IGFs and IGFBPs by prolactin in primary culture of fetal rat hepatocytes is influenced by maternal malnutrition. *Am. J. Physiol. Endocrinol. Metab. 291*:E835–E842.

45. Verhaeghe, J., Van Herck, E., Billen, J., Moerman, P., Van Assche, F.A., Giudice, L.C. (2003) Regulation of insulin-like growth factor-I and insulin-like growth factor binding protein-1 concentrations in preterm fetuses. *Am. J. Obstet. Gynecol. 188*:485–491.

46. Giudice, L.C., Martina, N.A., Crystal, R.A., Tazuke, S., Druzin, M. (1997) Insulin-like growth factor binding protein-1 at the maternal-fetal interface and insulin-like growth factor-I, insulin-like growth factor-II, and insulin-like growth factor binding

protein-1 in the circulation of women with severe preeclampsia. *Am. J. Obstet. Gynecol. 176*:751–757.

47. Grobman, W.A., Kazer, R.R. (2001) Serum insulin, insulin-like growth factor-I, and insulin-like growth factor binding protein-1 in women who develop preeclampsia. *Obstet. Gynecol. 97*:521–526.

48. Ingec, M., Gursoy, H.G., Yildiz, L., Kumtepe, Y., Kadanali, S. (2004) Serum levels of insulin, IGF-1, and IGFBP-1 in pre-eclampsia and eclampsia. *Int. J. Gynaecol. Obstet. 84*:214–219.

49. Takenaka, A., Komori, K., Morishita, T., Takahashi, S.I., Hidaka, T., Noguchi, T. (2000) Amino acid regulation of gene transcription of rat insulin-like growth factor-binding protein-1. *J. Endocrinol. 164*:R11–R16.

50. Casanello, P., Torres, A., Sanhueza, F., Gonzalez, M., Farias, M., Gallardo, V., Pastor-Anglada, M., San Martin, R., Sobrevia, L. (2005) Equilibrative nucleoside transporter 1 expression is downregulated by hypoxia in human umbilical vein endothelium. *Circ. Res. 97*:16–24.

51. Ahmad, S., Ahmed, A. (2004) Elevated placental soluble vascular endothelial growth factor receptor-1 inhibits angiogenesis in preeclampsia. *Circ. Res. 95*:884–891.

52. Underwood, L.E., Thissen, J.P., Lemozy, S., Ketelslegers, J.M., Clemmons, D.R. (1994) Hormonal and nutritional regulation of IGF-I and its binding proteins. *Horm. Res. 42*:145–151.

53. Maulik, D., Frances Evans, J., Ragolia, L. (2006) Fetal growth restriction: pathogenic mechanisms. *Clin. Obstet. Gynecol. 49*:219–227.

54. Leu, J.I., George, D.L. (2007) Hepatic IGFBP1 is a prosurvival factor that binds to BAK, protects the liver from apoptosis, and antagonizes the proapoptotic actions of p53 at mitochondria. *Genes Dev. 21*:3095–3109.

55. Neerhof, M.G., Thaete, L.G. (2008) The fetal response to chronic placental insufficiency. *Semin. Perinatol. 32*:201–205.

56. Kajimura, S., Aida, K., Duan, C. (2006) Understanding hypoxia-induced gene expression in early development: in vitro and in vivo analysis of hypoxia-inducible factor 1-regulated zebra fish insulin-like growth factor binding protein 1 gene expression. *Mol. Cell. Biol. 26*:1142–1155.

57. Coverley, J.A., Baxter, R.C. (1997) Phosphorylation of insulin-like growth factor binding proteins. *Mol. Cell. Endocrinol. 128*:1–5.

58. Liu, F., Zaidi, T., Iqbal, K., Grundke-Iqbal, I., Gong, C.X. (2002) Aberrant glycosylation modulates phosphorylation of tau by protein kinase A and dephosphorylation of tau by protein phosphatase 2A and 5. *Neuroscience. 115*:829–837.

59. Freeze, H.H., Aebi, M. (2005) Altered glycan structures: the molecular basis of congenital disorders of glycosylation. *Curr. Opin. Struct. Biol. 15*:490–498.

60. Baxter, R.C. (2000) Insulin-like growth factor (IGF)-binding proteins: interactions with IGFs and intrinsic bioactivities. *Am. J. Physiol. Endocrinol. Metab. 278*:E967–E976.

61. Westwood, M. (1999) Role of insulin-like growth factor binding protein 1 in human pregnancy. *Rev. Reprod. 4*:160–167.

62. Kelly, J.H., Darlington, G.J. (1989) Modulation of the liver specific phenotype in the human hepatoblastoma line Hep G2. *In Vitro Cell Dev. Biol. 25*:217–222.

63. Wilkening, S., Stahl, F., Bader, A. (2003) Comparison of primary human hepatocytes and hepatoma cell line Hepg2 with regard to their biotransformation properties. *Drug Metab. Dispos. 31*:1035–1042.

64. Maruyama, M., Matsunaga, T., Harada, E., Ohmori, S. (2007) Comparison of basal gene expression and induction of CYP3As in HepG2 and human fetal liver cells. *Biol. Pharm. Bull. 30*:2091–2097.

65. Sugawara, J., Suh, D.S., Faessen, G.H., Suen, L.H., Shibata, T., Kaper, F., Giaccia, A.J., Giudice, L.C. (2000) Regulation of insulin-like growth factor-binding protein-1 by nitric oxide under hypoxic conditions. *J. Clin. Endocrinol. Metab. 85*:2714–2721.

66. Westwood, M., Gibson, J.M., White, A. (1997) Purification and characterization of the insulin-like growth factor-binding protein-1 phosphoform found in normal plasma. *Endocrinology. 138*:1130–1136.

67. Raggiaschi, R., Gotta, S., Terstappen, G.C. (2005) Phosphoproteome analysis. *Biosci. Rep. 25*:33–44.

68. Collins, M.O., Yu, L., Coba, M.P., Husi, H., Campuzano, I., Blackstock, W.P., Choudhary, J.S., Grant, S.G. (2005) Proteomic analysis of in vivo phosphorylated synaptic proteins. *J. Biol. Chem. 280*:5972–5982.

69. Beck, E.J., Sorensen, R.G., Slater, S.J., Covarrubias, M. (1998) Interactions between multiple phosphorylation sites in the inactivation particle of a K+ channel. Insights into the molecular mechanism of protein kinase C action. *J. Gen. Physiol. 112*:71–84.

70. Johnson, L.N., Barford, D. (1993) The effects of phosphorylation on the structure and function of proteins. *Annu. Rev. Biophys. Biomol. Struct. 22*:199–232.

71. Johnson, L.N., O'Reilly, M. (1996) Control by phosphorylation. *Curr. Opin. Struct. Biol. 6*:762–769.

72. Jauniaux, E., Gulbis, B., Acharya, G., Gerlo, E. (1999) Fetal amino acid and enzyme levels with maternal smoking. *Obstet. Gynecol. 93*:680–683.

73. Bhatia, S., Farssen, G.H., Carland, G., Balise, R.L., Gargosky, S.E., Druzin, M., El-Sayed, Y., Wilson, D.M., Giudice, L.C. (2002) A longitudinal analysis of maternal serum insulin-like growth factor (IGF-I) and total and nonphosphorylated IGF-binding protein-1 in human pregnancies complicated by intrauterine growth restriction. *J. Clin. Endocrinol. Metab. 87*:1864–1870.

74. Frost, R.A., Tseng, L. (1991) Insulin-like growth factor-binding protein-1 is phosphorylated by cultured human endometrial stromal cells and multiple protein kinases *in vitro. J. Biol. Chem. 266*:18082–18088.

75. Koistinen, R., Angervo, M., Leinonen, P., Seppala, M. (1993) Phosphorylation of insulin-like growth factor-binding protein-1 from different sources. *Growth Regul. 3*:34–37.

76. Ankrapp, D.P., Jones, J.I., Clemmons, D.R. (1996) Characterization of insulin-like growth factor binding protein-1 kinases from human hepatoma cells. *J. Cell Biochem.* 60:387–399.

77. Uchiumi, T., Kohno, K., Tanimura, H., Hidaka, K., Asakuno, K., Abe, H., Uchida, Y., Kuwano, M. (1993) Involvement of protein kinase in environmental stress-induced activation of human multidrug resistance 1 (MDR1) gene promoter. *FEBS Lett. 326*:11–16.

78. Cushman, J.C., Bohnert, H.J. (1997) Molecular genetics of crassulacean acid metabolism. *Plant Physiol. 113*:667–676.

79. Gao, Z., Hwang, D., Bataille, F., Lefevre, M., York, D., Quon, M.J., Ye, J. (2002) Serine phosphorylation of insulin receptor substrate 1 by inhibitor κB kinase complex. *J. Biol. Chem. 277*:48115–48121.

80. Galetic, I., Andjelkovic, M., Meier, R., Brodbeck, D., Park, J., Hemmings, B.A. (1999) Mechanism of protein kinase B activation by insulin/insulin-like growth factor-1 revealed by specific inhibitors of phosphoinositide 3-kinase—significance for diabetes and cancer. *Pharmacol. Ther. 82*:409–425.

81. Nowrouzi, A., Yazdanparast, R. (2005) Alkaline phosphatase retained in HepG2 hepatocarcinoma cells vs. alkaline phosphatase released to culture medium: difference of aberrant glycosylation. *Biochem. Biophys. Res. Commun. 330*:400–409.

82. Lang, C.H., Nystrom, G.J., Frost, R.A. (1999) Regulation of IGF binding protein-1 in hep G2 cells by cytokines and reactive oxygen species. *Am. J. Physiol. 276(3 Pt 1)*:G719–G727.

83. Frost, R.A., Nystrom, G.J., Lang, C.H. (2000) Stimulation of insulin-like growth factor binding protein-1 synthesis by interleukin-1β: requirement of the mitogen-activated protein kinase pathway. *Endocrinology. 141*:3156–3164.

84. Siwanowicz, I., Popowicz, G.M., Wisniewska, M., Huber, R., Kuenkele, K.P., Lang, K., Engh, R.A., Holak, T.A. (2005) Structural basis for the regulation of insulin-like growth factors by IGF binding proteins. *Structure. 13*:155–167.

85. Buzzio, O.L., Lu, Z., Miller, C.D., Unterman, T.G., Kim, J.J. (2006) FOXO1A differentially regulates genes of decidualization. *Endocrinology. 147*:3870–3876.

86. Lee, M.S., Kim, M.S., Park, S.Y., Kang, C.W. (2006) Effects of betaine on ethanol-stimulated secretion of IGF-I and IGFBP-1 in rat primary hepatocytes: involvement of p42/44 MAPK activation. *World J. Gastroenterol. 12*:1718–1722.

87. Marchand, A., Tomkiewicz, C., Magne, L., Barouki, R., Garlatti, M. (2006) Endoplasmic reticulum stress induction of insulin-like growth factor-binding protein-1 involves ATF4. *J. Biol. Chem. 281*:19124–19133.

88. Hoybye, C., Hilding, A., Jacobsson, H., Thoren, M. (2002) Metabolic profile and body composition in adults with Prader-Willi syndrome and severe obesity. *J. Clin. Endocrinol. Metab. 87*:3590–3597.

89. Saeki, H., Hamada, M., Hiwada, K. (2002) Circulating levels of insulin-like growth factor-1 and its binding proteins in patients with hypertrophic cardiomyopathy. *Circ. J. 66*:639–644.

90. Bankowski, E., Sobolewski, K., Palka, J., Jaworski, S. (2004) Decreased expression of the insulin-like growth factor-I-binding protein-1 (IGFBP-1) phosphoisoform in pre-eclamptic Wharton's jelly and its role in the regulation of collagen biosynthesis. *Clin. Chem. Lab. Med. 42*:175–181.

91. Axelsson, J., Qureshi, A.R., Divino-Filho, J.C., Barany, P., Heimburger, O., Lindholm, B., Stenvinkel, P. (2006) Are insulin-like growth factor and its binding proteins 1 and 3 clinically useful as markers of malnutrition, sarcopenia and inflammation in end-stage renal disease? *Eur. J. Clin. Nutr. 60*:718–726.

CHAPTER 8

Summary and Perspectives

8.1. MATERNAL PLASMA PROTEIN CHANGES

8.1.1. Summary of findings

Maternal plasma proteome profiling of FGR pregnancies (Chapter 2) led to the successful identification of a variant of Hp α2 as changing in FGR. Despite this success, further broad profiling of the 2-D gels proved impossible due to the technical challenges of profiling un-depleted plasma on small format 2-D gels. To improve the proteomic analysis of the samples, optimizations to the methodology were carried out to maximize the spot resolution (Chapter 3). The depletion of albumin and IgG from the plasma, the adoption of large format 24 cm 2-D gels, and the use of more advanced software with the "same-spots" feature, made a substantial and measurable improvement in the resolution which proved to be significant and reproducible (Chapter 3). Using this optimized approach, a new experiment was undertaken with FGR mothers' plasma (n=12) and gestational age-matched controls (n=12). Though a further 15 proteins were found either increasing or decreasing, and subsequently identified by LC-MS/MS and NCBI database searching, no novel proteins of interest could be identified as changing with subsequent immunoblots or quantitative immunoassay analysis (Data not presented in this thesis).

Hp was therefore the only maternal protein of interest identified by 2-DGE. Hp is up-regulated by Il-1β, TNF-α, and particularly IL-6 in the liver (1, 2). It is also expressed in vascular endothelial cells and neutrophils (3) in response to TNF-α. The pro-angiogenic protein Hp is therefore induced in inflammation. The same inflammatory cytokines that up-regulate its expression are also powerful activators of vascular

endothelial inflammation, a process antecedent to angiogenesis. It appears highly plausible then that Hp expression may be related to localized vascular inflammation in the maternal placenta. The levels of inflammatory cytokines as well as markers of endothelial activation in the maternal plasma were therefore sought.

Inflammatory cytokines Il-1ß, Il-6, and TNF-α, as well as vascular endothelial activation markers E-selectin, VCAM-1, and ICAM-1, were measured in the maternal plasma (Chapter 6). Inflammatory cytokines were not increased in FGR. Interestingly, both E-selectin and VCAM-1 were increased relative to placental size. VCAM-1 was highly predictive of the placental weight and the fetus' birthweight for normal pregnancies, and also appeared to increase with gestational age. It was therefore suggested that VCAM-1 be assessed further for its potential as a biomarker of placental health (Chapter 6).

8.1.2. Significance of maternal plasma protein changes

Haptoglobin

Although, ELISA showed that Hp was not changed in overall levels between control and FGR (data not presented in this thesis), a careful study of the Hp α2 variants by Mikkat and others identified the structural differences between the variants, and confirmed the post-translational modifications (PTMs) responsible for variant 1's 2-fold decrease (4).
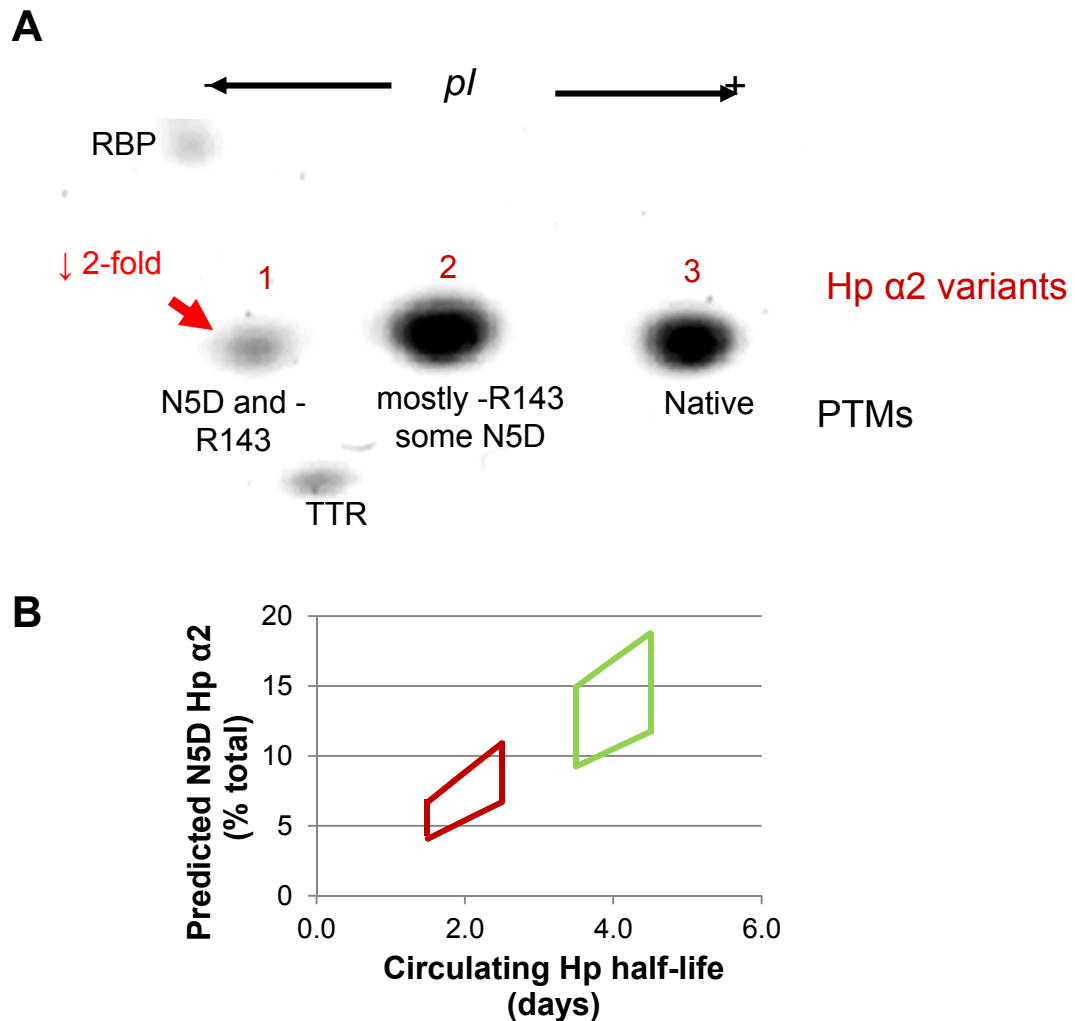
FIGURE 8.1. Hp structure and predicted life in maternal circulation. **(A)** The structure of the Hp α2 variants as worked out by Mikkat and others (2004). MS/MS analysis showed that variant 3 of haptoglobin (Hp) is native. Variant 2 of Hp is a mixture of α2 subunits either missing a C-terminal arginine at position 143 (-R143), or a smaller subset having an asparagine deamidation to an aspartic acid at position 5 (N5D). Variant 1 then contains both modifications. Cleavage of R143 takes place normally in the circulation by an unidentified carboxypeptidase. Variant 1 was found in chapter 2 to be reduced 2-fold in FGR mothers' plasma (p<0.006). **(B)** Deamidation of Asp takes place predictably over time in plasma proteins. Given the adjacent amino acids, Hp N5 has a predicted half-life of ~20 days before deamidation. Hp turnover in the circulation has normally a half-life of 4 days. The predicted proportion of Hp that is deamidated is graphed within a range of +/- 20%. Normal haptoglobin turnover (4 +/-0.5 days, green) and haptoglobin turnover of twice that rate (2 +/-0.5 days, red).

The Hp variant 1 contains two modifications (Figure 8.1A): a deamidation at Asn5 and a cleavage of C-terminal Arg143 (4). Arg143 is cleaved by a yet unidentified carboxypeptidase in the circulation (5). Deamidation takes place naturally and at a predictable rate, such that the half-life can be accurately inferred (6). Given the primary structure of Asn at the 5th amino acid, deamidation of Hp α2 is estimated with a half-life of ~20 days. Since the normal turnover of haptoglobin in the circulation is ~4 days (7), it can be estimated that 10-20% of Hp will be deamidated normally (Figure 8.1B, green). This is roughly in proportion to the distribution of the three variants by 2-DGE densitometry in controls (Figure 2.1 A and B). The 2-fold decrease in Hp α2 variant 1 in FGR may be accounted for by the doubling of the turnover rate of Hp, which would halve the proportion of deamidated Hp in circulation (Figure 8.1B, red). Alternatively, there could be decreased cleavage of Arg143 so that Hp may be more evenly divided between variants 2 and 3 (Figure 8.1A).

In either case (of increased Hp turnover, or increased Arg143 cleavage in the circulation), changing Hp PTMs are very likely attributable to functional changes of Hp in the maternal circulation. Although traditionally associated with an iron transportation function, Hp has been identified as having a major role in immunoregulation. Hp binds CD11b/CD18 (8), CD22 (9), and instigates a variety of immuno-inhibitory effects in T-cells (10), B cells (9), neutrophils (11), and macrophages (12). Together with the observation of its localization in the decidua at the maternal-fetal interface throughout pregnancy (13, 14, 15), this has led to the

speculation that Hp may be involved in suppressing the maternal immune response to the fetal tissues. Since vascular failure is of primary concern in placental insufficiency, it is of particular interest, that Hp is a potent inducer of angiogenesis., and has been associated with other vascular pathologies (16). Alterations in either its anti-immune or pro-angiogenic functions may therefore be associated with pathophysiological changes in FGR.

VCAM-1

Plasma levels of both soluble E-selectin and VCAM-1 are pro-angiogenic (17). VCAM-1 deletion is embryonic lethal in mice due to its importance in vascular formation in the placenta (18, 19). It is expressed from proliferating endothelial cells, and is required for blood vessel formation (20). That VCAM-1 expression correlates to placental weight in controls, and also increases with GA in controls, strongly indicates that VCAM-1 is functioning in normal vascular development. VCAM-1 expression increases in plasma as placental growth continues, and so changing levels of VCAM-1 in circulation in pregnancy most likely reflect changes in the placenta.

In FGR, VCAM-1 is more highly expressed before the prenatal period (i.e. <34 weeks). The levels in FGR are unrelated to increased placental weight, and decrease instead of increase with GA (Figure 6.6). Therefore its upregulation is in a manner unrelated to normal placental development. VCAM-1 is expressed only in very low amounts from endothelial cells in mature quiescent vasculature, but is upregulated in

angiogenesis, and is also strongly induced in inflammation and injury (20, 21). Thus, although in normal pregnancy VCAM-1 expression may be related to vascular development, in placental insufficiency, localized placental inflammation may lead to aberrantly upregulated levels of VCAM-1.

Maternal Vascular inflammation

Here we report evidence of maternal-vascular inflammation related to the placenta. Changes in oxygen conditions can cause inflammation. In placental insufficiency, maternal blood in the intervillous space, and blood returning to the mother's heart via the uterine veins, is higher than in normal pregnancies, as the fetal chorionic villi have failed to remove sufficient oxygen and nutrients from the maternal supply (22) (Figure 1.2.). The condition of supraoxic maternal-placental blood may be causing the localized inflammation. Oxygen-mediated inflammation may be analogous to reperfusion injury in the heart. In reperfusion injury, ROS mediated localized inflammation leads to endothelial expression of E-selectin, VCAM-1, and ICAM-1. Neutrophils roll and arrest on inflamed endothelial cells via cellular adhesion molecules ICAM-1 and VCAM-1 (23). Changing levels of oxygen or abnormally high ROS levels may then trigger inflammation; however, other factors could also be contributing. It has been shown, for example, that primary trophoblast cells from complicated pregnancies (FGR with preeclampsia) can induce endothelial activation in the maternal post-placental vessels by secretion of chymotrypsin-like proteases (24, 25).

Both Hp and CAM expression changes may therefore be related to inflammation. Other studies have shown increased inflammatory cytokine TNF-α in FGR mothers with placental insufficiency (26). As these changes are in the maternal circulation, vessel changes are unlikely to have any benevolent affect to maternal-fetal exchange in placental insufficiency. Nevertheless, the findings indicate that there are maternal vascular changes taking place in placental insufficiency. Most importantly however, the protein changes caused by vascular inflammation/activation may act as biomarkers, providing a basis for monitoring placental health in FGR with placental insufficiency.

8.1.3. Haptoglobin and VCAM-1 as biomarkers

The changing levels of both Hp and VCAM-1 in FGR compared to controls suggests they have potential as biomarkers of the disease. For a protein change to pass from the discovery phase to a biomarker with potential clinical relavence, validation criteria must be considered. Of primary interest are the sensitivity and specificity as well as the positive and negative predictive values of the protein change (27). Determination of these criteria involves large cohort studies with thousands of patients with a well defined pathology, and highly specific and quantitiative measurement's, most often done by ELISA.

The considerable effort and investment in the validation phase necessitates the carful prioritization and stratification of discovered markers. Selecting markers as

potential candidates then is critical, and should include primarily consideration of its potential specificity based on laboratory scale, highly specific immunobased measurement. The protein's levels should be chaning to as large a degree as possible between pathological and control patients. And finally, the potential biomarker should be resilient to variability inevitable with sample processing (27).

Although Hp and its modifications have a robust halflife (Figure 8.1), Hp may or may not prove to be highly specific to FGR given its changing levels in a variety of diseases. Detection of the identified specifiec PTM changes may prove more specific and predictive of FGF than overall protein changes. However, the detection of a single deamidation within the protein (in the absence of a highly specific antibody) presents challenges to its validation. As a subsequent study to assess the potential predictive value of Hp for placental insufficiency, the development of a Multiple Reaction Monitoring (MRM) assay should be developed. Mass spectrometric based MRM assays can rapidly select a known group of CID ions from a complex sample mixtures and digests and analyze for predetermined changes such as PTMs. As such they are highly sensitive and high-throughput, and therefore the development of an assay of the ratio of Hp ions related to its PTMs, compared to the ions produced in the absence of PTMs, could experimentally quantify the relative prevalence of variant 1 in FGR. Such a metod is practicable for larger scale validation that is required to assess the predictive sensitivity and specificity of the Hp protein modifications. Both the deamidation and the absence of the terminal arginine on Hp α2 could be considered. Currently, the detection of deamidated gliadin with a highly specific

antibody is being evaluated as a diagnostic test for Celiac disease (28, 29). For diagnostic purposes, a highly specific antibody to the Hp protein modification would also have to be developed, as mass-spectrometric based diagnostics are not yet broadly implemented by health care providers.

VCAM-1 antibodies are available, therefore an assessment of its specificity for placental insufficiency could be undertaken. As VCAM-1 is expressed only in developing or inflamed vessels, there is minimal baseline plasma expression originating from mature maternal vessels, and its blood plasma levels may therefore reflect placental changes very sensitively. Since VCAM-1 is increased <34 weeks in FGR but is decreased in the pre-perinatal period, there would be predictive value in monitoring VCAM-1 levels at multiple time points throughout pregnancy. A rapid increase in circulating VCAM-1 at a time point prior to 34 weeks followed by a decrease would indicated placental insufficiency, where continually increasing (or unchanging) VCAM-1 levels in the same time period would be normal. A large prospective study is therefore suggested.

Since the levels of VCAM-1 were increased to a larger degree between control and FGR after controlling for birthweight, the placental or fetal weight (which is estimated routinely by ultrasound) could be controlled for greater predictive power. Elevated levels of VCAM-1 based on standardized expected VCAM-1 levels for fetal size for a given fetal size prior to 34 weeks, the time period of both the greatest placental angiogenesis and the maximal separation of VCAM-1, may be a very sensitive means to distinguish SGA from FGR. Furthermore, the pre-perinatal period

would be a sufficiently early timepoint to identify FGR to facilitate fetal monitoring and potentially early delivery, which is currently the most effective intervention (30). The antecedent step in a subsequent validation study therefore, should be the measurement of VCAM-1 in a large sample group at time points coinciding with US examinations. Matching VCAM-1 levels with the estimated fetal size in control pregnancies would determine a baseline expression. The predictive power in terms of the sensitivity, specificity, false positive and negatives, of changing VCAM-1 levels in mothers that went on to develop FGR could then be determined, as well as the full extent of the biomarker's clinical utility.

8.2. FETAL PLASMA PROTEIN CHANGES

8.2.1. Summary of findings

Improved 2-DGE following immunodepletion (Chapter 3) identified several proteins in fetal plasma to be changing, including clusterin and fibrinogen (Chapter 4 supplemental). Targeted profiling of plasma proteins, using an *in vitro* model of liver secretion changes in hypoxia, was more successful. From our HepG2 cell culture model, transferrin and PAI-1 were added to fibrinogen and clusterin, as proteins shortlisted as both changing with hypoxic treatment, and functioning in a capacity of angiogenesis or blood vessel regulation (Chapter 4). These proteins were in fact found to have oxygen dependent fetal plasma expression, presumably because of hepatic secretion changes in *in utero* oxygen starvation (Chapter 4). As expected, the liver secretion of IGFBP-1, which functions in fetal growth regulation, was also found

to increase in hepatic secretion in hypoxia. Together this demonstrates that the liver is altering secretion of several key proteins in an oxygen-dependent manner in FGR.

PAI-1, fibrinogen, transferrin, and clusterin are upregulated in response to inflammation in an acute phase response. The hypothesis that placental inflammation was leading to increasing expression of these proteins was therefore evaluated as well. Inflammatory cytokines Il-1β, IL-6, and TNF-α, as well as markers of vascular inflammation, E-selectin, VCAM-1, and ICAM-1 in the fetal plasma were therefore measured in the effluent placental blood (Chapter 6). Although, highly-elevated levels of Il-1ß, IL-6, and TNF-α demonstrate that there is substantial fetal-placental inflammation (Chapter 6), no relationship existed between the levels of the cytokines and the levels of the hepatic secreted proteins in plasma (Data not presented in this thesis). However, it was found that the data nevertheless supports the theory that inflammation is at least partially brought on by chronic hypoxia in FGR, as levels of IL-6, TNF-α, and also ICAM-1 and E-selectin were correlated to blood gas conditions.

The expression of the hepatic proteins PAI-1, fibrinogen, transferrin, clusterin and IGFBP-1 then were hypoxic mediated. Although inflammatory cytokine levels were also related to levels of oxygen, IL-6 and TNF-α did not explain the hepatic protein secretion changes *in vivo*. The acute-phase like protein secretion changes in FGR were therefore directly mediated by hypoxia, and not through cytokine intermediaries. Acute phase-like secretion changes following hypoxic treatment of

hepatocytes has been described in the literature (31). The functional consequences of the most interesting hepatic protein secretion changes were therefore sought.

Angiogenesis - PAI-1

Since angiogenic regulation is central to the pathology of FGR, identifying changes in liver secretion associated with angiogenic function was crucial. It was shown, using the *in vitro* model, that liver secretions were inducing angiogenesis (Chapter 4). We therefore set out to discover whether fetal plasma exhibited the same angiogenic effect in relation to the levels of its hepatic secreted plasma proteins. The fetal plasma from hypoxic pregnancies not only induced angiogenesis, but did so in an oxygen-dependent manner (Chapter 5). Of the liver proteins analyzed, PAI-1 levels exhibited the strongest relationship with angiogenesis, and were also very strongly correlated with hypoxia (Chapters 4 and 5). Inhibition of plasma PAI-1 led to confirmation of its significant involvement in angiogenic regulation in the plasma (Chapter 5).

Although the increased angiogenic potential in plasma was related to hypoxia, the levels of both FGF-2 and VEGF did not change between control and FGR (Chapter 5). Their plasma levels correlated to the angiogenic-inducing potential of the plasma in an *in vitro* assay for normal (control) pregnancies, but did not account for the increased angiogenesis in FGR. This finding is consistent with other reports of unchanged VEGF levels in FGR (32, 33)**.** Since increasing angiogenesis is not explained

by either FGF-2 or VEGF, alternative, oxygen-dependent mechanisms of regulation, like PAI-1 upregulation, may well play a large role in vascular changes in FGR placenta *in utero*.

Fetal Growth - IGFBP-1

Our findings confirmed previous reports of increased IGFBP-1 secretion from HepG2 cells. In addition to its expression however, IGFBP-1's regulation of IGF-I is PTM-dependent. Since it is known that phosphorylation changes may affect IGFBP-1's binding affinity (34), we set out to determine if hypoxia affected its phosphorylation as well (Chapter 7). It was determined by 2-D blotting that not only hypoxia but additionally leucine deprivation led to increased secretion of highly phosphorylated variants from HepG2 cells. LC-MS/MS analysis revealed four serine phosphorylation sites: three known sites (pSer101, pSer119, and pSer169); as well as one novel site (pSer98). LC-MS further determined the site specific increases in phosphorylation. The highly phosphorylated IGFBP-1 isoforms had greater affinity for IGF-I, and inhibited IGF-I-stimulated cell proliferation more strongly. By binding to IGF-I with high affinity, IGFBP-1 sequesters IGF-I in the circulation, thereby limiting its bioavailability and growth promoting activity (34, 35). The finding here of IGFBP-1's increased phosphorylation in hypoxia may additionally modulate fetal growth in FGR *in vivo*.

8.2.2. Significance of fetal plasma protein changes

Liver secreted PAI-1 regulates angiogenesis in FGR

Given that the chorionic villi in FGR are compromised, it was unexpected that umbilical vein plasma induces angiogenesis in FGR at all, as it might be inhibitive of the process instead. That plasma PAI-1 had such a strong relationship with angiogenesis in hypoxic pregnancies was logical, given its regulation via HIF-1 and its known function in regulating the vasculature. Indeed, high circulating levels of PAI-1 are predictive of poor outcomes in many cancers because of their pro-angiogenic affects. PAI-1-deficient mice show reduced vascularization of both maternal and fetal placental tissues, where there are changes to the vasculature of the decidua and labyrinth (36). Altering levels of PAI-1 then may very well be directly implicated in the vascular changes in FGR of human pregnancies.

PAI-1 is upregulated via VEGF. In our experiments, PAI-1 very strongly correlated to circulating VEGF levels in controls only. There may therefore be a dual regulation such that in normal pregnancies PAI-1 is involved in a VEGF-mediated angiogenic mechanism, while in FGR cases, PAI-1 mediated angiogenesis is increased directly via its hypoxic upregulation. Angiogenesis follows endothelial migration which is driven by dynamic ECM changes. Regulation of the ECM is one of the antecedent and necessary steps in angiogenesis. PAI-1 is surmised to induce angiogenesis via stabilization of the ECM, tipping the balance towards a stable scaffold for endothelial proliferation and migration.

PAI-1 mediated angiogenesis is therefore inherently not directed, as locally secreted VEGF mediated angiogenesis might be; its increased levels regulate by simply creating pro-angiogenic conditions. Further, it functions counter to VEGF mediated secretion of proteases that break down the ECM. This could contribute to an elongated versus branched phenotype of the chorionic villi, as it is plausible that high levels of PAI-1 may favor non-sprouting (either proliferative or intercalative) over VEGF mediated sprouting angiogenesis, where more substantial ECM reorganization is perhaps necessary (Figure 1.4). PAI-1's pro-angiogenic effects would therefore function primarily in elongation, creating the poorly branched and excessively elongated chorionic villi phenotype, in the critical >25 week period, that is characteristic of FGR with ARED (Figure 1.3). It is theorized then, that PAI-1 is directly implicated in the fetal pathology through this proposed mechanism.

As plasma is in contact with all fetal and placental tissues, circulating PAI-1 levels are likely to exhibit their pro-angiogenic effect at the sites of greatest endothelial activity; the placental or fetal tissues undergoing vascular developmental changes. This may be particularly the case if the plasma expression levels are mediated primarily by liver secretions in hypoxia, and not by local endothelial expression. PAI-1 then, may contribute to vascular changes in the fetus that have long term effects. It is well known that FGR babies have increased risk hypertension, coronary heart disease and stroke (37, 38, 39). Hypoxic upregulation of plasma PAI-1 could mediate lasting vascular changes in the fetus itself, potentially compromising vascular health in later life in early development (DOHaD).

Although we have identified circulating levels of PAI-1 as having a critical function in plasma regulation of angiogenesis in FGR, it remains unclear whether its upregulation is a primary etiological factor, or is a consequence of hypoxia that exacerbates, or mitigates, the placental failure. It is furthermore not known if hepatic PAI-1 upregulation is sufficient to cause changes in vascular formation of the placenta on its own, as endothelial cell secretion likely has a significant role as well. Further study to determine what effect hepatic versus endothelial PAI-1 expression has on angiogenic regulation in FGR remains to be undertaken. The use of PAI-1 knockout mouse, or alternatively, a model with inducible PAI-1 expression (liver-specific or otherwise), would help resolve remaining questions as to whether upregulation of PAI-1 *in vivo* exacerbates or mitigates the placental vascular failure, and confirm that the liver has a role in placental vascular regulation. The use of murine models however is limiting because of the absence of chorionic villi. The drastically more efficient labyrinth vascular organization in mice, may not reveal the full significance of PAI-1 to maternal/fetal exchange. Therefore, the use of ewes or other animal models together with the administration of PAI-1 inhibitors and surgically induced fetal hypoxia, may better gauge the consequences of PAI-1 expression changes.

Vascular inflammation in the fetal-FGR placenta

The hepatic secreted proteins identified, PAI-1, fibrinogen, transferrin, and clusterin, are regulated in an acute phase response by inflammatory cytokines. Inflammatory cytokines furthermore are capable of inducing vascular inflammation. Vascular

remodeling changes in the FGR placenta may be induced directly by inflammation. For these reasons, we measured the fetal levels of inflammatory cytokines Il-1β, IL-6, and TNF-α, as well as markers of vascular inflammation, E-selectin, VCAM-1, and ICAM-1 in the fetal plasma (Chapter 6). The significant highly-elevated levels of Il-1ß, IL-6, and TNF-α demonstrate that there is very substantial fetal-placental inflammation. The data further shows that inflammation is at least partially brought on by chronic hypoxia.

It has been shown that chronic inflammation can lead to vascular changes and angiogenesis. Increased levels of endothelial activation markers E-selectin and especially ICAM-1 were all closely associated with inflammatory cytokine levels. TNF-α has been shown to prime endothelial cells for new sprouting of blood vessels (40). Murine models have shown that overexpression of TNF-α in the lung is sufficient to induce vascular changes (41), and that there is inflammation and immune-mediated angiogenesis following infection (42). Inflammation therefore has a very significant role in angiogenesis.

Early inflammation in the placenta may be disruptive to normal angiogenic processes causing endothelial dysfunction and leading to poorly branched vasculature. Alternatively, inflammation may be in response to hypoxia as a result from the failure of normal angiogenic processes earlier on. In such a scenario, inflammation may be a healing mechanism analogous to angiogenic reperfusion of tissues in wound healing or ischemic injury. Inflammation then may exacerbate the placental insufficiency, or

conversely, mitigate it. An assessment of the effect of fetal-placental vascular inflammation on vascular remodeling and angiogenesis is required.

Liver expression and phosphorylation of IGFBP-1

Secreted IGF-I, either localized or by liver in paracrine and endocrine fashions respectively, stimulates fetal growth via IGFRI activation of the MAPK cell signaling cascade (43). By binding to IGF-I with high affinity, IGFBP-1 sequesters IGF-I in the circulation, thereby limiting its bioavailability for binding to IGFRI, and functioning to limit fetal growth (44, 45). Here we were able to confirm using an *in vitro* model that its fetal liver synthesis is increased under hypoxic and nutrient-deprived conditions (46). IGFBP-1's regulation of IGF-I is also PTM-dependent. It has been proposed that IGFBP-1's phosphorylation blocks IGFBP-1 polymerization thereby increasing binding affinity for IGF-I (34). We were able to show that there is increased phosphorylation of hepatic secreted IGFBP-1 in conditions of hypoxia and leucine deprivation. Furthermore, the increased affinity for IGF-I by the highly phosphorylated variants suggests a further mechanism by which hepatic expression of IGFBP-1 may act to moderate fetal growth.

Although HIF-1 regulation of IGFBP-1 expression accounts for its upregulation in hypoxia, IGFBP-1 upregulation in amino acid deprivation reveals that an alternative regulatory mechanism is present in metabolic starvation. As the mTOR pathway is sensitive to several stress stimuli, including hypoxia and amino acid deprivation, it is likely that IGFBP-1 expression and possibly phosphorylation may be regulated via

mTOR. Preliminary data showing upregulation of IGFBP-1 expression in HepG2 cells following treatment with an mTOR inhibitor (rapamycin) has demonstrated this to be the case (data not shown in thesis).

mTOR exerts its kinase activity through complexing with Raptor (complex 1) or Rictor (complex 2) that have discrete downstream targets. As HIF-1 transcription is downstream of complex 1, IGFBP-1 may be upregulated via mTOR through its HRE. Alternatively, inhibition of complex 2 phosphorylation of AKT may lead to IGFBP-1 regulation via downstream FOXO transcription factors, which are known to regulate IGFBP-1 expression downstream of the insulin receptor. Characterization of phospho-variants of IGFBP-1 following rapamycin treatment will reveal mTOR's involvement in IGFBP-1 phosphorylation. Since phosphorylation of IGFBP-1 increases in both hypoxia and leucine deprivation, it is logical to expect that the kinases involved are also regulated through mTOR as well.

8.3. OVERALL CONCLUSIONS

Here it has been proven that the condition of placental insufficiency leads to both maternal and fetal plasma protein changes. Although, placental insufficiency originates in the pathological formation of the fetal-placental vasculature, it is apparent, based on these findings, that the pathological processes alter the contents of the maternal circulation as well. Changes in endothelial proteins VCAM-1 and E-selectin were detected in the mother's plasma, as well as PTM changes to angiogenic protein Hp, that together are suggestive vascular changes in the mother. It is logical

to theorize that these changes may be associated with the reduced exchange across the placenta, and corresponding intervillous conditions of abnormally abundant oxygen in placental insufficiency. These proteins' changing levels may be exploited as biomarkers. VCAM-1 changes in particular may be highly predictive of placental health problems. Validation of its changing levels in the disease could eventually lead to new diagnostic tools to facilitate monitoring placental development in pregnancy, which would improve clinical care, and ultimately fetal outcomes.

In the fetal circulation, the proteins proven to change with placental insufficiency are also related to the vasculature, and to the regulation of fetal growth. The expression of liver proteins was consistent with an acute phase-like change in liver secretion that takes place with inflammation. It was established that despite a large degree of inflammation, hypoxia was mediating acute phase-like protein changes directly. The functional consequences of the most significant liver secreted plasma protein changes were explored: The effect of increased PAI-1 expression`s on angiogenesis, and increased IGFBP-1 expression and phosphorylation on IGF-I mediated cellular growth, were demonstrated using *in vitro* experiments.

That FGR plasma is overwhelmingly pro-angiogenic despite the reduced vasculature is a novel finding. It is also especially significant in the context that normal vascular regulation via VEGF and FGF-2 is disrupted, as it suggests that other angiogenic regulatory mechanisms may be abnormally upregulated in FGR. Here, it was discovered that increased plasma levels of PAI-1 increased angiogenesis in plasma immediately effluent from the vascular-compromised placenta. PAI-1`s oxygen-

dependent levels in the fetal plasma are therefore of consequence to the angiogenic-inducing potential of the plasma itself. Characterizing the full extent of PAI-1 effects on placental angiogenesis, and indeed the vascular health of FGR newborns through adulthood, using animal models, may very well establish PAI-1 as a centrally important molecule in the vascular pathology of FGR. The altered secretion of PAI-1 from liver may have a regulatory role on vascular development in an analogous fashion to IGFBP-1 secretion's regulation of fetal growth.

Here increased IGFBP-1 phosphorylation at four specific sites was identified from liver secretions in hypoxia and leucine deprivation. Increased phosphorylation increased IGF-I affinity and restricted IGF-I mediated proliferation. The findings characterize an additional mechanism by which liver secretions may be regulating IGF-I mediated fetal growth. Reduced growth mitigates placental insufficiency by reducing the demands for metabolic substrates. It restricts growth to mitigate the effects of limited maternal/fetal exchange in placental insufficiency. The changes in IGFBP-1 phosphorylation identified here are therefore adaptive to placental insufficiency.

The fetus' ability to survive and very often thrive in later life, despite extreme *in utero* environments of deprivation, is evidence of a remarkable degree of adaptability. Here some important biochemical effectors circulating in the plasma that have roles in adaptation, or in regulating angiogenesis or fetal growth have been elucidated. The continuing investigation of their changing levels and their roles in FGR pathology will lead to new diagnostics, and help formulate a better understanding of the FGR

etiology that will eventually lead to effective interventions and better disease management.

8.4.   REFERENCES

1. Castell, J. V., Gomez-Lechon, M. J., David, M., Andus, T., Geiger, T., Trullenque, R., Fabra, R., and Heinrich, P. C. (1989) Interleukin-6 is the Major Regulator of Acute Phase Protein Synthesis in Adult Human Hepatocytes. *FEBS Lett. 242*, 237-239.

2. Oliviero, S., and Cortese, R. (1989) The Human Haptoglobin Gene Promoter: Interleukin-6-Responsive Elements Interact with a DNA-Binding Protein Induced by Interleukin-6. *EMBO J. 8*, 1145-1151.

3. Theilgaard-Monch, K., Jacobsen, L. C., Nielsen, M. J., Rasmussen, T., Udby, L., Gharib, M., Arkwright, P. D., Gombart, A. F., Calafat, J., Moestrup, S. K., Porse, B. T., and Borregaard, N. (2006) Haptoglobin is Synthesized during Granulocyte Differentiation, Stored in Specific Granules, and Released by Neutrophils in Response to Activation. *Blood. 108*, 353-361.

4. Mikkat, S., Koy, C., Ulbrich, M., Ringel, B., and Glocker, M. O. (2004) Mass Spectrometric Protein Structure Characterization Reveals Cause of Migration Differences of Haptoglobin Alpha Chains in Two-Dimensional Gel Electrophoresis. *Proteomics. 4*, 3921-3932.

5. Yang, F., Brune, J. L., Baldwin, W. D., Barnett, D. R., and Bowman, B. H. (1983) Identification and Characterization of Human Haptoglobin cDNA. *Proc. Natl. Acad. Sci. U. S. A. 80*, 5875-5879.

6. Robinson, N. E., and Robinson, A. B. (2001) Molecular Clocks. *Proc. Natl. Acad. Sci. U. S. A. 98*, 944-949.

7. Sadrzadeh, S. M., and Bozorgmehr, J. (2004) Haptoglobin Phenotypes in Health and Disorders. *Am. J. Clin. Pathol. 121 Suppl*, S97-104.

8. El Ghmati, S. M., Van Hoeyveld, E. M., Van Strijp, J. G., Ceuppens, J. L., and Stevens, E. A. (1996) Identification of Haptoglobin as an Alternative Ligand for CD11b/CD18. *J. Immunol. 156*, 2542-2552.

9. Hanasaki, K., Powell, L. D., and Varki, A. (1995) Binding of Human Plasma Sialoglycoproteins by the B Cell-Specific Lectin CD22. Selective Recognition of Immunoglobulin M and Haptoglobin. *J. Biol. Chem. 270*, 7543-7550.

10. Arredouani, M., Matthijs, P., Van Hoeyveld, E., Kasran, A., Baumann, H., Ceuppens, J. L., and Stevens, E. (2003) Haptoglobin Directly Affects T Cells and Suppresses T Helper Cell Type 2 Cytokine Release. *Immunology. 108*, 144-151.

11. Oh, S. K., Pavlotsky, N., and Tauber, A. I. (1990) Specific Binding of Haptoglobin to Human Neutrophils and its Functional Consequences. *J. Leukoc. Biol. 47*, 142-148.

12. Baseler, M. W., and Burrell, R. (1983) Purification of Haptoglobin and its Effects on Lymphocyte and Alveolar Macrophage Responses. *Inflammation. 7*, 387-400.

13. Olson, G. E., Winfrey, V. P., Matrisian, P. E., Melner, M. H., and Hoffman, L. H. (1997) Specific Expression of Haptoglobin mRNA in Implantation-Stage Rabbit Uterine Epithelium. *J. Endocrinol. 152*, 69-80.

14. Herrler, A., Krusche, C. A., Muller-Schottle, F., and Beier, H. M. (2004) Haptoglobin Expression and Release by Rabbit Oviduct and Endometrium, its Localization in Blastocyst Extra-Embryonic Matrix and Fluid during Preimplantation Time. *Hum. Reprod. 19*, 2730-2737.

15. Berkova, N., Lemay, A., Dresser, D. W., Fontaine, J. Y., Kerizit, J., and Goupil, S. (2001) Haptoglobin is Present in Human Endometrium and shows Elevated Levels in the Decidua during Pregnancy. *Mol. Hum. Reprod. 7*, 747-754.

16. Cid, M. C., Grant, D. S., Hoffman, G. S., Auerbach, R., Fauci, A. S., and Kleinman, H. K. (1993) Identification of Haptoglobin as an Angiogenic Factor in Sera from Patients with Systemic Vasculitis. *J. Clin. Invest. 91*, 977-985.

17. Koch, A. E., Halloran, M. M., Haskell, C. J., Shah, M. R., and Polverini, P. J. (1995) Angiogenesis Mediated by Soluble Forms of E-Selectin and Vascular Cell Adhesion Molecule-1. *Nature. 376*, 517-519.

18. Kwee, L., Baldwin, H. S., Shen, H. M., Stewart, C. L., Buck, C., Buck, C. A., and Labow, M. A. (1995) Defective Development of the Embryonic and Extraembryonic Circulatory Systems in Vascular Cell Adhesion Molecule (VCAM-1) Deficient Mice. *Development. 121*, 489-503.

19. Gurtner, G. C., Davis, V., Li, H., McCoy, M. J., Sharpe, A., and Cybulsky, M. I. (1995) Targeted Disruption of the Murine VCAM1 Gene: Essential Role of VCAM-1 in Chorioallantoic Fusion and Placentation. *Genes Dev. 9*, 1-14.

20. Garmy-Susini, B., Jin, H., Zhu, Y., Sung, R. J., Hwang, R., and Varner, J. (2005) Integrin alpha4beta1-VCAM-1-Mediated Adhesion between Endothelial and Mural Cells is Required for Blood Vessel Maturation. *J. Clin. Invest. 115*, 1542-1551.

21. Ulyanova, T., Scott, L. M., Priestley, G. V., Jiang, Y., Nakamoto, B., Koni, P. A., and Papayannopoulou, T. (2005) VCAM-1 Expression in Adult Hematopoietic and

Nonhematopoietic Cells is Controlled by Tissue-Inductive Signals and Reflects their Developmental Origin. *Blood. 106*, 86-94.

22. Ahmed, A., and Kilby, M. D. (1997) Hypoxia Or Hyperoxia in Placental Insufficiency? *Lancet. 350*, 826-827.

23. Bowden, R. A., Ding, Z. M., Donnachie, E. M., Petersen, T. K., Michael, L. H., Ballantyne, C. M., and Burns, A. R. (2002) Role of alpha4 Integrin and VCAM-1 in CD18-Independent Neutrophil Migration Across Mouse Cardiac Endothelium. *Circ. Res. 90*, 562-569.

24. Yang, G., Chang, L., Alexander, J. S., Groome, L. J., and Yuping, W. (2009) Chymotrypsin-Like Protease (Chymase) Mediates Endothelial Activation by Factors Derived from Preeclamptic Placentas. *Reprod. Sci. 16*, 905-913.

25. Wang, Y., Zhang, Y., Lewis, D. F., Gu, Y., Li, H., Granger, D. N., and Alexander, J. S. (2003) Protease Chymotrypsin Mediates the Endothelial Expression of P- and E-Selectin, but Not ICAM and VCAM, Induced by Placental Trophoblasts from Pre-Eclamptic Pregnancies. *Placenta. 24*, 851-861.

26. Bartha, J. L., Romero-Carmona, R., and Comino-Delgado, R. (2003) Inflammatory Cytokines in Intrauterine Growth Retardation. *Acta Obstet. Gynecol. Scand. 82*, 1099-1102.

27. Lescuyer, P., Hochstrasser, D., and Rabilloud, T. (2007) How Shall we use the Proteomics Toolbox for Biomarker Discovery? *J. Proteome Res. 6*, 3371-3376.

28. Villalta, D., Tonutti, E., Prause, C., Koletzko, S., Uhlig, H. H., Vermeersch, P., Bossuyt, X., Stern, M., Laass, M. W., Ellis, J. H., Ciclitira, P. J., Richter, T., Daehnrich, C., Schlumberger, W., and Mothes, T. (2010) IgG Antibodies Against Deamidated Gliadin Peptides for Diagnosis of Celiac Disease in Patients with IgA Deficiency. *Clin. Chem. 56*, 464-468.

29. Prause, C., Ritter, M., Probst, C., Daehnrich, C., Schlumberger, W., Komorowski, L., Lieske, R., Richter, T., Hauer, A. C., Stern, M., Uhlig, H. H., Laass, M. W., Zimmer, K. P., and Mothes, T. (2009) Antibodies Against Deamidated Gliadin as New and Accurate Biomarkers of Childhood Coeliac Disease. *J. Pediatr. Gastroenterol. Nutr. 49*, 52-58.

30. Han, V. K. M., Seferovic, M. D., Albion, C. D., and Gupta, M. B. (2012) Intrauterine Growth Restriction: Intervention Strategies, in *Neonatology: A practical approach to neonatal diseases* (G. Buinocore, R. Bracci, and M. Weindling, Eds.) pp 89-93, Springer-Verlag Italia.

31. Wenger, R. H., Rolfs, A., Marti, H. H., Bauer, C., and Gassmann, M. (1995) Hypoxia, a Novel Inducer of Acute Phase Gene Expression in a Human Hepatoma Cell Line. *J. Biol. Chem. 270*, 27865-27870.

32. Khaliq, A., Dunk, C., Jiang, J., Shams, M., Li, X. F., Acevedo, C., Weich, H., Whittle, M., and Ahmed, A. (1999) Hypoxia Down-Regulates Placenta Growth Factor, Whereas Fetal Growth Restriction Up-Regulates Placenta Growth Factor Expression: Molecular Evidence for "Placental Hyperoxia" in Intrauterine Growth Restriction. *Lab. Invest. 79*, 151-170.

33. Malamitsi-Puchner, A., Boutsikou, T., Economou, E., Sarandakou, A., Makrakis, E., Hassiakos, D., and Creatsas, G. (2005) Vascular Endothelial Growth Factor and Placenta Growth Factor in Intrauterine Growth-Restricted Fetuses and Neonates. *Mediators Inflamm. 2005*, 293-297.

34. Jones, J. I., Busby, W. H.,Jr, Wright, G., Smith, C. E., Kimack, N. M., and Clemmons, D. R. (1993) Identification of the Sites of Phosphorylation in Insulin-Like Growth Factor Binding Protein-1. Regulation of its Affinity by Phosphorylation of Serine 101. *J. Biol. Chem. 268*, 1125-1131.

35. Watson, C. S., Bialek, P., Anzo, M., Khosravi, J., Yee, S. P., and Han, V. K. (2006) Elevated Circulating Insulin-Like Growth Factor Binding Protein-1 is Sufficient to Cause Fetal Growth Restriction. *Endocrinology. 147*, 1175-1186.

36. Labied, S., Blacher, S., Carmeliet, P., Noel, A., Frankenne, F., Foidart, J. M., and Munaut, C. (2011) Transient Reduction of Placental Angiogenesis in PAI-1-Deficient Mice. *Physiol. Genomics. 43*, 188-198.

37. Jarvis, S., Glinianaia, S. V., Torrioli, M. G., Platt, M. J., Miceli, M., Jouk, P. S., Johnson, A., Hutton, J., Hemming, K., Hagberg, G., Dolk, H., Chalmers, J., and Surveillance of Cerebral Palsy in Europe (SCPE) collaboration of European Cerebral Palsy Registers. (2003) Cerebral Palsy and Intrauterine Growth in Single Births: European Collaborative Study. *Lancet. 362*, 1106-1111.

38. Barker, D. J. (1998) In Utero Programming of Chronic Disease. *Clin. Sci. (Lond). 95*, 115-128.

39. Jornayvaz, F. R., Selz, R., Tappy, L., and Theintz, G. E. (2004) Metabolism of Oral Glucose in Children Born Small for Gestational Age: Evidence for an Impaired Whole Body Glucose Oxidation. *Metabolism. 53*, 847-851.

40. Sainson, R. C., Johnston, D. A., Chu, H. C., Holderfield, M. T., Nakatsu, M. N., Crampton, S. P., Davis, J., Conn, E., and Hughes, C. C. (2008) TNF Primes Endothelial Cells for Angiogenic Sprouting by Inducing a Tip Cell Phenotype. *Blood. 111*, 4997-5007.

41. Baluk, P., Yao, L. C., Feng, J., Romano, T., Jung, S. S., Schreiter, J. L., Yan, L., Shealy, D. J., and McDonald, D. M. (2009) TNF-Alpha Drives Remodeling of Blood Vessels and Lymphatics in Sustained Airway Inflammation in Mice. *J. Clin. Invest. 119*, 2954-2964.

42. Aurora, A. B., Baluk, P., Zhang, D., Sidhu, S. S., Dolganov, G. M., Basbaum, C., McDonald, D. M., and Killeen, N. (2005) Immune Complex-Dependent Remodeling of the Airway Vasculature in Response to a Chronic Bacterial Infection. *J. Immunol. 175*, 6319-6326.

43. Bauman, D. E. (1999) Bovine Somatotropin and Lactation: From Basic Science to Commercial Application. *Domest. Anim. Endocrinol. 17*, 101-116.

44. Watson, C. S., Bialek, P., Anzo, M., Khosravi, J., Yee, S. P., and Han, V. K. (2006) Elevated Circulating Insulin-Like Growth Factor Binding Protein-1 is Sufficient to Cause Fetal Growth Restriction. *Endocrinology. 147*, 1175-1186.

45. Martina, N. A., Kim, E., Chitkara, U., Wathen, N. C., Chard, T., and Giudice, L. C. (1997) Gestational Age-Dependent Expression of Insulin-Like Growth Factor-Binding Protein-1 (IGFBP-1) Phosphoisoforms in Human Extraembryonic Cavities, Maternal Serum, and Decidua Suggests Decidua as the Primary Source of IGFBP-1 in these Fluids during Early Pregnancy. *J. Clin. Endocrinol. Metab. 82*, 1894-1898.

46. Averous, J., Maurin, A. C., Bruhat, A., Jousse, C., Arliguie, C., and Fafournoux, P. (2005) Induction of IGFBP-1 Expression by Amino Acid Deprivation of HepG2 Human Hepatoma Cells Involves both a Transcriptional Activation and an mRNA Stabilization due to its 3'UTR. *FEBS Lett. 579*, 2609-2614.
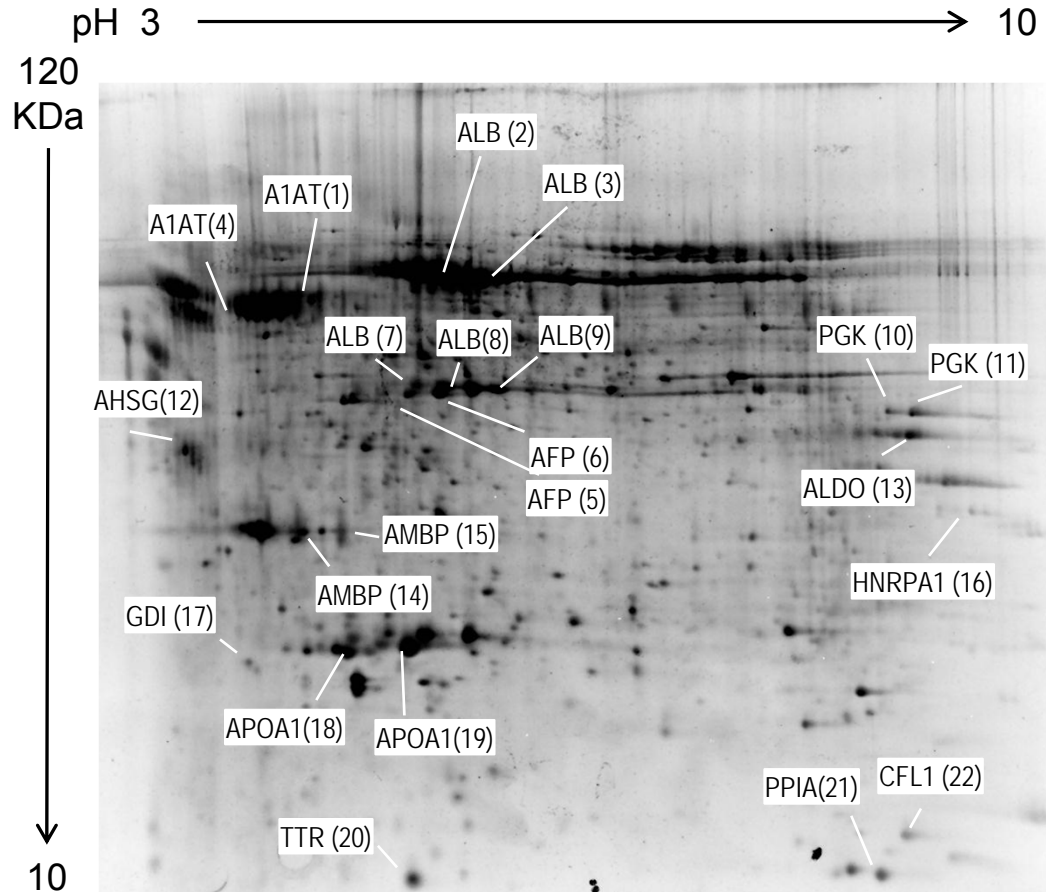
SUPPLEMENTAL FIGURE 4.1. Representative 2-D gel illustrating pH 3-10NL of conditioned media from HepG2 cells treated with O_2 concentrations of either 1%, 4% or 20% (ambient air). Proteins indicated are top scoring hits of spots identified following in-gel digestion and LC-MS/MS identification of the spots. Proteins spots indicated are not significantly changing by ANOVA . Complete MS data are listed in Supplemental Table 4.1.

Supplemental Table 4.1. LC-MS/MS identification of the protein spots from HepG2 conditioned media in Supplemental Figure 4.1.

Spot ID	Accession	Description	Score	Peptides
1	IPI00553177	Alpha-1-antitrypsin	201	6
	IPI00032220	Angiotensinogen	195	4
	IPI00295542	Nucleobindin-1	59	2
2	IPI00022443	Alpha-fetoprotein	69	2
	IPI00022434	Putative uncharacterized protein albumin	62	4
3	IPI00022434	Putative uncharacterized protein albumin	125	8
4	IPI00553177	Alpha-1-antitrypsin	427	17
	IPI00032220	Angiotensinogen	123	4
	IPI00031121	Carboxypeptidase E precursor	96	4
	IPI00030702	Isocitrate dehydrogenase [NAD] α, mitochondrial	42	1
	IPI00022431	Alpha-2-HS-glycoprotein like	40	2
	IPI00216773	Albumin	38	1
5	IPI00216773	Albumin	51	3
6	IPI00216773	Albumin	69	2
7	IPI00216773	Albumin	61	2
8	IPI00216773	Albumin	94	4
9	IPI00216773	Albumin	90	4
10	IPI00290460	Eukaryotic translation initiation factor 3 subunit G	73	1
	IPI00169383	Phosphoglycerate kinase 1	247	10
11	IPI00169383	Phosphoglycerate kinase 1	64	2

Table Continued…

SUPPLEMENTAL TABLE 4.1 Continued.

Spot ID	Accession	Description	Score	Peptides
12	IPI00553177	Alpha-1-antitrypsin	144	6
	IPI00022213	Gastricsin	58	1
13	IPI00465439	Fructose-bisphosphate aldolase A	162	6
	IPI00418262	Fructose-bisphosphate aldolase C like	77	3
14	IPI00010896	Chloride intracellular channel protein 1	382	7
	IPI00022426	Alpha-1-microglobulin/bikunin precursor	108	3
15	IPI00022426	Alpha-1-microglobulin/bikunin precursor	69	2
16	IPI00386854	Heterogeneous nuclear ribonucleoproteins A2/B1	77	1
17	IPI00003815	Rho GDP-dissociation inhibitor 1	109	4
18	IPI00021841	Apolipoprotein A-I	256	9
19	IPI00021841	Apolipoprotein A-I	149	10
20	IPI00022432	Transthyretin	183	5
21	IPI00419585	Peptidyl-prolyl cis-trans isomerase A	123	4
22	IPI00022432	Cofilin 1 (non-muscle)	183	5
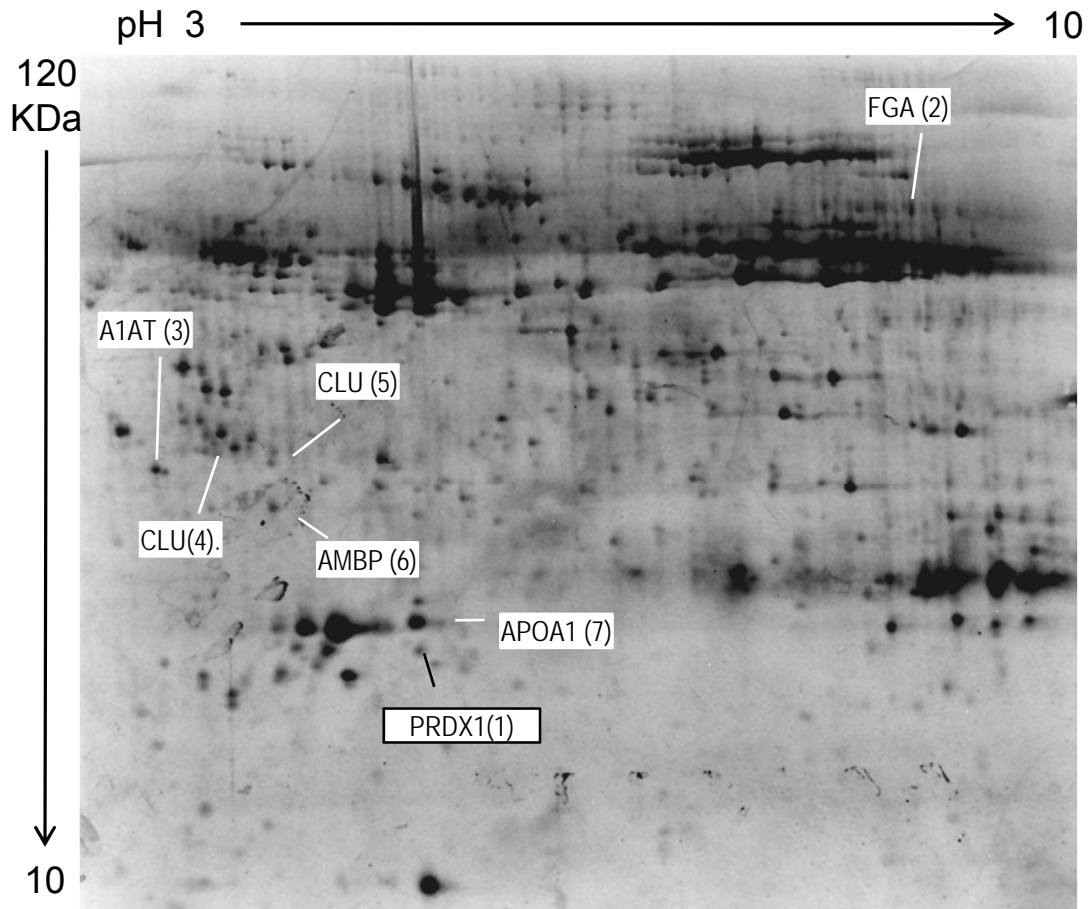
SUPPLEMENTAL FIGURE 4.2. A representative 2-D gel showing pH 3-10NL of fetal cord plasma after albumin and IgG depletion. Twelve FGR and twelve matching gestational-age control fetal plasma samples (Figure 4.6 and Table 4.2) were separated by 2-DGE after albumin and IgG depletion. Densitometric software analysis compared changes by paired t-test (p<0.05) between control and FGR groups.   Proteins indicated are top scoring hits of significantly changing spots identified by LC-MS/MS. Black borders indicates increasing spot, while lines indicated decreasing spots in FGR compared to controls.   Complete MS and quantitative data are listed in Supplemental Table 4.2.

SUPPLEMENTAL TABLE 4.2. Densitometric fold change and LC-MS/MS identification of the protein spots significantly increasing or decreasing as shown in Supplemental Figure 4.2. Proteins for which subsequent ELISA was performed on the fetal cord plasma are in bold.

Spot ID	Accession	Description	Score	Peptides	Change	paired t-test (p)
1	IPI00027350	Peroxiredoxin-2	102	2	1.93	0.026
	IPI00022434	Putative uncharacterized protein ALB	62	4		
2	IPI00029717	**Fibrinogen alpha chain**	**145**	**6**	**-2.19**	**0.020**
	IPI00554676	Hemoglobin subunit gamma-2	103	3		
3	IPI00553177	Isoform 1 of Alpha-1-antitrypsin	120	2	-1.59	0.012
4	IPI00291262	**Clusterin**	**74**	**4**	**-1.81**	**0.038**
5	IPI00291262	**Clusterin**	**212**	**4**	**-1.46**	**0.034**
6	IPI00022426	Protein AMBP	65	2	-1.19	0.027
7	IPI00021841	Apolipoprotein A-I	170	7	-1.15	0.047
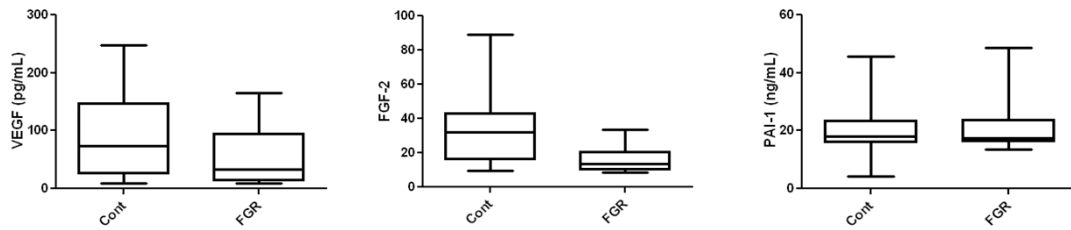
Supplemental Figure 5.1. Maternal plasma levels of vascular regulating proteins from mothers of FGR pregnancies with placental insufficiency compared to controls. Although VEGF and FGF-2 appear modestly decreased in FGR, no significant differences are present by t-test. Whiskers indicate range.

A

B
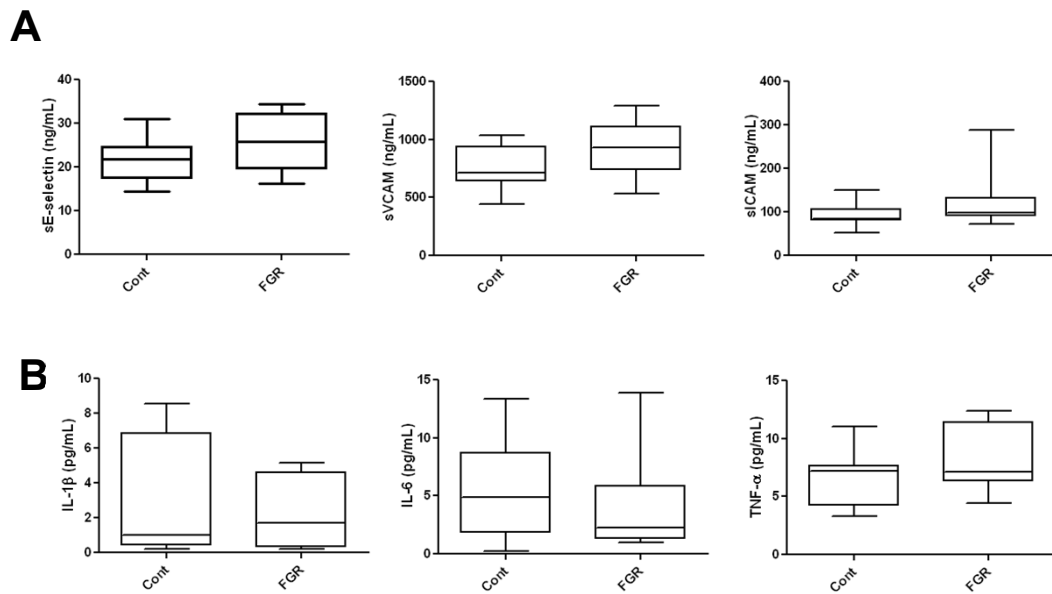
SUPPLEMENTAL FIGURE 6.1. Maternal   plasma levels of proteins in FGR samples compared to controls. **(A)** Endothelial activation/inflammation markers **(B)** Inflammatory cytokines. Whiskers indicate range.

ELSEVIER LICENSE
TERMS AND CONDITIONS

Aug 30, 2011

This is a License Agreement between Maxim D Seferovic ("You") and Elsevier ("Elsevier") provided by Copyright Clearance Center ("CCC"). The license consists of your order details, the terms and conditions provided by Elsevier, and the payment terms and conditions.

All payments must be made in full to CCC. For payment instructions, please see information listed at the bottom of this form.

Supplier	Elsevier Limited
	The Boulevard,Langford Lane
	Kidlington,Oxford,OX5 1GB,UK
Registered Company Number	1982084
Customer name	Maxim D Seferovic
Customer address	800 commissioners Rd S.
	London, ON N5Y 3G8
License number	2738770853267
License date	Aug 30, 2011
Licensed content publisher	Elsevier
Licensed content publication	Seminars in Perinatology
Licensed content title	Fetal growth restriction due to placental disease
Licensed content author	Ahmet A Baschat,Kurt Hecher
Licensed content date	February 2004
Licensed content volume number	28
Licensed content issue number	1
Number of pages	14
Start Page	67
End Page	80
Type of Use	reuse in a thesis/dissertation
Portion	figures/tables/illustrations
Number of figures/tables/illustrations	1
Format	both print and electronic
Are you the author of this Elsevier article?	No
Will you be translating?	No
Order reference number	
Title of your thesis/dissertation	Maternal and fetal plasma proteome changes in fetal growth restriction
Expected completion date	Dec 2011
Estimated size (number of pages)	300

Elsevier VAT number	GB 494 6272 12
Permissions price	0.00 USD
VAT/Local Sales Tax	0.0 USD / 0.0 GBP
Total	**0.00 USD**

Terms and Conditions

INTRODUCTION

1. The publisher for this copyrighted material is Elsevier. By clicking "accept" in connection with completing this licensing transaction, you agree that the following terms and conditions apply to this transaction (along with the Billing and Payment terms and conditions established by Copyright Clearance Center, Inc. ("CCC"), at the time that you opened your Rightslink account and that are available at any time at http://myaccount.copyright.com).

GENERAL TERMS

2. Elsevier hereby grants you permission to reproduce the aforementioned material subject to the terms and conditions indicated.

3. Acknowledgement: If any part of the material to be used (for example, figures) has appeared in our publication with credit or acknowledgement to another source, permission must also be sought from that source. If such permission is not obtained then that material may not be included in your publication/copies. Suitable acknowledgement to the source must be made, either as a footnote or in a reference list at the end of your publication, as follows:

"Reprinted from Publication title, Vol /edition number, Author(s), Title of article / title of chapter, Pages No., Copyright (Year), with permission from Elsevier [OR APPLICABLE SOCIETY COPYRIGHT OWNER]." Also Lancet special credit - "Reprinted from The Lancet, Vol. number, Author(s), Title of article, Pages No., Copyright (Year), with permission from Elsevier."

4. Reproduction of this material is confined to the purpose and/or media for which permission is hereby given.

5. Altering/Modifying Material: Not Permitted. However figures and illustrations may be altered/adapted minimally to serve your work. Any other abbreviations, additions, deletions and/or any other alterations shall be made only with prior written authorization of Elsevier Ltd. (Please contact Elsevier at permissions@elsevier.com)

6. If the permission fee for the requested use of our material is waived in this instance, please be advised that your future requests for Elsevier materials may attract a fee.

7. Reservation of Rights: Publisher reserves all rights not specifically granted in the combination of (i) the license details provided by you and accepted in the course of this licensing transaction, (ii) these terms and conditions and (iii) CCC's Billing and Payment terms and conditions.

8. License Contingent Upon Payment: While you may exercise the rights licensed immediately upon issuance of the license at the end of the licensing process for the transaction, provided that you have disclosed complete and accurate details of your proposed use, no license is finally effective unless and until full payment is received from you (either by publisher or by CCC) as provided in CCC's Billing and Payment terms and conditions. If full payment is not received on a timely basis, then any license preliminarily granted shall be deemed automatically revoked and shall be void as if never granted. Further, in the event that you breach any of these terms and conditions or any of CCC's Billing and Payment terms and conditions, the license is automatically revoked and shall be void as if never granted. Use of materials as described in a revoked license, as well as any use of the materials beyond the scope of an unrevoked license, may constitute copyright infringement and publisher reserves the right to take any and all action to protect its copyright in the materials.

9. Warranties: Publisher makes no representations or warranties with respect to the licensed material.

10. Indemnity: You hereby indemnify and agree to hold harmless publisher and CCC, and their respective officers, directors, employees and agents, from and against any and all claims arising out of your use of the licensed material other than as specifically authorized pursuant to this license.

11. No Transfer of License: This license is personal to you and may not be sublicensed, assigned, or transferred by you to any other person without publisher's written permission.

12. No Amendment Except in Writing: This license may not be amended except in a writing signed by both parties (or, in the case of publisher, by CCC on publisher's behalf).

13. Objection to Contrary Terms: Publisher hereby objects to any terms contained in any purchase order, acknowledgment, check endorsement or other writing prepared by you, which terms are inconsistent with these terms and conditions or CCC's Billing and Payment terms and conditions. These terms and conditions, together with CCC's Billing and Payment terms and conditions (which are incorporated herein), comprise the entire agreement between you and publisher (and CCC) concerning this licensing transaction. In the event of any conflict between your obligations established by these terms and conditions and those established by CCC's Billing and Payment terms and conditions, these terms and conditions shall control.

14. Revocation: Elsevier or Copyright Clearance Center may deny the permissions described in this License at their sole discretion, for any reason or no reason, with a full refund payable to you. Notice of such denial will be made using the contact information provided by you. Failure to receive such notice will not alter or invalidate the denial. In no event will Elsevier or Copyright Clearance Center be responsible or liable for any costs, expenses or damage incurred by you as a result of a denial of your permission request, other than a refund of the amount(s) paid by you to Elsevier and/or Copyright Clearance Center for denied permissions.

LIMITED LICENSE

The following terms and conditions apply only to specific license types:

15. **Translation**: This permission is granted for non-exclusive world **English** rights only unless your license was granted for translation rights. If you licensed translation rights you may only translate this content into the languages you requested. A professional translator must perform all translations and reproduce the content word for word preserving the integrity of the article. If this license is to re-use 1 or 2 figures then permission is granted for non-exclusive world rights in all languages.

16. **Website**: The following terms and conditions apply to electronic reserve and author websites:

Electronic reserve: If licensed material is to be posted to website, the web site is to be password-protected and made available only to bona fide students registered on a relevant course if:
This license was made in connection with a course,
This permission is granted for 1 year only. You may obtain a license for future website posting,
All content posted to the web site must maintain the copyright information line on the bottom of each image,
A hyper-text must be included to the Homepage of the journal from which you are licensing at http://www.sciencedirect.com/science/journal/xxxxx or the Elsevier homepage for books at http://www.elsevier.com , and
Central Storage: This license does not include permission for a scanned version of the material to be stored in a central repository such as that provided by Heron/XanEdu.
17. **Author website** for journals with the following additional clauses:
All content posted to the web site must maintain the copyright information line on the bottom of each image, and
he permission granted is limited to the personal version of your paper. You are not allowed to download and post the published electronic version of your article (whether PDF or HTML, proof or final version), nor may you scan the printed edition to create an electronic version,
A hyper-text must be included to the Homepage of the journal from which you are licensing at http://www.sciencedirect.com/science/journal/xxxxx , As part of our normal production process, you will receive an e-mail notice when your article appears on Elsevier's online service ScienceDirect (www.sciencedirect.com). That e-mail will include the article's Digital Object Identifier (DOI). This number provides the electronic link to the published article and should be included in the posting of your personal version. We ask that you wait until you receive this e-mail and have the DOI to do any posting.
Central Storage: This license does not include permission for a scanned version of the material to be stored in a central repository such as that provided by Heron/XanEdu.
18. **Author website** for books with the following additional clauses:
Authors are permitted to place a brief summary of their work online only.
A hyper-text must be included to the Elsevier homepage at http://www.elsevier.com
All content posted to the web site must maintain the copyright information line on the bottom of each image
You are not allowed to download and post the published electronic version of your chapter, nor may you scan the printed edition to create an electronic version.
Central Storage: This license does not include permission for a scanned version of the material to be stored in a central repository such as that provided by Heron/XanEdu.

19. **Website** (regular and for author): A hyper-text must be included to the Homepage of the journal from which you are licensing at http://www.sciencedirect.com/science/journal/xxxxx. or for books to the Elsevier homepage at http://www.elsevier.com
20. **Thesis/Dissertation**: If your license is for use in a thesis/dissertation your thesis may be submitted to your institution in either print or electronic form. Should your thesis be published commercially, please reapply for permission. These requirements include permission for the Library and Archives of Canada to supply single copies, on demand, of the complete thesis and include permission for UMI to supply single copies, on demand, of the complete thesis. Should your thesis be published commercially, please reapply for permission.
21. **Other Conditions**:

v1.6

Gratis licenses (referencing $0 in the Total field) are free. Please retain this printable license for your reference. No payment is required.

If you would like to pay for this license now, please remit this license along with your payment made payable to "COPYRIGHT CLEARANCE CENTER" otherwise you will be invoiced within 48 hours of the license date. Payment should be in the form of a check or money order referencing your account number and this invoice number RLNK0. Once you receive your invoice for this order, you may pay your invoice by credit card. Please follow instructions provided at that time.

Make Payment To:
Copyright Clearance Center
Dept 001
P.O. Box 843006
Boston, MA 02284-3006

For suggestions or comments regarding this order, contact Rightslink Customer Support:

ELSEVIER LICENSE
TERMS AND CONDITIONS

Aug 30, 2011

This is a License Agreement between Maxim D Seferovic ("You") and Elsevier ("Elsevier") provided by Copyright Clearance Center ("CCC"). The license consists of your order details, the terms and conditions provided by Elsevier, and the payment terms and conditions.

All payments must be made in full to CCC. For payment instructions, please see information listed at the bottom of this form.

Supplier	Elsevier Limited The Boulevard,Langford Lane Kidlington,Oxford,OX5 1GB,UK
Registered Company Number	1982084
Customer name	Maxim D Seferovic
Customer address	800 commissioners Rd S. London, ON N5Y 3G8
License number	2738911028625
License date	Aug 30, 2011
Licensed content publisher	Elsevier
Licensed content publication	Placenta
Licensed content title	Aspects of Human Fetoplacental Vasculogenesis and Angiogenesis. II. Changes During Normal Pregnancy
Licensed content author	P. Kaufmann,T.M. Mayhew,D.S. Charnock-Jones
Licensed content date	February-March 2004
Licensed content volume number	25
Licensed content issue number	2-3
Number of pages	13
Start Page	114
End Page	126
Type of Use	reuse in a thesis/dissertation
Portion	figures/tables/illustrations
Number of figures/tables/illustrations	1
Format	both print and electronic
Are you the author of this Elsevier article?	No
Will you be translating?	No
Order reference number	
Title of your thesis/dissertation	Maternal and fetal plasma proteome changes in fetal growth restriction
Expected completion date	Dec 2011
Estimated size (number of pages)	300

Elsevier VAT number	GB 494 6272 12
Permissions price	0.00 USD
VAT/Local Sales Tax	0.0 USD / 0.0 GBP
Total	**0.00 USD**

Terms and Conditions

INTRODUCTION

1. The publisher for this copyrighted material is Elsevier. By clicking "accept" in connection with completing this licensing transaction, you agree that the following terms and conditions apply to this transaction (along with the Billing and Payment terms and conditions established by Copyright Clearance Center, Inc. ("CCC"), at the time that you opened your Rightslink account and that are available at any time at http://myaccount.copyright.com).

GENERAL TERMS

2. Elsevier hereby grants you permission to reproduce the aforementioned material subject to the terms and conditions indicated.

3. Acknowledgement: If any part of the material to be used (for example, figures) has appeared in our publication with credit or acknowledgement to another source, permission must also be sought from that source. If such permission is not obtained then that material may not be included in your publication/copies. Suitable acknowledgement to the source must be made, either as a footnote or in a reference list at the end of your publication, as follows:

"Reprinted from Publication title, Vol /edition number, Author(s), Title of article / title of chapter, Pages No., Copyright (Year), with permission from Elsevier [OR APPLICABLE SOCIETY COPYRIGHT OWNER]." Also Lancet special credit - "Reprinted from The Lancet, Vol. number, Author(s), Title of article, Pages No., Copyright (Year), with permission from Elsevier."

4. Reproduction of this material is confined to the purpose and/or media for which permission is hereby given.

5. Altering/Modifying Material: Not Permitted. However figures and illustrations may be altered/adapted minimally to serve your work. Any other abbreviations, additions, deletions and/or any other alterations shall be made only with prior written authorization of Elsevier Ltd. (Please contact Elsevier at permissions@elsevier.com)

6. If the permission fee for the requested use of our material is waived in this instance, please be advised that your future requests for Elsevier materials may attract a fee.

7. Reservation of Rights: Publisher reserves all rights not specifically granted in the combination of (i) the license details provided by you and accepted in the course of this licensing transaction, (ii) these terms and conditions and (iii) CCC's Billing and Payment terms and conditions.

8. License Contingent Upon Payment: While you may exercise the rights licensed immediately upon issuance of the license at the end of the licensing process for the transaction, provided that you have disclosed complete and accurate details of your proposed use, no license is finally effective unless and until full payment is received from you (either by publisher or by CCC) as provided in CCC's Billing and Payment terms and conditions. If full payment is not received on a timely basis, then any license preliminarily granted shall be deemed automatically revoked and shall be void as if never granted. Further, in the event that you breach any of these terms and conditions or any of CCC's Billing and Payment terms and conditions, the license is automatically revoked and shall be void as if never granted. Use of materials as described in a revoked license, as well as any use of the materials beyond the scope of an unrevoked license, may constitute copyright infringement and publisher reserves the right to take any and all action to protect its copyright in the materials.

9. Warranties: Publisher makes no representations or warranties with respect to the licensed material.

10. Indemnity: You hereby indemnify and agree to hold harmless publisher and CCC, and their respective officers, directors, employees and agents, from and against any and all claims arising out of your use of the licensed material other than as specifically authorized pursuant to this license.

11. No Transfer of License: This license is personal to you and may not be sublicensed, assigned, or transferred by you to any other person without publisher's written permission.

12. No Amendment Except in Writing: This license may not be amended except in a writing signed by both parties (or, in the case of publisher, by CCC on publisher's behalf).

13. Objection to Contrary Terms: Publisher hereby objects to any terms contained in any purchase order, acknowledgment, check endorsement or other writing prepared by you, which terms are inconsistent with these terms and conditions or CCC's Billing and Payment terms and conditions. These terms and conditions, together with CCC's Billing and Payment terms and conditions (which are incorporated herein), comprise the entire agreement between you and publisher (and CCC) concerning this licensing transaction. In the event of any conflict between your obligations established by these terms and conditions and those established by CCC's Billing and Payment terms and conditions, these terms and conditions shall control.

14. Revocation: Elsevier or Copyright Clearance Center may deny the permissions described in this License at their sole discretion, for any reason or no reason, with a full refund payable to you. Notice of such denial will be made using the contact information provided by you. Failure to receive such notice will not alter or invalidate the denial. In no event will Elsevier or Copyright Clearance Center be responsible or liable for any costs, expenses or damage incurred by you as a result of a denial of your permission request, other than a refund of the amount(s) paid by you to Elsevier and/or Copyright Clearance Center for denied permissions.

LIMITED LICENSE

The following terms and conditions apply only to specific license types:

15. **Translation**: This permission is granted for non-exclusive world **English** rights only unless your license was granted for translation rights. If you licensed translation rights you may only translate this content into the languages you requested. A professional translator must perform all translations and reproduce the content word for word preserving the integrity of the article. If this license is to re-use 1 or 2 figures then permission is granted for non-exclusive world rights in all languages.

16. **Website**: The following terms and conditions apply to electronic reserve and author websites:

Electronic reserve: If licensed material is to be posted to website, the web site is to be password-protected and made available only to bona fide students registered on a relevant course if:
This license was made in connection with a course,
This permission is granted for 1 year only. You may obtain a license for future website posting,
All content posted to the web site must maintain the copyright information line on the bottom of each image,
A hyper-text must be included to the Homepage of the journal from which you are licensing at http://www.sciencedirect.com/science/journal/xxxxx or the Elsevier homepage for books at http://www.elsevier.com , and
Central Storage: This license does not include permission for a scanned version of the material to be stored in a central repository such as that provided by Heron/XanEdu.
17. **Author website** for journals with the following additional clauses:
All content posted to the web site must maintain the copyright information line on the bottom of each image, and
he permission granted is limited to the personal version of your paper. You are not allowed to download and post the published electronic version of your article (whether PDF or HTML, proof or final version), nor may you scan the printed edition to create an electronic version,
A hyper-text must be included to the Homepage of the journal from which you are licensing at http://www.sciencedirect.com/science/journal/xxxxx , As part of our normal production process, you will receive an e-mail notice when your article appears on Elsevier's online service ScienceDirect (www.sciencedirect.com). That e-mail will include the article's Digital Object Identifier (DOI). This number provides the electronic link to the published article and should be included in the posting of your personal version. We ask that you wait until you receive this e-mail and have the DOI to do any posting.
Central Storage: This license does not include permission for a scanned version of the material to be stored in a central repository such as that provided by Heron/XanEdu.
18. **Author website** for books with the following additional clauses:
Authors are permitted to place a brief summary of their work online only.
A hyper-text must be included to the Elsevier homepage at http://www.elsevier.com
All content posted to the web site must maintain the copyright information line on the bottom of each image
You are not allowed to download and post the published electronic version of your chapter, nor may you scan the printed edition to create an electronic version.
Central Storage: This license does not include permission for a scanned version of the material to be stored in a central repository such as that provided by Heron/XanEdu.

19. **Website** (regular and for author): A hyper-text must be included to the Homepage of the journal from which you are licensing at http://www.sciencedirect.com/science/journal/xxxxx. or for books to the Elsevier homepage at http://www.elsevier.com
20. **Thesis/Dissertation**: If your license is for use in a thesis/dissertation your thesis may be submitted to your institution in either print or electronic form. Should your thesis be published commercially, please reapply for permission. These requirements include permission for the Library and Archives of Canada to supply single copies, on demand, of the complete thesis and include permission for UMI to supply single copies, on demand, of the complete thesis. Should your thesis be published commercially, please reapply for permission.
21. **Other Conditions**:

v1.6

ELSEVIER LICENSE
TERMS AND CONDITIONS

Aug 30, 2011

This is a License Agreement between Maxim D Seferovic ("You") and Elsevier ("Elsevier") provided by Copyright Clearance Center ("CCC"). The license consists of your order details, the terms and conditions provided by Elsevier, and the payment terms and conditions.

All payments must be made in full to CCC. For payment instructions, please see information listed at the bottom of this form.

Supplier	Elsevier Limited
	The Boulevard,Langford Lane
	Kidlington,Oxford,OX5 1GB,UK
Registered Company Number	1982084
Customer name	Maxim D Seferovic
Customer address	800 commissioners Rd S.
	London, ON N5Y 3G8
License number	2738771292305
License date	Aug 30, 2011
Licensed content publisher	Elsevier
Licensed content publication	Placenta
Licensed content title	Aspects of Human Fetoplacental Vasculogenesis and Angiogenesis. I. Molecular Regulation
Licensed content author	D.S Charnock-Jones,P Kaufmann,T.M Mayhew
Licensed content date	February-March 2004
Licensed content volume number	25
Licensed content issue number	23
Number of pages	11
Start Page	103
End Page	113
Type of Use	reuse in a thesis/dissertation
Intended publisher of new work	other
Portion	figures/tables/illustrations
Number of figures/tables/illustrations	1
Format	both print and electronic
Are you the author of this Elsevier article?	No
Will you be translating?	No
Order reference number	
Title of your thesis/dissertation	Maternal and fetal plasma proteome changes in fetal growth restriction
Expected completion date	Dec 2011

Estimated size (number of pages)	300
Elsevier VAT number	GB 494 6272 12
Permissions price	0.00 USD
VAT/Local Sales Tax	0.0 USD / 0.0 GBP
Total	**0.00 USD**

Terms and Conditions

INTRODUCTION

1. The publisher for this copyrighted material is Elsevier. By clicking "accept" in connection with completing this licensing transaction, you agree that the following terms and conditions apply to this transaction (along with the Billing and Payment terms and conditions established by Copyright Clearance Center, Inc. ("CCC"), at the time that you opened your Rightslink account and that are available at any time at http://myaccount.copyright.com).

GENERAL TERMS

2. Elsevier hereby grants you permission to reproduce the aforementioned material subject to the terms and conditions indicated.

3. Acknowledgement: If any part of the material to be used (for example, figures) has appeared in our publication with credit or acknowledgement to another source, permission must also be sought from that source. If such permission is not obtained then that material may not be included in your publication/copies. Suitable acknowledgement to the source must be made, either as a footnote or in a reference list at the end of your publication, as follows:

"Reprinted from Publication title, Vol /edition number, Author(s), Title of article / title of chapter, Pages No., Copyright (Year), with permission from Elsevier [OR APPLICABLE SOCIETY COPYRIGHT OWNER]." Also Lancet special credit - "Reprinted from The Lancet, Vol. number, Author(s), Title of article, Pages No., Copyright (Year), with permission from Elsevier."

4. Reproduction of this material is confined to the purpose and/or media for which permission is hereby given.

5. Altering/Modifying Material: Not Permitted. However figures and illustrations may be altered/adapted minimally to serve your work. Any other abbreviations, additions, deletions and/or any other alterations shall be made only with prior written authorization of Elsevier Ltd. (Please contact Elsevier at permissions@elsevier.com)

6. If the permission fee for the requested use of our material is waived in this instance, please be advised that your future requests for Elsevier materials may attract a fee.

7. Reservation of Rights: Publisher reserves all rights not specifically granted in the combination of (i) the license details provided by you and accepted in the course of this licensing transaction, (ii) these terms and conditions and (iii) CCC's Billing and Payment terms and conditions.

8. License Contingent Upon Payment: While you may exercise the rights licensed immediately upon issuance of the license at the end of the licensing process for the transaction, provided that you have disclosed complete and accurate details of your proposed use, no license is finally effective unless and until full payment is received from you (either by publisher or by CCC) as provided in CCC's Billing and Payment terms and conditions. If full payment is not received on a timely basis, then any license preliminarily granted shall be deemed automatically revoked and shall be void as if never granted. Further, in the event that you breach any of these terms and conditions or any of CCC's Billing and Payment terms and conditions, the license is automatically revoked and shall be void as if never granted. Use of materials as described in a revoked license, as well as any use of the materials beyond the scope of an unrevoked license, may constitute copyright infringement and publisher reserves the right to take any and all action to protect its copyright in the materials.

9. Warranties: Publisher makes no representations or warranties with respect to the licensed material.

10. Indemnity: You hereby indemnify and agree to hold harmless publisher and CCC, and their respective officers, directors, employees and agents, from and against any and all claims arising out of your use of the licensed material other than as specifically authorized pursuant to this license.

11. No Transfer of License: This license is personal to you and may not be sublicensed, assigned, or transferred by you to any other person without publisher's written permission.

12. No Amendment Except in Writing: This license may not be amended except in a writing signed by both parties (or, in the case of publisher, by CCC on publisher's behalf).

13. Objection to Contrary Terms: Publisher hereby objects to any terms contained in any purchase order, acknowledgment, check endorsement or other writing prepared by you, which terms are inconsistent with these terms and conditions or CCC's Billing and Payment terms and conditions. These terms and conditions, together with CCC's Billing and Payment terms and conditions (which are incorporated herein), comprise the entire agreement between you and publisher (and CCC) concerning this licensing transaction. In the event of any conflict between your obligations established by these terms and conditions and those established by CCC's Billing and Payment terms and conditions, these terms and conditions shall control.

14. Revocation: Elsevier or Copyright Clearance Center may deny the permissions described in this License at their sole discretion, for any reason or no reason, with a full refund payable to you. Notice of such denial will be made using the contact information provided by you. Failure to receive such notice will not alter or invalidate the denial. In no event will Elsevier or Copyright Clearance Center be responsible or liable for any costs, expenses or damage incurred by you as a result of a denial of your permission request, other than a refund of the amount(s) paid by you to Elsevier and/or Copyright Clearance Center for denied permissions.

LIMITED LICENSE

The following terms and conditions apply only to specific license types:

15. **Translation**: This permission is granted for non-exclusive world **English** rights only unless your license was granted for translation rights. If you licensed translation rights you may only translate this content into the languages you requested. A professional translator must perform all translations and reproduce the content word for word preserving the integrity of the article. If this

license is to re-use 1 or 2 figures then permission is granted for non-exclusive world rights in all languages.

16. **Website**: The following terms and conditions apply to electronic reserve and author websites:

Electronic reserve: If licensed material is to be posted to website, the web site is to be password-protected and made available only to bona fide students registered on a relevant course if:

This license was made in connection with a course,

This permission is granted for 1 year only. You may obtain a license for future website posting,

All content posted to the web site must maintain the copyright information line on the bottom of each image,

A hyper-text must be included to the Homepage of the journal from which you are licensing at http://www.sciencedirect.com/science/journal/xxxxx or the Elsevier homepage for books at http://www.elsevier.com , and

Central Storage: This license does not include permission for a scanned version of the material to be stored in a central repository such as that provided by Heron/XanEdu.

17. **Author website** for journals with the following additional clauses:

All content posted to the web site must maintain the copyright information line on the bottom of each image, and

he permission granted is limited to the personal version of your paper. You are not allowed to download and post the published electronic version of your article (whether PDF or HTML, proof or final version), nor may you scan the printed edition to create an electronic version,

A hyper-text must be included to the Homepage of the journal from which you are licensing at http://www.sciencedirect.com/science/journal/xxxxx , As part of our normal production process, you will receive an e-mail notice when your article appears on Elsevier's online service ScienceDirect (www.sciencedirect.com). That e-mail will include the article's Digital Object Identifier (DOI). This number provides the electronic link to the published article and should be included in the posting of your personal version. We ask that you wait until you receive this e-mail and have the DOI to do any posting.

Central Storage: This license does not include permission for a scanned version of the material to be stored in a central repository such as that provided by Heron/XanEdu.

18. **Author website** for books with the following additional clauses:

Authors are permitted to place a brief summary of their work online only.

A hyper-text must be included to the Elsevier homepage at http://www.elsevier.com

All content posted to the web site must maintain the copyright information line on the bottom of each image

You are not allowed to download and post the published electronic version of your chapter, nor may you scan the printed edition to create an electronic version.

Central Storage: This license does not include permission for a scanned version of the material to be stored in a central repository such as that provided by Heron/XanEdu.

19. **Website** (regular and for author): A hyper-text must be included to the Homepage of the journal from which you are licensing at http://www.sciencedirect.com/science/journal/xxxxx. or for books to the Elsevier homepage at http://www.elsevier.com

20. **Thesis/Dissertation**: If your license is for use in a thesis/dissertation your thesis may be submitted to your institution in either print or electronic form. Should your thesis be published commercially, please reapply for permission. These requirements include permission for the Library and Archives of Canada to supply single copies, on demand, of the complete thesis and include permission for UMI to supply single copies, on demand, of the complete thesis. Should your thesis be published commercially, please reapply for permission.

21. **Other Conditions**:

v1.6

WG: Permission request

From: **Essenpreis, Alice, Springer DE**
Sent: September-15-11 8:27:40 AM
To:

Hello,

Thank you for your e-mail.

With reference to your request to reprint in your thesis material on which Springer Science and Business Media control the copyright, permission is granted, free of charge, for the use indicated in your enquiry. Licenses are for one-time use only with a maximum distribution equal to the number that you identified in the licensing process.

This License includes use in an electronic form, provided it is password protected or on the university's intranet, destined to microfilming by UMI and University repository. For any other electronic use, please contact Springer at

The material can only be used for the purpose of defending your thesis, and with a maximum of 100 extra copies in paper.

Although Springer holds copyright to the material and is entitled to negotiate on rights, this license is only valid, provided permission is also obtained from the (co) author (address is given with the chapter) and provided it concerns original material which does not carry references to other sources (if material in question appears with credit to another source, authorization from that source is required as well). Permission free of charge on this occasion does not prejudice any rights we might have to charge for reproduction of our copyrighted material in the future.

Springer Science + Business Media reserves all rights not specifically granted in the combination of (i) the license details provided by you and accepted in the course of this licensing transaction, (ii) these terms and conditions and (iii) CCC's Billing and Payment terms and conditions.

Please include the following copyright citation referencing the publication in which the material was originally published. Where wording is within brackets, please include verbatim.

"With kind permission from Springer Science+Business Media: <book title, chapter title, volume, year of publication, page, name(s) of author(s), figure number(s), and any original (first) copyright notice displayed with material>."

This license is personal to you and may not be sublicensed, assigned, or transferred by you to any other person without Springer Science + Business Media's written permission.

Kind regards,

—

Alice Essenpreis

Springer

Rights and Permissions

—

Tiergartenstrasse 17 | 69121 Heidelberg GERMANY

www.springer.com/rights

—

Von: **Im Auftrag von** Maxim Seferovic
Gesendet: Dienstag, 30. August 2011 16:27
An: Permissions Heidelberg, Springer DE
Betreff: Permission request

Dear springer,

I would like permission to reproduce a version of a figure from:

Benirschke K, Kaufmann P. Pathology of the human placenta. 4th ed. New York: Springer Verlag, 2000 947 pp.

I am using a modified version of this figure taken from a review article that was reproduced with your permission by the origional author:

Kaufmann P, Mayhew TM, Charnock-Jones DS. (2004) Aspects of human fetoplacental vasculogenesis and angiogenesis. II. Changes during normal pregnancy. Placenta. 2004 Feb-Mar;25(2-3):114-26.

I have already obtained permission from the publishers of "Placenta" however require that of Springers, since the origional material was in your book.

I am reproducing this in my PhD thesis/dissertation: "Maternal Plasma Proteome Changes in Fetal Growth Restriction" to be completed before December 2011. Fewer than 10 copies will be made for the purposes of evaluation and completion of the degree.

The University of Western Ontatio,
800 Commissioners Rd E,
London, On
Canada.
N6C 2V5

Thank You
Maxim Seferovic

Copyright Clearance Center

RightsLink®

Title: Role of ductus venosus in distribution of umbilical blood flow in human fetuses during second half of pregnancy

Author: Maria Bellotti, Giancarlo Pennati, Camilla De Gasperi, Frederick C. Battaglia, Enrico Ferrazzi

Publication: Am J Physiol- Heart and Circulatory Physiology

Publisher: The American Physiological Society

Date: Sep 1, 2000

Copyright © 2000, The American Physiological Society

Logged in as:
Maxim Seferovic
Account #:
3000442836

LOGOUT

Permission Not Required

Permission is not required for this type of use.

BACK | CLOSE WINDOW

SPRINGER LICENSE
TERMS AND CONDITIONS

This is a License Agreement between Maxim D Seferovic ("You") and Springer ("Springer") provided by Copyright Clearance Center ("CCC"). The license consists of your order details, the terms and conditions provided by Springer, and the payment terms and conditions.

All payments must be made in full to CCC. For payment instructions, please see information listed at the bottom of this form.

License Number	2738780580821
License date	Aug 30, 2011
Licensed content publisher	Springer
Licensed content publication	Clinical Proteomics
Licensed content title	Altered proteome profiles in maternal plasma in pregnancies with fetal growth restriction
Licensed content author	Madhulika B. Gupta
Licensed content date	Jan 1, 2006
Volume number	2
Issue number	3
Type of Use	Thesis/Dissertation
Portion	Full text
Number of copies	5
Author of this Springer article	Yes and you are the sole author of the new work
Order reference number	
Title of your thesis / dissertation	Maternal and fetal plasma proteome changes in fetal growth restriction
Expected completion date	Dec 2011
Estimated size(pages)	300
Total	**0.00 USD**

Terms and Conditions

Introduction
The publisher for this copyrighted material is Springer Science + Business Media. By clicking "accept" in connection with completing this licensing transaction, you agree that the following terms and conditions apply to this transaction (along with the Billing and Payment terms and conditions established by Copyright Clearance Center, Inc. ("CCC"), at the time that you opened your Rightslink account and that are available at any time at http://myaccount.copyright.com).
Limited License
With reference to your request to reprint in your thesis material on which Springer Science and Business Media control the copyright, permission is granted, free of charge, for the use indicated in your enquiry. Licenses are for one-time use only with a maximum distribution equal to the number that you identified in the licensing process.
This License includes use in an electronic form, provided it is password protected or on the university's intranet, destined to microfilming by UMI and University repository. For any other electronic use, please contact Springer at (permissions.dordrecht@springer.com or permissions.heidelberg@springer.com)
The material can only be used for the purpose of defending your thesis, and with a maximum of 100 extra copies in paper.
Although Springer holds copyright to the material and is entitled to negotiate on rights, this license is only valid, provided permission is also obtained from the (co) author (address is given with the

article/chapter) and provided it concerns original material which does not carry references to other sources (if material in question appears with credit to another source, authorization from that source is required as well). Permission free of charge on this occasion does not prejudice any rights we might have to charge for reproduction of our copyrighted material in the future.
Altering/Modifying Material: Not Permitted
However figures and illustrations may be altered minimally to serve your work. Any other abbreviations, additions, deletions and/or any other alterations shall be made only with prior written authorization of the author(s) and/or Springer Science + Business Media. (Please contact Springer at permissions.dordrecht@springer.com or permissions.heidelberg@springer.com)
Reservation of Rights
Springer Science + Business Media reserves all rights not specifically granted in the combination of (i) the license details provided by you and accepted in the course of this licensing transaction, (ii) these terms and conditions and (iii) CCC's Billing and Payment terms and conditions.
Copyright Notice:
Please include the following copyright citation referencing the publication in which the material was originally published. Where wording is within brackets, please include verbatim.
"With kind permission from Springer Science+Business Media: <book/journal title, chapter/article title, volume, year of publication, page, name(s) of author(s), figure number(s), and any original (first) copyright notice displayed with material>."
Warranties: Springer Science + Business Media makes no representations or warranties with respect to the licensed material.
Indemnity
You hereby indemnify and agree to hold harmless Springer Science + Business Media and CCC, and their respective officers, directors, employees and agents, from and against any and all claims arising out of your use of the licensed material other than as specifically authorized pursuant to this license.
No Transfer of License
This license is personal to you and may not be sublicensed, assigned, or transferred by you to any other person without Springer Science + Business Media's written permission.
No Amendment Except in Writing
This license may not be amended except in a writing signed by both parties (or, in the case of Springer Science + Business Media, by CCC on Springer Science + Business Media's behalf).
Objection to Contrary Terms
Springer Science + Business Media hereby objects to any terms contained in any purchase order, acknowledgment, check endorsement or other writing prepared by you, which terms are inconsistent with these terms and conditions or CCC's Billing and Payment terms and conditions. These terms and conditions, together with CCC's Billing and Payment terms and conditions (which are incorporated herein), comprise the entire agreement between you and Springer Science + Business Media (and CCC) concerning this licensing transaction. In the event of any conflict between your obligations established by these terms and conditions and those established by CCC's Billing and Payment terms and conditions, these terms and conditions shall control.
Jurisdiction
All disputes that may arise in connection with this present License, or the breach thereof, shall be settled exclusively by the country's law in which the work was originally published.
Other terms and conditions:
v1.2

Gratis licenses (referencing $0 in the Total field) are free. Please retain this printable license for your reference. No payment is required.

If you would like to pay for this license now, please remit this license along with your payment made payable to "COPYRIGHT CLEARANCE CENTER" otherwise you will be invoiced within 48 hours of the license date. Payment should be in the form of a check or money order referencing your account number and this invoice number RLNK0. Once you receive your invoice for this order, you may pay your invoice by credit card. Please follow instructions provided at that time.

Make Payment To:
Copyright Clearance Center
Dept 001
P.O. Box 843006
Boston, MA 02284-3006

For suggestions or comments regarding this order, contact Rightslink Customer Support:

SPRINGER LICENSE
TERMS AND CONDITIONS

Aug 30, 2011

This is a License Agreement between Maxim D Seferovic ("You") and Springer ("Springer") provided by Copyright Clearance Center ("CCC"). The license consists of your order details, the terms and conditions provided by Springer, and the payment terms and conditions.

All payments must be made in full to CCC. For payment instructions, please see information listed at the bottom of this form.

License Number	2738780661819
License date	Aug 30, 2011
Licensed content publisher	Springer
Licensed content publication	Clinical Proteomics
Licensed content title	Altered proteome profiles in maternal plasma in pregnancies with fetal growth restriction
Licensed content author	Madhulika B. Gupta
Licensed content date	Jan 1, 2006
Volume number	2
Issue number	3
Type of Use	Thesis/Dissertation
Portion	Figures
Author of this Springer article	Yes and you are the sole author of the new work
Order reference number	
Title of your thesis / dissertation	Maternal and fetal plasma proteome changes in fetal growth restriction
Expected completion date	Dec 2011
Estimated size(pages)	300
Total	**0.00 USD**

Terms and Conditions

Introduction
The publisher for this copyrighted material is Springer Science + Business Media. By clicking "accept" in connection with completing this licensing transaction, you agree that the following terms and conditions apply to this transaction (along with the Billing and Payment terms and conditions established by Copyright Clearance Center, Inc. ("CCC"), at the time that you opened your Rightslink account and that are available at any time at http://myaccount.copyright.com).
Limited License
With reference to your request to reprint in your thesis material on which Springer Science and Business Media control the copyright, permission is granted, free of charge, for the use indicated in your enquiry. Licenses are for one-time use only with a maximum distribution equal to the number that you identified in the licensing process.
This License includes use in an electronic form, provided it is password protected or on the university's intranet, destined to microfilming by UMI and University repository. For any other electronic use, please contact Springer at (permissions.dordrecht@springer.com or permissions.heidelberg@springer.com)
The material can only be used for the purpose of defending your thesis, and with a maximum of 100 extra copies in paper.
Although Springer holds copyright to the material and is entitled to negotiate on rights, this license is only valid, provided permission is also obtained from the (co) author (address is given with the article/chapter) and provided it concerns original material which does not carry references to other sources (if material in question appears with credit to another source, authorization from that

source is required as well). Permission free of charge on this occasion does not prejudice any rights we might have to charge for reproduction of our copyrighted material in the future.
Altering/Modifying Material: Not Permitted

However figures and illustrations may be altered minimally to serve your work. Any other abbreviations, additions, deletions and/or any other alterations shall be made only with prior written authorization of the author(s) and/or Springer Science + Business Media. (Please contact Springer at permissions.dordrecht@springer.com or permissions.heidelberg@springer.com)
Reservation of Rights

Springer Science + Business Media reserves all rights not specifically granted in the combination of (i) the license details provided by you and accepted in the course of this licensing transaction, (ii) these terms and conditions and (iii) CCC's Billing and Payment terms and conditions.
Copyright Notice:

Please include the following copyright citation referencing the publication in which the material was originally published. Where wording is within brackets, please include verbatim.
"With kind permission from Springer Science+Business Media: <book/journal title, chapter/article title, volume, year of publication, page, name(s) of author(s), figure number(s), and any original (first) copyright notice displayed with material>."
Warranties: Springer Science + Business Media makes no representations or warranties with respect to the licensed material.
Indemnity

You hereby indemnify and agree to hold harmless Springer Science + Business Media and CCC, and their respective officers, directors, employees and agents, from and against any and all claims arising out of your use of the licensed material other than as specifically authorized pursuant to this license.
No Transfer of License

This license is personal to you and may not be sublicensed, assigned, or transferred by you to any other person without Springer Science + Business Media's written permission.
No Amendment Except in Writing

This license may not be amended except in a writing signed by both parties (or, in the case of Springer Science + Business Media, by CCC on Springer Science + Business Media's behalf).
Objection to Contrary Terms

Springer Science + Business Media hereby objects to any terms contained in any purchase order, acknowledgment, check endorsement or other writing prepared by you, which terms are inconsistent with these terms and conditions or CCC's Billing and Payment terms and conditions. These terms and conditions, together with CCC's Billing and Payment terms and conditions (which are incorporated herein), comprise the entire agreement between you and Springer Science + Business Media (and CCC) concerning this licensing transaction. In the event of any conflict between your obligations established by these terms and conditions and those established by CCC's Billing and Payment terms and conditions, these terms and conditions shall control.
Jurisdiction

All disputes that may arise in connection with this present License, or the breach thereof, shall be settled exclusively by the country's law in which the work was originally published.
Other terms and conditions:
v1.2

Gratis licenses (referencing $0 in the Total field) are free. Please retain this printable license for your reference. No payment is required.

If you would like to pay for this license now, please remit this license along with your payment made payable to "COPYRIGHT CLEARANCE CENTER" otherwise you will be invoiced within 48 hours of the license date. Payment should be in the form of a check or money order referencing your account number and this invoice number RLNK0. Once you receive your invoice for this order, you may pay your invoice by credit card. Please follow instructions provided at that time.

Make Payment To:
Copyright Clearance Center
Dept 001
P.O. Box 843006
Boston, MA 02284-3006

For suggestions or comments regarding this order, contact Rightslink Customer Support:

ELSEVIER LICENSE
TERMS AND CONDITIONS

Aug 30, 2011

This is a License Agreement between Maxim D Seferovic ("You") and Elsevier ("Elsevier") provided by Copyright Clearance Center ("CCC"). The license consists of your order details, the terms and conditions provided by Elsevier, and the payment terms and conditions.

All payments must be made in full to CCC. For payment instructions, please see information listed at the bottom of this form.

Supplier	Elsevier Limited
	The Boulevard,Langford Lane
	Kidlington,Oxford,OX5 1GB,UK
Registered Company Number	1982084
Customer name	Maxim D Seferovic
Customer address	800 commissioners Rd S.
	London, ON N5Y 3G8
License number	2738780827176
License date	Aug 30, 2011
Licensed content publisher	Elsevier
Licensed content publication	Journal of Chromatography B
Licensed content title	Quantitative 2-D gel electrophoresis-based expression proteomics of albumin and IgG immunodepleted plasma
Licensed content author	Maxim D. Seferovic,Violet Krughkov,Devanand Pinto,Victor K.M. Han,Madhulika B. Gupta
Licensed content date	01 April 2008
Licensed content volume number	865
Licensed content issue number	1-2
Number of pages	6
Start Page	147
End Page	152
Type of Use	reuse in a thesis/dissertation
Intended publisher of new work	other
Portion	full article
Format	both print and electronic
Are you the author of this Elsevier article?	Yes
Will you be translating?	No
Order reference number	
Title of your thesis/dissertation	Maternal and fetal plasma proteome changes in fetal growth restriction
Expected completion date	Dec 2011
Estimated size (number of pages)	300

Elsevier VAT number	GB 494 6272 12
Permissions price	0.00 USD
VAT/Local Sales Tax	0.0 USD / 0.0 GBP
Total	**0.00 USD**

Terms and Conditions

INTRODUCTION

1. The publisher for this copyrighted material is Elsevier. By clicking "accept" in connection with completing this licensing transaction, you agree that the following terms and conditions apply to this transaction (along with the Billing and Payment terms and conditions established by Copyright Clearance Center, Inc. ("CCC"), at the time that you opened your Rightslink account and that are available at any time at http://myaccount.copyright.com).

GENERAL TERMS

2. Elsevier hereby grants you permission to reproduce the aforementioned material subject to the terms and conditions indicated.

3. Acknowledgement: If any part of the material to be used (for example, figures) has appeared in our publication with credit or acknowledgement to another source, permission must also be sought from that source. If such permission is not obtained then that material may not be included in your publication/copies. Suitable acknowledgement to the source must be made, either as a footnote or in a reference list at the end of your publication, as follows:

"Reprinted from Publication title, Vol /edition number, Author(s), Title of article / title of chapter, Pages No., Copyright (Year), with permission from Elsevier [OR APPLICABLE SOCIETY COPYRIGHT OWNER]." Also Lancet special credit - "Reprinted from The Lancet, Vol. number, Author(s), Title of article, Pages No., Copyright (Year), with permission from Elsevier."

4. Reproduction of this material is confined to the purpose and/or media for which permission is hereby given.

5. Altering/Modifying Material: Not Permitted. However figures and illustrations may be altered/adapted minimally to serve your work. Any other abbreviations, additions, deletions and/or any other alterations shall be made only with prior written authorization of Elsevier Ltd. (Please contact Elsevier at permissions@elsevier.com)

6. If the permission fee for the requested use of our material is waived in this instance, please be advised that your future requests for Elsevier materials may attract a fee.

7. Reservation of Rights: Publisher reserves all rights not specifically granted in the combination of (i) the license details provided by you and accepted in the course of this licensing transaction, (ii) these terms and conditions and (iii) CCC's Billing and Payment terms and conditions.

8. License Contingent Upon Payment: While you may exercise the rights licensed immediately upon issuance of the license at the end of the licensing process for the transaction, provided that you have disclosed complete and accurate details of your proposed use, no license is finally effective unless and until full payment is received from you (either by publisher or by CCC) as provided in CCC's Billing and Payment terms and conditions. If full payment is not received on a timely basis, then any license preliminarily granted shall be deemed automatically revoked and shall be void as if never granted. Further, in the event that you breach any of these terms and conditions or any of CCC's Billing and Payment terms and conditions, the license is automatically revoked and shall be void as if never granted. Use of materials as described in a revoked license, as well as any use of the materials beyond the scope of an unrevoked license, may constitute copyright infringement and publisher reserves the right to take any and all action to protect its copyright in the materials.

9. Warranties: Publisher makes no representations or warranties with respect to the licensed material.

10. Indemnity: You hereby indemnify and agree to hold harmless publisher and CCC, and their respective officers, directors, employees and agents, from and against any and all claims arising out of your use of the licensed material other than as specifically authorized pursuant to this license.

11. No Transfer of License: This license is personal to you and may not be sublicensed, assigned, or transferred by you to any other person without publisher's written permission.

12. No Amendment Except in Writing: This license may not be amended except in a writing signed by both parties (or, in the case of publisher, by CCC on publisher's behalf).

13. Objection to Contrary Terms: Publisher hereby objects to any terms contained in any purchase order, acknowledgment, check endorsement or other writing prepared by you, which terms are inconsistent with these terms and conditions or CCC's Billing and Payment terms and conditions. These terms and conditions, together with CCC's Billing and Payment terms and conditions (which are incorporated herein), comprise the entire agreement between you and publisher (and CCC) concerning this licensing transaction. In the event of any conflict between your obligations established by these terms and conditions and those established by CCC's Billing and Payment terms and conditions, these terms and conditions shall control.

14. Revocation: Elsevier or Copyright Clearance Center may deny the permissions described in this License at their sole discretion, for any reason or no reason, with a full refund payable to you. Notice of such denial will be made using the contact information provided by you. Failure to receive such notice will not alter or invalidate the denial. In no event will Elsevier or Copyright Clearance Center be responsible or liable for any costs, expenses or damage incurred by you as a result of a denial of your permission request, other than a refund of the amount(s) paid by you to Elsevier and/or Copyright Clearance Center for denied permissions.

LIMITED LICENSE

The following terms and conditions apply only to specific license types:

15. **Translation**: This permission is granted for non-exclusive world **English** rights only unless your license was granted for translation rights. If you licensed translation rights you may only translate this content into the languages you requested. A professional translator must perform all translations and reproduce the content word for word preserving the integrity of the article. If this license is to re-use 1 or 2 figures then permission is granted for non-exclusive world rights in all languages.

16. **Website**: The following terms and conditions apply to electronic reserve and author websites:

Electronic reserve: If licensed material is to be posted to website, the web site is to be password-protected and made available only to bona fide students registered on a relevant course if:

This license was made in connection with a course,

This permission is granted for 1 year only. You may obtain a license for future website posting,

All content posted to the web site must maintain the copyright information line on the bottom of each image,

A hyper-text must be included to the Homepage of the journal from which you are licensing at http://www.sciencedirect.com/science/journal/xxxxx or the Elsevier homepage for books at http://www.elsevier.com , and

Central Storage: This license does not include permission for a scanned version of the material to be stored in a central repository such as that provided by Heron/XanEdu.

17. **Author website** for journals with the following additional clauses:

All content posted to the web site must maintain the copyright information line on the bottom of each image, and

he permission granted is limited to the personal version of your paper. You are not allowed to download and post the published electronic version of your article (whether PDF or HTML, proof or final version), nor may you scan the printed edition to create an electronic version,

A hyper-text must be included to the Homepage of the journal from which you are licensing at http://www.sciencedirect.com/science/journal/xxxxx , As part of our normal production process, you will receive an e-mail notice when your article appears on Elsevier's online service ScienceDirect (www.sciencedirect.com). That e-mail will include the article's Digital Object Identifier (DOI). This number provides the electronic link to the published article and should be included in the posting of your personal version. We ask that you wait until you receive this e-mail and have the DOI to do any posting.

Central Storage: This license does not include permission for a scanned version of the material to be stored in a central repository such as that provided by Heron/XanEdu.

18. **Author website** for books with the following additional clauses:

Authors are permitted to place a brief summary of their work online only.

A hyper-text must be included to the Elsevier homepage at http://www.elsevier.com

All content posted to the web site must maintain the copyright information line on the bottom of each image

You are not allowed to download and post the published electronic version of your chapter, nor may you scan the printed edition to create an electronic version.

Central Storage: This license does not include permission for a scanned version of the material to be stored in a central repository such as that provided by Heron/XanEdu.

19. **Website** (regular and for author): A hyper-text must be included to the Homepage of the journal from which you are licensing at http://www.sciencedirect.com/science/journal/xxxxx. or for books to the Elsevier homepage at http://www.elsevier.com

20. **Thesis/Dissertation**: If your license is for use in a thesis/dissertation your thesis may be submitted to your institution in either print or electronic form. Should your thesis be published commercially, please reapply for permission. These requirements include permission for the Library and Archives of Canada to supply single copies, on demand, of the complete thesis and include permission for UMI to supply single copies, on demand, of the complete thesis. Should your thesis be published commercially, please reapply for permission.

21. **Other Conditions**:

v1.6

Copyright Clearance Center

RightsLink

Home | Account Info | Help

ACS Publications
High quality. High impact.

Title: Altered Liver Secretion of Vascular Regulatory Proteins in Hypoxic Pregnancies Stimulate Angiogenesis in vitro

Author: Maxim D. Seferovic et al.

Publication: Journal of Proteome Research

Publisher: American Chemical Society

Date: Apr 1, 2011

Copyright © 2011, American Chemical Society

Logged in as:
Maxim Seferovic
Account #:
3000442836

LOGOUT

No charge permission and attribution

Permission for this particular request is granted for print and electronic formats at no charge. Figures and tables may be modified. Appropriate credit should be given. Please print this page for your records and provide a copy to your publisher. Requests for up to 4 figures require only this record. Five or more figures will generate a printout of additional terms and conditions. Appropriate credit should read: "Reprinted with permission from {COMPLETE REFERENCE CITATION}. Copyright {YEAR} American Chemical Society." Insert appropriate information in place of the capitalized words.

BACK | CLOSE WINDOW

Granted - Copyright Permission Request

From:
Sent: August-30-11 9:17:37 AM
To:
Cc:

The Endocrine Society
8401 Connecticut Avenue, Suite 900
Chevy Chase, MD 20815-5817

www.endo-society.org
TIN Number: 73-0531256

Form was submitted by: maxseferovic@hotmail.com

Original author to publish in a Dissertation.

Date: August 30, 2011
Reference Number:

Name: Maxim Seferovic
Organization: The University of Western Ontario
Department:
Address: 800 Commissioners Rd E
City, State and Postal Code: London, Ontario N5y 3G8
Country: Canada
Phone:
Fax:
Email:

Journal: Endocrinology
Author Name: M. Seferovic
Title: Hypoxia and leucine deprivation induce human IGFBP-1 hyper-phosphorylation and increase its biological activity.
Year: 2009
Volume: 10
Page Range: 220-31
Figure Reproduction:
Figure Number(s): Fig 1, Fig 2, Fig 3, Fig 4, Fig 5, Fig 6, Table 1, Table 2
Where will the figures appear:
- Dissertation
- Title: Maternal and fetal plasma proteome changes in fetal growth restriction

The Endocrine Society grants permission to reproduce tables/figures Fig 1, Fig 2, Fig 3, Fig 4, Fig 5, Fig 6, Table 1 and Table 2 from the selected article stated above contingent upon the following conditions: 1) That you give proper credit to the author(s) and to include in your citation, the title of journal, title of article, volume, issue number, date, and page numbers. 2) That you include the statement *Copyright 2009, The Endocrine Society*. Please understand that permission is granted for one-time use only. Permission must be requested separately for future editions, revisions, translations, derivative works, and promotional pieces.

Office of Research Ethics

The University of Western Ontario
Room 4180 Support Services Building, London, ON, Canada N6A 5C1

Website: www.uwo.ca/research/ethics

Use of Human Subjects - Ethics Approval Notice

Principal Investigator: Dr. M.B. Gupta	**Review Level:** Expedited
Review Number: 08422E	**Revision Number:** 6
Review Date: January 20, 2010	**Approved Local # of Participants:** 78

Protocol Title: Clinical significance of IGFBP-1 Phosphoisoforms and other proteins in intrauterine growth restriction (IUGR).

Department and Institution: Paediatrics, London Health Sciences Centre

Sponsor:

Ethics Approval Date: January 20, 2010   **Expiry Date:** December 31, 2015

Documents Reviewed and Approved: Revised Study End Date

Documents Received for Information:

This is to notify you that The University of Western Ontario Research Ethics Board for Health Sciences Research Involving Human Subjects (HSREB) which is organized and operates according to the Tri-Council Policy Statement: Ethical Conduct of Research Involving Humans and the Health Canada/ICH Good Clinical Practice Practices: Consolidated Guidelines; and the applicable laws and regulations of Ontario has reviewed and granted approval to the above referenced revision(s) or amendment(s) on the approval date noted above. The membership of this REB also complies with the membership requirements for REB's as defined in Division 5 of the Food and Drug Regulations.

The ethics approval for this study shall remain valid until the expiry date noted above assuming timely and acceptable responses to the HSREB's periodic requests for surveillance and monitoring information. If you require an updated approval notice prior to that time you must request it using the UWO Updated Approval Request Form.

During the course of the research, no deviations from, or changes to, the protocol or consent form may be initiated without prior written approval from the HSREB except when necessary to eliminate immediate hazards to the subject or when the change(s) involve only logistical or administrative aspects of the study (e.g. change of monitor, telephone number). Expedited review of minor change(s) in ongoing studies will be considered. Subjects must receive a copy of the signed information/consent documentation.

Investigators must promptly also report to the HSREB:

a) changes increasing the risk to the participant(s) and/or affecting significantly the conduct of the study;
b) all adverse and unexpected experiences or events that are both serious and unexpected;
c) new information that may adversely affect the safety of the subjects or the conduct of the study.

If these changes/adverse events require a change to the information/consent documentation, and/or recruitment advertisement, the newly revised information/consent documentation, and/or advertisement, must be submitted to this office for approval.

Members of the HSREB who are named as investigators in research studies, or declare a conflict of interest, do not participate in discussion related to, nor vote on, such studies when they are presented to the HSREB.

Chair of HSREB: Dr. Joseph Gilbert
FDA Ref. #: IRB 00000940

Ethics Officer to Contact for Further Information			
☐ Janice Sutherland	☐ Elizabeth Wambolt	☐ Grace Kelly	☐ Denise Grafton

This is an official document. Please retain the original in your files.   cc: ORE File
LHRI

UWO HSREB Ethics Approval - Revision
V.2008-07-01 (rptApprovalNoticeHSREB_REV)   08422E   Page 1 of 1

MAXIM D. SEFEROVIC - CURRICULUM VITAE

EDUCATION

Doctor of Philosophy, Biochemistry (2011)
University of Western Ontario, Children's Health Research Institute

Bachelor of Medical Sciences (Honours), Biochemistry (2005)
University of Western Ontario

SCHOLARSHIPS

Alexander Graham Bell Canada Graduate Scholarship (2009-2011)
Natural Science and Engineering Research Council of Canada

Graduate Scholarship (2008-2009)
Department of Paediatrics, University of Western Ontario

AWARDS

HUPO Travel Award, Genome Canada (2009)

Publication incentive, Department of Biochemistry (2008)

Best Talk, Dept. of Paediatrics Research Day (2008)

Travel Award, Children's Health Research Institute (2007)

Dean's List Honour Student (2000/2005)

EXPERIENCE

Graduate Research Thesis, (2006 - Present)
Dept. of Biochemistry, University of Western Ontario

Teaching Assistant, (2008, 2009)
Dept. of Biochemistry, University of Western Ontario

Visiting Research Student, (Summer 2008)
National Research Council - Institute for Marine Biosciences, Halifax, NS

BMSc. Research Thesis, (2004 - 2005)
Dept. of Biochemistry, University of Western Ontario

Mineral and mycotoxin analyst, (2003 - 2004)
Cargill Animal Nutrition, North American Regional Laboratory, Strathroy, ON

PUBLICATIONS

Journal Articles

Seferovic, M.D., Han, V.K.M., and Gupta, M.B. Maternal and fetal vascular inflammation in placental insufficiency: VCAM-1 as a marker of placental health. *In Preparation.*

Seferovic, M.D., Han, V.K.M., and Gupta, M.B. Oxygen dependent increase in fetal-placental plasma PAI-1 stimulates angiogenesis in placental insufficiency. *In Preparation.*

Seferovic, M.D., Pinto, D., Chen, C., and Gupta, M.B. (2011). Altered Liver Secretion of Vascular Regulatory Proteins in Hypoxic Pregnancies Stimulate Angiogenesis *in vitro. Journal of Proteome Research*. *10* (4):1495–1504.

Seferovic, M.D., Ali, R., Kamei, H., Liu, S., Khosravi, J.M., Nazarian, S., Han, V.K.M., Duan, C., and Gupta, M.B. (2009). Hypoxia and leucine deprivation induce human IGFBP-1 hyper-phosphorylation and increase its biological activity. *Endocrinology.* 150(1):220-31.

Seferovic, M.D., Krughkov, V., Pinto, D., Han V.K.M., and Gupta, M.B. (2008). Quantitative 2-D gel electrophoresis-based expression proteomics of albumin and IgG immunodepleted plasma. *Journal of Chromatography B*. 865(1-2): 147-52.

Gupta, M.B., Seferovic, M.D., Liu, S., Gratton, R., Doherty-Kirby, A., Lajoie, G., and Han, V.K.M. (2006). Haptoglobin α2 in maternal plasma from pregnancies with fetal growth restriction. *Clinical Proteomics*. 2(3-4): 169-184.

Book Chapters

Han, V.K.M., Seferovic, M.D., Albion, C.D., and Gupta, M.B. Intrauterine growth restriction: Intervention strategies. In, *Neonatology: A practical approach to neonatal diseases.* Buonocore, G., Bracci, R., Weindling, M., (Eds). Springer-Verlag Italia, 2012:89-93.